An investigation into perceived motion paths by means of the Slalom Illusion

GHEORGHES, Tamara

Available from Sheffield Hallam University Research Archive (SHURA) at:

http://shura.shu.ac.uk/22408/

SHEFFIELD HALLAM UNIVERSITY

An Investigation into Perceived Motion Paths by Means of the Slalom Illusion

---

By

Tamara Nicoleta Gheorghes (BSc, MSc)

A thesis submitted to the Faculty in partial fulfilment of the requirements for

Doctor of Philosophy

in

Psychology

Faculty of Development & Society

Department of Psychology, Sociology & Politics

April 2018

Abstract

When a dot moves horizontally across a set of tilted lines of alternating orientations, the dot appears to be moving up and down along its trajectory. This perceptual phenomenon, known as the 'slalom illusion' (Cesaro & Agostini, 1998), reveals a mismatch between the veridical motion signals and the subjective percept of the motion trajectory which has not been comprehensively explained. In the context of the current thesis, the slalom illusion was used as a paradigm to investigate the integration of the brief and localised motion signals that are initially encoded by the visual cortex into the overall illusory percept that is subjectively perceived by human observers. It was observed that the slalom illusion also occurs when part of the dot trajectory is occluded by another object, with an increased magnitude, and that it occurs both when the eyes follow the dot and when the gaze remains fixated. The latter finding was replicated in foveal and in peripheral vision. An inverse stimulus display, whereby a dot trajectory that in reality was sinusoidal in shape moved across a set of vertical lines, did not result in the expected inverse effect of an underestimated trajectory amplitude. A theoretical view on the slalom illusion was developed, positing that the illusion is not rooted in the earliest phase of visual processing, and that the human visual system only interprets trajectories after the fact - that is, after the input motion signals have been registered for a period of time - rather than on-line as the motion signals arrive. Moreover, it was proposed that straight trajectories in particular are sensitive to perceptual biases and illusions, due to the propensity of neurons in thevisual cortex to encode the transients of motion direction over a constant motion direction. In conclusion, the slalom illusion reveals that human visual perception of the trajectory of a moving object is an active inferential process, in which it is more important to form a coherent interpretation consistent with prior knowledge of realistic object motion, than it is to perceive the input motion signals accurately. Through systematic manipulation of the elements of the slalom display, the properties of this process can be investigated.

Table of contents

Acknowledgements

I dedicate this thesis to the memory of my mother, Tatiana, whose determined and persistent spirit is what I will always aspire to.

I would like to thank my supervisors, Dr John Reidy and Dr Paul Richardson, for their continuous support, trust, and encouragement. Their kind disposition and thoughtful feedback have helped me overcome all the inherent challenges throughout this process.

I also want to acknowledge the support I received from Sheffield Hallam University's Psychology, Sociology and Politics department and its Doctoral Researchers community.

I want to thank Maarten for his patience and support during the writing stage of this thesis.

Finally, I want to thankmy closest: Raluca, Radu, and Ioana, without whom I would have found this journey much more difficult.

1. Chapter 1 - General introduction

1.1. Introduction

1.1.1. Motion as a Gestalt

In 1912, Max Wertheimer published an experiment which marked a new beginning for the study of human visual perception. Using a tachitoscopic wheel, two identical line stimuli were flashed in quick succession. As the inter-stimulus interval (ISI) decreased, the subjective percept changed from that of two alternating stimuli, to a perception of a stimulus apparently moving between both positions, to two simultaneous stimuli flashing (Wagemans et al., 2012). This is known as *apparent motion*. The phenomenon of interest, however, occurred when the ISI was decreased slightly below the apparent motion stage: the subjects perceived the motion, but without the moving object which would have produced it. Wertheimer named this *phi motion*, or pure motion.

This finding is historically significant, in that it is generally considered to have created the field of Gestalt psychology. A 'Gestalt' is often described as a whole (in Wertheimer's case, pure motion) that is more than the sum of its constituent parts (the stimulus positions). But the phenomenon of phi motion to Gestalt psychologists revealed a more fundamental truth: that the wholes constitute the fundamental units of perception, rather than the parts, and that the brain is geared towards a direct holistic analysis of the stimulus input (Wertheimer, 1912).

Wertheimer's finding is also of singular importance for the study of motion perception itself. Decades before the identification of cortical areas functionally specialised in visual motion perception (Dubner & Zeki, 1971; Allman & Kaas, 1971), Wertheimer's psychophysical and clinical work already suggested that motion as it is analysed by the

visual system cannot be reduced to a succession of object positions and is processed separately from other aspects of the stimulus.

1.1.2. Motion as a local signal

This conceptualisation of motion as a holistic Gestalt is, however, specific to the experimental paradigm of Wertheimer (1912). In other circumstances, the resulting brief motion signal could instead constitute a part from which a larger whole is constructed. When the dot is displaced to a nearby position, the apparent motion is indeed an added Gestalt quality of perceiving the whole stimulus sequence, as opposed to perceiving two separate dots. But if the dot then continues to be displaced to a third and a fourth position, the apparent motions between each two dot positions can instead be seen as the elementary local signals, which combine to form a more complex motion trajectory. Thus, what is called the parts and what is called the whole depends on the perspective taken.

As an example, consider a ball thrown through the air and filmed at a rate of 24 frames per second. The physical stimulus to the observer consists of a sequence of static images, showing the ball at different positions. The relevant global interpretation of this video fragment, however, will be in terms of the trajectory described by the ball – to which each apparent motion between consecutive frames is only a momentary local signal. In this situation, the apparent motion is no longer the overall Gestalt in the stimulus.

Perceived trajectories, too, can then have holistic properties that are more than the sum of the motion signals in the display. An early example was reported by Michotte (1946), who created experimental displays containing two distinct objects. One object followed a straight trajectory up to the second, stationary object. At this moment, the first object stopped moving and the second object started moving along a continued straight trajectory. The subjective percept of the first object transferring its motion and

launching the second object is then an example of a Gestalt at the level of the object trajectory. Importantly, this causality is not only added to the perception of the whole trajectory, but changes the perception of the local motion signals, too. For example, Parovel and Casco (2006) report that the speed of the second object is overestimated when causality is perceived. The general problem of how the local motion signals of a moving object are integrated into the perception of a global trajectory is the subject of the current thesis, and is investigated by means of the *slalom illusion*, as described in the next section.

1.1.3. Overall goal of the thesis

The experimental paradigm used to investigate the local-global integration of object trajectories in this thesis is the *slalom illusion* (Cesàro & Agostini, 1998), whereby a dot following a straight horizontal motion path appears to move smoothly up and down as it intersects with a sequence of alternatingly tilted lines (Figure 1.1). That is, the global trajectory interpretation is qualitatively different from the local motion signals from which it is constructed.
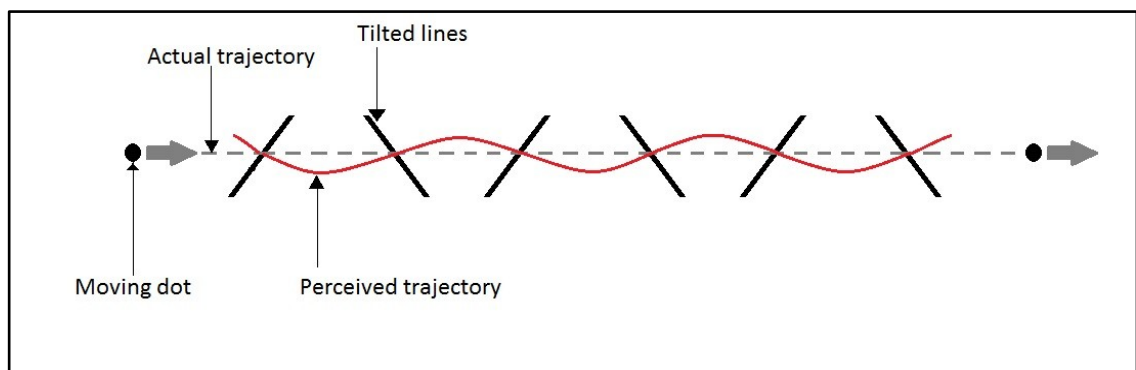
*Figure 1.1.*Schematic representation of the slalom illusion. The moving dot follows a straight trajectory, but due to its intersection with the tilted lines, the perceived trajectory is sinusoidal.

4

In section 2 and 3 of this chapter, the neuroanatomy and neural dynamics of visual processing, and motion processing in particular, will be discussed to provide a general context to the experiments performed in this thesis. The perceptual completion of occluded objects (section 4) and current knowledge on the mechanisms of motion integration (section 5) will be introduced, and broadened with a discussion of the role of eye movements (section 6). The slalom illusion, its determinants and its relation to other visual illusions will be discussed in detail in section 7, and in section 8 the specificaims of the current research will be set out.

1.2. Neurophysiology of the perception of form and motion

1.2.1. Organisation of the visual system

Figure 1.2 illustrates the visual processing stream as it proposed to exist in the human brain. As light falls on the retina of both eyes, the neurons of the optical nerve transmit electrical signals to the Lateral Geniculate Nucleus (LGN) of the thalamus, in the middle of the brain. Three anatomically distinct types of processing layers exist in LGN: parvocellular, sensitive to colour and visual detail, magnocellular, sensitive to contrast and low spatial frequencies, and koniocellular, which is heterogeneous in its functional properties. The output of LGN projects to the primary visual cortex (V1) at the back of the brain, responsible for analysing several important local characteristics of the input image, such as orientation (Hubel & Wiesel, 1959), spatial frequency (Campbell & Robson, 1968), and motion direction (Hubel & Wiesel, 1968).
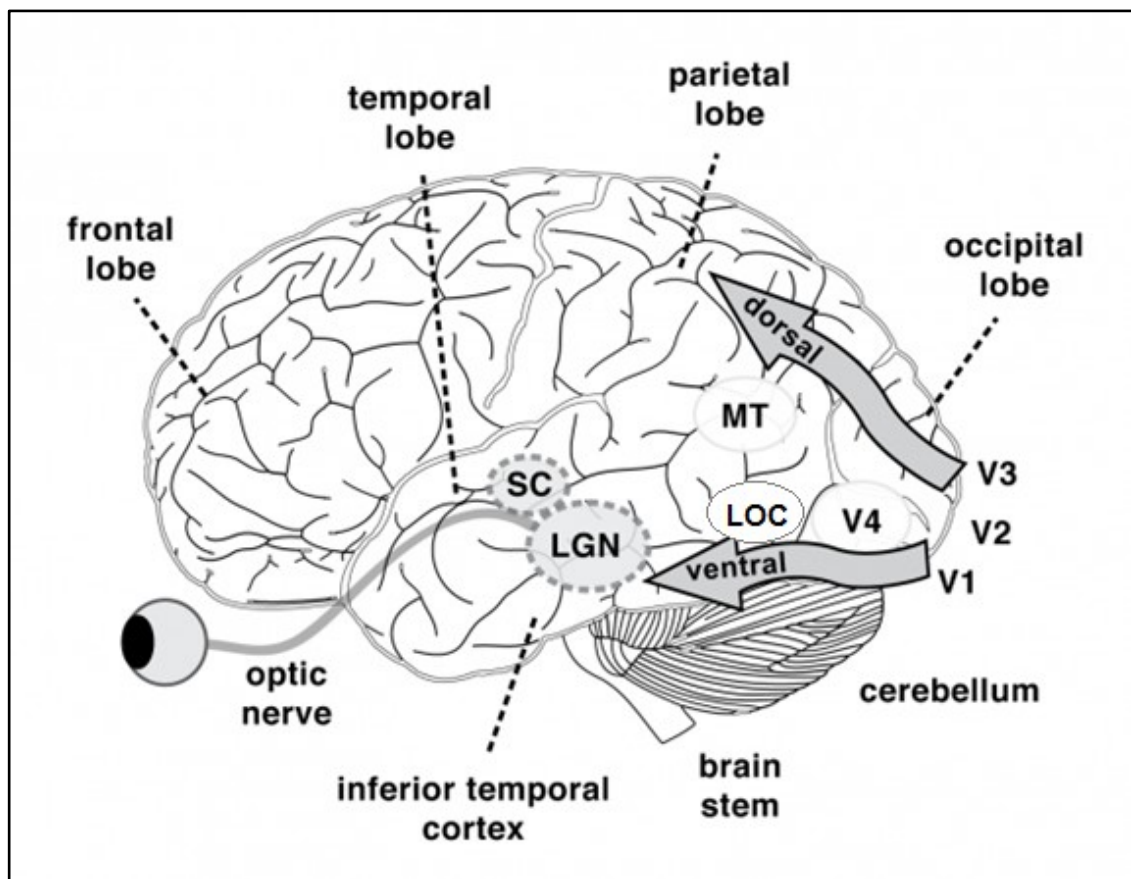
Figure 1.2. Neuroanatomical regions principally associated with visual perception (adapted from Montemayor & Haladijan, 2015).

The layout of V1 is *retinotopic*, with neighbouring locations on the retina being represented by neighbouring neurons in primary visual cortex, and organised in a *columnar* manner for local edge orientation. That is, each layer in a column represents a specific orientation, and each column represents a specific retinal location. V1 neurons represent local information because they have a small *receptive field* – the region on the retina that can be stimulated to change the activity in the neuron. They represent a stimulus characteristic, such as orientation, because they are *tuned* or *selective* to it. That is, their *response strength,* measured in the number of spikes per second, is high for a specific orientation, and much lower for other orientations.

The outputs of V1 are then projected to the next stages of visual processing, V2 and V3, where increasingly complex properties of the input are analysed, by neurons with increasingly larger receptive fields. After this stage, visual processing increasingly splits into the *ventral* and the *dorsal* stream, classically said to respectively represent the *what*and the *where* of the visual stimulus (Ungerleider & Mischkin, 1982; Goodale & Milner, 1992). The ventral stream projects to area V4 and the lateral occipital complex(LOC), where object form is analysed and object recognition occurs. The dorsal stream projects to areas MT and MST, responsible for motion, and into parietal cortex where object localisation takes place in preparation of visually driven actions. Whereas the separation between the two streams is not absolute and the interaction between their brain regions is ubiquitous (Schenk & McIntosh, 2010), as a large-scale model of functional organisation it continues to shape scientific thought about the visual system.

1.2.2. Motion perception

Early single-unit recordingson primates,whereby a micro-electrode is used to measure the electrical activity of single neurons,revealed that the middle temporal visual area (MT, also known as V5) plays a prominent role in the perception of visual motion (Dubner & Zeki, 1971; Allman & Kaas, 1971). Indeed, MT was one of the first areas in which the functional specialisation of the primate brain was so clearly demonstrated. Lesion studies have further shown that in absence of area MT, motion perception is severely compromised, to the extent that the visual world is perceived as a sequence of snapshots rather than a smooth flow of movement (Zihl, Von Cramon, & Mai, 1983; Newsome & Paré, 1988; MacLeod et al., 1996; Marcar, Zihl, & Cowey, 1997). In humans, the equivalent area is situated around the ascending limb of the temporal sulcus

(ITS) and is part of a larger motion-sensitive complex called MT+, functionally comprising both monkey area MT and monkey area MST.

The inputs of area MT originate mainly in the magnocellular layers of the LGN. These cells are sensitive to contrast and low spatial frequencies, but not colour and visual detail. The projection of LGN towards MT occurs chiefly through layer 4B of V1. Neurons in this lamina are specifically tuned to the motion of local oriented edges, as well as speed and binocular disparity (Orban, Kennedy, & Bullier, 1986; Movshon & Newsome 1996; Prince, Pointon, Cumming, & Parker, 2000). Separate from this main pathway directly from V1 into MT, there are also minor pathways going indirectly through V2 and V3 (Maunsell & Van Essen 1983; DeYoe & Van Essen, 1985), partially mediated by parvocellular LGN, and direct pathways from koniocellular cells of LGN and from the pulvinar nuclei in the thalamus. Indeed, despite being dominated by cortical inputs, MT remains partially functional even after the complete removal of V1 and the absence of conscious vision that is associated with such a lesion (Rodman, Gross, & Albright, 1989).

Area MT itself is, like V1, organised in a retinotopic fashion. There is a strong emphasis on the central part of the visual field, accounting for more than half of the total MT surface (Van Essen, Maunsell, & Bixby, 1981). Within this retinotopic map, Albright, Desimone, and Gross (1984) have demonstrated a strong columnar organization, with each column of neurons representing a preferred direction of motion. The strength of responses in area MT can also be related to the binocular disparity of the visual input (DeAngelis & Newsome, 1999), and to the speed of the motion (Liu & Newsome, 2003). The final determinant of neuronal responses is stimulus size: MT neurons are especially sensitive to smaller objects. This dependence on size is caused by centre-surround suppression, which is a common mechanism in visual cortex, whereby neurons are

especially active if other cells with a similar selectivity to a visual property (for instance, motion direction) at different locations in the retinotopic map are not active (Allman, Miezin, & McGuinness, 1985). In area MT, it allows the segmentation of a moving object from the background, based on their different motion vectors.

The specialisation of MT into motion processing comes at the cost of insensitivity to visual detail and colour. The adequate processing of moving objects can therefore not rely solely on MT, and must involve the integration of its signals with those of differently specialised brain areas. A relevant example of such an interaction is with the lateral occipital complex (LOC) in the ventral stream, which represents object shapeinstead (Kourtzi & Kanwisher, 2001).

The output signals of area MTproject into the *medial superior temporal area (MST)* of the brain, which in humans is considered part of the MT+ complex. Whereas MT is a retinotopic area, MST increasingly represents motion in the outside world as it relates to action. For instance, MST neurons display strong directional selectivity to a moving stimulus even when the gaze follows the stimulus, so that its projection is stabilised on the retina (Newsome et al., 1988). If an action into the outside world, such as manual interception of the object, is to be based on its motion representation in the visual cortex, this transformation from eye-centred (retinotopic) coding to world-centred (spatiotopic) coding of position information is necessary. In other studies, the role of MST in the representation of optic flow has been demonstrated. MST helps disambiguate self-movement from real motion in the outside world, aiding navigation (Duffy, 1998).

1.3. Dynamics of visual processing

The visual processing streams described, from early areas with small receptive fields encoding simple features to later areas with larger receptive fields encoding more complex features, are examples of feed-forward processing. Visual input signals propagate fast through the hierarchy, reaching IT cortex for object recognition within 100 ms in monkeys (Vogels, 1999; Keysers, Xiao, Földiák, & Perrett, 2001) and the corresponding areas in 150 – 200 ms in humans (Thorpe, Fize, & Marlot, 1996; Liu, Harris, & Kanwisher, 2002; Löw et al., 2003). However, substantial feedback connections exist as well in the visual cortex, sending signals back from higher-level visual areas to lower-level areas after the initial feedforward sweep (DeYoe & Van Essen, 1988; Bar, 2003). It is generally held that this feedback activity plays a key role in the emergence of awareness in visual perception (Enns & DiLollo, 2000; Lamme & Roelfsema, 2000; Tong, 2003). According to some accounts, feedback connections only apply attentional modulation to the visual input (MacKnik & Martinez-Conde, 2008), whereas others have maintained that feedforward processing acts quickly on the coarse low spatial frequency content of the scene, and the feedback activity serves to later fill in the fine details (Bullier, 2001; Hochstein & Ahissar, 2002; Bar, 2003).

An alternative interpretation of feedback activity was offered by Murray, Kersten, Olshausen, Schrater, and Woods (2002) in the context of form-from-motion. In an fMRI study, they presented participants with a display of randomly positioned dots. In the crucial condition, these dots were in fact placed on the surface of an invisible transparent cube, of which the shape became apparent when it was rotated. As a control condition, dots moving at similar velocities were positioned randomly in space. As expected, the control condition evoked activity in primary visual cortex (V1) and motion areas (MT+). The crucial cube condition, on the other hand, was strongly

associated with increased responses in the LOC, responsible for representing object shape, and at the same time it was associated with decreased responses in the V1 and MT+ activity. The authors posit that the global stimulus at the level of LOC is 'explaining away' its constituent parts – when the whole can explain the visual input array, there is no longer a need for a strong representation of the parts. This finding is reminiscent of the classical work of Navon (1977). In Experiment 3 of his landmark paper, 'Forest Before Trees', the author constructed a large letter stimulus that was made up out of a set of smaller letters, either identical or different from the global shape. Whereas the identification of the global letter was not hindered by the identity of the smaller letters, the smaller letters were significantly harder to identify when different from the global one. This ties in both with the suppression of the neuronal activity of 'parts' by the 'whole', and with the Gestalt notion that the holistic analysis is dominant in visual processing (Wertheimer, 1912).

This view has been formalised in the *predictive coding* framework (Rao & Ballard, 1999; Friston, 2010; Clark, 2013). Feed-forward processing is said to quickly generate predictions about the visual stimulus in high-level visual areas, based on prior knowledge built up through experience with the visual world. These predictions are sent back to earlier visual areas, who continue to encode only those aspects of the stimulus not explained by the prediction. That is, they essentially encode error signals with regard to the predictions generated by higher-level areas. In an iterative process, the error signal is propagated along feed-forward connections again until the optimal prediction - with the smallest error signal - is reached and the low-level neuronal activity is minimal.

Predictive coding is closely related to a view of visual processing as *hierarchical Bayesian inference* (Lee & Mumford, 2003). Applying Bayes' theorem, the probability

that a visual input stems from a certain object or a certain motion, can be computed by combining the probabilities of the visual input occurring, the object/motion occurring, and the probability that the object/motion would produce that visual input. The first is given by the initial feedforward processing, whereas the latter two require prior knowledge that is iteratively integrated into the neuronal code, fine-tuning the prediction of the object/motion until its probability given the visual input is maximal.

Predictive coding is not mutually exclusive with the earlier accounts that feedback connections apply attentional modulation, or that a quick, coarse representation of the visual scene is typically reached before conscious awareness of the details arises. Instead, it provides a generalised framework for understanding the goal of the cortical dynamics of the visual system, and how it could concretely be achieved.

1.4. Perceptual completion

To understand why an iterative and probabilistic approach is required for the visual system to analyse a stimulus, it suffices to consider the inputs it is confronted with in the real world. Whereas experimental displays often contain a small number of isolated objects with simple properties, such as a dot moving along straight trajectories, realistic objects are subject to effects of distance, viewpoint and lighting, and are often part of a rich scene. This causes them to be viewed against a cluttered background, and to be occluded from view by other objects – partially or completely, temporarily or permanently. In such circumstances, it is perhaps reasonable to suggest that the visual system is required to make approximate inferences about what is being viewed and constantly checks them against the incoming visual inputs. Different fields within vision science investigate each of these challenges. In this section, the focus is on the problem

that will hold the greatest relevance to the current thesis – the perceptual completion of wholes for which not all the parts are visible.

1.4.1. Modal and amodal completion

Perceptual completion phenomena can be subdivided into two categories, modal and amodal completion, which partly rely on different mechanisms (Murray, Foxe, Javitt, & Foxe, 2004; Singh, 2004; Albert, 2007). *Modal* completion is the perception of a visual input that is, in reality, not present. It does not involve occlusion, but does require a context to be extrapolated for the completion to occur. A well-known example is the perceptual filling-in of the blind spot of the retina, which is permanently present yet only consciously detectable by the observer in specific experimental setups. The brightness, colour and texture of this filled-in visual blindspot are extrapolated from a narrow surrounding region contiguous to the border of the blind spot (Spillmann, Otte, Hamburger, & Magnussen, 2006). *Amodal* completion (Michotte, Thinès, & Crabbé, 1964) is the inferred perception of (parts of) an object that is physically present, but occluded by another object. This is a very common situation in real-life visual perception, as objects in a scene are often not visible in their entirety. Inferring the shape of an object that is partially hidden is an integral part of vision.

The exact mechanisms driving the percept of the ultimately completed figure are still largely unknown, or researched only in the context of a specific experimental stimulus. The underlying general principles, however, are often proposed to be simplicity or likelihood. Theoretical frameworks relying on the *simplicity* principle (for instance, Hochberg & McAlister, 1953; Leeuwenberg & Boselie, 1988) in essence can be reduced to the principle of Occam's razor: in absence of further information, the most parsimonious explanation is preferable. In terms of information theory (Shannon, 1948)

13

this is often conceptualised as Minimum Description Length – the representation of the stimulus which requires the least space to describe (Van der Helm, 2014). For example, the simplest completion of a circle partially occluded by another circle in Figure 1.3 is a continuation of the circular contour, rather than a straight line.
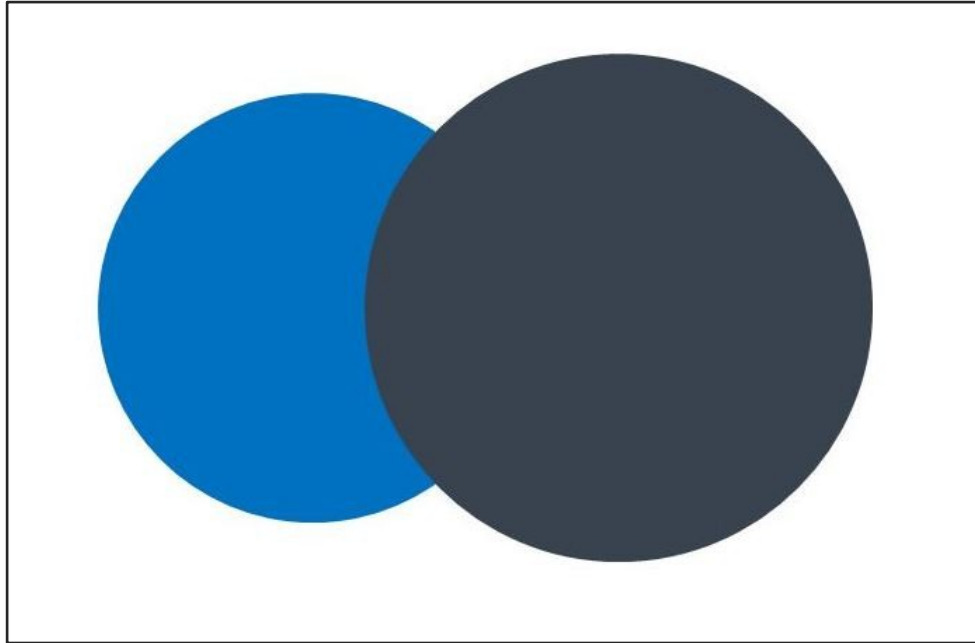
Figure 1.3. The blue figure is perceptually completed as a circle even though any other contour could be present behind the occluding circle.

Likelihood theories of perceptual completion (Helmholtz, 1924; MacKay, 2003; Feldman, 2009), on the other hand, draw on Bayes' theorem: the preferable interpretation of the distal stimulus is that, which given all prior and current knowledge, is the most likely to have given rise to the current visual input. Often, this coincides with those visual shapes that are most common in the real world. Continuing the example of the occluded circle, likelihood accounts of perceptual completion posit that a continuation of the circular contour is perceived because circles commonly occur in the real world, and because it is unlikely that the occlusion would coincidentally

coincide with the straight segment of the contour. This view relates closely to the predictive coding framework discussed in section 3.

In the next section, a particular type of modal completion - *illusory contours* - is introduced.

1.4.2.   Illusory contours

Contours or edges are an important part of the visual input, as they often delineate the visual projection of a physical object and thus allow its segmentation from the background. As Hubel and Wiesel (1959) demonstrated through their electrophysiological investigations of the primary visual cortex of the cat, the selective processing of oriented local edges lies at the very basis of the brain's visual analysis of its retinal input. In subsequent visual areas, much of the neuronal activity is likewise related to the integration and parsing of the full spatial extent of contours (Desimone, Schein, Moran, & Ungerleider, 1985). Contours are typically defined by changes in luminance and colour, with the area on one side of the contour being lighter or chromatically different than the area on the other side. Indeed, this is what many neurons in early visual cortex are tuned to (Pearson & Kingdom, 2002; Friedman, Zhou, & von der Heydt, 2003; Sumner, Anderson, Sylvester, Haynes, & Rees, 2008). The visual system is equally capable, however, of extracting object contours from experimental displays that are defined by more complex structures, such as changes in texture (Tapia, Breitmeyer, & Jacob, 2011).

Of particular interest is the phenomenon of *illusory* or *subjective* contours, where no visual cue is present around the location of the perceived contour, but rather the contour is inferred from the context. Already in the beginning of the last century, Schumann (1900) presented this phenomenon in a set-up where a "white rectangle with sharply

defined contours appears, which objectively are not there"(Figure 1.4) (as cited in Lesher, 1995, p. 279). Schumann indicated two properties of the illusory contours, namely that they require sharp edges around regions of homogenous luminance, and that they result in a brightening of the inside of the figure. However, the phenomenon did not attract a great deal of interest within the scientific community at the time.
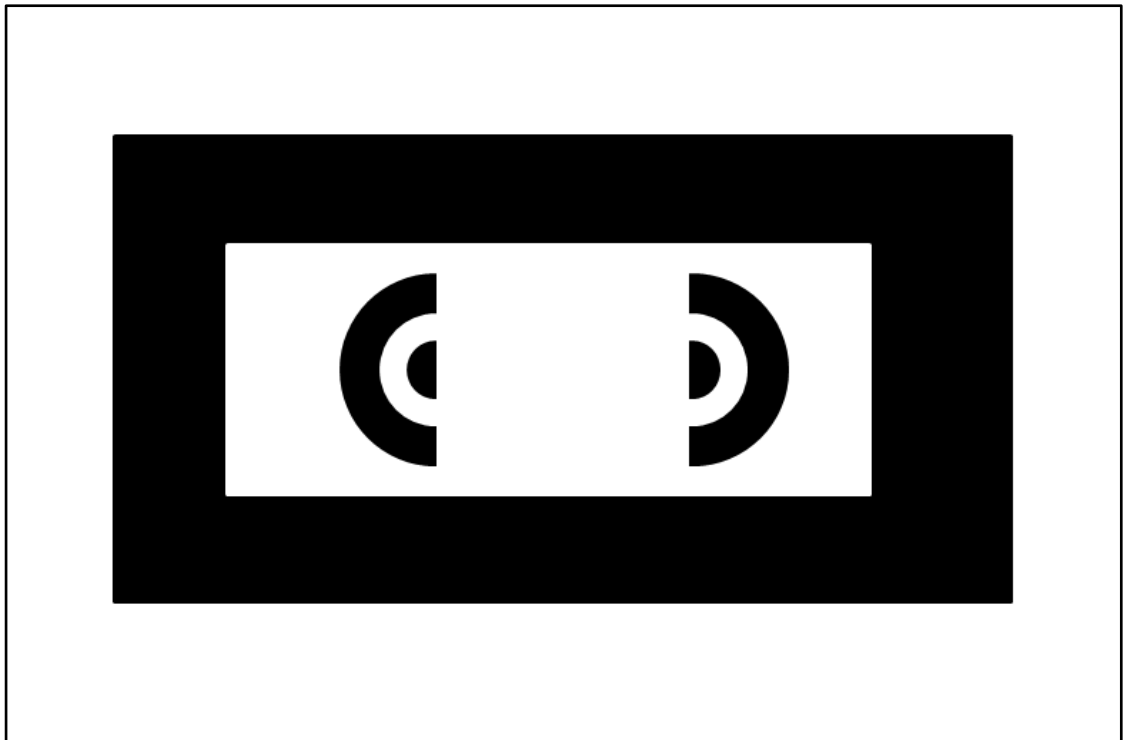
Figure 1.4. The Schumann figure: A white square is perceived in the centre of the display despite it not being objectively there.

Half a century later, Kanizsa (1955) produced clearer depictions of the same phenomenon (Figure 1.5) using three circular *inducers* with a triangular 'cut-out'. In his seminal paper from 1976, Kanizsa defines illusory contours as illusory edges or surface in the absence of any local variations in luminance in the display, and attributes to them the following additional properties: (1) that the illusory-contoured region appears brighter than the background, despite it having the same physical properties, and (2) that

16

the illusory-contoured region appears to be superimposed on the other figures in the set-up.
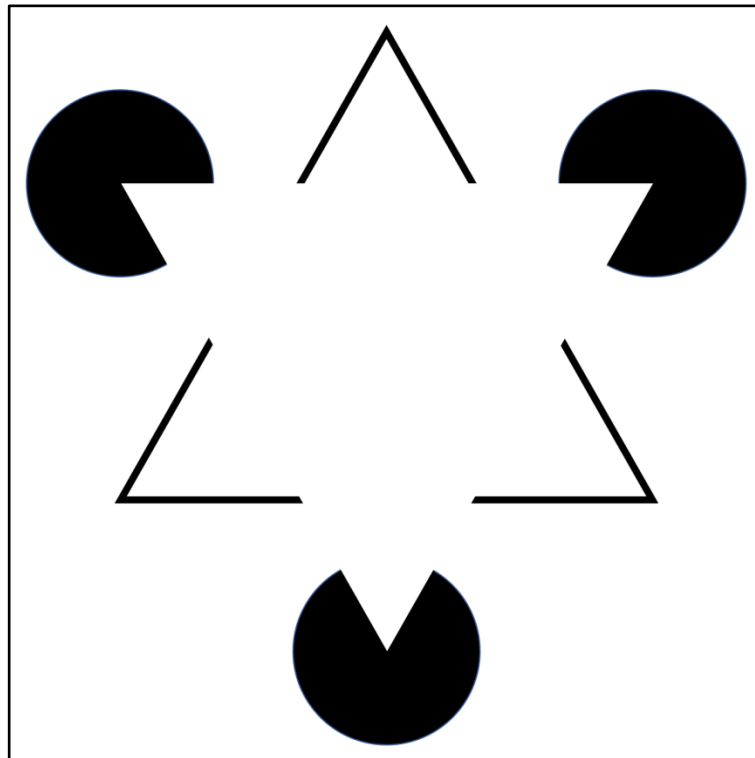
Figure 1.5. Kanizsa triangle: An illusory white triangle is perceived in the centre of the display.

The Kanizsa triangle is an example of both modal and amodal completion. The perceived superimposed white triangle is modally completed so as to occlude the inducers. It does not exist in the physical local features of the display, but is inferred from the context. The inducers are amodally completed, and are inferred to be circles occluded by the modally completed superimposed triangle. Similarly, the second triangle with real contours is amodally completed to be occluded by the white triangle. A similar and perhaps even more potent example can be found in the Koffka cross (Figure 1.6). Here, a strong percept of a circular occluder on the centre of a cross is

induced, when in reality no circular shape is present, or even directly suggested by the terminated lines.
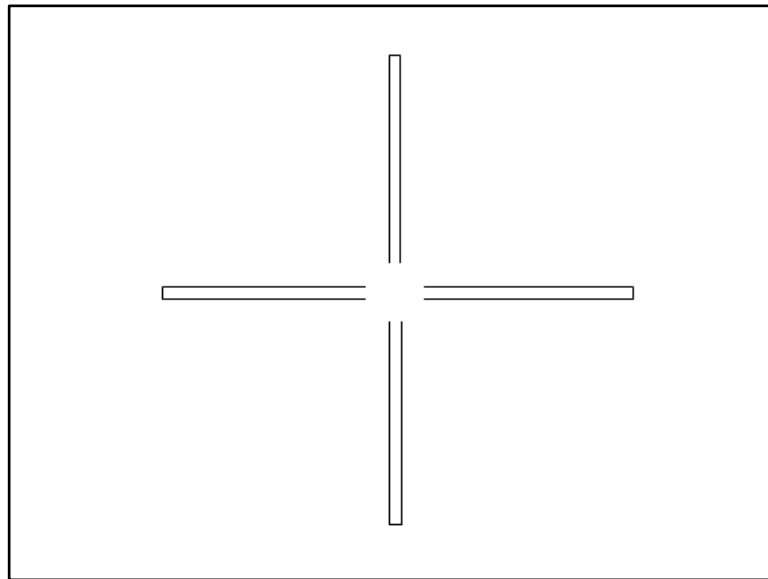
*Figure 1.6.*Koffka cross: A white circle is perceived as occluding the intersection of the two intersecting lines of a cross.

In terms of the mechanisms behind the formation of subjective contours, the theoretical framework is rather disjointed (Albert, 2007), but theories proposed thus-far can largely be grouped into three categories. In *interpolation* accounts (Grossberg & Mingolla, 1985), the illusory contour is said to form in an attempt to close the gap between the visible edges of the inducers. Closely related but subtly different, *extrapolation* accounts (Williams & Jacobs, 1997) attribute the emergence of the contour to an illusory extension of the inducer edges, meeting each other across the gap. The *figural feedback* theory (Carman & Welch, 1992), finally, proposes that the visible illusory contours arise as the result of higher visual areas identifying a large triangularfigure in the middle of the Kanizsa display, and feeding back their signals to the earlier visual cortex responsible for local contour detection. However, these three explanations are not necessarily mutually exclusive (Halko, Mingolla, & Somers, 2008).

Neurophysiological studies on illusory contours have shown that both the primary visual cortex (V1) and the secondary visual cortex (V2) respond to subjective contours, even when no physical edge is present within the receptive field of the neuron(von der Heydt, Peterhans, Baumgartner, 1984 ; Grosof, Shapley, & Hawken, 1993; Murray & Herrmann, 2013). Furthermore, Lee and Nguyen (2001) were able to show that while both V1 and V2 neurons can respond to illusory contours, the V1 responses are significantly delayed compared to normal V1 responses with real contours *and* to V2 responses with illusory contours. This suggests that V2 responses to illusory contours are fed back to V1, and lends further support to the figural feedback theory. Since illusory contours elicit V1 responses, they seem to be similar to real contours in phenomenology, function, and location of neuronal encoding.

Whereas experimental demonstrations such as the Kanizsa triangle could appear to be entirely artificial, they are likely to rely on and thus expose the same mechanisms that are responsible for everyday contour, object and scene perception. When a clear, continuous luminance-defined boundary is not readily available, the contour must be integrated over weak or fragmented visual information. In humans, there is evidence that the perception of illusory contours is present from early infancy (Ghim, 1990; Johnson & Aslin, 1998; Otsuka & Yamaguchi, 2003), and even in newborn babies (Valenza & Bulf, 2007). There is also considerable evidence coming from studies on animals suggesting that the illusory contours are perceived by other mammals such as macaque monkeys (Peterhans & von der Heydt, 1989), cats (De Weerd, Vandenbussche, De Bruyn, & Orban, 1990) and mice (Okuyama-Uchimura & Komai, 2016). Moreover, the illusory contours are perceptible by other animal classes such as birds (Zanforlin, 1981; Nieder & Wagner, 1999) and even fish (Sovrano & Bisazza, 2009), demonstrating that the ability to perceive illusory edges is widespread in the animal kingdom.

1.5. Mechanisms of motion integration

The introduction in section 1 set out the general goal of the current thesis: to investigate how local motion signals are combined into a percept of a global trajectory. In section 2, the neurophysiological loci of motion perception were introduced, with special attention to the encoding of motion direction, and the specialised motion processing area MT+. In this section, the current knowledge on functional mechanisms in the visual system that could support the motion integration process will be discussed in more detail.

1.5.1. The aperture problem

The neurons representing motion direction at the level of V1 have small receptive fields (Fennema & Thompson, 1979), and therefore cannot represent the motion of the entire object, but only fragments of edges. This exposes V1 to the *aperture problem*, illustrated in Figure 1.7. When the movement of a straight line is seen through a circular aperture, such that its end-points are concealed, the true direction of motion cannot be determined (Stumpf, 1911; Wallach, 1935). Any direction of motion is a valid interpretation of the stimulus, except the direction parallel to the line (which would not produce any perceptible motion). In psychophysical experiments, the reported perceived direction of motion is found to be orthogonal to the orientation of the line (Wallach, 1935; Wuerger, Shapley, & Rubin, 1996). This interpretation corresponds to the line motion with the lowest speed of the possible alternatives.
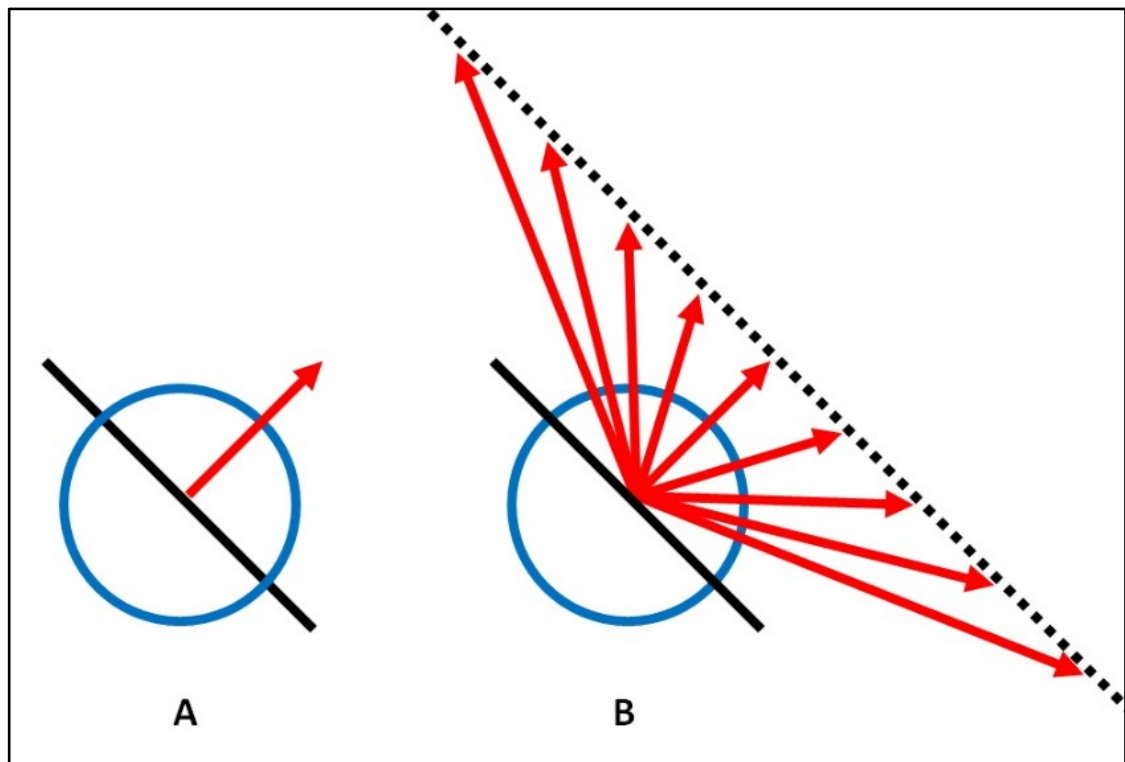
Figure 1.7. The aperture problem: When the movement of a line is viewed through an aperture occluding its endpoints, the true direction of motion cannot be determined. The perceived direction of motion (A) corresponds to the shortest motion vector, whereas all other motion directions (B) imply a higher speed (adapted from Aaen-Stockdale & Thompson, 2012).

V1 neurons faced with the aperture problem are therefore unable to separately encode the direction and the speed of the edge visible within their receptive field (Adelson & Movshon, 1982). Two possible solutions exist to this challenge. First, some neurons will have the endpoints of long edges within their receptive field, and can therefore encode the true motion direction. Indeed, it has been found that specific subpopulation of end-stopped V1 neurons is sensitive to this information, that project directly to area MT (Sceniak, Hawken, & Shapley, 2001; Pack, Livingstone, Duffy, & Born, 2003). Second, the true motion direction of the object to which the edges belong can be determined by aggregating V1 motion signals. Movshon, Adelson, Gizzi, and Newsome

(1985) investigated this using a *plaid* motion stimulus (Figure 1.8), in which two sets of parallel lines move across each other in different directions. At the level of V1, neurons respond only to these two component motion directions. In area MT however, where receptive field sizes are up to ten times larger than in V1 (Maunsell & Van Essen, 1987), a large proportion of cells will represent the intermediate motion direction in which observers subjectively perceive the entire plaid pattern to be coherently moving. That is, the visual system is able to solve the aperture problem arising in V1 and infer object motion through integration of local motion signals, when the experimental display is unsuitable to be analysed by end-stopped neurons.
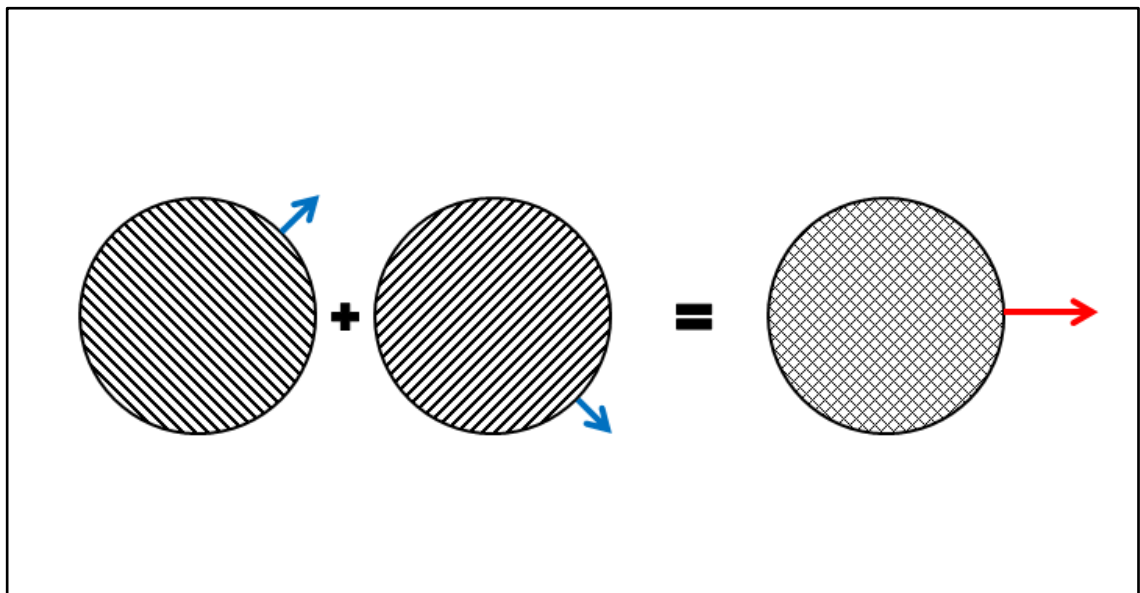
*Figure 1.8.*Schematic illustration of the plaid stimulus. Two sets of parallel lines move across each other in different directions (blue). The perceived direction of the resulting plaid stimulus (red) is the average of the two individual component directions.

Note that the integrated motion signals in area MT do not manifest themselves immediately. Neuronal response immediately after the stimulus onset tend to correspond to the motion directions of the component motions, whereas signals 60-100

ms after stimulus onset start to reflect the direction of the integrated motion (Recanzone & Wurtz, 1999; Pack & Born, 2001; Pack, Berezovskii, & Born, 2001).

1.5.2. Theoretical approaches

The simplest model for the spatial integration of local motion signals encoded by V1 neurons with different receptive fields is *vector averaging* (Adelson & Movshon, 1982; Wilson, Ferrera, & Yo, 1992; Yo & Wilson, 1992). A 'motion vector' corresponds to the combined properties of the speed and the direction of motion. By averaging the motion vectors of the individual components, a single motion estimate can be reached. In the case of the plaid stimuli, this will (because of the aperture problem) be the average of the motion directions orthogonal to the component line orientations, weighted by their speed. Alternatively, an *intersection-of-constraints* (IOC) solution can be computed (Fennema & Thompson, 1979; Stone, Watson, & Mulligan, 1990; Simoncelli & Heeger, 1998): since, given the aperture problem of Figure 1.7, each possible direction of a motion component is associated with a certain speed, a globally coherent motion direction can be found for which both sets of parallel lines in the plaid stimulus would have the same speed. Probabilistic Bayesian models inferring the most *likely* global motion direction from the component motions can be considered an extension of the IOC approach (Weiss, Simoncelli & Adelson, 2002), taking into account such parameters as the reliability of the visual information on each motion component and high-level expectations following from the perceptual context.

These large-scale spatial motion integration processes are especially relevant at low visual contrast, or in general when the available information is weak and uncertain (Tadin & Lappin, 2005; Sceniak, Ringach, Hawken, & Shapley, 1999). This suggests that, while scientifically interesting, they do not necessarily reflect the main role of area

MT in everyday visual processing. Indeed, integrating all motion signals in the visual field into a single direction cannot be the only function of area MT: the observer must remain capable of distinguishing the different motion directions of different objects, or the movement of an object relative to the background. The selective tuning of MT neurons for binocular disparity information (DeAngelis & Newsome, 1999) and its strong centre-surround suppression mechanisms (Allman et al., 1985) are likely to play an important role in this.

Visual signals are not only integrated in the spatial domain, but also in the temporal domain. The period over which a neuron combines its inputs is called the *temporal integration window*. Geisler (1999), for instance, observed that even when presented with end-stopped motion, many V1 neurons still largely confound the orientation and the (orthogonal) motion direction of an edge. He notes, however, that the temporal integration window typically observed for V1 neurons suffices to encode the change in stimulus position as brief *motion streaks*. The motion direction of an object can then be inferred from the oriented spatial signals it leaves behind in the neural code of V1, without the need for component motions to be combined at a later stage. Later studies confirmed that motion direction discrimination shares characteristics with orientation discrimination of lines (Geisler, Albrecht, Crane, & Stern, 2001; Edwards & Crane, 2007; Alais, Apthorp, Karmann, & Cass, 2011).

In area MT, individual neurons have a temporal integration window of tens of milliseconds for component motion signals (Bair & Movshon, 2004; Hasson, Yang, Vallines, Heeger, & Rubin, 2008; Kumbhani, El-Shamayleh, & Movshon, 2015). In psychophysical studies, motion integration windows have been found to last from 100 ms for simple dot stimuli (Burr, 1981) up to several seconds for weakly coherent large-scale patterns (Watamaniuk & Sekuler, 1992; Burr & Santoro, 2001), which are more

likely to require the coordinated effort of motion-sensitive neurons across a large spatial scale.

1.5.3. Trajectory perception

The current thesis is focused on the motion integration process as it pertains to a single dot object, moving along a trajectory through space and time. The aperture problem does not strictly speaking apply to a dot stimulus, since it is end-stopped even within the limited receptive field size of V1 neurons. However, many V1 neurons still confound motion direction with their preferred edge orientation, and the integration mechanisms discussed above might therefore still apply – be it motion streaks, vector averaging, or intersection of constraints. These mechanisms describe the perception of a single direction of motion, however. In the case of trajectory perception, the motion vector can change over time, and the shape of the path described through visual space is to be integrated from the local motion vectors.

Whereas the detection of changes in motion *direction* is known to depend strongly on the initial direction of the motion, the detection of changes in *speed* of motion does not depend on the initial speed of motion (Sekuler, Sekuler, & Sekuler, 1990; Dzhafarov, Sekuler, & Allik, 1993; Hohnsbein & Matteef, 1998). The overall accuracy of trajectory perception is high when it is presented within a clear visual context (Verghese, Watamaniuk, McKee, & Grzywacz, 1999). However, when the same trajectory is viewed without a visual context, the performance of perceiving the shape of the trajectory accurately sharply decreases (Verghese & McKee, 2002). In particular, the total length of the trajectory is underestimated (Kerzel, 2003; Sinico, Parovel, Casco, & Anstis, 2009), and the ending location of a motion trajectory is often overestimated (Freyd & Finke, 1984; Hubbard, 1995). For instance, if a dot moves rightward from

position A to position B, and then disappears, participants will indicate the dot to have stopped moving at a position to the right of B. This effect is known as *representational momentum*, and is indicative of the predictive nature of object trajectories, both with regard to the future motion direction and the future object position. Indeed, it has been found repeatedly that the motion of an object biases the position estimate of that object in the direction of the motion (Whitney, 2002; Maus, Fischer, & Whitney, 2013; Nishida & Johnston, 1999; McGraw, Whitaker, Skillen, & Chung, 2002), and that the visual system is biased to perceive the moving object as continuing on its current path (Watamaniuk, 2005; Davies, Chaplin, Rosa, & Yu, 2016).

Trajectory perception, and motion perception in general, isrelated to action. The interception of a falling ball, for instance, requires an accurate estimate and prediction of its visual trajectory (Zago, McIntyre, Senot, & Lacquaniti, 2009). However, a more immediate form of motor action that very often accompanies trajectory perception is eye movements: when attending to a moving object, human observers tend to follow it with their gaze. An important consequence of this behaviour is that the motion of the object, as it is being kept in central vision, will be largely neutralised in its projection on the fovea. In the next section, the discussion is on the interplay between eye movements and visual perception in general, and trajectory perception in particular.

1.6. Eye movements and retinal eccentricity

1.6.1. The retina and human scene exploration behaviour

The visual field is the total area visible to both eyes during any fixation (Gibson, 1950), and it covers approximately 200-220 degrees visual angle (Harrington, 1981). Visual acuity, the ability to observe fine details in a visual scene, depends on the position of the

stimuli in our visual field, with objects placed in central vision being perceived in much greater detail (Anstis, 1974). The anatomical structure of the human retina is such that there is a disproportionate concentration of cones, the photoreceptive cells specialised in colour perception, in the fovea centralis, which is a small region in the centre of the retina. Moreover, despite the fovea spanning only 5 degrees of the visual field, it is subserved by approximately 30% of the primary visual cortex (Schira, Tyler, Breakspear, & Spehar, 2009). It can then be understood why in central (or foveal) vision acuity is considerably higher than in peripheral vision.

Because of the limited extent of the fovea, human observers must move their eyes in order to view specific parts of the visual scene in detail. The typical sequence observed during scene exploration is an alternation of fixations of 150 - 500 ms, when the gaze remains relatively stable, and saccades of 20 – 100 ms, during which the gaze position is rapidly changed (Bahill, Clark, & Stark, 1975; Wilming et al., 2017). As a consequence the projection of the visual scene will be displaced across the retina, but human observers do not consciously perceive these displacements. Yet, when a similar retinal motion is induced by a moving stimulus instead of an eye movement, the same displacement is easily detected (Bridgeman, Hendry, & Stark, 1975). It has been suggested that a copy of the motor signals which drive the eye movements is sent to visual areas, to compensate for the retinal motion signals induced by saccadic eye movements (Sperry, 1950; von Holst & Mittelstaedt, 1950; Gauthier, Nommay, & Vercher, 1990; Souman & Freeman, 2008). The terms efference copy, extra-retinal signals and re-afferent signals are commonly used to indicate such neuronal activity. The exact mechanisms that allow the saccade-induced displacement to be compensated are still the subject of scientific debate, however (Irwin, Yantis, & Jonides, 1983; Bridgeman, Heijden, & Velichkovsky, 1994; Melcher, 2005; Cavanagh, Hunt, Afraz, & Rolfs, 2010; Zirnsak & Moore, 2014).

1.6.2. Smooth pursuit eye movements

Next to fixations and saccades, the third type of commonly observed eye movements is referred to as *smooth pursuit* (Rashbass, 1961; Robinson, 1965; Keller & Heinen, 1991; Krauzlis & Stone, 1999), and can only be initiated when a smoothly moving visual stimulus is available to follow with the gaze. Human observers are capable of following targets with speeds up to 30° per second (Lisberger, Morris, & Tychsen, 1987), and are more accurate at horizontal trajectories than vertical or diagonal trajectories (Rottach et al., 1996).

To initiate and maintain tracking, the motor control of smooth pursuit eye movements must be closely related to visual motion signals. Two phases can be identified. During the initial 100 ms of motion, the stimulus moves across the retina, and a retinal signal drives the eye movement (Lisberger & Westbrook, 1985). In the next phase, the stimulus is accurately being tracked. The properties of tracking behaviour are not based on a low-level motion signal, but instead share their properties with those of high-level perceptual judgments of motion (Yasui & Young, 1975; Beutter & Stone, 1998; Stone & Krauzlis, 2003). Indeed, smooth pursuit eye movements continue when the stimulus traverses behind an occluder, although at a reduced speed when the occlusion period becomes longer (Becker & Fuchs, 1985; Pola & Wyatt, 1997). The locus of this link between perception and action is proposed to be area MST (Dürsteler & Wurtz, 1988; Komatsu & Wurtz, 1989; Pack, Conway, Born, & Livingstone, 2006).

Since retinal motion is neutralised during the tracking phase of smooth pursuit, motion areas must integrate an efference copy of the eye movements themselves to encode the motion of the target that is being followed. Whereas area MT is retinotopic in organisation, area MST is largely spatiotopic and continues to respond when a stimulus is stabilised on the retina (Newsome, Wurtz, & Komatsu, 1988; Thier & Ilg, 2005; Ilg,

2008). It is thus proposed that MST integrates retinal and extraretinal signals to enable continued pursuit and allow the conscious perception of motion, despite the absence of a retinal motion signal. Indeed, the properties of trajectory perception are independent of the presence of eye movements (Dzhafarov et al., 1993; Krukowski, Pirog, Beutter, Brooks, & Stone, 2003).

1.6.3. Motion perception in foveal and peripheral vision

The position of the gaze also determines in which part of the visual field a stimulus will be processed. Visual acuity declines rapidly with retinal eccentricity (Anstis, 1974). Although human observers are not typically conscious of this during normal behaviour, it can be easily experienced by keeping the gaze fixed on a single point in space while directing visual attention away from foveal vision. Other differences between foveal and peripheral vision have been found in the processing of visual information; for example, it has been shown that the estimated size of objects in peripheral vision is smaller when compared to foveal vision (Baldwin, Burleigh, Pepperell, & Ruta, 2016), and that the mechanisms of contour integration are different beyond 10 degrees of retinal eccentricity (Hess & Dakin, 1997, Hess & Field, 1999).

Visual information from outside foveal vision is important, however, since it is this information that will be used to decide where to direct the gaze next. Given that saccadic eye movements are made multiple times per second, a continuous analysis of the visual periphery is required to plan the next eye movement. Motion in particular is a strong cue to attract the gaze towards a peripheral location, to bring it into the fovea for detailed analysis (Dorr, Martinez, Gegenfurtner, & Barth, 2010; Mital, Smith, Hill, & Henderson, 2011). Indeed, the peripheral retina is encoded by large field motion neurons (Cleland & Levick, 1974; Walsh & Polley, 1985), which makes it relatively

more sensitive to moving stimuli than the fovea (Edwards & Nishida 2004). Fahle and Wehrhahn (1991) showed that motion sensitivity in the periphery is especially high for horizontal and centrifugal motion and less so for vertical and centripetal motion. The latter finding could potentially be related to the properties of the ubiquitous optic flow motion signals that are generated during self-movement, which is typically centrifugal.

Finally, some motion phenomena are unique to peripheral vision. In the Peripheral Drift illusion (Faubert & Herbert, 1999), a static image is presented that in the fovea indeed appears to be static. However when eye movements occur, the layout of the figure will stimulate specifically the motion detectors in peripheral vision, and cause an illusory impression of motion. In reality, the only motion occurring is the movement of the eyes. These eye movements are then not fully compensated for by the efference copy of the eye movement motor signals, and the retinal motion signals are instead assigned to the static stimulus. In the Furrow illusion (Anstis, 2012; see Chapter 6), a dot is shown to traverse vertically across a diagonally striped pattern, alternatingly white and black in colour. In foveal vision the vertical trajectory is perceived accurately, whereas in peripheral vision the dot will appear to move diagonally instead. These examples indicate that motion and trajectory perception can operate differently at different locations of the visual field.

1.7. The slalom illusion

1.7.1. Original findings

No perceptual registration is trusted more than visual perception, as evidenced in several expressions of the English language ('I saw it with my own eyes!'). However, this is a false impression. Perception does not directly reflect reality, but entails an

elaborate reconstruction of it, based on intricate mechanisms and strong assumptions. On almost all occasions, this will result in a convincing, veridical impression of the visual world, which serves the action goals of the observer. Only in a select few artificial displays, namely visual illusions, does the process of visual perception break down, potentially revealing the underlying mechanisms of visual perception.

To investigate the mechanisms of the integration of local motion signals into a coherent trajectory, the current thesis will focus on the *slalom illusion,* a kinetic illusion of direction, whereby the straight trajectory of a dot crossing a pattern of tilted lines is perceived as being sinusoidal (see Figure 1.1 onpage 4). This illusion was first reported by Cesàro and Agostini (1998), who have conducted three experiments in order to test the effects of: the angle of intersection; the speed of the moving dot (as well as the interaction between the speed and the angle of intersection); and the distance between the tilted lines on the magnitude of the illusion. Ten experimentally naive participants were employed for each of the experiments, and the apparatus was the same throughout.

In the first experiment, five different patterns were presented, corresponding to the following incidence angles: 30°, 37°, 45°, 53°, and 60°. The tilted lines were black solid lines with a thickness of .27 mm and displayed on a white background. Each pattern, presented in the centre of the screen, consisted of 13 tilted lines (six and a half modules), with a distance at the base of the line of 18.6 mm intra-module and 9.3 mm inter-module. Figure 1.1 illustrates the general layout of the slalom display. A *module* was defined as two tilted lines positioned such that are closest at the top and farthest at the bottom. The translating dot had a diameter of .54 mm and moved horizontally from left to right along a straight trajectory of 230 mm at a constant velocity of 19 mm/sec (1.55°/sec). After completing its trajectory from left to right, the pattern disappeared and was replaced with a vertical line the length of which participants had to adjust in order

to report the perceived magnitude of the illusion. The experimental design was within-subjects, with 20 randomised trials for each participant (four repetitions per condition). The results led the authors to conclude that the illusion is angle-dependent and that the magnitude of the illusion is inversely proportional to the size of the angle.

In the second experiment, a 3x3 within participantsdesign was employed, combining the size of the angle (30°, 45°, 60°) and the speed of the moving dot (0.78°/sec, 1.55°/sec, and 3.11°/sec). The number of trials per participants was 36 (nine conditions repeated four times). Results showed that both the angle of intersection and the speed of the moving dot independently affect the magnitude of the illusion, but no effect was found for the interaction between the two factors. The illusion was shown to be inversely proportional with the speed of the moving dot in the given range of velocities.

Finally, the third experiment presented participants with three different patterns where the distance between the middle of the tilted lines in each module was manipulated as to correspond to the following values: 13.3mm, 18.6mm, and 23.9mm. Throughout all three conditions, the angle of incidence was 30°, and the velocity was 1.55°/sec. There were 15 trials per participant (five repetitions for each condition). The magnitude of the illusion was shown to vary with the distance between the tilted lines, in an inversely-proportional manner with the given range. Thus, the amplitude of the perceived sinusoidal trajectory was largest when the distance between the tilted lines was smallest.

In the slalom illusion, the perceived trajectory of the dot bends to cross the lines perpendicularly. Cesàro and Agostini (1998) propose that there are local distortions of the direction of the dot motion, occurring around the time of the line crossings. The sinusoidal trajectory perceived is then proposed to be the result of an integration of these local distortions with the straight trajectory. That is, there is a perceptual tendency for the moving dot to continue along the deviant perpendicular path, but as its physical

trajectory is straight, the final result would be a compromise between the two. Having identified three factors which affect the magnitude of the illusion (the size of the angle of intersection, the velocity of the dot, and the distance between the tilted lines), the authors also showed that the magnitude of the illusion is inversely proportional with each of the tested factors in their given range for these experimental set-ups. However, there was not a sufficiently wide range of values to definitely conclude an inverse relationship with the three tested factors. Thus, it is possible that a specific speed of the dot, angle of intersection, and distance between modules could be reached that would result in an even greater magnitude of the illusion.

Cesàro and Agostini's explanation for the slalom illusion is based on the similarities between this effect and a number of similar illusions present in the literature, both of orientation (static illusions) and of direction (kinetic illusions). Indeed, there are numerous illusions that are based on the angle of intersection, and so the authors argue that a common mechanism could be used to explain them. Furthermore, they propose, in line with Swanston (1984), that a possible interaction between the system responsive to movement direction and that responsive to orientation might be responsible for the effect. Although the authors speak of the local distortions occurring due to a perceptual normalisation towards a right angle, they do not attempt an explanation as to why this may be the case, pointing solely on the abundance of illusions that rely on the same phenomenon. Moreover, the local-global integration mechanism is invoked without a comprehensive account of how this happens.

Despite the tentative nature of the explanation that Cesàro and Agostini provide for the effect, they presented a kinetic illusion of direction which makes for an appropriate experimental paradigm to investigate the integration of local motion signals into a global trajectory, as it occurs in high-acuity foveal vision, and can be induced with a

sparse display of which the visual elements can be precisely controlled. This combination of properties found in the slalom illusion has not been studied before in the context of motion integration.

1.7.2. Related geometric illusions

Geometric illusions are illusions caused by the geometrical properties of an object in the display (shape, length, orientation, etc.). Wundt (1898) made the first attempt to classify geometric illusions and divided them into two classes: illusions of extent and illusions of direction. Coren & Girgus (1978) used a factor analytic technique to generate a classification scheme, and proposed five classes: (1) shape and direction illusions, (2) size contrast illusions, (3) overestimation illusions, (4) underestimation illusions, and (5) frame of reference illusions.

Four of the most famous geometric illusions of direction are the Wundt, Poggendorff, Hering, and Zollner illusions (Figure 1.9). In all of these illusions, static lines that should have been straight or parallel, appear as bent (Wundt, Hering) or at an angle with each other (Poggendorff, Zollner). The Poggendorff and Zollner illusion have both been shown to not only occur when the crossing lines causing the illusion are drawn as full lines, but also when they are induced as subjective contours (Tibber, Melmoth, & Morgan, 2008); for the Hering and Wundt illusion comparable data are not available.
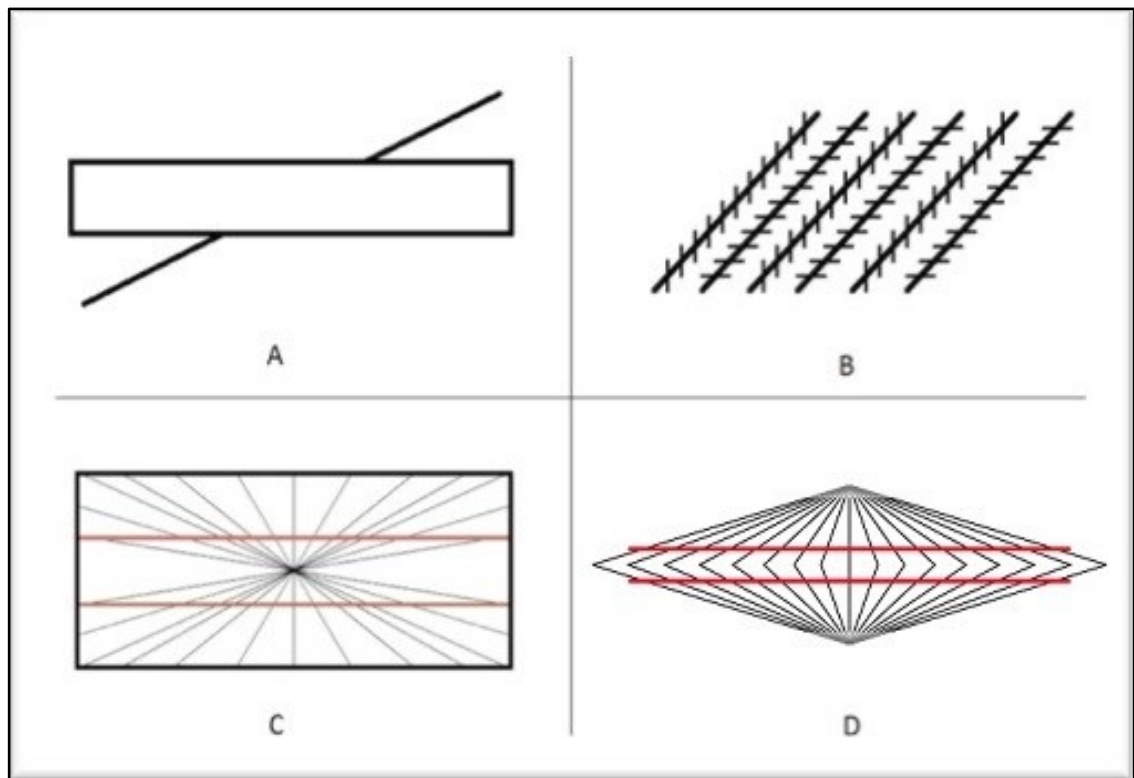
Figure 1.9. Illustration of four classic geometric illusions of direction: (A) Poggendorff illusion, (B) Zollner illusion, (C) Hering illusion, and (D) Wundt illusion.

The slalom illusion can be compared to these four classic geometric illusions. Whereas the Poggendorff is an illusion of angle on a discontinuous line, the slalom illusion pertains to the shape of the trajectory along a continuous path. The Zollner illusion also is not an illusion of the shape of the line, but of the relative orientations of multiple lines. The Wundt and the Hering illusions, on the other hand, do affect the shape of a straight line. All four illusions are static, however, whereas the slalom illusion requires a moving object.

Kinetic versions of these illusions have been reported in the literature. Fineman and Melingonis (1977) created a kinetic Poggendorff illusion using a cardboard cut-out for the vertical occluder, and a moving light source behind a diagonal slit as the moving stimulus. The illusion was observed to be even stronger than under static conditions.

Wenderoth and Johnson (1983) replicated these findings using a computer-driven display screen. Watamaniuk (2005), however, could not replicate the misalignment illusion in a small experiment with four participants. A hybrid variant, with a static line segment on one end and a disappearing moving dot on the other end, did produce the effect. Khuu (2012; Khuu & Kim, 2013) replicated a variant of the Zollner illusion in a kinetic display, whereby a small group of dots moved vertically across a parallel set of tilted lines. The direction of motion appeared tilted away from the orientation of the lines. Smeets and Brenner (2004) instructed their participants to make a hand movement across the background lines of the Hering illusion, and found that this motor action was biased similarly to the perception of a static line in the classic illusion. In conclusion, the available evidence appears to suggest that geometric illusions of static line shape and orientation generalise to kinetic variants. As discussed in section 2 of this chapter, early visual cortex strongly confounds the encoding of orientation and of motion direction. For this reason, it is not entirely surprising that common mechanisms could underlie geometric illusions of both static lines and dot motion along a trajectory (Swanston, 1984).

Another phenomenon closely related to the slalom illusion is the Squirming Illusion (Ito & Yang, 2013). When a continuous zig-zag line is shown in the periphery of the visual field, a dot moving in a straight line across it appears to follow the zig-zag contour instead. This effect is opposite to that of the slalom illusion, where the dot is proposed to intersect with the tilted lines at a perpendicular angle. In Chapter 6, the relation between both of these illusions will be investigated in greater detail.

1.7.3. The angle of intersection

Explanations of geometric illusions of direction often rely on the angle between two lines. In particular, they are often consistent with a bias towards perceiving *perpendicular angles*. In the Poggendorff illusion (Figure 1.9.A), the perceived misalignment between both parts of the diagonal line is then caused by each line appearing to be slightly more vertical than it veridically is. In the Zollner illusion (Figure 1.9.B), the tilt of each longer parallel line is biased towards an orientation perpendicular to its intersection with the smaller line segments. In the Herring (Figure 1.9.C) and Wundt illusions (Figure 1.9.D), the shape of the line itself is bent to better conform to perpendicular intersection angles. Similarly, in the slalom illusion, Cesàro and Agostini (1998) suggest that the angles of intersection between the dot and the tilted lines are perceptually corrected towards perpendicularity (Figure 1.10).
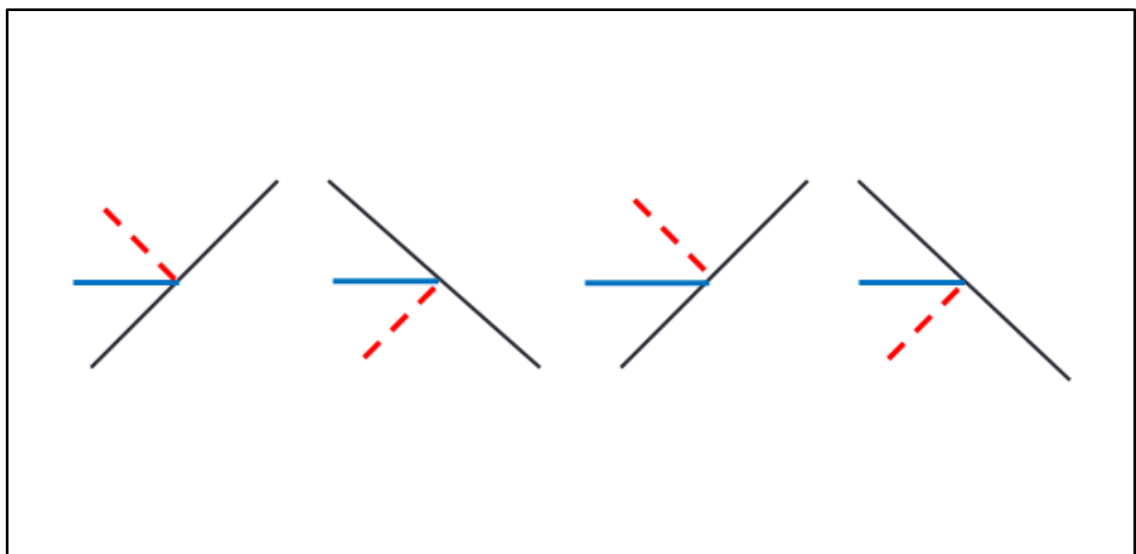

Figure 1.1. Illustration of the perceptual correction of the angle of intersection in the slalom illusion. The actual angle of intersection between the straight trajectory of the dot and the tilted lines is depicted in blue, and the perceptually corrected angle of 90°is depicted in red.

This bias towards perpendicularity is reminiscent of the aperture problem discussed in section 1.5.1, but since it also occurs in static displays it cannot be explained by the inherent ambiguity of local motion signals. Instead, Blakemore, Carpenter, and Georgeson (1970; Parker, 1974) propose that the bias is differently rooted in primary visual cortex. Because the tuning of V1 neurons to line orientations is gradual rather than very specific, a neuron optimally responsive to a given orientation will in fact also generate signals, but more weakly, when stimulated with lines that have similar orientations. To achieve a more orientation-specific overall response, V1 neurons exhibit *lateral inhibition*, whereby each neuron will generate an inhibitive response towards neurons that have a slightly different orientation tuning around the same retinal location. This will cause two lines that intersect at an acute angle to be repelled from each other, because these neighbouring orientation responses will be suppressed in favour of more dissimilar orientations. This could explain the bias away from acute angles, towards perpendicularity.

However, other authors offer instead a Bayesian view on the perpendicularity bias (Nundy, Lotto, Coppola, Shimpi, & Purves, 2000; Changizi, 2001; Changizi & Widders, 2002; Howe & Purves, 2005), relying on the statistics of the real world. In the Bayesian proposition, the visual system attempts to infer the veridical properties of the physical stimulus from its projection on the retina. Angles that are veridically perpendicular not only occur often in our everyday experience, but are also often seen under viewpoints that cause them to appear acute or obtuse. Therefore, angles that are projected as acute or obtuse are relatively speaking more likely to actually be perpendicular, and the inference of the veridical visual angle is biased towards perpendicularity.

Therefore, whereas the lateral inhibition explanation reduces the angle bias to a by-product of the finer mechanics of the early visual cortex, the Bayesian view posits it is a

direct reflection of real-world experiences, and a consequence of optimal inference. Both hypotheses are not mutually exclusive, however, and their effects could be additive to each other. In either case, it appears likely that, as proposed by Cesàro and Agostini (1998), the angle of intersection and the bias towards perpendicularity play a crucial role in the slalom illusion, too.

1.8. Goals of the current thesis

The programme of research presented in this thesis was designed to investigate the integration of local motion signals into a global trajectory, by means of the slalom illusion. In this illusion, there is a marked discrepancy between the veridical local inputs of a constant horizontal motion direction, and the final percept of a constantly changing direction. In particular, the original paper on the slalom illusion (Cesàro & Agostini, 1998) placed great emphasis on the local distortions in motion direction around the points of intersection between the trajectory and the tilted lines.

Since the original paper is the only one to date investigating the slalom effect, and no other illusions combine all the elements of the slalom illusion (a single object moving on a trajectory of illusory shape, in foveal vision), many empirical and theoretical uncertainties still exist about the nature and the mechanisms of the slalom illusion that could directly reflect on the nature and mechanism of trajectory perception in general. The following aspects were investigated in the current thesis: (a) If the origin of the slalom illusion is local, does the slalom illusion then indeed depend on the local properties of the points of intersection between the trajectory and the tilted lines? (b) Is the angle of intersection indeed the sole driving factor behind the slalom illusion? (c) Does the slalom illusion occur if the trajectory is not continuously available, but to be completed behind an occluder, similar to the kinetic Poggendorff illusion? (d) Does a

constant magnitude of the slalom illusion require the occlusion time to be consistent with the real length of the trajectory, or the illusory length of the trajectory? (e) Does the slalom illusion depend on the viewing strategy and the retinal position of the stimulus display?

The investigation into these questions is presented over six additional chapters, as follows:

In **Chapter 2**, two main manipulations are applied. First, instead of real contours for the tilted lines, illusory contours formed by Kanizsa-like inducers are employed. If the local distortions underlying the slalom illusion are low-level and immediate on the image level, it is predicted that illusory tilted lines do not serve as inducers of the slalom illusion. Second, the contrast of real contours is manipulated. If the slalom illusion is rooted in biases in early visual cortex, contrast-dependence is predicted.

In **Chapter 3**, part of the trajectory is occluded to elicit amodal completion of the trajectory. The empirical question is asked whether this prevents the slalom occlusion from occurring, and if not then whether it affects the magnitude of the illusion. In a theoretical view where trajectory perception is a high-level phenomenon, it is expected that amodal completion will occur, and that the partial occlusion of the veridical, horizontal trajectory will give more weight to the biased signals, and increase the magnitude.

In **Chapter 4**, the speed of the moving dot during occlusion is manipulated. It is hypothesised that, similar to findings in the apparent motion literature (Korte, 1915), shorter ISIs could lead to shorter inferred trajectory lengths, and therefore a reduced magnitude of the illusion.

In **Chapter 5**, the reverse slalom illusion is presented to participants, where the magnitude of a veridically sinusoidal trajectory is to be estimated against a background

of tilted or vertical lines of interception to the trajectory. Following the suggestion of Cesàro and Agostini (1998) that the angle of intersection drives the slalom illusion, a decreased magnitude is expected. In a follow-up experiment, it is tested whether the magnitude of a sinusoidal trajectory can be accurately estimated in the absence of the illusion-inducing lines.

In **Chapter 6**, the observers' eye movement patterns and positions on the slalom stimulus display are manipulated. If the slalom illusion arises at a level of visual processing where retinal signals and extra-retinal signals (the efference copy) have already been combined, it is expected that the viewing strategy does not affect the occurrence of the illusion. The magnitude of the illusion at different retinal eccentricities is measured, and the occurrence of the slalom illusion in the periphery is distinguished from that of the related squirming illusion.

Finally, in **Chapter 7** a general discussion is offered on the entirety of the empirical results in the context of local-global integration processes and motion perception. In addition, suggestions are made for future research.

2. Chapter 2 - Subjective contours

2.1. Introduction

The slalom illusion has robustly produced a potent visual effect in the case of strongly-defined contours (Cesàro & Agostini, 1998). In section 1.7.1 of the general introduction, the broader context was provided for Cesàro and Agostini's proposed explanation of the slalom illusion, according to which the local distortions in motion direction signals at the points of intersection between the horizontal dot trajectory and the tilted lines integrate into a global percept of a sinusoidal trajectory. In particular, these local distortions could be rooted in the V1 mechanisms proposed by Blakemore et al. (1970), who reported that neurons encoding edge orientation and motion direction signals in primary visual cortex are biased towards perpendicular angles of intersection.

However, not all contours that are subjectively perceived are also locally present in the image. As discussed in section 1.4.2 of the general introduction, illusory contours such as those induced by the Kanizsa triangle (Kanizsa, 1976) preserve many of the properties of real contours, both phenomenologically and functionally. In the neuronal responses of V1 and V2, illusory (or subjective) contours are eventually encoded similarly to real contours, following feedback signals from higher-level visual areas (von der Heydt et al., 1984; Lee & Nguyen, 2001). This brings forward an interesting question: does the slalom illusion still occur if the inducing tilted lines are only subjectively present, similar to the contours of the Kanizsa triangle? That is, when the physical intersections between the oriented lines and the dot trajectory – proposed by Cesàro and Agostini (1998) to give rise to the local distortions in motion direction underlying the slalom illusion – are therefore absent?

The general question of whether illusory contours can induce the perceptual phenomena apparent with real contours has previously been addressed in a number of papers on static geometric illusions. The Poggendorff illusion, in particular, has in a number of studies been adapted to a version where the real contours of the inducing rectangle are replaced with Kanizsa-like illusory ones (Figure 2.1). The misalignment effect typical of the illusion was robustly replicated in a number of studies (Gregory, 1972; Meyer & Garges, 1979; Westheimer & Wehrhahn, 1997; Tibber et al., 2008).
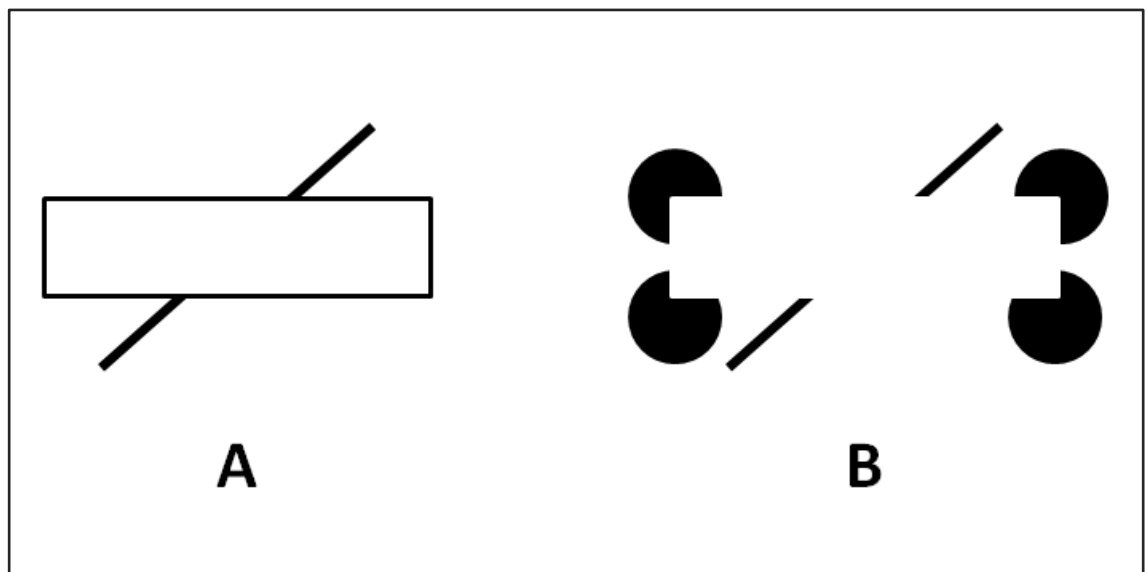
Figure 2.1. Illustrations of the Poggendorff effect in the original first-order contours version (A), and in the illusory lines adaptation (B).

One study (Day, Dickinson, & Jory, 1977) did not confirm the effectiveness of illusory contours as inducers to the Poggendorff illusion. Their data showed no difference between illusory contour conditions and a control condition consisting of only an oblique line (without the rectangle). However, the authors themselves point out that the oblique line of their display interfered with the Kanizsa elements inducing the illusory contours and might therefore have negated the expected effect. Given the robust effect

subsequently found in the more carefully controlled study of Meyer and Garges (1979), the importance of the negative finding of Day et al. (1977) should therefore not be overstated due to this confound.

It can therefore be concluded that Kanizsa-like subjective contours are capable of driving the Poggendorff effect. However, despite the repeated replication of this phenomenon, it has also been found that the magnitude of the misalignment bias is smaller in subjective-contour Poggendorff displays, when compared to the bias that can be observed using a classical display with real contours. Tibber et al. (2008) suggest that the attenuation in the Poggendorff effect when driven by subjective contours could be explained by the lower salience of the subjective contours. That is, that subjective contours are detected by a smaller subset of cortical neurons in the early visual areas than real contours and that, consequently, lateral inhibition between orientations columns in V1 is weaker than when the entire stimulus is defined by real contours. In the study of Westheimer & Wehrhahn, 1997), the authors additionally included experimental conditions where the contrast of the display was reduced, both for the real-contour and the subjective-contour variants of the Poggendorff illusion. Although the subjective contours elicited a weaker misalignment bias than the real contours, the full size of the effect was in both cases reached at a very low level of stimulus contrast. The response strength of V1 neurons is however strongly dependent on stimulus contrast (Carandini, 2007), as are psychophysical tasks relying on low-level orientation discrimination mechanisms (Wehrhahn & Westheimer, 1990). This then suggests that the magnitude of the misalignment bias does not simply depend on the response strength of V1 neurons. Therefore, the weakened misalignment bias in subjective contour conditions similarly cannot simply be reduced to a weaker V1 response to subjective contours, as compared to real contours.

The literature also registers that the kinetic version of the Poggendorff illusion, where the oblique line is replaced by an oblique dot trajectory, produces the misalignment bias typically found in the static Poggendorff display (Fineman & Melingonis, 1977; Wenderoth & Johnson, 1983). However, a recent search of published papers revealed that no combination of the two factors (kinetic instead of static and subjective/illusory instead of real contours) has been tested with the Poggendorff effect, or any other illusion of direction. It remains therefore an outstanding question whether subjective contours are capable of maintaining kinetic illusions of direction.

In the current study, the kinetic nature of the slalom illusion will therefore be combined with the illusory type of contours. In addition, the contrast of the real-contour tilted lines will be manipulated. If the mechanisms of the slalom illusion are similar to those of the Poggendorff illusion, it can be expected that the slalom illusion can be replicated using subjective-contour displays, but possibly at a decreased magnitude of the illusion. In the real-contour conditions, the contrast of the tilted lines should then also not affect the magnitude of the illusion.

This would suggest that the slalom illusion is not simply rooted in momentary local distortions of motion direction early in the visual processing stream, but that higher-level contour representations interact with the signals of motion direction. If, on the other hand, subjective contours fail to elicit the slalom illusion and contrast manipulations strongly affect its magnitude when using real contours for the tilted lines, then it can be concluded that the slalom illusion is rooted in low-level interactions between the motion direction of the dot and the orientation of the tilted line edges – as originally suggested by Cesàro and Agostini (1998).

2.2. Experiment 1

Since visual illusions are prone to large inter-individual differences (Genç, Bergmann, Singer, &Kohler, 2011; Schwarzkopf, Song & Rees, 2011), one requirement of this study was to sample a larger group of participants than Cesàro and Agostini (1998) used in their experiments (n=10). To gain access to a larger sample, the first experiment was performed on a computer tablet (see Methods section for details) that could easily be transported to locations outside of the psychophysics laboratory.

The preliminary theory of Cesàro and Agostini was used as the working hypothesis for this study. In line with their interpretation of the slalom illusion as being rooted in momentary local interactions between the dot motion and the line orientations, it was predicted that black tilted lines will elicit the largest magnitude in the illusory modulation of the dot trajectory. Next, it was hypothesised that contrast-reduced version of the same tilted lines will result in a decreased magnitude of the slalom illusion. Finally, it was expected that the subjective-contour version of the stimulus display will result in a strongly reduced magnitude of the illusion, which within the limits of the statistical power provided by the current study (see Methods for details) is no longer distinguishable from a control condition with vertical instead of tilted lines.

If these predictions do not hold true, the original theory of Cesàro and Agostini (1998), whereby local distortions in the early visual system are the cause of the slalom illusion, must be revisited.

2.2.1. Methods

2.2.1.1. Participants

Opportunity sampling was carried out during a science open-day event at Sheffield Hallam University. A total of 67 participants with normal or corrected-to-normal vision were recruited. All participants were naïve as to the purpose of the experiment. Apart from having normal or corrected-to-normal vision and an age of at least 18 years old, no other exclusion criteria have been applied to recruiting participants.

2.2.1.2. Design

A repeated-measures design was employed, with one independent variable, 'background'. The independent variable had four levels: *original slalom* (black inducing lines), *illusory lines* (subjective contours), *reduced contrast* (grey inducing lines), and *control* (vertical black lines instead of tilted ones). The dependent variable, *illusion magnitude*, was operationalised as the difference between the highest and the lowest points in the reported perceived trajectory of the moving dot, measured in pixels.

2.2.1.3. Apparatus and stimuli

The experiment was programmed in Java and presented on a Samsung Galaxy Tab 3 tablet with a 1.1" screen and a resolution of 1280 x 800 pixels. The experimental display (Figure 2.2) consisted of the *background*, meaning the static stimuli, and the *moving dot*, which moved across the background. Across all four conditions, the dot measured 2 mm and moved at the speed of 10 cm/sec. The background consisted of six lines (three modules) and seven ovals elongated on the horizontal axis. Throughout the four conditions, the ovals were placed in the same positions and had the same dimension of 1.7 cm for the long axis and .7 cm for the short axis. The lines were 3.5 cm long and 2 mm wide across all conditions. The angle of intersection for all the tilted lines was 15°.

The angle of intersection is smaller than the 30°-60° range used by Cesàro & Agostini (1998), but it was chosen as to suit the experimental setup on the new apparatus; moreover, it provides evidence on whether the slalom illusion is maintained at a considerably lower angle of intersection. Although the black ovals were an essential part of the stimuli solely in the illusory lines condition, they were maintained throughout all the conditions as a measure of control. The oval shape, which is a deviation from the classic Kanizsa inducing circles, was used in order to maintain a larger part of the trajectory visible; had the full circles had been used, the moving dot would have intersected the inducers, providing valid reference points for estimating the real trajectory of the dot, and thus affecting the illusion setup. The centre of the experimental display is centred with the centre of the screen in all four conditions.
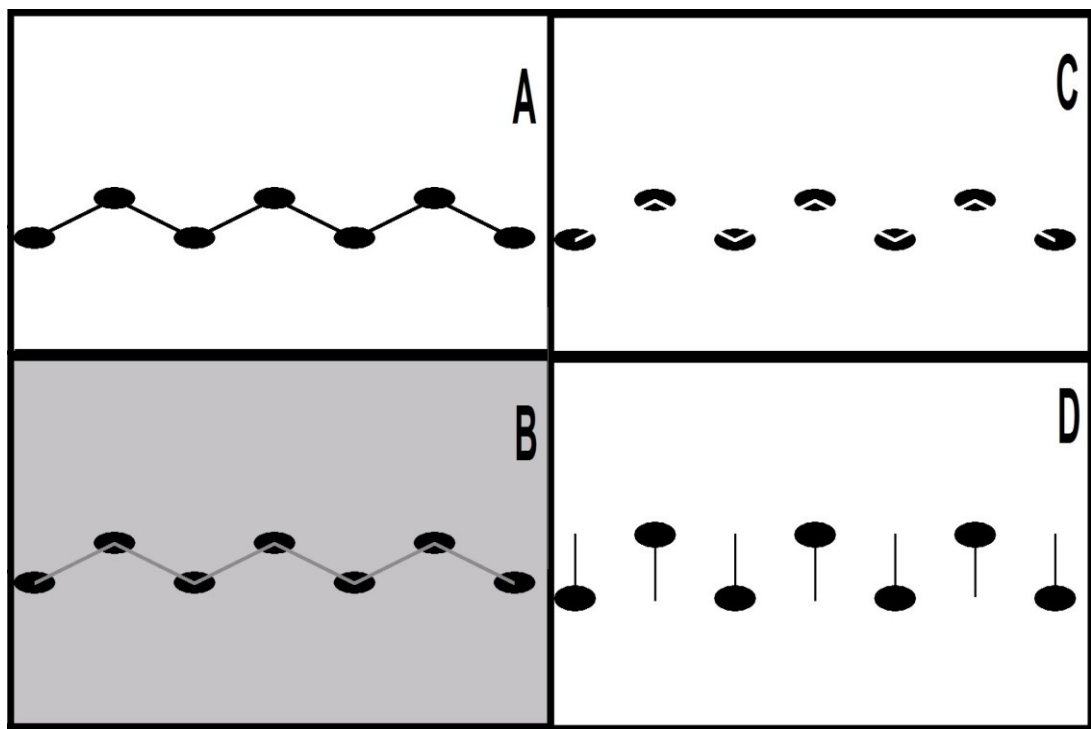
Figure 2.2. Schematic illustration of the four experimental conditions: *original slalom* (A), *reduced contrast* (B), *illusory lines* (C), and *control* (D).

In the original slalom condition (Figure 2.2.A), the tilted lines were black. In the 'reduced contrast' condition (Figure 2.2.B), the luminance (L) was manipulated so that the tilted lines were a darker shade of grey (L = 185), whereas the background was a lighter shade of grey (L = 131). The Michelson Contrast, measuring the relation between the spread and the sum of the two luminances, $(L_{max} - L_{min}) / (L_{max} + L_{min})$, is equal to .17. In the 'illusory lines' condition (Figure 2.2.C), the tilted lines were induced in a Kanizsa fashion, with the edges of the illusory line placed inside the black ovals. In the 'control' condition (Figure 2.2.D) the lines were placed vertically, creating a 90° angle of intersection. Participants' answers were collected as drawings of the perceived trajectories, participants made these drawings by using their finger, in a designated area on the screen of the computer tablet (Figure 2.3).
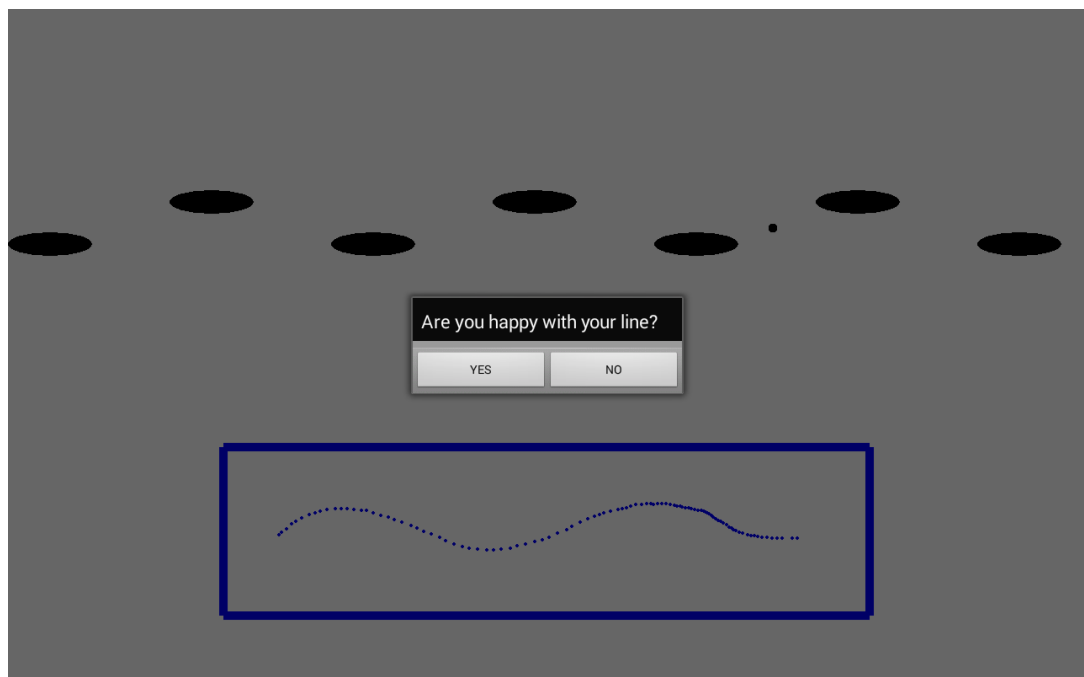
Figure 2.3. Printscreen (in reduced dimension) including the answer input display. The blue rectangle represents the area where the drawing had to be made, and the blue dot line is an example of an inputted answer.

2.2.1.4. Procedure

Ethical approval for the project, including all the experiments presented in the thesis, was obtained from the Faculty Research Ethics Committee (reference AM/KW/21C-2014) prior to collecting any data (Appendix 1). All the research included in this project was conducted in accordance with the Declaration of Helsinki.

During an open-day event at the university, a 'pop-up' research laboratory was organised. Participants were recruited through opportunity sampling from the people attending the open-day event. The purpose of the experiment was explained and participants were asked to read through an information sheet (Appendix 2). When they agreed to take part in the experiment, they were asked to read and to sign a consent form (Appendix 3). All participants were offered the chance to ask questions and were made aware of their rights as participants. Once the participants agreed to partake, they were invited in to the experimental room, where they were sat at a table and were handed a computer tablet. The experimenter demonstrated how to complete the task and assisted them through a trial run consisting of five repetitions. In these trial exercises, the background of the moving dot consisted of the black ovals alone, without any lines. Participants were also instructed to use their index finger and draw in the designated box on the screen their perceived trajectory of the dot, focusing on the amplitude of the trajectory. The stimuli were concurrently present on the screen so that participants would not rely on memory alone and were able check whether the drawing corresponds with their perception. Participants could delete their answer if not content with how representative the drawing was, and only confirm as the correct answer a drawing that was satisfyingly descriptive of the perceived trajectory. Following the eventual clarifications when required, the participants were left alone to complete the task. There were five repetitions per condition, resulting in a total number of 20 trials which were randomised in terms of

order. The typical length of the experiment was ten minutes, and no breaks were introduced in the task. After completion, participants were fully debriefed as to the phenomenon investigated and were encouraged to make any comments relating to their experience, as well as to ask any further questions. All the data were anonymised prior to being statistically analysed.

2.2.2. Results

The dependent variable, illusion magnitude, was calculated as the difference in pixels between the highest and the lowest points on the trajectories as drawn by the participants. Per combination of participant and background condition, the mean magnitude response was computed in preparation for repeated-measures statistical tests.

Boxplots (Appendix 4) indicate three possible outliers among the participants in at least one of the four background conditions and the computed Z-scores, using ±3.29 (Tabachnick & Fidell, 2007) as the cut-off, confirm all three of them ($z_1 = 3.92$, $z_2 = 5.09$, $z_3 = 4.12$). After removing the outliers, the distribution was analysed: the skewness statistic (Appendix 5) shows that the data are not normally distributed for the illusory lines condition (skewness = 1.225, SE = .299) and the control condition (skewness = 1.278, SE = .299). These two conditions have the lowest means, but relative to these means, they have a larger proportion of participants giving high amplitude answers (see histograms in Appendix 6). Transforming the data into their natural logarithms would have introduced skewness into the initially normally distributed conditions, so no such transformation was applied. The decision was made to rely on the general robustness of the ANOVA to violations of the assumption of normality (Schmider, Ziegler, Danay, Beyer, & Bühner, 2010).

The mean amplitudes and standard deviations are presented in Table 1. As expected, the largest illusion magnitude was reported in the original slalom condition, whereas the lowest illusion magnitude was reported in the control condition. Out of the remaining 64 participants, 52 reported the effect in the expected direction when comparing the control condition to the original slalom condition.

Table 1

Mean Magnitudes and Standard Deviations (in Pixels) for the Four Background Conditions

	Means	SDs
Original slalom illusion	24.73	1.76
Reduced contrast	23.77	1.53
Illusory lines	17.45	7.47
Control	17.14	9.18

The effect of background on the perception of the trajectory was analysed using a repeated-measures ANOVA. The null hypothesis of sphericity was rejected (W = .75, *p* = .003), so a Greenhouse-Geisser correction was applied to the repeated-measures ANOVA. The results show that the background had a significant effect on the perception of the dot trajectory [F (2.49, 156.85) = 26.18, *p* <.001, η_p^2 = .294]. G*Power (Faul, Erdfelder, Buchner, & Lang, 2009) was used to determine the statistical power of the repeated measures ANOVA. Given the η_p^2 = .294 for the effect size, an alpha-level .05 and a total of 64 participants, the statistical power was estimated to be .997.
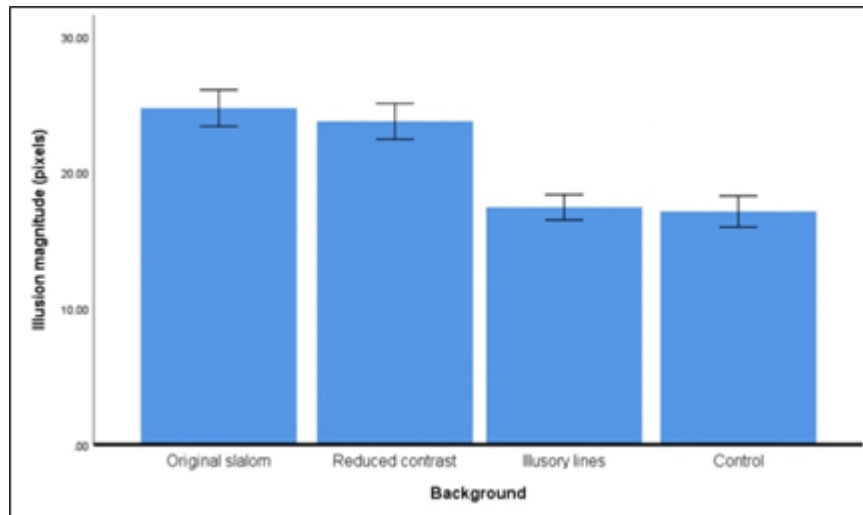
Figure 2.4. Mean magnitudes and standard errors (in pixels) for the four background conditions.

In order to investigate the differences between the four conditions, Bonferroni-corrected post-hoc pairwise comparisons were performed. No significant differences were recorded between the original slalom condition and the reduced contrast condition (mean difference (mdif) = .97, p>.999) and between the illusory lines condition and the control condition (mdif = .309, p>.999). However, the illusion magnitude was significantly larger in the original slalom condition compared with both the control condition (mdif = 7.59, p<.001) and the illusory lines condition (mdif = 7.29, p<.001). Also, the illusion magnitude was significantly larger in the reduced contrast condition when compared with the control condition (mdif = 6.63, p<.001) and the illusory lines condition (mdif = 6.32, p<.001).

2.2.3. Discussion

The original slalom illusion of Cesàro and Agostini (1998) was replicated using a large group of participants, in a slalom display configuration which was modified to allow the direct comparison between real and illusory tilted line inducers. Instead of disjointed

tilted lines, a zigzag pattern was used. The speed of the dot was increased to 100 mm/s compared to the maximum speed found in the original study (38 mm/s), although these values cannot be compared in terms of visual degrees per second, since the current experiment was done on a tablet and participants were free to position themselves at any distance from the display. The angle of intersection was decreased to 15°, whereas the minimal angle used in the original study was 30°. For the purpose of inducing subjective contours in other conditions, oval shapes occluded the endpoints of the tilted lines.

The *magnitude* of the slalom illusion observed was 50% of the vertical extent of the tilted lines, whereas Cesàro and Agostini observed effects up to 25% of the vertical extent. However, Cesàro and Agostini report the amplitude of the sinusoidal path, whereas in the current study the maximal vertical difference in the trajectory is measured, which corresponds to twice the amplitude. Therefore, the effect sizes are similar to the original study, despite the tablet response method and the differences in dot speed (which would have reduced the effect) and intersection angle (which would have amplified the effect). The expected *direction* of the effect was found in most participants in the original slalom condition, with 81% of the participants perceiving a larger magnitude in the original slalom condition than in the control condition. Although inter-individual differences (Genç et al., 2011; Schwarzkopf et al., 2011) could account for some of the remaining 22%, there is also the possibility that the methodological limitations of this experiment may have been a factor. The lack of control on how the participants looked at the display, with no fixed distance to or position of the tablet, could have prevented some participants from observing the effect. Moreover, the response method was not constrained, but involved a free-form finger drawing on the tablet. This might have precluded an accurate measurement of the perceived trajectory.

The reduced contrast condition elicited the slalom effect to a magnitude comparable to that of the original slalom condition, and significantly above the control condition. The illusory line condition, on the other hand, showed no effect that was statistically distinguishable from the control condition. Regarding the predictions put forward prior to the experiment,one could not be not supported (namely, that contrast reduction did not reduce the effect), whereas the other two predictions are supported: the original slalom illusion was replicated and the illusory lines did eliminate the effect.

It could be argued that the subjective contours induced in the current experiment were not salient enough to elicit the slalom illusion. Differently from the classic Kanizsa triangle, there was not segregation of a closed figure from the background, but only isolated line contours, since this is also what was used in the original slalom illusion. Replacing line contours with a closed figure in the current experiment would have introduced additional differences between this experimental setup and the original study on the slalom illusion, whereas the goal here was to keep the stimulus display as similar as possible to that used to generate the known results from the literature. An additional reason why the subjective contours proved impotent in this kinetic visual illusion could be that participants were instructed to follow the dot with their eyes. That is, the subjective contours were not in foveal vision until the dot crossed them. Taking together the implication that Kanizsa-like illusions are stronger when visually attended or in foveal vision (Li, Cave & Wolfe, 2008) and the fact that subjective contours require processing time in feedback loops to manifest themselves in visual cortex (Lee & Nguyen, 2001), they may not have manifested themselves quickly and saliently enough in the current kinetic setup given the speed of the dot. In the methodology of the next experiment, the properties of the stimulus display will be adapted so as to increase the perceptual strength of the illusory contours.

Finally, while the reported magnitude of the slalom illusion in the real-contour condition with tilted lines was large, it is also clear that even in the vertical line control condition, a large sinusoidal amplitude is reported. Cesàro and Agostini did not include a control condition in their study, so the comparison cannot be made whether this is a deviant finding. Potentially, the alternating placement of the ovals at the top and the bottom of the display suggested a sinusoidal trajectory to the participants even in the control condition, where the illusory contours were not present. In the next experiment, this confounding factor will be addressed, and a distinction will be made between the effect of the placement of the Kanizsa inducers and the effect of the vertical control lines.

2.3. Experiment 2

2.3.1. Introduction

Even though the findings of Experiment 1 were statistically valid, replication was sought under the controlled conditions of a classical psychophysics laboratory setup. A CRT screen at a fixed distance was used, and responses were measured using an adaptive probe line. The salience of the subjective contours was increased by using a larger stimulus display with a larger angle of intersection, which allowed the vertical size of the tilted lines modules to be larger and the Kanizsa inducers to be circular, rather than oval. Moreover, the control condition was split into two separate control conditions, one with circles that did not induce subjective contours, and one with real vertical lines. It can then be observed whether the large amplitude of the perceived trajectory in the control condition of Experiment 1 was due to the placement of the circles (if it is not replicated in the vertical line condition), the tablet response method

(if it is not replicated in either control condition), or neither (if it is replicated in both control conditions of Experiment 2).

2.3.2. Methods

2.3.2.1. Participants

Thirty participants were recruited, mainly through the Sheffield Hallam University's Psychology credit scheme, as a course requirement for first year Psychology undergraduates. All participants were undergraduate or postgraduate students and were naïve as to the phenomenon investigated. The inclusion criteria for the sample were having normal or corrected-to-normal vision and being at least 18 years old.

2.3.2.2. Design

Similar to Experiment 1, a repeated-measures design was employed with a single independent variable, *background*. The independent variable had five conditions, three of which were also present in the first experiment:*original slalom* (black inducing lines), *illusory lines* (subjective contours), and *reduced contrast* (grey inducing lines). There were two control conditions: *control lines* (black vertical lines without any circles) and *control circles* (black circles without any lines). The dependent variable, *illusion amplitude*, was operationalised as the height of the response line, measured in pixels.

2.3.2.3. Apparatus and stimuli

The experiment was programmed in Psychtoolbox-3 for MATLAB (Brainard, 1997; Pelli, 1997; Kleiner, Brainard, & Pelli, 2007) and presented on a NEC MultiSync FP2141sb 22" CRT monitor. The viewable area of the monitor was 406 x 304.6 mm. The experiment was run with a spatial resolution of 1600 x 1200 pixels and a temporal resolution of 85 Hz. Similar to the first experiment, the display consisted of the

background, meaning the static stimuli, and the *moving dot* which moved across the background. Unlike the first experiment, the inducing elements for the illusory lines were full circles, not ovals. That is because the salience of the illusory lines in the first experiment may potentially not have worked so well due to the reduced height of the inducers. As in this second experiment a larger screen was used, the stimuli were larger in size, allowing thus for sufficient height between the inducers to accommodate the trajectory of the dot without intersecting the inducers. In all five conditions the dot was black, had a diameter of 2 mm, and moved at the speed of 5 cm/sec. The speed was reduced compared to the first experiment in order to produce an experimental setup closer to the original Cesàro & Agostini study, as well as to adapt the stimuli to the apparatus described above. For the same reasons, other properties of the stimuli were modified compared to the first experiment. Moreover, the control condition in the first experiment was replaced with two, more sophisticated, control conditions in the present experiment, as to account separately for the angle of intersection and the inducers. Excluding the control conditions, the background consisted of seven modules comprising 14 tilted lines placed on 15 inducing circles. Throughout the three experimental conditions, the circles were placed in the same positions and had the same diameter of 1cm. All lines were 3 cm long and 2 mm wide. The angle of intersection for all the tilted lines was 40°. The centre of the experimental display was centred with the centre of the screen.

In the *original slalom* condition (Figure 2.5.A), the tilted lines were black. In the *reduced contrast* condition (Figure 2.5.B), the tilted lines were grey (L = 127.5), whereas the background was white (L = 255). The Michelson Contrast wasequal to .33. In the *illusory lines* condition (Figure 2.5.C), the tilted lines were induced in a Kanizsa fashion, with the edges of the illusory lines placed inside the black circles. In the *control lines* condition (Figure 2.5.D), the lines were placed vertically, creating a 90° angle of

intersection, and there were no circles. In the *control circles* condition (Figure 2.5.E), there were no lines, only the black circles.
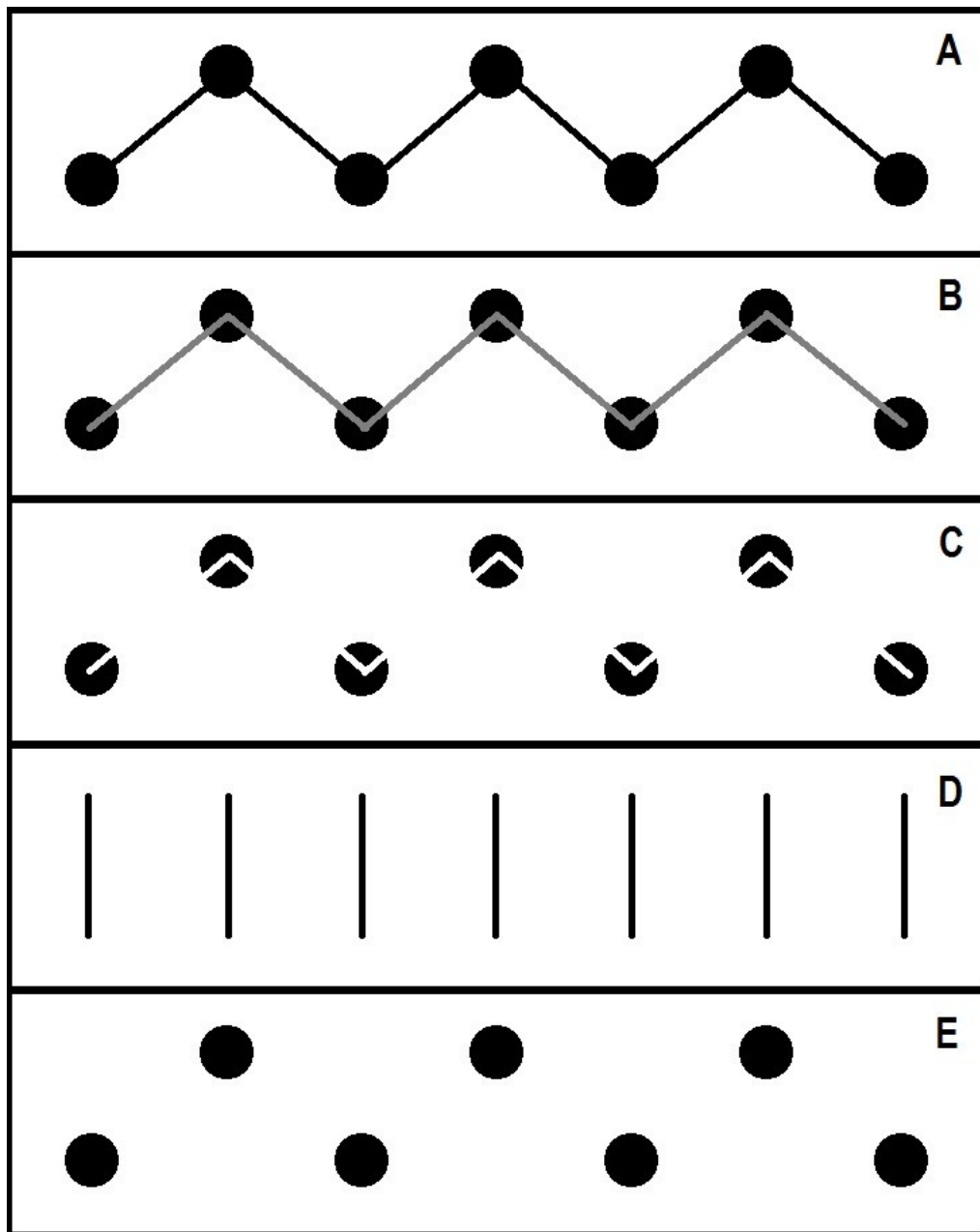

Figure 2.5. Illustration of the five experimental conditions: *original slalom* (A), *reduced contrast* (B), *illusory lines* (C), *control lines* (D), and *control circles* (E). These illustrations are representative of the displays, but not the actual displays.

2.3.2.4.   Procedure

Participants were recruited through the participation credit system in place for first year Psychology undergraduates. A description of the experiment was provided and following the signing up for the experiment, participants were able to choose one of the available proposed timeslots of 30 minutes. Upon arrival at the psychophysics laboratory at the date and time chosen, they were provided with information sheets (Appendix 2) and consent forms (Appendix 3) which they had to sign prior to commencing the experiment. All participants were informed about their rights as per the university ethics guideline and the Declaration of Helsinki. Before starting the experimental task, participants were assisted by the experimenter in a trial run consisting of ten repetitions. This made the participants familiar with the task, which consisted of following the moving dot, which moved back and forth continuously across the background. A chin rest was used, placed at 60 cm from the monitor. Participants were asked to report whether, and if so - how much, the trajectory of the moving dot deviated from a straight one (the slalom effect). In order to answer, participants had to alter the height of a vertical line placed at the centre-bottom of the display. The response line had a starting height randomly assigned from 1 to 20 pixels and, in order to be adjusted, the participants had to press the up arrow key (to increase the size) and the down arrow key (to decrease size). The line was present concomitantly with the stimuli and participants could take as long as they wished before pressing the space bar, which confirmed that they are satisfied that the height of the response line corresponded to the perceived vertical deviation. Once the answer was given, the following trial commenced immediately. There were ten repetitions per condition, meaning that there were 50 trials in total. The trials were randomised in terms of order. The participants completed the task at their own pace, having the choice of proceeding with the trials as they found comfortable, and the duration of the task was on average 30 minutes. Upon completion participants were fully debriefed as to the phenomenon investigated and were

encouraged to make any comments relating to their experience or to ask any further questions.

2.3.3. Results

From the length of the response line for each trial, the mean amplitude response was computed per combination of participant and background condition, in preparation for repeated-measures statistical tests.

Boxplots (Appendix 7) indicated four possible outliers among the participants in at least one of the five background conditions, but the computed Z-scores confirm only two ($z_1 = 3.94$, $z_2 = 3.32$). After removing the outliers, the skewness statistic (Appendix 8) and histograms (Appendix 9) show that the data are not normally distributed in any of the five conditions. The data were transformed into their natural logarithms and the distributions were thus normalised (Appendix 10).

The means and standard deviations presented in Table 2 refer to the data after the removal of the two outliers and prior to the transformation into the natural logarithms. The largest illusion magnitude was reported in the reduced contrast condition, whereas the lowest illusion magnitude was reported in the control lines condition.

Table 2
Mean Amplitudes and Standard Deviations for the Five Background Conditions (in Pixels)

	Means	SDs
Original slalom	8.40	6.68
Reduced contrast	8.54	7.08
Illusory lines	2.88	2.62
Control lines	2.19	1.77
Control circles	2.69	2.23

The effect of background on the perception of the trajectory was analysed using a repeated-measures ANOVA. All the inferential statistics were calculated based on the computed natural logarithms.

The null hypothesis of sphericity was rejected (W = .19, $p < .001$), so a Greenhouse-Geisser correction was applied to the repeated-measures ANOVA. The results show that the background had a significant effect on the perception of the dot trajectory [$F_{(2.03, 54.75)} = 84.60$, $p < .001$, $\eta_p^2 = .758$]. G*Power (Faul et al., 2009) was used to determine the statistical power of the repeated-measures ANOVA. Given the $\eta_p^2 = .758$ for the effect size, an alpha-level .05 and a total sample of 28, the statistical power was estimated to be $> .999$.
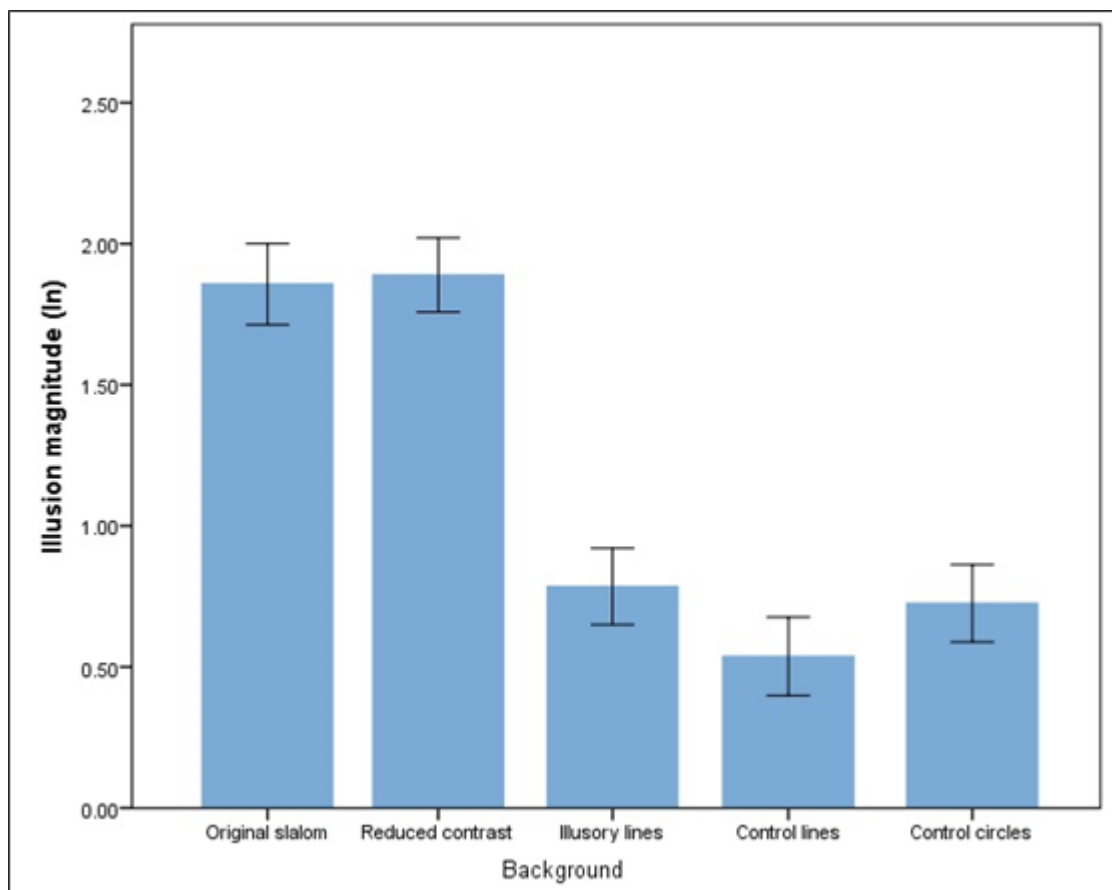

Figure 2.6. Mean amplitudes and standard errors for the experimental conditions of Experiment 2.

In order to investigate the differences between the five conditions, Bonferroni-corrected post-hoc pairwise comparisons were performed. No significant difference was recorded between the original slalom condition and the reduced contrast condition (mdif = -.03, $p>.999$). Similarly, no significant difference was found between the two control conditions (mdif = .19, $p = .076$) or between the illusory lines condition and the control circles condition (mdif = -.06, $p>.999$). Contrary to the results of Experiment 1, the illusion magnitude was significantly larger in the illusory lines condition when compared to the control lines condition (mdif = -.25, $p = .044$). The illusion magnitude was significantly larger in the original slalom condition compared with both of the control conditions (circles mdif =1.13, $p<.001$; lines mdif = 1.32, $p<.001$) and the illusory lines condition (mdif = 1.07, $p<.001$). Also, the illusion magnitude was significantly larger in the reduced contrast condition when compared with the two control conditions (circles mdif = 1.16, $p<.001$; lines mdif = 1.35, $p<.001$) and the illusory lines condition (mdif = 1.11, $p<.001$).

2.3.4. Discussion

The results of the first experiment were replicated in a psychophysical laboratory, where the procedure could be controlled better. All participants in the second experiment perceived the magnitude of the trajectory deviation to be larger in the original slalom condition than in the control conditions. The angle of intersection tested in Experiment 2 (40°) was also tested by Cesàro and Agostini, whereas the speed of 50 mm/s (at a viewing distance of 60 cm) was similar to their maximum speed of 38 mm/s (at a viewing distance of 70 cm). From Figure 6 in Cesàro and Agostini (1998), a reported relative illusory amplitude of around 12.5% (1 mm amplitude for a vertical extent of the inducing lines of 8 mm) could then be expected. Indeed, in the current experiment, a

reported amplitude of 8.4 pixels for a vertical extent of 76 pixels for the tilted lines resulted in a similar relative illusion magnitude for the classic slalom condition (11%). Contrary to Experiment 1, where the amplitude of the control condition accounted for 70% of the amplitude of the classic slalom illusion, in Experiment 2 this ratio was only 26% for the lines, and 32% for the circles. No significant difference was found between the line and the circle control conditions. This implies that the large illusory amplitude of the control condition of Experiment 1 is mainly to be ascribed to the methodology used in the tablet experiment.

All the significant differences between the four conditions of Experiment 1 were replicated in Experiment 2. However, despite the absence of a significant difference between the control line condition and the control circle condition, the illusory line condition resulted in significantly higher reported amplitude when compared to the control line condition, but not when compared to the control circle condition. This could suggest that the salience of the subjective contours had indeed increased in Experiment 2 as compared to the setup of Experiment 1, although the mean difference in amplitude remains small. However, it could also be argued that the control circle condition is more closely matched to the illusory line condition, and constitutes a better baseline for the effect of the general layout of the visual display.

It can be concluded that both the original slalom effect and the significant findings of the current study are robust to replication. The controlled psychophysical setup allowed more reliable measurements, both with regard to the baseline amplitude response in the control conditions and with regard to the consistency of the direction of the effect between participants. An effect of the illusory lines condition is present as compared to the vertical line control condition, but this could be ascribed to the layout of the contour-inducing Kanizsa circles in the former condition.

2.4. General discussion

The slalom effect of Cesàro and Agostini (1998) was replicated. In Experiment 1, it was demonstrated that a low-barrier portable experimental setup can be used to measure the slalom effect, requiring only a few minutes of each participant's time. In Experiment 2, a classical psychophysics laboratory setup was used to successfully support the validity of these results. Indeed, the measurements of Experiment 1 and Experiment 2 are consistent with each other, despite considerable differences in the presentation mode, experimental environment, response collection and number of repetitions in each condition. These findings thus appear to be robust, and generalise across experimental setups.

No prior literature existed that explored the determinants of the slalom illusion, other than the dot speed, the interception angle and the distance between the tilted lines (Cesàro & Agostini, 1998). Cesàro and Agostini, however, did conjecture that the illusion is based on local distortions of motion direction at the points of intersection with the tilted black lines, whereby the interception angle is biased towards perpendicularity. At the same time, a number of studies performed on the Poggendorff illusion (Gregory, 1972; Meyer & Garges, 1979; Westheimer & Wehrhahn, 1997; Tibber et al., 2008) were able to show that the misalignment bias associated with the Poggendorff illusion generalised to displays based on subjective contours instead of real contours. Since the Poggendorff illusion is also a geometric illusion of angle and its effect has been shown to generalise to a kinetic variant with a dot trajectory instead of a static oblique line (Fineman & Melingonis, 1977; Wenderoth & Johnson, 1983), the question arose whether the slalom illusion could also be elicited using subjective contours.

In Experiment 1, illusory contours could not be shown to elicit the slalom illusion to a greater magnitude than could be observed in the control condition. In Experiment 2, where measurements were more carefully collected, this was only the case relative to one of the two control conditions. Relative to the vertical line controls, there was a small but significant improvement. The alternate explanation that can be offered here is that the spatial layout of the circles for the illusory line condition was better matched by the control circle condition, and that, consequently, their placement explains the observed amplitude in the illusory line condition. However, this hypothesis is not supported by the data, due to the absence of a significant difference between the two conditions that were meant to allow statistical inference on this effect – the control line and control circle conditions. While the evidence is weak, it is still possible that the illusory lines were effective. Indeed, Westheimer and Wehrhahn (1997; Tibber et al., 2008) did report that, while present, the Poggendorff effect was considerably decreased when elicited with a Kanizsa figure. A similar decrease might have taken place in the current experiments, to a level that is only just above that of the control line condition.

In both of the current experiments, it was also found that a reduction of the contrast of the tilted lines did not result in a weakening of the slalom illusion. The reduction in contrast under which the slalom illusion was still maintained is not negligible: in the first experiment for instance, Michelson contrast was reduced to .17. This supports the findings of Westheimer and Wehrhahn (1997) using contrast manipulations on the Poggendorff illusion, who similarly observed that the misalignment bias associated with this illusion was already maximal at low contrast levels (Michelson contrast 0.1).

The predictions derived from the theoretical notions of Cesàro and Agostini, formulated prior to the experiment, have therefore not been confirmed. While the evidence for eliciting the slalom illusion by means of subjective contours is relatively weak, the

illusion does remain invariant to contrast manipulations. Conversely, these findings also do not completely confirm the observations made on the Poggendorff illusion, where subjective contours were effective while the illusion similarly remained invariant to contrast manipulations. This then raises the question is the slalom illusion rooted in local distortions at the points of intersection between the dot trajectory and the tilted lines? On balance, there is more evidence for contrast invariance in the current results, than for the ineffectiveness of subjective contours in eliciting the slalom illusion. Not only was a small significant effect of illusory contours observed, but whereas contrast can be easily controlled in a stimulus display, the perception of subjective contours can be fragile and dependent on multiple stimulus parameters that are seldom comparable between studies. For instance, Day et al. (1977) did not find that subjective contours induce the Poggendorff illusion, whereas Meyer and Garges (1979) did. One of the differences between these studies was that Day et al. used four Kanizsa inducers, whereas Meyer and Garges used six, making thus the subjective contour more salient.

The contrast invariance of the slalom illusion is at odds with the hypothesis that the slalom illusion is based on local distortions in motion direction at the points of intersection. The strength of response in V1 neurons, where such local distortions would be situated, has been demonstrated to be strongly dependent on the stimulus contrast (Albrecht, 1995; Carandini, Heeger & Movshon, 1997). It would then follow that the distorted directional signals would also be reduced in their salience and importance when the contrast of the tilted lines is reduced, but this was not the case in the current experiment, or in comparable experiments on the static Poggendorff illusion. This would put the locus of the slalom illusion later in the visual processing stream. The invariance of visual perception to contrast has been proposed to occur gradually from area V1 to area LOC (Avidan et al., 2002; Murray & He, 2006). If it is the case that higher-level visual form areas are responsible for the observed geometric angle biases in

both moving dots and static lines, however, theories that attribute a bias towards perpendicular angles to low-level lateral inhibition between V1 orientation columns (Blakemore et al., 1970) might have to be revisited.

Having performed this study on the local origins of the slalom illusion, the next chapter will investigate whether the biased signals of motion direction can also integrate into a global trajectory percept behind an occluding closed figure.

2.5. Summary

Two experiments were conducted using a different experimental setup, and consistently replicated the robust effect found with the original slalom illusion. Subjective tilted lines could not conclusively be shown to elicit the slalom illusion. Under conditions of a strong reduction in contrast for the tilted lines, however, the full effect was maintained. It therefore appears unlikely that the slalom illusion is rooted in local distortions early in the visual processing stream.

3. Chapter 3 - Occluded trajectory

3.1. Introduction

In their original report on the slalom effect, Cesàro and Agostini (1998) proposed that local distortions at the intersections of the dot trajectory and the tilted lines give rise to an illusory sinusoidal modulation of the dot's straight and horizontal path of movement through the stimulus display. From the experiments of the previous Chapter, it was concluded that the distorted signals at the root of the slalom illusion are however not to be situated at the earliest stages of the visual processing stream. Regarding the determinants and mechanisms of the *integration* of local motion signals into the globally perceived trajectory, Cesàro and Agostini offer no detailed insights. This integration process will be the focus of the current chapter. As discussed in section 5 of Chapter 1, motion integration processes over space and time have been widely studied in the vision sciences, but less often so in the context of a single-object trajectory.

In the current study, the properties of the integration process of the dot trajectory were investigated through the use of an occlusion manipulation, whereby parts of the global trajectory were hidden from the observer's view, to be completed amodally. The occlusion manipulation can naturally be applied to the slalom display by filling the space in between the pairs of tilted inducing lines, forming solid triangular shapes. Figure 3.1 on page 77 illustrates this: the tilted lines now also serve as the onset and offset locations of the occluded parts of the trajectory. Numerous studies have shown that an occlusion manipulation does not impact on the ability of the observers to perceive a continuous trajectory (Burke, 1952; Michotte et al., 1964; Watamaniuk & McKee, 1995), even when testing infants as young as four months old (Bremner et al., 2005). A particularly strong indication that human observers naturally complete

69

occluded trajectories can be found in the literature on smooth pursuit eye movements. As discussed in section 6 of the general introduction chapter, normal exploration of a visual scene happens through an alternation of fast saccadic eye movements and steady fixational periods, but the oculomotor system is also capable of continuous eye movements when a smoothly moving stimulus is available to be followed (Keller & Heinen, 1991). Smooth pursuit eye movements continue when the stimulus traverses behind an occluder, although at a reduced speed when the occlusion period becomes longer (Becker & Fuchs, 1985; Pola & Wyatt, 1997). This indicates that accounting for the occluded parts of an object's trajectory is indeed a fundamental capability of the visual system. Area MST has been proposed to form the necessary spatiotopic link between motion analysis and eye movement control (Newsome et al., 1988; Thier & Ilg, 2005; Ilg, 2008).

It is unclear what the effect of a partial occlusion of the dot trajectory on the magnitude of the slalom illusion would be, because the mechanisms by which the trajectory is integrated from the local motion signals into a coherent whole are unknown.

The kinetic variant of the Poggendorff illusion, introduced in section 7.2 of Chapter 1, bears similarities to the slalom illusion display however. Both the Poggendorff illusion and the slalom illusion are geometric illusions in which the angle of intersection is implicated as the causal factor. The kinetic variant of the Poggendorff display contains a dot trajectory, similar to the classic slalom illusion, and the occluded variant of the slalom illusion the trajectory is only partly visible, similar to the Poggendorff illusion. The main difference between both displays is that whereas the slalom illusion pertains to the *shape* of a trajectory, the Poggendorff illusion is focused on the *misalignment* of two straight segment of a trajectory, that are never perceived to form a coherent whole.

An initial study by Fineman and Melingonis (1977) created the kinetic Poggendorff illusion using a cardboard cut-out for the vertical occluder, and a moving light source behind a diagonal slit as the moving stimulus. It was observed that the misalignment of the two segments perceived in the static Poggendorff illusion was even greater under kinetic conditions. Wenderoth and Johnson (1983) included a similar condition in the third experiment of their paper, this time using a computer-driven display screen, and replicated these findings. When Watamaniuk (2005) revisited the kinetic Poggendorff illusion on a modern psychophysical setup, however, the misalignment illusion was absent in all four participants, whereas the static variant on the same display did produce the classic Poggendorff effect. The author suggests that the results of these earlier studies were affected by methodological shortcomings. Interestingly, a hybrid variant which combined a static line segment on the lower part of the diagonal with an upward moving dot on the upper part did produce the misalignment illusion, but a complementary display where the upward moving dot covered the lower part of the trajectory did not. The author concludes it is specifically the disappearance of the moving dot behind the occluding rectangle which generates a more accurate perception of its continued trajectory, instead of the misalignment illusion typical of the Poggendorff display.

The empirical evidence on the kinetic Poggendorff illusion is therefore inconclusive, with the earlier studies suggesting a slight increase, and the newer study a strong decrease. What does this imply for the predicted effect on the slalom illusion? Contrary to the Poggendorff display, the slalom display is always kinetic in nature, and what is to be compared here is occlusion versus non-occlusion, instead of kinetic versus static. The equivalent of the findings of Fineman and Melingonis (1977) and Wenderoth and Johnson (1983) in their kinetic occlusion condition would still result in a biased trajectory perception across an occluder in the slalom illusion, although the magnitude

71

of the slalom effect relative to the original slalom display cannot be predicted. The equivalent of the findings of Watamaniuk (2005) would imply a strong reduction in the magnitude of the trajectory modulation, since these results suggest that the angle of intersection does *not* bias the trajectory of a moving dot across an occluder.

In terms of theoretical interpretation, Watamaniuk (2005) explains the findings in his experiment through a proposed cascade of sequentially activated motion detectors along the trajectory, generating an accurate predictive signal for the re-appearance of the dot (Grzywacz, Watamaniuk, & Mckee, 1995), which is not present when at least the lower part of the diagonal is static. If this mechanism of facilitatory propagation would be present in the occluded slalom illusion, it would then be expected for the straight dot trajectory to propagate in a linear fashion behind the occluder. It does prompt the question, however, why this cascade of detectors of linear motion would not be effective in the classic slalom display. On the basis of the slalom illusion itself being easily replicable, this theoretical view then seems unlikely. Should it nevertheless be found that the findings of Watamaniuk (2005) do generalise from the kinetic Poggendorff to the occluded slalom illusion, however, an interesting challenge to existing theoretical frameworks will have presented itself.

A second, theoretically separatereason to expect a reduced or absent slalom illusion can also be put forward. Under conditions of occlusion, research on apparent motion has repeatedly shown that the visual system prefers a shortest-path interpretation for the stimulus (Sigman & Rock, 1974; Anstis & Ramachandran, 1985; Yantis, 1995). That is, a straight line between the onset and the offset position of the dot. If this finding generalises to the occluded parts of a continuously moving dots, the magnitude of the slalom illusion could similarly be predicted to decrease.

Alternatively, theories of motion integration often propose that the integration from local motion signals into a single motion direction occurs through an averaging or summing of the individual motion vectors (see section 1.5.2 of the general introduction), whereby the local motion signals are continuously pooled together into the consciously perceived coherent motion direction (Wilson et al., 1992; Yo & Wilson, 1992; Amano, Edwards, Badcock, & Nishida, 2009; Amano et al., 2012). Typically, motion stimuli with a larger spatial extent, such as plaid stimuli, have been employed in these studies, requiring participants to combine multiple motion components that are simultaneously present in the display. The spatio-temporal integration window for such motion displays has been found to measure around one degree in visual angle and 100 ms in time (Sceniak et al., 2001; Hawken, Shapley, & Grosof, 1996). In the slalom display, only a single moving dot is present, however. A vector averaging mechanism would therefore necessarily have to operate *sequentially* on the local motion signals, within the spatio-temporal window of integration. To predict the slalom effect from a large number of horizontal motion signals and a small number of distorted motion signals, it would furthermore have to be assumed that the motion signal around the points of intersection is stronger or more salient because of the presence of the oriented edge. The slalom effect then arises naturally – as strong, distorted signals are summed with weak, linear signals across the integration window, a smoothly modulated motion direction arises, which gives rise to an illusory displacement of the dot on a sinusoidal trajectory. Under conditions of occlusion, a large part of the veridical horizontal motion signal is not present, and therefore no longer adds to the vector summation solution in the integration window. The distorted signals at the intersections are still present, however. As a consequence, it could be expected that in the partial absence of the corrective horizontal motion signals, the inferred trajectory of the dot in the occluded slalom display would be dominated more strongly by its most recent motion signal: the distorted signal at the

point of intersection. The magnitude of the illusion could then be expected to increase. This can be rephrased in the concepts of the predictive coding framework (see section 3 of the general introduction): The amplitude of the global interpretation of the trajectory would be strengthened by partial occlusion, because the error between this illusory interpretation and the (veridical) horizontal local motion signals is reduced by their partial absence.

A second group of motion integration theories proposes that global solutions can be reached through an intersection of constraints (IOC), rather than summation of signals (Adelson & Movshon, 1982; Simoncelli & Heeger, 1998). These theories look at what the possible global solutions are given the divergent motion information present within the integration window, and which interpretations fit the constraints. A variant of this view can be formulated for the current study. If it is supposed that the strongest constraints are posed by the distorted local signals of motion direction at the points of intersection with the tilted lines, the slalom illusion could then be produced by connecting these directional signals in a manner that is smooth enough to form a continuous trajectory. In this view, it can be argued that partially occluding the trajectory should not affect the extremes of the constraints, and therefore should not affect the magnitude of the slalom illusion.

Through the inclusion of an occlusion condition, critical evidence is collected on the likelihood that each of these accounts of integration in motion perception are indeed driving the slalom illusion.

3.2. Experiment 1

3.2.1. Introduction

In the first experiment, an occlusion condition was introduced and compared to both the original slalom condition (tilted lines), and a control condition (vertical lines). As illustrated in Figure 3.1, the occlusion was created by filling the space between each pair of lines of which the top endpoints are tilted towards each other, forming black triangles. The specific comparison being made here, between a dot crossing a set of lines at an angle, and a dot crossing a similar set of lines but with intermittent occlusion, was not revealed to have an equivalent in the existing literature, even in other types of stimulus display. Therefore, no specific prediction was madefrom previous empirical research.

To summarise the theoretical accounts put forward in the introduction, a strong reduction in the effect by partial occlusion could be interpreted as a shortest-path completion of the trajectory, or alternatively as predictive propagation of the predominantly horizontal motion signal. While the former explanation might share mechanisms with static stimulus displays, the latter is inherently based on the motion contents of the slalom illusion. An increased slalom effect can be interpreted as supporting a vector summation view, with continuous integration of the motion signals. When the corrective information of the straight trajectory is missing for 50% of the display duration time, the distorted signals at the line intersections gain a greater weight in the final integration. A constant manifestation of the illusion across occluded and non-occluded trials can be interpreted as an intersection-of-constraints mechanism, where the illusion is based on the motion direction information at the points of intersection only, rather than on a continuous integration of all motion inputs.

3.2.2. Methods

3.2.2.1. Participants

During a science open-day event at the university, a total of 67 participants were recruited through opportunity sampling. The same participants have been tested for this experiment as for Experiment 1, Chapter 2. All participants were over 18 years old at the time of testing and had normal or corrected-to-normal vision. No other exclusive criteria have been used. All participants were naïve as to the purpose of the experiment.

3.2.2.2. Design

A repeated-measures design was employed, with one independent variable, 'background'. The independent variable had three levels: *original slalom* (black inducing lines), *occluders* (black triangles),and *control* (vertical black lines instead of tilted ones). The dependent variable, *illusion magnitude*, was operationalised as the difference between the highest and the lowest points in the reported perceived trajectory of the moving dot, measured in pixels.

3.2.2.3. Apparatus and stimuli

The apparatus was the same as the one described in Experiment 1 of Chapter 2: the experimental task was programmed in Java and presented on a Samsung Galaxy Tab 3 tablet with a 1.1" screen and a resolution of 1280 x 800 pixels. In order to allow for direct comparisons with Experiment 1 of Chapter 2, a similar display layout was used. The experimental display consisted of the *background*, meaning the static stimuli, and the *moving dot,* which moved across the background. The stimuli were also similar to those described in Experiment 1 of Chapter 2, with the exception of the newly-introduced occluding triangles condition (Figure 3.1), where the triangles resulted from the tilted lines of the original slalom condition were filled in with the same colour of

the black tilted lines. The moving dot, thus, disappeared behind these occluders and was only visible in between the black triangles. Across all three conditions, the same properties of the moving dot and angle of intersection were maintained as in Experiment 1 Chapter 2, as follows: the dot measured 2 mm and moved at the speed of 10 cm/sec, and the angle of intersection for all the tilted lines, including the edges of the occluding triangles, was 15°. The centre of the experimental display is centred with the centre of the screen in all four conditions.

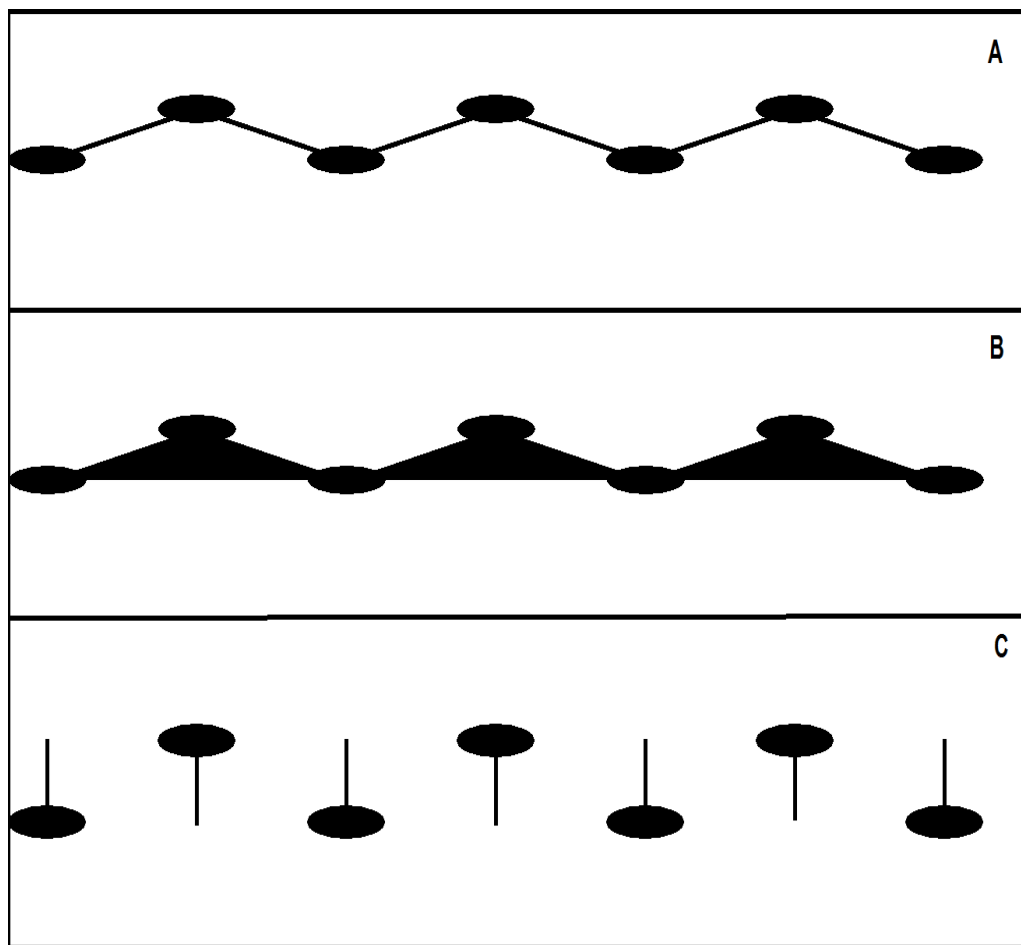*Figure 3.1.* Schematic representation of the three background conditions: *original slalom* (A), *occluders* (B), and *control* (C).

3.2.2.4.   Procedure

The procedure was the same as the one described in Experiment 1 from Chapter 2 (page 50).

3.2.3. Results

The dependent variable, illusion magnitude, was calculated as the difference in pixels between the highest and the lowest points on the trajectories as drawn by the participants. Per combination of participant and background condition, the mean magnitude response was computed in preparation for repeated-measures statistical tests.

Boxplots (Appendix 11) indicate five possible outliers among the participants in at least one of the three background conditions. However, the computed Z-scores confirm only two outliers ($z_1 = 5.10$, $z_2 = 3.56$). After removing the outliers, the skewness statistic (Appendix 12) shows that the data wereskewness levels were within normal parametersin the two experimental conditions (original slalom skewness = .617, SE = .297; occluding triangles skewness = .609, SE = .297), and skewed in the control condition (skewness = 1.922, SE = .297) (see histograms in Appendix13). Relying on the general robustness of the ANOVA to violations of the assumption of normality (Schmider et al., 2010), the data was analysed using parametric tests.

The means and standard deviations are presented in Table 3.1. The largest illusion magnitude was reported in the occluding triangles condition, whereas the lowest illusion magnitude was reported in the control condition. Out of 65 participants, 47 reported a higher magnitude in the occluding triangles condition when compared to the original slalom condition.

Table 3.1
Mean Magnitudes and Standard Deviations (Measured in Pixels) for the Three Background Conditions

	Means	SDs
Original slalom	25.40	11.95
Occluding triangles	32.18	16.06
Control	17.88	1.87

The effect of background on the perception of the trajectory was analysed through a one-way analysis of variance. The independent variable, background, was a within-participants factor with three levels (original illusion vs occluded condition vs control). The dependent variable was the magnitude of the perceived motion of the dot and was measured in pixels.

The null hypothesis of sphericity was rejected ($W = .83$, $p = .002$), so a Greenhouse-Geisser correction was applied to the repeated-measures ANOVA. The results show that the background has a significant effect on the perception of the dot trajectory [$F (1.70, 108.99) = 42.99$, $p < .001$, $\eta_p^2 = .402$]. G*Power (Faul et al., 2009) was used to determine the statistical power of the repeated-measures ANOVA. Given the $\eta_p^2 = .402$ for the effect size, an alpha-level .05 and a total of 65 participants, the statistical power was estimated at $> .999$.

In order to investigate the differences between the three conditions, Bonferroni-corrected post-hoc pairwise comparisons were performed. In the occluding triangles condition the magnitude of the illusion was significantly higher than both in the original slalom condition (mdif $= 6.79$, $p < .001$) and in the control condition (mdif $= 14.31$, $p < .001$). In the slalom condition, the magnitude of the illusion was significantly larger than in the control condition (mdif $= 7.52$, $p < .001$).
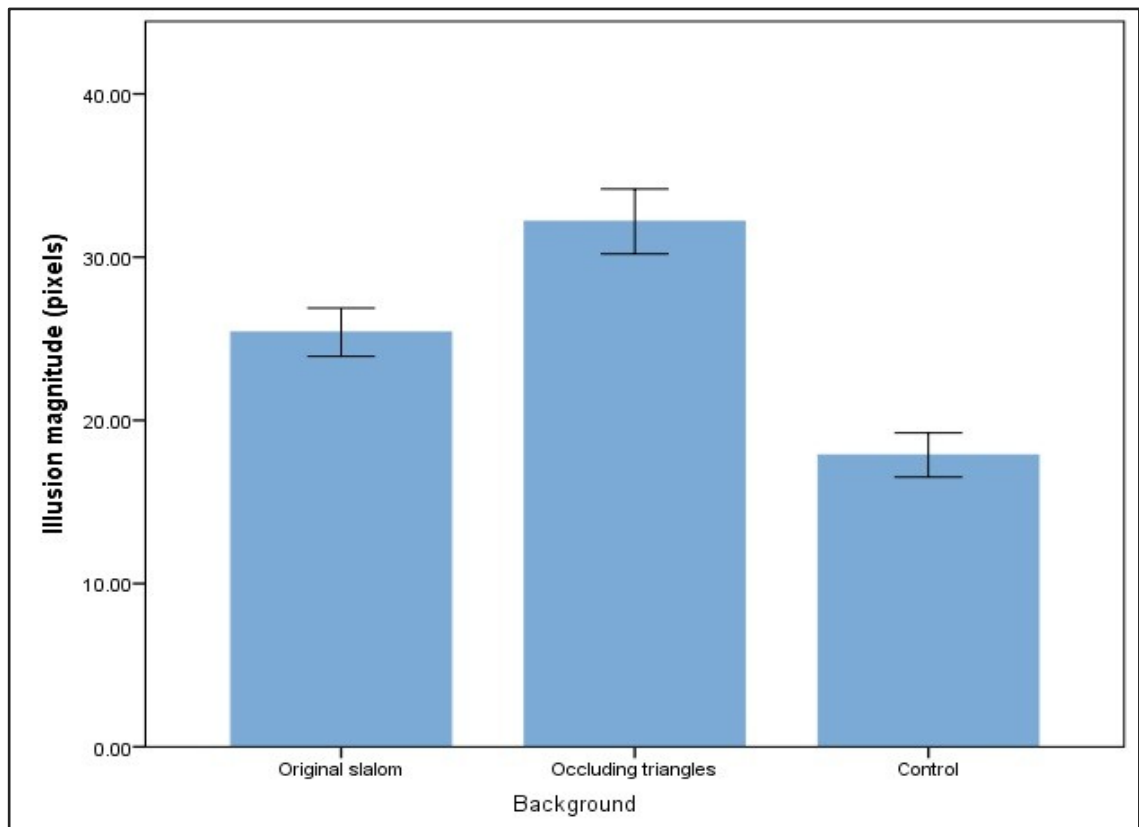
Figure 3.2. Mean magnitudes and standard errors (in pixels) for the three background conditions.

3.2.4. Discussion

The slalom illusion was present as in the original findings of Cesàro and Agostini (1998), and its magnitude increased further when half of the trajectory was intermittently occluded with black triangles. According to the theoretical views put forward at the beginning of this chapter, this finding provides supporting evidence for a vector-summation account of local-global integration in the slalom illusion, whereby motion signals are continuously combined within the motion integration window, and the partial removal of the horizontal trajectory increased the relative weight of the distorted signals at the points of intersection. These theoretical implications are discussed in more detail in the general discussion.

The occlusion condition resulted in a larger perceived amplitude on top of the classical slalom effect in the large majority of the participants. Because these data were collected in an environment that did not allow for a great degree of experimental control, such variability is to be expected. Indeed, in Chapter 2 it was similarly observed that the direction of the classic slalomeffect could be replicated more reliably in a psychophysical laboratory than using the tablet display and response method. In Experiment 2 of the current chapter, the occlusion effect will therefore be assessed again, applying more stringent methodological control.

3.3. Experiment 2

3.3.1. Introduction

In the second experiment, participants were tested under more controlled conditions in a laboratory, using a chin rest, a CRT monitor, and an adaptive probe line for collecting the responses. If the results of Experiment 1 of the current study are replicated, the classic slalom effect is predicted to be observed, as well as an increased magnitude of the illusion for the occlusion condition with black triangles. Because the oval elements at the endpoints of the tilted lines in Experiment 1 were only present to make the visual displays consistent with the methodology of Chapter 2, and the current Experiment 2 was instead performed separately from these experiments, the ovals were removed.

Possibly, the occlusion condition differed in more aspects from the original slalom condition, than only the intermittent occlusion of the trajectory. The occluding black triangles introduced a new visual element into the display: the horizontal line which forms the base of the triangles. It can be argued that the presence of this line could be sufficient to induce the larger illusory amplitude of the illusion under the occlusion

condition of Experiment 1. To control for this confounding factor, two additional

conditions were introduced in Experiment 2. In the transparent triangles condition, the

base of the triangle is completed with a black line identical in width to the tilted lines.

The dot remains visible as it traverse the triangle, and no occlusion occurs. If the mere

presence of the triangle object is responsible for the increase in the slalom illusion, it

should be replicated in this condition as well. It is, however, expected that this will not

occur. To the contrary, since the base of the triangle provides a strong reference line for

the horizontal trajectory, it could reduce the magnitude of the slalom illusion.

In the grey triangles condition, the black triangles and their contour lines are reduced in

contrast to a shape lighter in colour, in front of which the dot traverses without

occlusion. Through this manipulation, it was investigated whether the effect observed in

the occlusion condition of Experiment 1 could rely specifically on the presence of a

filled triangle instead of a contour drawing of a triangle. In particular, it could be argued

that the dot has two points of intersection with each contour of the transparent triangles:

once on the left side, and once on the right side of the line. In the occluding condition

employing black triangles, there is only a single point of intersection. It is however

unclear in what manner this would by itself result in an increased slalom effect, and

therefore it is not expected that the effect of the occluding black triangles would be

replicated in the non-occluding grey triangles condition. Since it was found in

Experiment 1 of Chapter 2 that the contrast of the inducing lines does not affect the

magnitude of the slalom illusion, it can instead be predicted that the grey triangles

condition will result in a magnitude of the illusion that is comparable to the similarly

non-occluding transparent triangles condition.

3.3.2. Methods

3.3.2.1. Participants

Thirty participants were recruited through the Sheffield Hallam University's Psychology credit scheme. All participants were undergraduate students and were naïve as to the phenomenon investigated. The inclusion criteria for the sample were having normal or corrected-to-normal vision and being at least 18 years old.

3.3.2.2. Design

A repeated-measures design was employed, with a single independent variable, *background*. The independent variable had five conditions, three of which replicate those in the first experiment: *original slalom* (black inducing lines), *occluding triangles* (black triangles), and *control* (vertical lines). The additional two conditions were: *grey triangles* and *transparent triangles*. The dependent variable, *illusion amplitude*, was operationalised as the height of the response line, measured in pixels.

3.3.2.3. Apparatus and stimuli

The experiment was programmed in Psychtoolbox-3 for MATLAB (Brainard, 1997; Pelli, 1997; Kleiner et al., 2007) and presented on a NEC MultiSync FP2141sb 22" CRT monitor. The viewable area of the monitor was 406 x 304.6 mm. The experiment was run with a spatial resolution of 1600 x 1200 pixels and a temporal resolution of 85 Hz. The properties of the stimuli were in line with those presented in Experiment 2 of Chapter 2 with respect to the dot size, trajectory, and angle of intersection. However, the modules were modified from both the previous study (Chapter 2) and the first experiment of the present study, as to remove the circles placed at the intersections of the inducing lines. This way, the experimental setup was more similar to the original Cesàro & Agostini display. In all five conditions the moving dot was black, had a

diameter of 2 mm, and moved at the speed of 5 cm/sec. The angle of intersection for all the tilted lines was 40°. In the three triangle conditions (occluding, grey and transparent), the background consists of 7 isosceles triangles, with the base of 4.6 cm and the two equal edges (the tilted lines) of 3 cm. The triangles were placed at 1 cm distance from each other. The occluding triangles (Figure 3.3.B) were black and hid the trajectory of the dot when it intersected their surface. The grey triangles (Figure 3.3.C) had a mid-grey luminance of 127 RGB and do not occlude the trajectory of the dot, as the black dot crosses in front of them. The transparent triangles (Figure 3.3.D) have a black contour of 1 mm, but are not filled, and the trajectory of the dot is visible when it translates them. The original slalom condition (Figure 3.3.A) consists of a series of 7 modules of two tilted lines corresponding to the edges of the triangles from the triangles conditions; the distance between the modules is 1 cm and the tilted lines are 1 mm thick and 2.5 cm long. The vertical lines in the control condition (Figure 3.3.E) were black, 1 mm thick and 2 cm long. The centre of the experimental display was centred with the centre of the screen in all conditions.
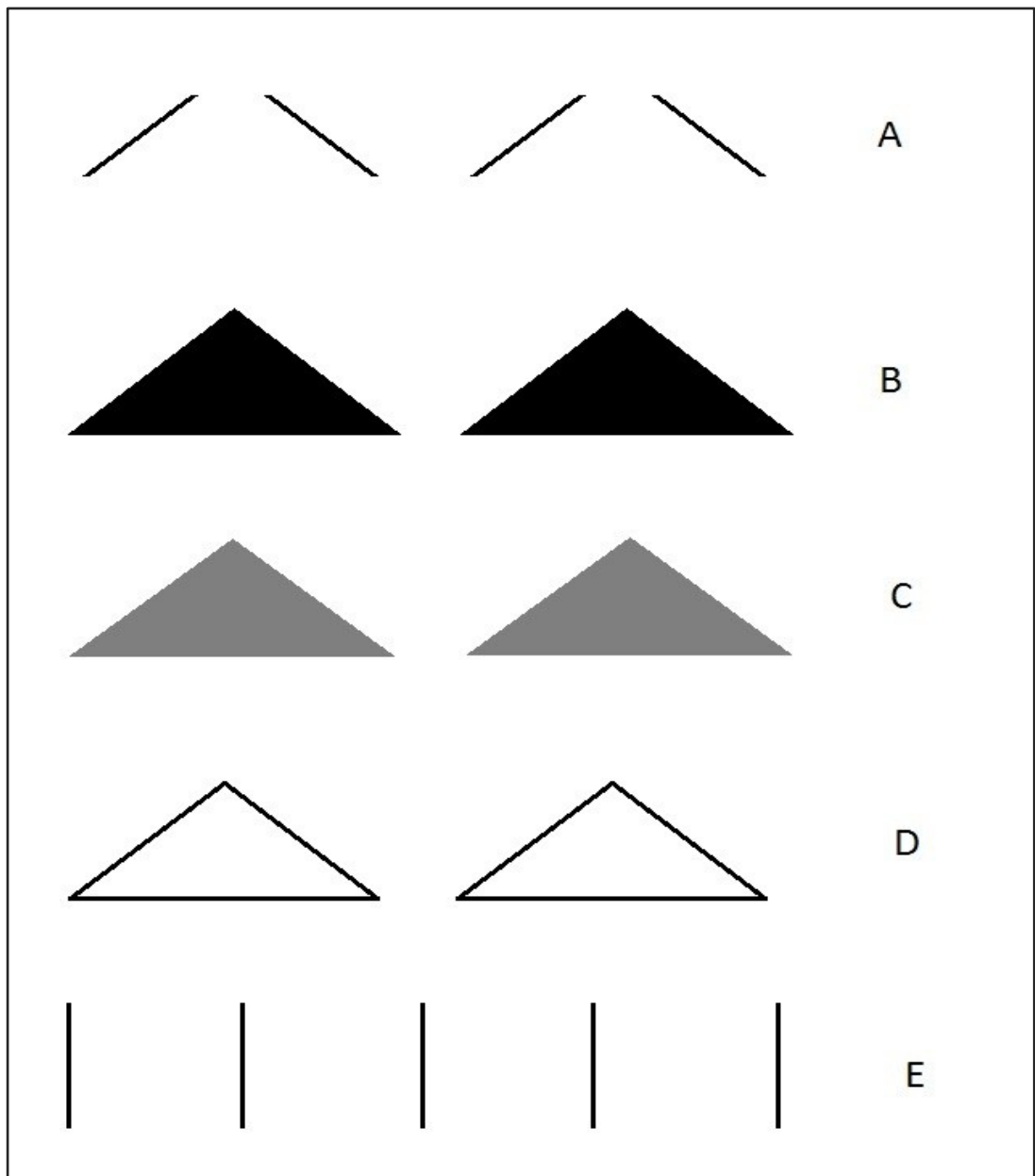
Figure 3.3. Illustration of the five experimental conditions: *original slalom* (A), *occluding triangles* (B), *grey triangles* (C), *transparent triangles* (D), and *control* (E). These illustrations are representative of the displays, but not the actual displays.

3.3.2.4. Procedure

The procedure was identical to the one described in the Experiment 2 of Chapter 2 (page 60).

3.3.3. Results

From the length of the response line for each trial, the mean amplitude response was computed per combination of participant and background condition, in preparation for repeated-measures statistical tests.

Boxplots (Appendix 14) indicated three possible outliers among the participants in at least one of the five background conditions, and the computed Z-scores confirmed two of them ($z_1 = 3.71$, $z_2 = 3.70$). After the outliers were removed, the histograms (Appendix 15) and the skewness statistic (Appendix 16) show that the data are not normally distributed in any of the five conditions. All the data were transformed into their natural logarithms, which lead to the normalisation of the distributions in preparation for the parametric tests (Appendix 17).

The means and standard deviations presented in Table 3.2 refer to the data after the removal of the two outliers and prior to the transformation into natural logarithms. The largest illusion magnitude was reported in the occluding triangles condition, whereas the lowest illusion magnitude was reported in the control condition. The direction of the effect was very consistent in this experiment, with all the remaining 28 participants reporting a larger magnitude in the original slalom condition than in the control condition.

Table 3.2
Means Magnitudes and Standard Deviations for the Five Background Conditions (Measured in Pixels)

	Means	SDs
Original slalom	8.10	6.76
Occluding triangles	11.88	7.75
Grey triangles	5.37	5.09
Transparent triangles	6.59	5.81
Control	1.91	1.30

The effect of background on the perception of the trajectory was analysed using a repeated-measures ANOVA. The independent variable, background, was a within-participants factor with five levels and the dependent variable was the amplitude of the illusion. All the inferential statistics were calculated based on the computed natural logarithms.

The null hypothesis of sphericity was rejected ($W = .21$, $p<.001$), so a Greenhouse-Geisser correction was applied to the repeated-measures ANOVA. The results show that the background had a significant effect on the perception of the dot trajectory [$F (2.99, 8.73) = 86.12$, $p <.001$, $\eta_p^2 = .761$]. G*Power (Faul et al., 2009) was used to determine the statistical power of the repeated-measures ANOVA. Given the $\eta_p^2 = .761$ for the effect size, an alpha-level .05 and a total of 28 participants, the statistical power was estimated at $>.999$.
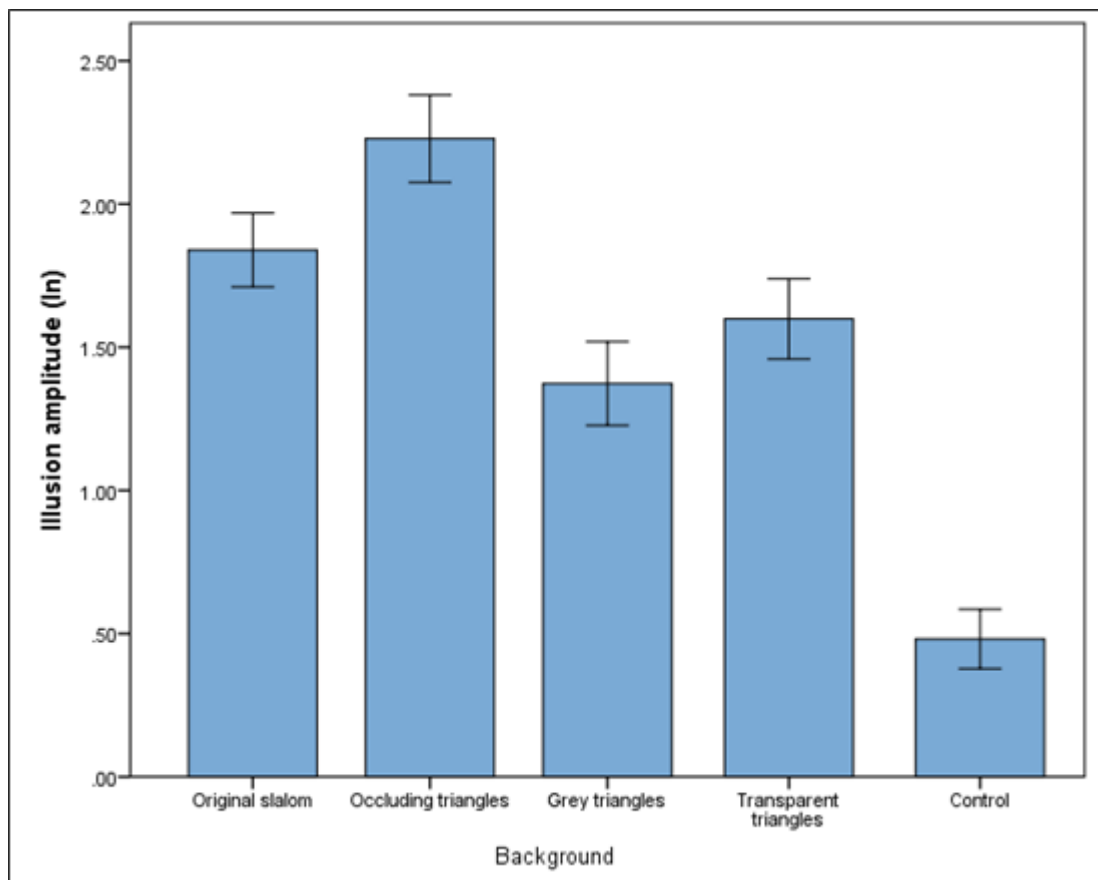

*Figure 3.4.*Mean amplitudes and standard errors for the five background conditions.

In order to investigate the differences between the five conditions, Bonferroni-corrected post-hoc pairwise comparisons were performed. The illusion amplitude was significantly larger in the occluding triangles condition compared with all other conditions: original slalom (mdif = .39, p = .006), grey triangles (mdif = .86, $p<$.001), transparent triangles (mdif = .63, $p<$.001), and control (mdif = 1.75, $p<$.001). In the control condition, the magnitude of the illusion was significantly smaller than in all the other conditions: original slalom (mdif = -1.36, $p<$.001), grey triangles (mdif = -.89, $p<$.001), and transparent triangles (mdif = -1.12, $p<$.001). In the original slalom condition, the amplitude of the illusion was significantly larger when compared to the grey triangles (mdif = .47, p = .001) and transparent triangles (mdif = .24, $p<$.001). There was no difference in the illusion magnitude between the grey triangles and transparent triangles conditions (mdif = -.23, p = .187).

3.3.4. Discussion

The classic slalom illusion was replicated, as was the increased magnitude of the slalom illusion under conditions of partial occlusion of the dot trajectory. In the more controlled laboratory set-up of this experiment, the large majority of the participants displayed the occlusion effect in this direction. As in the Experiment 1 of this study, this is interpreted as supporting evidence for a vector summation account of the local-global integration process in the slalom illusion.

The grey triangles condition was statistically indistinguishable from the transparent triangles condition. This invariance to contrast, and indeed to the difference between a filled triangle and a contour outline of a triangle, is consistent with the findings of contrast invariance of Chapter 2. This again suggests that the motion signals of the dot do not interact with an early, low-level representation of the inducing lines, but that

higher-level processing has already taken place before the initial distorted signals of motion direction arise. While the interaction might still occur at a low anatomical level in the visual hierarchy, feedback signals from higher level areas must at least have added invariance to the contour representation (Lee & Nguyen, 2001).

The non-occluding grey triangles and transparent triangles did not result in an increased slalom effect. To the contrary, the slalom effect was reduced, but still present, in both conditions. This convincingly demonstrates that the occlusion effect was not caused by the mere presence of closed triangular objects, as opposed to paired sets of tilted lines as in the classic slalom illusion. On the reason for the reduced slalom effect, it might be speculated that the presence of the base of the triangle perhaps provided a more useful frame of reference for the estimation of the veridical trajectory than the tilted lines of the original slalom display. However, it is worth pointing out that this did not prevent the slalom illusion from still occurring.

3.4. General discussion

The studies presented here demonstrate a novel effect: the slalom illusion is amplified by the partial occlusion of its dot trajectory. This effect could not be explained by the mere presence of either filled geometric shapes or contour outlines thereof – occlusion appears to have been a necessary condition.

Compared to the results obtained using the kinetic Poggendorff display, the current data are congruent with the findings of Fineman and Melingonis (1977) and Wenderoth and Johnsson (1983). In both cases, it was observed that a strong Poggendorff illusion of displacement could still occur when the dot traversed behind an occluding rectangle. The results of Watamaniuk (2005), who noted an absence of the Poggendorff

misalignment in kinetic conditions, did not generalise to the occluded slalom display. Little support is found for the theoretical account of facilitatory propagation as a mechanism for the global integration of the dot trajectory, which would, as noted in the introduction of this chapter, also appear to be at odds with the existing empirical evidence on the slalom illusion. If the dot trajectory indeed results in a propagating facilitation of a cascade of motion detectors, its horizontal course must be easily deflected by the tilted inducing lines - in which case the proposed propagating effect of motion direction cannot be strong. This is not to discard predictive effects in motion perception entirely, however. For instance, in the *flash-lag effect* (Nijhawan, 2002), a static stimulus briefly flashed alongside a moving stimulus always appears to lag behind the moving stimulus, whereas in reality they are spatially aligned. This demonstrates convincingly that the visual system attempts to predict where a moving stimulus is going. However, the mechanisms behind such predictive effects do not result in an extrapolation towards a straight path in the context of the slalom illusion.

Similarly, the hypothesis that the dot trajectory would be completed according to a shortest-path solution can be rejected, as this would similarly have resulted in a reduced magnitude of the slalom illusion. Shortest-path solutions appear to occur more readily in the literature on apparent motion, where a percept of motion is induced by flashing a dot at two successive locations (Anstis & Ramachandran, 1985; Ramachandran & Anstis, 1986; Akselrod, Herzog, & Öğmen, 2014), than in a visual display containing continuous motion. The completion of the dot trajectory in the current study is then more similar to static demonstrations of amodal completion, where it is evident that the shortest-path solution is often not preferable. Consider the example of a circle of which one quadrant is occluded by a superimposed shape: it will be completed as a circle, not as a partial circle with one straight segment exactly coinciding with the occluding shape. This occurs because the visible part of the contour imposes a strong prior on what the

occluded part could look like (Singh & Fulvio, 2005; see also section 4.2 of the general introduction). Possibly, such shape priors also apply to the trajectories reported in the current experiments.

Cesàro and Agostini (1998) suggest that the points of intersection between the dot trajectory and the tilted lines are the most plausible cause for the illusory trajectory modulation observed in the slalom illusion. Indeed, the tendency towards perceiving right angles is often proposed to lie at the basis of many geometric illusions, including the Poggendorff illusion (Morgan, 1999). The intersection-of-constraints account put forward for the slalom illusion posited that the observer's perception of the dot trajectory is governed by a solution which satisfies fully these extremes of the local signals of motion direction, as observed at the points of intersection. The proportion of the visible trajectory which is not distorted is then of little importance, as these horizontal motion signals do not define a boundary to the range of motion directions observed. The results of the current experiments contradict such a view, as indeed they clearly demonstrated an amplified illusion when the proportion of the visible horizontal trajectory decreases.

This suggests a continuous integration of the local motion signals, in congruence with the vector summation account of local-global integration. As the veridical information of the straight horizontal trajectory is partly absent, the distorted motion directions gain a greater weight, and the amplitude of the trajectory modulation increases. In other words, the entire trajectory contributes to the global interpretation, not only the strong signals with the most extreme motion direction at the points of intersection. As proposed in the introduction of this chapter, these findings can be framed within the predictive coding theory (Rao & Ballard, 1999) - also discussed in section 3 of the general introduction. Partial occlusion in this view supports the interpretation of a

higher-amplitude sinusoidal trajectory, because it decreases the error signals between this global interpretation and the incoming local horizontal motion signals – due to the reduced availability of such signals.

If the slalom effect can be explained in such a general framework as predictive coding, the question arises as to whether the slalom illusion itself could also occur more generally, such as in a static version, without these specific summation mechanisms of motion. However, no illusion is visible in a static slalom display, where the dot trajectory is replaced by a horizontal line. Static geometric illusions of angle that do affect the apparent shape of a continuous line, like the Hering illusion, require a more dense visual display, with more intersecting angles, than the relatively sparse slalom illusion. It is therefore suggested that motion illusions are far more susceptible to biased global interpretations, since they explicitly require integration mechanisms over time of their transient local signals, such as vector summation, whereas static lines remain visible for the entire display duration. That is, their local signals continuously provide a mismatch with the illusory global interpretation, whereas the local signals of motion illusions are fleeting and cannot be revisited.

Finally, a spontaneous observation made by a number of participants in the occluded condition of Experiment 2 can be reported on. Instead of perceiving the movement speed of the slalom illusion to be consistent and predictable, it was indicated that the dot appeared to 'jump out' from behind the black triangle upon re-appearance, faster than expected. While these observations are anecdotal in nature and were not formalised in the experimental design, one can confirm this impression by looking at a full stimulus sequence in the occluding triangles condition. It is proposed that this finding is congruent with the perceptual expectation of a greater modulation of the trajectory amplitude behind the occluder. Because the occluded trajectory is, as a result, expected

to be longer in length, a constant dot speed would also result in an overestimation of the total time of occlusion. The re-appearance of the dot would then occur sooner than expected.

At this point, it is worth highlighting that the local-global integration of a trajectory does not consist of one single process or mechanism. Rather, it involves the integration of transient signals of motion directions within a motion integration window, for which the continuous summation or averaging of motion vectors is indeed a strong candidate. These mechanisms are specific for motion perception. On the other hand, the *shape* of the trajectory is to be inferred from the perceived positions of the moving object. This stage of the integration process might well share mechanisms and pathways with the perception of static contours and shapes, which also manifest themselves in phenomena of amodal completion. The spontaneous observation reported in the previous paragraph might well relate to this second stage of integration – the shape described by the trajectory. Expectations about this shape might then have been fed back into predictions about the local position and speed of the moving dot, causing surprise upon its re-appearance. In the next chapter, this phenomenon will be investigated more closely.

3.5. Summary

Two experiments were conducted using a different experimental setup, and both consistently found that partial occlusion of the dot trajectory increases the slalom illusion. This effect was not caused by the mere presence of triangular objects, and it was evinced that the slalom illusion was invariant to the low-level characteristics of the inducing tilted lines. It was proposed that these results are best explained by a continuous summation of the local motion signals, whereby partial occlusion increases

the relative importance of the distorted signals at the points of intersection between the

dot trajectory and the tilted lines.

4. Chapter 4 - Inter-stimulus interval

4.1. Introduction

In the occluded conditions of Experiments 1 and 2 in Chapter 3, the moving dot of the slalom illusion display disappeared at the left side of the black triangle, and then re-appeared at the right side. The illusory trajectory of the slalom illusion was found to be completed across these occluders. The time interval between these offset and onset events was determined by the constant horizontal speed of the veridical dot trajectory, and remained consistent with the shortest-path solution of a straight trajectory, even though a longer, sinusoidal trajectory was subjectively perceived by the participants. This experimental sequence of a first stimulus followed by a second stimulus, interrupted by a short inter-stimulus interval (ISI), is reminiscent of the phenomenon of *apparent motion*. Instead of a veridically moving dot interrupted by occlusion, in the apparent motion paradigm two static dots are shown at different positions and different moments in time. The movement of the dot is then perceptually inferred from its rapid displacement from the first position to the second position (Figure 4.1). For this to occur, the inter-stimulus interval (ISI) should be of an intermediate duration: if it is too short, two stimuli will appear to be flashing simultaneously, and if it is too long the first and the second stimulus will appear to be separate and sequential.

Korte (1915) investigated the effect of stimulus intensity, distance and ISI on the phenomenon of apparent motion, and summarised his results in three laws. First, larger distances require larger stimulus salience for the apparent motion illusion to occur. Second, larger ISIs require larger intensities. Third, larger distances require larger ISIs for apparent motion to be perceived. The latter result is especially noteworthy: the apparent motion illusion's lower ISI limit is not just bound by the visual system's

discrimination thresholds for the order of appearance in sequentially flashing stimuli, but also and more importantly by the maximum speed the visual system can assume for the object's motion, given the distance it had to travel.
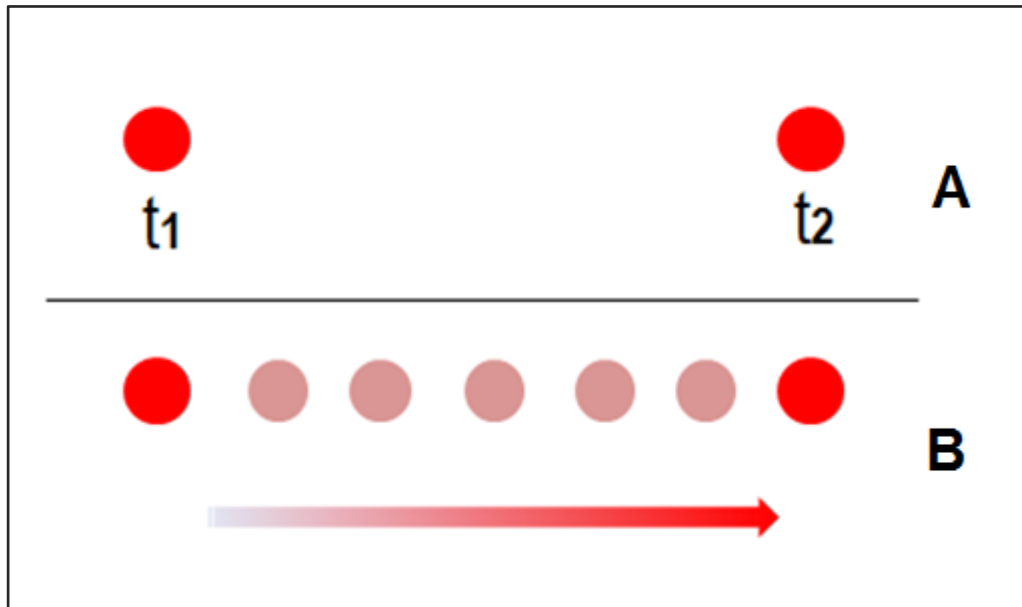

*Figure 4.1.*Illustration of apparent motion. When two objects (the red circles) are presented at different times (A), if the ISI is neither too short nor too long, the two objects are perceived as a single one moving between the two positions (B).

The perceived path of apparent motion is typically found to be a straight line between the first and the second position (Anstis & Ramachandran, 1985; Akselrod et al., 2014). However, in specific experimental contexts there have been observations to the contrary. Shepard and Zare (1983) briefly flashed a curved grey path in the ISI of an apparent motion display, and observed that the object appeared to have moved along that path. In addition, Korte's third law generalised to this curved apparent trajectory of motion: not the linear distance between the sequential stimuli, but the length of the curved path determined the minimal ISI needed for the perception of apparent motion. This could be seen as an instance of the tunnel effect (Burke, 1952; Michotte et al., 1964). When a

continuously moving object moves behind an elongated occluder, its trajectory is amodally completed to follow the shape of the occluder.

The study of Shepard and Zare (1983) did not necessarily constitute amodal completion, however. Whereas the tunnel effect relies on a persistently present occluder, Shepard and Zare only flashed the curved path briefly during the ISI of the apparent motion display. This could be seen as a priming of the curved trajectory, just prior to the appearance of the second stimulus. To address this discrepancy, Kim, Feldman, and Singh (2012) introduced a curved occluder constantly present on the screen into an apparent motion display. The authors observed that at short ISIs (less than 200 ms for a three to nine visual degree separation) participants predominantly perceived a straight path. As the ISIs increased, however, so did the proportion of curved responses. This can be seen as a generalisation of Korte's third law to the shape of the trajectory, as in this case the curved shape was associated with a longer distance; as mentioned previously, Korte (1915) described how the minimum ISI required to perceive any apparent motion is longer for greater stimulus distances. Kim et al. (2012) observed that a greater perceived trajectory length, independent of the stimulus distance, also requires longer ISIs (as well as experimental conditions conducive to a curved interpretation). In one of their experiments, Kim et al. (2012) confirm that their results can be ascribed to amodal completion rather than shape priming.
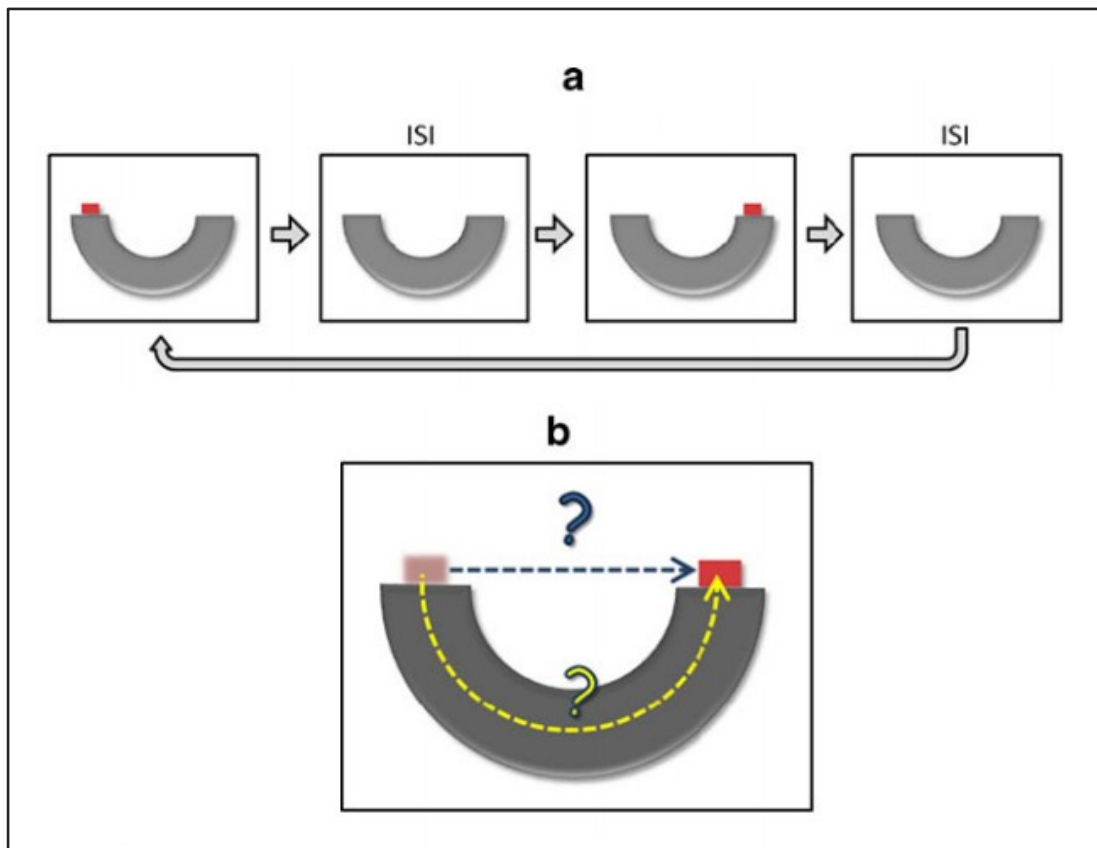
Figure 4.2. Adapted illustration of the stimuli from Kim et al. (2012), showing the stimuli used to demonstrate that when using a curved occluder, if the ISI was increased, the path of the object between the ends of the occluders was more likely to be perceived as curved.

In a follow-up study, Kim, Feldman, & Singh (2013) extended their displays with context objects suggesting different types of *causes* for the (apparent) motion of the object, such as being bounced or launched by another moving object. Some of these causal events were consistent with a curved trajectory, whilst others were consistent with a straight trajectory. The authors observed that the causality of the apparent motion suggested by the context objects strongly affected the perception of the shape of the trajectory as being either curved or straight, even if the crucial context information was provided only *after* the appearance of the second apparent motion stimulus. These

findings are at odds with the intuitive experience human observers have of visual perception, namely that we perceive things on-line, as they are happening. Rather, these results lend support to the concept of postdiction in visual perception (as opposed to prediction). In this view, a perceptual interpretation imposes itself retroactively on past inputs, reinterpreting them before they have reached conscious perception (Eagleman & Sejnowski, 2000; 2003). Applied to apparent motion, the perceived trajectory is then strongly based on information received *after* the moving object has completed its illusory path, that is, after the second apparent motion stimulus.

To summarise, trajectory perception is bound by constraints of plausibility as a function of speed (ISI), and can be affected by postdictive interpretations. In the previous chapter, it was observed that the slalom illusion was increased in magnitude by a partial occlusion of the dot trajectory, and attributed this effect to the partial absence of corrective horizontal motion inputs to the illusory perception of a sinusoidal path. In addition, however, several participants spontaneously reported that the dot appeared to 'jump out' from behind each occluder, earlier than they had expected. Similar to the studies on apparent motion and amodal completion discussed above, participants were required to infer the trajectory of a moving object without being able to perceive it. To gain further insights in the mechanisms involved in the global integration process of the sinusoidal trajectory, the central ISI parameter of these apparent motion studies was manipulated in the current experiment.

It was postulated in the discussion of Chapter 3 that the dot reappeared faster than expected, because the illusory curvature of the slalom trajectory caused it to be interpreted as longer than the veridical, horizontal trajectory. At constant dot speed, it follows that the actual occlusion time will therefore be shorter than the expected occlusion time. Three different views can be formulated on how this reported

phenomenon relates to the increased magnitude of the slalom illusion in the occluded conditions. First, the 'jumping out' of the dot could be only a *by-product* of the occluded slalom illusion, caused by the mismatch between the subjectively completed trajectory and the real trajectory, and the expected re-appearance times from behind the occluder that are associated with each. If this hypothesis is true, manipulating ISI should not affect the size of the occluded slalom illusion, even if it could affect the magnitude of the 'jumping out' phenomenon.

Second, the 'jumping out' phenomenon could itself have caused the increased reported magnitude of the slalom illusion in the occluded conditions of Experiments 1 and 2 in Chapter 3. The mere perceptual surprise associated with the early re-appearance of the dot could have led to a less accurate amplitude response. That is, participants might have expected the dot to travel behind the occluder for a longer time because they expected the trajectory to be sinusoidal and therefore longer than it veridically was. This will be called the *discontinuity* hypothesis. Prolonging the ISI should then weaken the occluded slalom illusion, since the mismatch between the real and the expected re-appearance time is decreased, and shortening the ISI should strengthen it.

Both of these hypothetical views are predictive: a certain re-appearance time was expected, and it mismatched the actual re-appearance time. Analogous to the literature discussed above, however, a postdictive view on trajectory perception in the occluded slalom illusion could also be taken. Under the *postdictive* hypothesis, the time of re-appearance itself will be used as a source of information to interpret the trajectory of the dot as it would have occurred before its re-appearance from occlusion. That is, longer ISIs will lead to longer and therefore more curved sinusoidal trajectories, with a higher amplitude. Shorter ISIs, on the other hand, will lead to an interpretation of a shorter and less curved occluded trajectory, with a smaller amplitude.

In this experiment, a comparison of the classic slalom illusion to the occluded slalom illusion will again be made. In addition, the ISI of the dot stimulus during occlusion (the duration of the occlusion) will be manipulated, so that it is either shorter or longer than would have resulted from a constant horizontal dot speed. The results will allow us to distinguish between the three hypotheses proposed above: the by-product hypothesis would predict no effect of the ISI manipulation, the discontinuity hypothesis would predict the magnitude of the illusion to increase with lower ISIs, and the postdictive hypothesis would predict the magnitude of the illusion to increase with higher ISIs.

4.2. Methods

4.2.1. Participants

A sample of 17 participants was recruited through the Sheffield Hallam University's Psychology credit scheme as well as through opportunity sampling from the general student population. All participants were undergraduate or postgraduate students and were naive as to the phenomenon investigated. The inclusion criteria for participants were having normal or corrected-to-normal vision and being at least 18 years old.

4.2.2. Design

A repeated-measures design was employed, with one independent variable, condition. The independent variable had four levels: *original slalom* (black tilted lines), *original ISI* (occluding triangles with constant speed of the dot), *long ISI* (occluding triangles with increased ISIs), and *short ISI* (occluding triangles with decreased ISIs). The dependent variable is the amplitude of the illusion, operationalised as the height of the response line, measured in pixels.

4.2.3. Apparatus and stimuli

The experiment was programmed in Psychtoolbox-3 for MATLAB (Brainard, 1997; Pelli, 1997; Kleiner et al., 2007) and presented on a NEC MultiSync FP2141sb 22" CRT monitor. The viewable area of the monitor was 406 x 304.6 mm. The experiment was run with a spatial resolution of 1600 x 1200 pixels and a temporal resolution of 85 Hz. In all four conditions the moving dot is black, has a diameter of 2 mm, and the angle of intersection for all the tilted lines is 40°. The stimuli for the three occluded conditions are based on those used in the second experiment from study 2, consisting of 7 black isosceles triangles, with the base of 4.6 cm and the two equal edges (the tilted lines) of 3 cm. The triangles are placed at 1 cm distance from each other. The black triangles hide the trajectory of the dot when it intersects their surface, but the dot has a different speed behind the occluder, depending on the experimental condition, relating to different ISIs (see Figure 4.3). In line with the experiments conducted in previous chapters, the speed of the moving dot in the visible parts of the trajectory was 5 cm/s. In the experimental conditions, the speed of the occluded parts of the trajectory was maintained, increased by 50%, or decreased by 50%, depending on the condition. This led to a decreased or an increased ISI, respectively. The following conditions were created: (1) in the *original ISI* condition, the dot travels all the time at a speed of 5 cm/s (ISI of 470 ms), (2) in the *long ISI* condition the dot moves at a speed of 5 cm/s whilst visible and 2.5 cm/s whilst behind the occluders (ISI of 235 ms), and (3) in the *short ISI* condition, the dot moves at a speed of 5 cm/s whilst visible and at a speed of 7.5 cm/s whilst behind the occluders (ISI of 705 ms). Similar to the second experiment from the second study, the original slalom condition consists of a series of 7 modules of two tilted lines; the distance between the modules is 1 cm and the tilted lines are 1 mm thick and 2.5 cm long. The speed of the moving dot in the original slalom condition is constantly 5 cm/s. The centre of the experimental display is centred with the centre of the screen in all conditions.
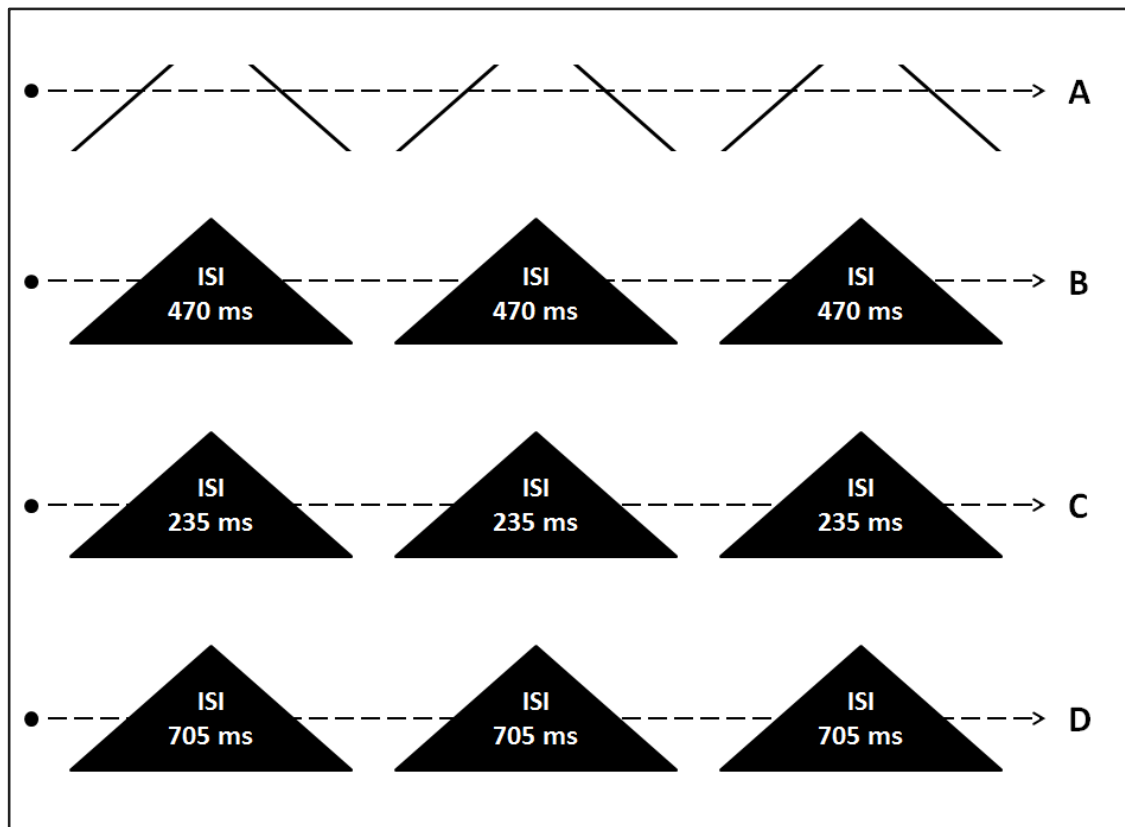
Figure 4.3. Illustration of the four experimental conditions: *original slalom* (A), *original ISI* (B), short ISI (C), and long ISI (D). In all conditions, the dot is moving at the same speed (5 cm/s) on the visible parts of the trajectory.

4.2.4. Procedure

The procedure was similar to that described in the previous laboratory experiments: participants were provided with information sheets (Appendix 2) and consent forms (Appendix 3) and had to give their informed consent prior to commencing the experiment. All participants were informed about their rights as per the university ethics guideline and the Declaration of Helsinki. Before starting the experimental task, participants were assisted by the experimenter in a trial run consisting of ten repetitions of the experimental trials randomised in terms of condition. This made the participants familiar with the task, which required, as in the previous experiments, to follow the

moving dot back and forth continuously across the background. A chin rest was used, placed at 60 cm from the monitor. Participants were asked to report whether, and if so - how much, the trajectory of the moving dot deviated from a straight one (the slalom effect). In order to answer, participants had to alter the height of a vertical line placed at the centre-bottom of the display. The response line had a starting height randomly assigned from 1 to 20 pixels and, in order to be adjusted, the participants had to press the up arrow key (to increase the size) and the down arrow key (to decrease size). The line was present concomitantly with the stimuli and participants could take as long as they wished before pressing the space bar, which confirmed that they were satisfied that the height of the response line corresponded to the perceived vertical deviation. Once the answer was given, the following trial commenced immediately. There were ten repetitions per condition, meaning that there were 40 trials in total. The trials were randomised in terms of order. Participants completed the experimental task at their own pace, and the duration was about 30 minutes on average, without any breaks. Upon completion, participants were fully debriefed as to the phenomenon investigated and were encouraged to make any comments relating to their experience or to ask any further questions.

4.3. Results

From the length of the response line for each trial, the mean amplitude response was computed per combination of participant and background condition, in preparation for repeated-measures statistical tests.

Boxplots (Appendix 18) indicate one possible outlier in the original slalom and short ISI conditions, but the computed Z-scores show that no outlier existed when using 3.29 as the cut-off point. The histograms (Appendix 19) and the skewness statistic (Appendix

20) show that the data are normally distributed in all three occluded conditions, but skewed in the original slalom condition. Because of the different patterns of distribution across the conditions, the data was not transformed. Relying on the general robustness of the ANOVA to violations of the assumption of normality (Schmider et al., 2010), the data was analysed using parametric tests.

The means and standard deviations are presented in Table 4.1. The largest amplitude was reported in the original ISI condition, whereas the lowest amplitude was reported in the short ISI condition.

Table 4.1
Mean Amplitudes and Standard Deviations for the Four Background Conditions (Measured in Pixels)

	Means	SDs
Original slalom	4.33	1.73
Original ISI	7.56	2.51
Long ISI	6.84	2.31
Short ISI	3.72	1.20

The effect of the experimental manipulation on the perception of the trajectory was analysed using repeated-measures ANOVA. The independent variable was a within-participants factor with four levels (*original slalom* vs *original ISI* vs *long ISI* vs *short ISI*), whereas the dependent variable was the reported amplitude of the trajectory, measured in pixels.

The null hypothesis of sphericity was rejected (W = .43, p = .028), so a Greenhouse-Geisser correction was applied to the repeated-measures ANOVA. The results show that the background had a significant effect on the perception of the dot trajectory [F (2.04, 32.65) = 44.80, p <.001, η_p^2 = .737]. G*Power (Faul et al., 2009) was used to determine the statistical power of the repeated measures ANOVA. Given the η_p^2 = .737 for the effect size, an alpha-level .05 and a total of 17 participants, the statistical power was estimated at >.999.
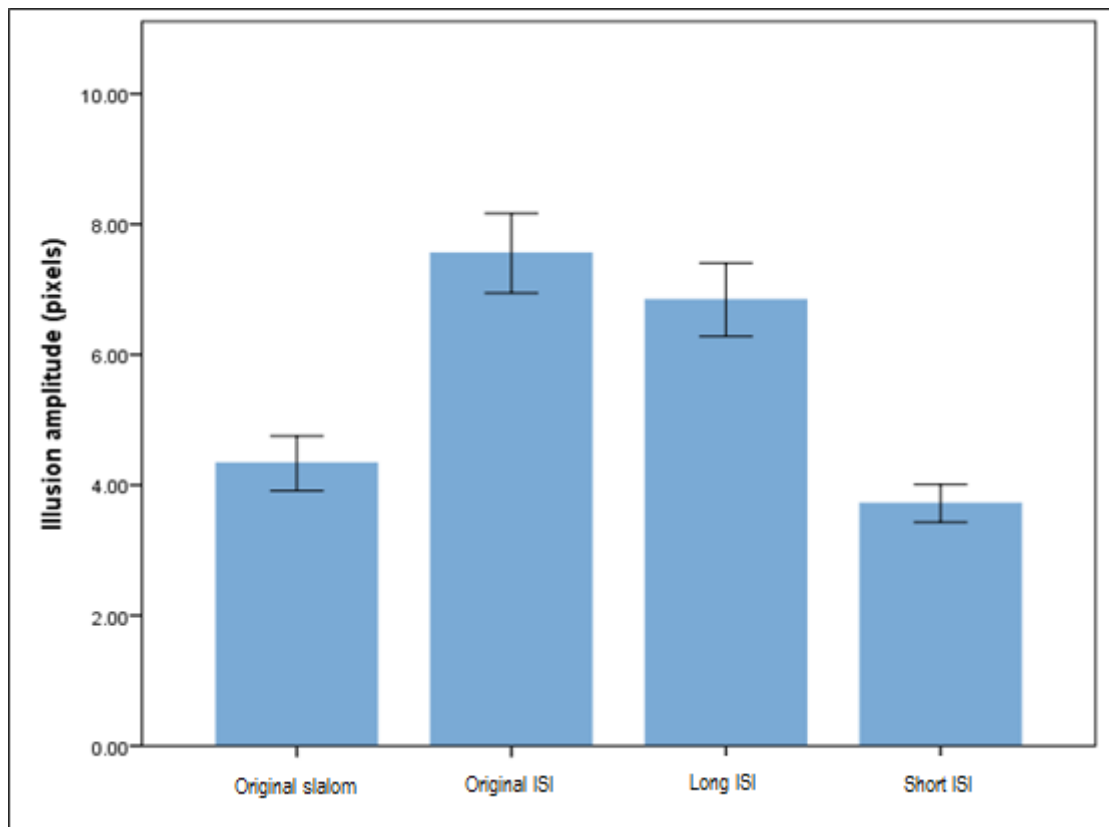
Figure 4.4. Mean amplitudes and standard errors for the four experimental conditions.

In order to investigate the differences between the four conditions, Bonferroni-corrected post-hoc pairwise comparisons were performed. The illusion magnitude was significantly larger in the original ISI condition compared with the original slalom condition (mdif = 3.22, p <.001) and short ISI condition (mdif = 3.84, p <.001). Also, the illusion magnitude was significantly larger in the long ISI condition compared with the original slalom condition (mdif = 2.51, p <.001) and short ISI condition (mdif = 3.12, p <.001). There was no difference in the illusion magnitude between the original ISI and the long ISI conditions (mdif = .72, p = .336) or between the original slalom and the short ISI conditions (mdif = .61, p = .091).

4.4. Discussion

In line with the main finding from the previous chapter, it was evinced that partially occluding the dot trajectory increases the slalom illusion. The effect of the ISI manipulations however was mixed: the long-ISI condition did not affect the occluded slalom illusion, whereas the short-ISI condition reduced it to the level of the classical, non-occluded slalom illusion. This clearly contradicts both predictions of the discontinuity hypothesis, according to which the short-ISI condition should increase the occluded slalom illusion, and the long-ISI condition should decrease it. The by-product hypothesis was refuted in the short-ISI condition, where the slalom effect was strongly decreased, but not in the long-ISI condition. The postdictive hypothesis was similarly partially refuted, since it had predicted the long-ISI condition to increase the slalom effect.

These results therefore require a more nuanced interpretation. The reduction of the perceived trajectory magnitude under short-ISI conditions is a strong effect, which appears to point at a postdictive interpretation of a smaller trajectory modulation as a function of the observed re-appearance time. This would result in a more consistent interpretation of the global trajectory. Indeed, it has previously been found that human observers prefer interpretations of smooth trajectories at a continuous speed over trajectories that are strongly variable in their speed and direction (Scherzer & Ekroll, 2009). At the same time, this explanation cannot account for all the empirical findings. First, long-ISI conditions did not increase the occluded slalom effect, as would also have been expected from the postdictive hypothesis. Second, the original finding inspiring this study was anecdotal evidence of a 'jumping out' effect. If the visual system successfully postdictively interprets the occluded trajectory amplitude to match

the re-appearance time of the dot, then this effect should not have occurred to begin with.

It therefore appears that multiple variables go into the neural equation for trajectory perception and that while each of these variables imposes a distribution of likelihoods for all of the trajectory amplitudes that could reasonably be perceived, none of the variables by itself determines the outcome. One such variable is the angle of intersection of the trajectory with the tilted line inducers which, as shown by Cesàro and Agostini (1998), strongly influences the slalom illusion. However, the angle of intersection also limits the amplitude the trajectory could *maximally* have, regardless of the duration of the ISI. Another relevant variable into the equation is the perceived motion direction during the visible part of the trajectory, which will bias the perception of the trajectory towards a more horizontal and straight perception (see Chapter 3). And, as mentioned, a general bias towards smoother trajectories could play a role (Scherzer & Ekroll, 2009). In the compromise of what is likely according to all of these input signals and biases of the visual system, it is then indeed not guaranteed that all constraints can be fully satisfied simultaneously. That is, even if postdictive effects bias the perceived amplitude in a certain direction to achieve consistency in the global interpretation, residual discontinuities, such as the 'jumping out' effect, could still occur. This view could formally be captured in a Bayesian framework, where the probabilities of all prior expectations and the strengths of all current observations combine into the perceived interpretation of the stimulus, within a given spatio-temporal integration window. Such frameworks have been applied to great effect in many areas of visual perception, including perception of ambiguous motion direction (Weiss et al., 2002).

These findings are in alignment with the literature on apparent motion. In particular, Korte's third law and its generalization to apparent motion trajectories (Kim et al., 2012)

appear to hold true in the current experiment as well, as far as the original-ISI and the short-ISI conditions are concerned. That is, motion along a shorter path requires a shorter ISI. But whereas studies on apparent motion, due to the nature of the paradigm, investigated the ISIs necessary for *qualitatively*different perception to be enabled, the current study has provided evidence of similar effects on the *quantitative* magnitude of a trajectory shape modulation. Indeed, a shared neuronal basis between apparent motion and continuous trajectory perception has previously been suggested (Larsen, Madsen, Lund, & Bundesen, 2006; Muckli, Kohler, Kriegeskorte, & Singer, 2005).

4.5. Summary

It was found that shortening the ISI in the occluded slalom illusion can decrease the slalom effect to the level of the non-occluded slalom illusion. According to the hypothesis proposed, the perceived amplitude of the trajectory can be affected in a postdictive manner by the observed re-appearance time of the dot after occlusion. However, other sources of information on the trajectory, such as the angle of intersection, impose limits on the degree to which ISI can affect the occluded slalom illusion. The final, postdictive, interpretation of the trajectory is likely to be a balanced compromise between all of these constraints, which may in future work be captured in a Bayesian framework.

5. Chapter 5 - Inverted slalom illusion

5.1. Introduction

The slalom illusion has been proposed to be rooted in local biases of motion direction, arising at the points of intersection between the horizontal dot trajectory and the tilted line inducers (Cesàro & Agostini, 1998). In particular, the angle of intersection between the trajectory and the tilted lines plays a crucial role, as discussed in detail in section 7.3 of the General Introduction. In the experiments of the current thesis the angle of intersection has not been manipulated systematically, but it could nevertheless be repeatedly shown in the experimental results of Chapters 2 to 4 that tilted lines elicit a greater perceived trajectory amplitude than vertical lines. Cesàro and Agostini (1998) did systematically manipulated the angle of intersection in their Experiment 1, and found a near-linear decrease in the illusion magnitude in the range between 30 and 55 degrees of angle. In addition, the authors demonstrated in their Experiment 2 a monotonic dependence on the speed of the dot motion, an effect that did not interact with the angle of intersection effect. Central to the angle of intersection hypothesis is the assumption that the visual system is strongly biased towards perceiving more perpendicular angles, necessitating in the interpretation of the dot trajectory a greater deviation from the veridical horizontal path as the tilt angle of the lines becomes more horizontal.

The bias towards perpendicular angles has a long empirical and theoretical history within the vision sciences. It was first noted in the context of the *aperture problem*, which was previously discussed in section 5.2 of the General Introduction. When a moving line is seen through a circular aperture, such that its end-points are concealed, the veridical motion direction of the line cannot be determined (Stumpf, 1911; Wallach,

1935, Wuerger et al., 1996). Indeed, any direction of motion is a valid interpretation of the stimulus, except the direction parallel to the line, which would not produce any perceptible motion. Each potential motion direction of the line, however, is associated with a different speed (see Figure 1.7 in Chapter 1). When faced with such a line stimulus of which the end-points are not visible, observers consistently report to perceive a direction of motion that is *perpendicular* to the orientation of the line. This perception also coincides with the singular solution which has the slowest associated speed of motion for the line object. The aperture problem received renewed interest when it was shown to be relevant to the early visual cortex, where the receptive fields of individual direction-sensitive motion neurons are too small to perceive the movement of a full moving object, and instead encode only the orientation and motion direction of a limited segment of an oriented edge (Adelson & Movshon, 1982). Similar to the classical aperture problem, the activity of these neurons cannot be used to determine the true motion direction of the oriented edge. To determine the true motion direction of an object, either an integration of motion signals over a larger number of cells must take place, or the perception of motion must be driven by those cells that do perceive and code the end-points of edges, and therefore do not suffer from the aperture problem (Pack et al., 2003).

The perpendicularity bias in angle perception also occurs, however, in static displays with line intersections. Here, the aperture problem does not apply, since there is no motion. Several classical geometric illusions are proposed to be based on this mechanism. In the Poggendorff illusion (Figure 5.1A), the perceived misalignment between both parts of the diagonal line are then rooted in a perception of these lines as being slightly more vertical than they veridically are. In support of this hypothesis, Morgan (1999) shows that the Poggendorff illusion disappears when the point of intersection is locally made perpendicular, while maintaining the same global

111

configuration. In the Zollner illusion (Figure 5.1 B), the tilt of each parallel line is biased towards an orientation perpendicular to its intersection with a series of smaller line segments. The alternation of the orientation of these segments between the lines then causes them to not appear parallel. In the Herring (Figure 5.1C) and Wundt (Figure 5.1D) illusions, the geometry of a line is itself bent to better conform to a proposed expectation of perpendicular angles of intersection. Finally, in the Tilt Illusion (Figure 5.2) (Gibson & Radner, 1937; Clifford, 2014), no direct intersection is present, but the orientation of the middle grating is still biased towards perpendicularity with the tilted surrounding grating.
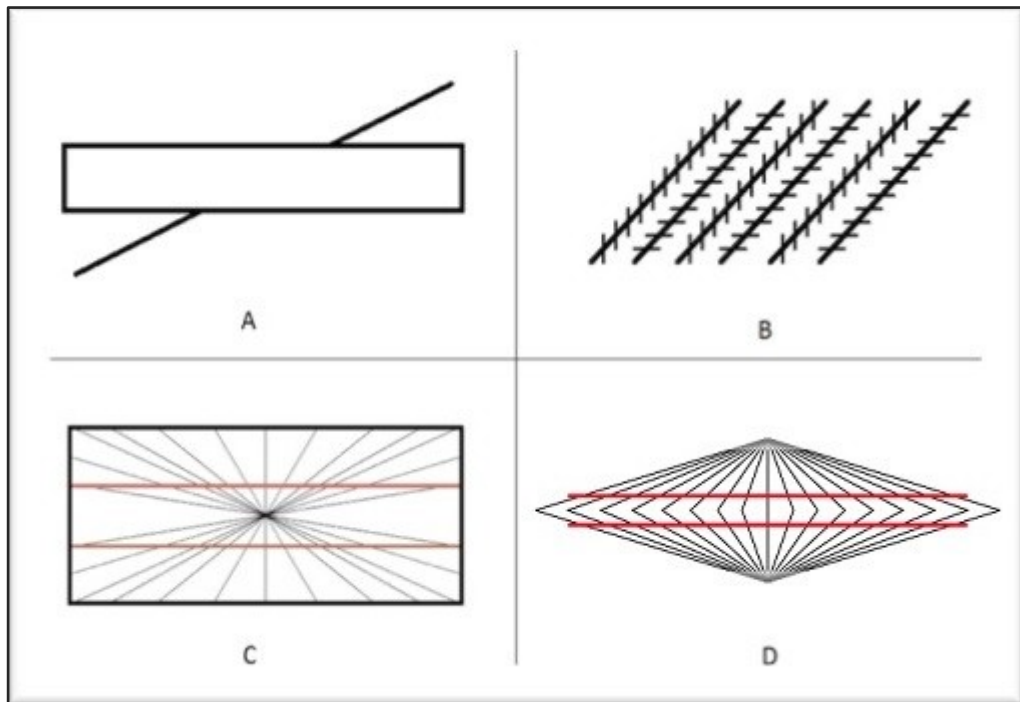

Figure 5.1. Illustration of geometric illusions dependent on the angle of intersection: (A) Poggendorff illusion, (B) Zollner illusion, (C) Herring illusion, and (D) Wundt illusion.
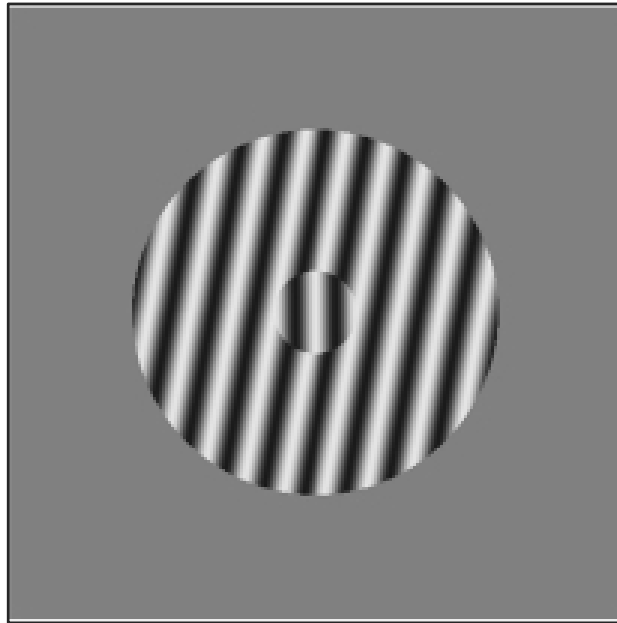
Figure 5.2. The Tilt illusion, whereby the orientation of the middle grating is perceptually biased towards perpendicularity in relation to the surrounding grating.

Kinetic versions of these static geometric illusions, where the straight line is replaced by a straight dot trajectory, exist in the case of Poggendorff (Fineman & Melingonis, 1977; Wenderoth & Johnson, 1983) and the Zollner (Khuu, 2012; Khuu & Kim, 2013) illusions. Note that in trajectory motion displays, the aperture problem would also not be relevant, because a dot stimulus is necessarily end-stopped and does not suffer from motion direction ambiguity in the same manner as a line does.

Blakemore et al. (1970) systematically tested the perception of the angle between two intersecting lines in isolation, and found that indeed observers tend to underestimate obtuse angles and overestimate acute angles. This is equivalent to a bias towards perpendicularity. The authors propose that this bias follows from lateral inhibition between orientation columns in V1 (see Section 2.1 of the General introduction). When activated, orientation columns suppress neighbouring columns that represent similar orientations, so that the orientation column with the greatest activation stands out even

more from other columns that are stimulated less by the orientation of the stimulus line. When two oriented lines are presented in close vicinity of each other, they will then suppress each other's responses, and orientation columns in between the orientations of the lines will be doubly suppressed. If the final line orientation perception of the observer is achieved by aggregating responses across all orientation column responses, the intersecting lines will then appear to be repelled from each other's orientation. Again, this is equivalent to a bias towards perpendicularity. The root cause of the perpendicularity bias would then lie in the desire of orientation-sensitive neurons to achieve a narrow, more specific response to the orientation of the edge in their receptive field, through suppression of weaker neighbouring orientation responses. Other explanations of the bias in angle perception, however, take a high-level probabilistic view on this problem. The visual system is then proposed to attempt an inference on the most likely veridical angle in the distal stimulus, based on its proximal projection on the retina (Nundy et al., 2000; Changizi, 2001; Changizi & Widders, 2002; Howe & Purves, 2005). The general argument of these studies is that veridically perpendicular angles will in real-world three-dimensional perception often be projected on the retina as being either acute or obtuse. Assuming that perpendicular or near-perpendicular angles are more likely to occur in the physical world (for instance, the angle between trees and the horizon), the visual system then has grounds to interpret projected angles as being more perpendicular than they are. This can be understood as hierarchical Bayesian inference, a framework introduced in Chapter 3 of the general introduction.

5.2. Experiment 1

If the angle of intersection is the main determinant of the slalom illusion, it should be possible to invert the direction of the illusion, by letting a sinusoidal dot trajectory move

across a set of vertical line stimuli. The bias towards perpendicularity would then predictably result in a locally more horizontal angle of intersection (figure 5.3). Therefore, the trajectory amplitude can be expected to be underestimated when compared to a control condition with tilted lines, which do form an unbiased perpendicular angle with the sinusoidal dot trajectory.
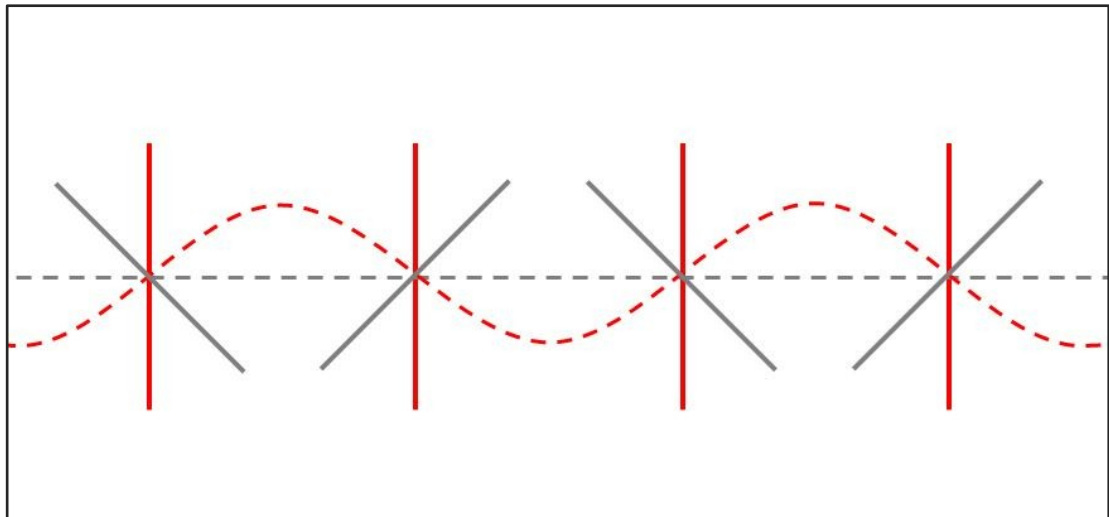

Figure 5.3. The original slalom display (in grey) can be manipulated such that the trajectory becomes sinusoidal and the inducing lines become vertical, whilst the angle of intersection is maintained, leading to an inverted slalom display (in red).

In Chapter 3, it was concluded that partial occlusion of the dot trajectory amplified the illusory effect elicited, because less veridical motion information was available to counteract the perpendicularity bias. A similar condition will be introduced in the current study, for which it is then hypothesised that the illusory effect will also increase. That is, the sinusoidal amplitude will be *under*estimated to a greater degree. Finally, a control condition without intersecting lines will be included to test the baseline accuracy of participants for reporting the amplitude of sinusoidal paths.

5.2.1. Methods

5.2.1.1. Participants

The experiment was conducted with 40 participants recruited from the general student population of Sheffield Hallam University. All participants were undergraduate or postgraduate students and were naive as to the phenomenon investigated. The inclusion criteria were having normal or corrected-to-normal vision and being at least 18 years old.

5.2.1.2. Design

A repeated-measures design was employed, with one independent variable, *background*. The independent variable had four levels: *inverted slalom* (black vertical lines), *inverted occluded* (black squares), *inverted control* (tilted lines) and *blank* (white background). The dependent variable is the amplitude of the illusion, operationalised as the height of the response line, measured in pixels.

5.2.1.3. Apparatus and stimuli

The experiment was programmed in Psychtoolbox-3 for MATLAB (Brainard, 1997; Pelli, 1997; Kleiner et al., 2007) and presented on a NEC MultiSync FP2141sb 22" CRT monitor. The viewable area of the monitor was 406 x 304.6 mm. The experiment was run with a spatial resolution of 1600 x 1200 pixels and a temporal resolution of 85 Hz. In all four conditions the moving dot is black, has a diameter of 2 mm and traverses the trajectory one way in 5.9 seconds (this corresponds to a horizontal speed of 6.5 cm/s).The trajectory of the dot is sinusoidal, with an amplitude of 10 pixels, its phase equals 0 (meaning that it starts in the middle of the vertical range of the trajectory), and a frequency of 7 (corresponding to 7 modules).

116

The background for the moving dot depends on the experimental condition, as follows: in the *inverted slalom* condition, there are 7 modules each of two vertical lines (Figure 5.4.A), in the *inverted occluded* condition, there are 7 black squares (Figure 5.4.B) in the *inverted control* condition there are 7 modules of lines tilted at 45° (Figure 5.4.C), and in the *blank* condition the dot moves across a white, blank, background (Figure 5.4.D).
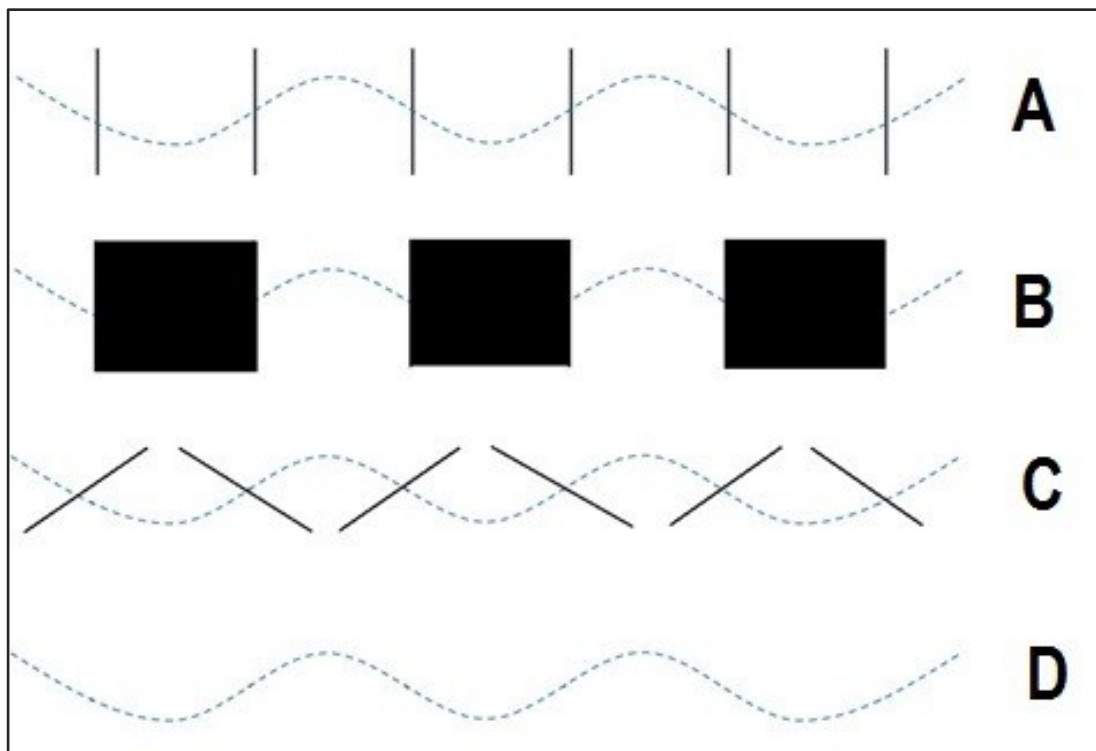

*Figure 5.4.*The four types of background corresponding to the four experimental conditions: *inverted slalom* (A), *inverted occluded* (B), *inverted control* (C), and *blank* (D).

All lines, including the vertical edges of the squares, have been placed at the points where $\sin(x) = 0$, leading to the following angles of intersection: in the *inverted slalom* and *inverted occluded* conditions, the angle of intersection is 45°, whereas in the

117

inverted control, the angle of intersection is 90°. The centre of the experimental display is centred with the centre of the screen in all conditions.

5.2.1.4. Procedure

The procedure was similar to that described in the previous laboratory experiments: participants were provided with an information sheet (Appendix 2) and a consent form (Appendix 3), and after giving their informed consent, they were given the instructions for completing the experimental task, as well as a practice run consisting of 5 trials in order to get familiar with the task. The task, as in the previous experiments, consisted of following the moving dot, which moved back and forth continuously across the background. A chin rest was used, placed at 60 cm from the monitor. Participants were asked to report whether, and if so - how much, the trajectory of the moving dot deviated from a straight horizontal one. In order to answer, participants had to alter the height of a vertical line placed at the centre-bottom of the display. The response line had a starting height randomly assigned from 1 to 20 pixels and, in order to be adjusted, the participants had to press the up arrow key (to increase the size) and the down arrow key (to decrease size). The line was present concomitantly with the stimuli and participants could take as long as they wished before pressing the space bar, which confirmed that they are satisfied that the height of the response line corresponded to the perceived vertical deviation. Once the answer was given, the following trial commenced immediately. There were ten repetitions per condition, meaning that there were 40 trials in total. The trials were randomised in terms of order. Participants completed the experimental task at their own pace, and the duration was 30 minutes on average. Upon completion, participants were fully debriefed as to the phenomenon investigated and were encouraged to make any comments relating to their experience or to ask any further questions.

5.2.2. Results

From the length of the response line for each trial, the mean amplitude response was computed per combination of participant and background condition, in preparation for repeated-measures statistical tests.

Boxplots (Appendix 21) revealed no potential outliers and the computed Z-scores confirmed this. Histograms (Appendix 22) suggest relatively normal distributions across the four conditions, and this was confirmed by the skewness statistic (Appendix 23). The means and standard deviation are presented in Table 5.1. Contrary to what was predicted, the largest amplitude was reported in the inverted occluded condition, whereas the lowest perceived amplitude was reported in the blank condition.

Table 5.1.
Mean Amplitudes and Standard Deviations for the Four Background Conditions
(Measured in Pixels)

	Means	SDs
Inverted slalom	11.90	4.28
Inverted occluded	13.12	4.59
Inverted control	11.65	4.66
Blank	7.73	3.61

The effect of background on the perception of the trajectory was analysed using a repeated measures ANOVA. The independent variable, background, had four levels (*inverted slalom* vs *inverted occluded* vs *inverted control* vs *blank*), whereas the dependent variable was the reported amplitude of the perceived trajectory.

The null hypothesis of sphericity was rejected (W = .63, p = .003), so a Greenhouse-Geisser correction was applied. The results show that the background has a significant effect on the perception of the dot trajectory [F (2.44, 95.20) = 5.99, p <.001, η_p^2 = .567]. G*Power (Faul et al., 2009) was used to determine the statistical power of the

119

repeated measures ANOVA. Given the $\eta_p^2 = .567$ for the effect size, an alpha-level .05 and a total of 17 participants, the statistical power was estimated at >.999.

In order to investigate the differences between the four conditions, Bonferroni-corrected post-hoc pairwise comparisons were performed. In the inverted occluded condition, the amplitude was significantly higher than in all three other conditions: inverted slalom (mdif = 1.22, p = .002), inverted control (mdif = 1.47, p = .043), and blank (mdif = 5.39, p<.001). The amplitude reported for the blank condition was significantly lower than for inverted slalom (mdif = -4.16, p<.001) and inverted control (mdif = -3.92, p<.001). No significant difference was found between the inverted slalom condition and the inverted control condition (mdif = .25, p>.999).
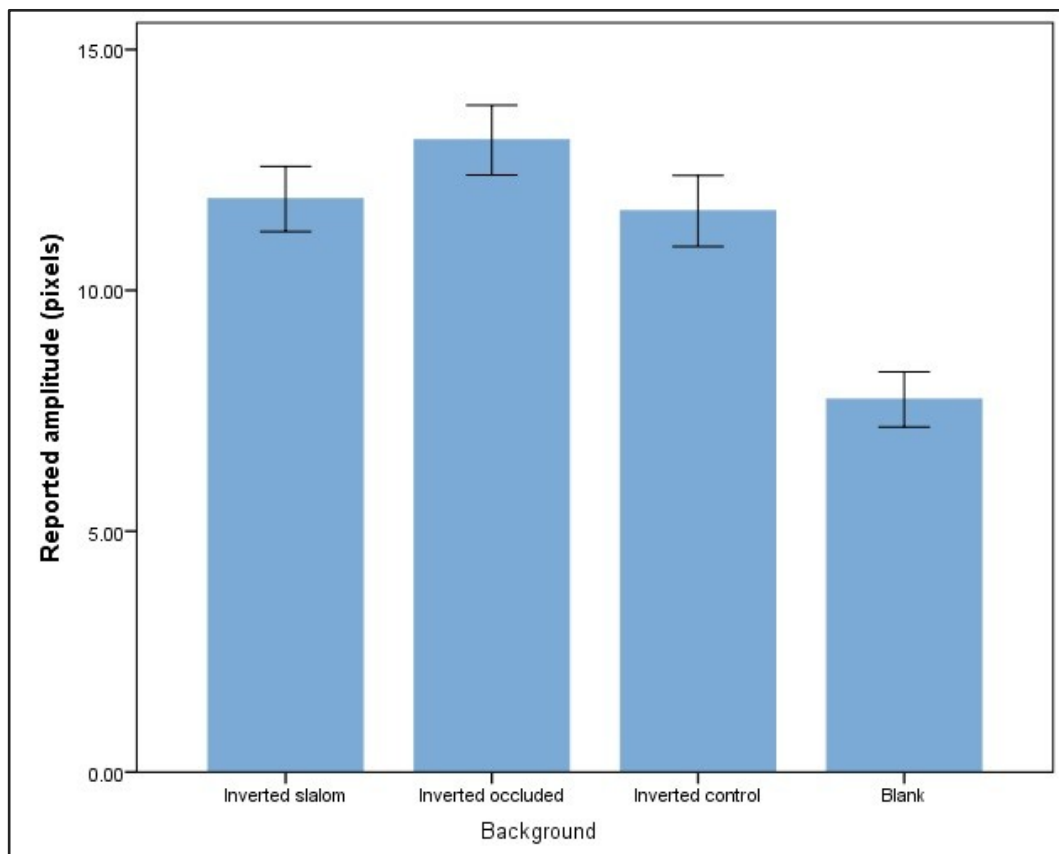

Figure 5.5. The mean amplitudes and standard errors for the four background conditions.

In order to investigate whether the perceived amplitudes in each of the conditions were overestimated or underestimated relative to the real amplitude of the trajectory of 10 pixels, four one-sample two-tailed t-tests were performed. Bonferroni corrections were applied, meaning that the alpha level of the hypothesis test was reduced to .0125 (.05/4). Results showed that in the inverted slalom [$t(39) = 2.80$, $p = .008$] and the inverted occluded [$t(39) = 4.30$, $p<.001$] conditions, the amplitude of the trajectory was significantly overestimated by participants, whereas in the blank condition it was significantly underestimated [$t(39) = 3.97$, $p<.001$]. In the inverted control condition, no significant difference with regard to the real amplitude of the trajectory was observed [$t(39) = 2.24$, $p = .031$].

5.2.3. Discussion

The results show that the inverted slalom display with vertical line inducers did not affect the perceived amplitude of the trajectory, when compared to a control condition with tilted line inducers. The hypothesis that the causal mechanism of the slalom illusion relies solely on a bias towards perpendicularity in the angle of intersection between the dot trajectory and the line inducers can therefore not be confirmed, as the slalom illusion does not generalise to the reverse situation, where a significant reduction in perceived amplitude would have been expected. At the same time, however, Cesàro and Agostini (1998) provided strong evidence supporting at least the dependence of the strength of the slalom illusion on the angle of intersection, and the bias towards perpendicular in angles is known to exist in the visual system (Blakemore et al., 1970). Moreover, it is strongly implied in explanatory theories of several related static and kinetic illusions.

The first possibility to consider is that while the slalom illusion relates to the angle of intersection, it is not caused by it. Indeed, the orientation of the inducing lines, and therefore the angle of intersection, also correlates with either the vertical extent of the lines, or the length of the lines. That is, if the vertical extent of the line is controlled to be constant, the length of the line must necessarily depend on the tilt of the line. In the study of Cesàro and Agostini (1998), the vertical extent was indeed kept constant, and the horizontal extent and line length therefore co-varied with the angle. Sharper angles, which induced a stronger illusion, were necessarily created using longer lines. While this could reasonably be put forward as a confounding factor, there are arguments against it. In Chapter 2 of the current thesis, results showed that inducing subjective contours using Kanizsa markers around their end-points did not elicit a clear slalom illusion. The spatial layout of the display and the length of the lines remained constant, but the local intersections with the dot trajectory were removed. This suggests a role for the intersections with the lines, rather than only the dimensions of the lines. Moreover, the horizontal extent and the length of the lines were also manipulated in the current experiment (inverted slalom vs inverted control conditions), but this did not lead to a changed perception of the amplitude of the sinusoidal trajectory. While a potential confound of line length cannot be strictly ruled out, it appears unlikely that this would be the causal mechanism behind an effect as strong as the slalom illusion.

The second possibility is that the angle of intersection does drive the slalom illusion, but only when the dot trajectory follows a straight path, rather than a veridically sinusoidal path. The explanatory mechanism behind this could be proposed to be *adaptation*. The visual system has evolved to represent transients in stimuli, rather than constant stimuli (Emerson & Gerstein, 1977). Constant stimulation leads to perceptual fading (Tulunay-Keesey, 1982), negative afterimages (Kelly & Martinez-Uriegas, 1993), and, in the case of exposure to a field with constant motion direction, motion after-effects in the

opposite direction. The latter phenomenon is also known as the waterfall illusion, as it occurs when looking away after prolonged fixation on a waterfall. However, these phenomena are often attributed to neuronal fatigue and gradual desensitisation (Pirenne, Compbell, Robson, & Mackay, 1958; Anstis, Verstraten, & Mather, 1998). Even though adaptation after-effects to motion have been reported after short exposure durations (Glasser, Tsui, Pack, & Tadin, 2011), more commonly they require a continued stimulation of several seconds (Price & Prescott, 2012). In the context of the slalom illusion, it appears unlikely that neuronal fatigue would occur so quickly. However, a number of single-cell studies on direction-sensitive motion cells in macaque MT cortex have also demonstrated the existence of short-term adaptation, within tens of milliseconds (Priebe, Churchland, & Lisberger, 2002; Priebe & Lisberger, 2002; Perge, Borghuis, Bours, Lankheet, & van Wezel, 2005). Rather than suffering from neuronal fatigue, MT cells appear to exhibit an inherently biphasic response, whereby a strong initial response to their preferred direction is quickly followed by a lowered firing rate and a stronger response to non-preferred directions. To sustain a maximal firing pattern, transient motion direction signals are required. In the case of the slalom illusion, it can be hypothesised that the constant motion direction of the dot then quickly leads to decreased neuronal responses for that direction in the MT cortex. In its rapidly adapted state, with neurons looking to respond more strongly to non-horizontal directions, the visual system becomes especially sensitive to directional signals that are biased away from the horizontal directions, as they occur at the tilted line intersections in the original slalom illusion. In the inverted slalom illusion of the current study, however, the motion signal is not constant in direction, and therefore short-term adaptation would not occur. The motion direction signal could still be biased around the points of intersection, but relative to the full trajectory of the dot, its weight in the total MT neuronal activity is then strongly reduced. According to this hypothesis, the original slalom illusion is then

fundamentally caused by a combination of the visual system's preference for perpendicular angles, *and* its preference for transient motion directions over constant motion directions.

In addition to the main finding of interest, the results also showed that all displays containing lines elicit a consistent overestimation of the sinusoidal amplitude. In case of the occlusion condition, this effect was even significantly increased. Possibly, the vertical extent of the dot trajectory was biased towards the vertical extent of the other elements in the display, and this illusion was amplified by the partial absence of the veridical path information. This explanation is similar to the explanation previously put forward in Chapter 3, on why the occlusion conditions amplified the amplitude of the slalom illusion. Since the vertical extent of the stimulus was kept constant in all conditions, however, no further evidence for this hypothesis can be offered. Finally, in the Blank condition, the amplitude of the sinusoidal trajectory was systematically underestimated by the participants. This effect will be explored further in the next experiment.

5.3. Experiment 2

In Experiment 1 of this study, when the sinusoidal dot trajectory was shown in isolation, without any lines or occluding elements, the amplitude was underestimated by on average 25%. It is unclear whether this occurred because observers were not able to accurately perceive the sinusoidal dot trajectory at all, or whether such an underestimation bias exists systematically. Moreover, it is possible that the bias only occurs in the context of the experimental set-up of Experiment 1, where trials without visual reference were intermixed with trials where the amplitude of the sinusoidal path could be compared to the position of other static objects much more easily. In the

current experiment, it will be tested whether the underestimation of the amplitude of sinusoidal trajectories is a general phenomenon, by studying it in isolation and for different amplitudes.

5.3.1. Methods

5.3.1.1. Participants

A sample of 24 participants was recruited from the general student population of Sheffield Hallam University. All participants were undergraduate or postgraduate students and were naive as to the phenomenon investigated. The inclusion criteria for participants were having normal or corrected-to-normal vision and being at least 18 years old.

5.3.1.2. Design

A repeated-measures design was employed, with one independent variable, *real amplitude*. The independent variable has four levels: *5 pixels*, *10 pixels*, *15 pixels*, and *20 pixels*. The dependent variable is the perceived amplitude of the illusion, operationalised as the height of the response line, measured in pixels.

5.3.1.3. Apparatus and stimuli

The experiment was programmed in Psychtoolbox-3 for MATLAB (Brainard, 1997; Pelli, 1997; Kleiner et al., 2007) and presented on a NEC MultiSync FP2141sb 22" CRT monitor. The viewable area of the monitor was 406 x 304.6 mm. The experiment was run with a spatial resolution of 1600 x 1200 pixels and a temporal resolution of 85 Hz. In all four conditions the moving dot was black, had a diameter of 2 mm and traversed the trajectory one way in 5.9 seconds. Like in the first experiment of this study, the trajectory of the dot was sinusoidal, with its phase equalling 0 (meaning that it started in

the middle of the vertical range of the trajectory), and a frequency of 7. The background

for the moving dot was blank across all four conditions, but the amplitude of the dot,

depending on the condition was: 5 pixels, 10 pixels, 15 pixels, or 20 pixels. The centre

of the experimental display was centred with the centre of the screen in all conditions.

5.3.1.4. Procedure

The procedure was the same as the one described in the first experiment of this chapter.

5.3.2. Results

From the length of the response line for each trial, the mean amplitude response was

computed per combination of participant and background condition, in preparation for

repeated-measures statistical tests.

Boxplots (Appendix 24) indicate two possible outliers among the participants in the 5

pixels condition. However, the computed Z-scores confirm only one outliers ($z_1 = 3.91$).

After removing the outlier, the skewness statistic (Appendix 25) shows that the data are

normally distributed in three out of the four experimental conditions, with a skewed

distribution for the 5 pixels condition (see histograms in Appendix 26).

The means and standard deviations are presented in Table 5.2. As expected, the largest

perceived amplitude was reported in the 20 pixels condition, whereas the lowest

perceived amplitude was reported in the 5 pixels condition.

Table 5.2.
*Mean Response Amplitudes and Standard Deviations for the Four Amplitude
Conditions(Measured in Pixels)*

	Means	SDs
5 pixels	3.03	1.15
10 pixels	7.29	2.85
15 pixels	11.78	3.59
20 pixels	16.10	4.20

5.3.2.1. Differences between the four conditions

The effect of the real amplitude on the perception of the trajectory was analysed. The independent variable, real amplitude, is a within-participants factor with four levels.

The null hypothesis of sphericity was rejected (W = .13, $p<.001$), so a Greenhouse-Geisser correction was applied to the repeated-measures ANOVA. The results show that the real amplitude has a significant effect on the perception of the dot trajectory [F (1.41, 31.00) = 178.73, $p <.001$, $\eta_p^2 = .890$]. G*Power (Faul et al., 2009) was used to determine the statistical power of the repeated measures ANOVA. Given the $\eta_p^2 = .890$ for the effect size, an alpha-level .05 and a total of 22 retained participants, the statistical power was estimated to be larger than .999.

In order to investigate the differences between the four conditions, Bonferroni-corrected post-hoc pairwise comparisons were performed. As expected, there were significant differences between all the combinations of the four conditions, with each real amplitude level being correctly reported as significantly larger or smaller than the lower and higher levels respectively. Thus, the highest level of the real amplitude, 20 pixels, was perceived as significantly higher than the three other levels: 15 pixels (mdif = 4.32, $p<.001$), 10 pixels (mdif = 8.81, $p<.001$), and 5 pixels (mdif = 13.07, $p<.001$). Conversely, the lowest level of real amplitude, 5 pixels, was perceived as significantly lower than the three other levels: 10 pixels (mdif = -4.26, $p<.001$), 15 pixels (mdif = -8.75, $p<.001$), and 20 pixels (mdif = -13.07, $p<.001$). Finally, the middle real amplitude values of 10 and 15 pixels were perceived as different, with the 10 pixels level significantly lower than the 15 pixels level (mdif = -4.49, $p<.001$).
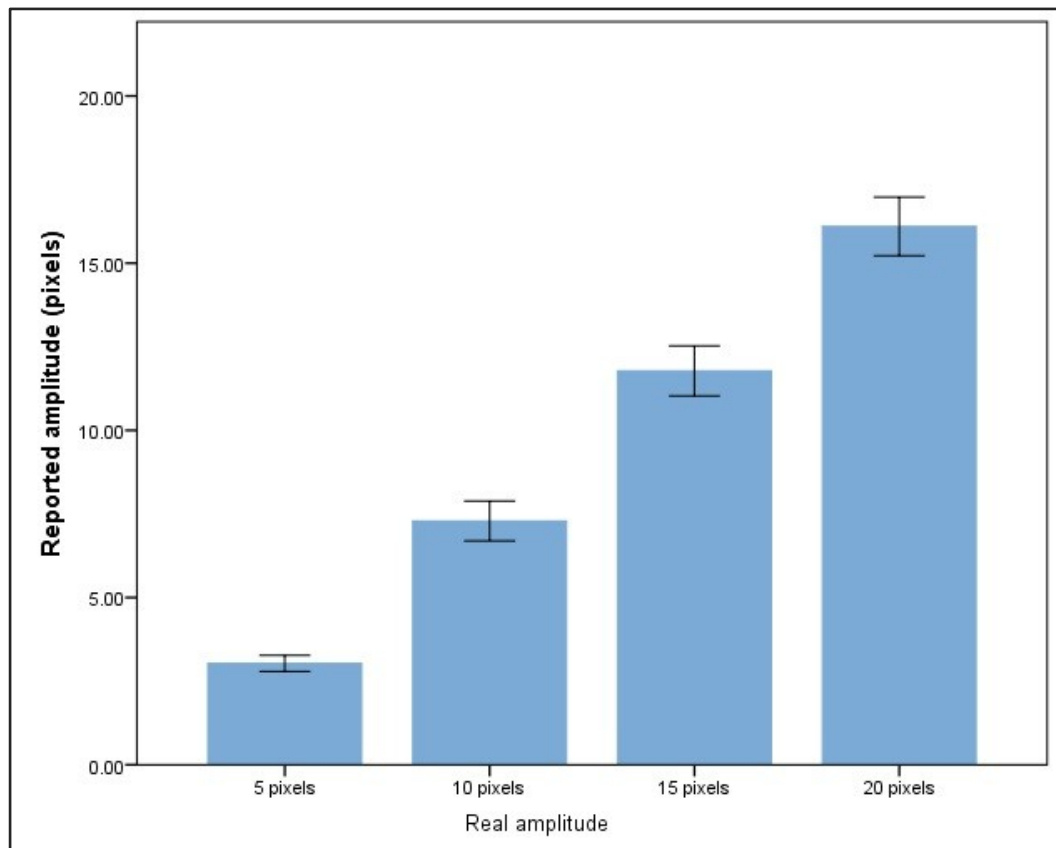
*Figure 5.6.*The perceived amplitude reported for the four levels of real amplitude with standard errors, both measured in pixels.

5.3.2.2. Differences between real and perceived amplitudes

Four one-sample t-tests were performed in order to investigate the differences between the real amplitude and the perceived amplitude of the trajectory of the dot. In each case, the perceived magnitude was significantly lower than the real amplitude, as follows:

In all four conditions, the perceived amplitude was significantly lower than the real amplitude (all ts > 4.30, all ps < .001).

5.3.2.3. Differences in underestimation between conditions

In order to quantify the proportional impact of the previously reported underestimations on each of the four experimental levels, four variables were computed as the ratio between the perceived and the real amplitudes. The means and standard deviations are

128

presented in Table 5.3 and show that the highest perceived/real amplitude ratio was in

the 20 pixels condition, whereas the lowest amplitude ratio was in the 5 pixels condition.

Table 5.3
Means and Standard Deviations for the Amplitude Ratios in Each of the Four Conditions

	Means	SDs
5 pixels	.61	.23
10 pixels	.73	.29
15 pixels	.79	.24
20 pixels	.80	.21

A repeated-measures ANOVA was performed to investigate the differences between the

resulting variables. The null hypothesis of sphericity was rejected (W = .15, $p<.001$), so

a Greenhouse-Geisser correction was applied. The results show that there is an effect of

the real amplitude on the degree of underestimation [F (1.62, 35.60) = 7.44, p = .004,

η_p^2 = .253]. G*Power (Faul et al., 2009) was used to determine the statistical power of

the repeated measures ANOVA. Given the η_p^2 = .253 for the effect size, an alpha-

level .05 and a total of 17 participants, the statistical power was estimated at .66.

Bonferroni corrected post-hoc pairwise comparisons reveal that in the 5 pixels condition,

the underestimation ratio is significantly larger than in the 15 pixels condition (mdif = -

.18, p = .038) and in the 20 pixels condition (mdif = -.20, p = .025). No other significant

differences were found between the remaining pairwise comparisons.

5.3.3. Discussion

The amplitudes of sinusoidal dot trajectories without visual reference objects along their

path were systematically underestimated. The findings from the current experiment

suggest, however, that observers retain the ability to discriminate between different

amplitudes, as is shown by the dependence of responses on the physical characteristics

of the trajectory. Although the absolute magnitude of the underestimation increased with increasing amplitude, as a ratio to the real amplitude it decreased. That is, the relative underestimation is largest for trajectories with small amplitudes.

Underestimation of motion paths has previous been observed using linear and circular trajectories (Sinico et al., 2009; Nakajima & Sakaguchi, 2016). The explanations offered by these authors are rooted in a vector summation of the motion speeds and directions within the motion integration window, whereby motion signals around the extremities of the motion path, where the motion direction reverses, cancel each other out. As a result, the motion path appears smaller than it physically is. Indeed, this could also be a plausible explanation for the current experiments. An additional role might be played by the instruction to the participants to follow the dot with their gaze. When observers engage in smooth pursuit eye movement to follow a moving stimulus, the extent of the eye movement when compared to the extent of the stimulus trajectory is comparable in the horizontal direction, but reduced in the vertical direction (Rottach et al., 1996). If the perception of the trajectory is biased by the eye movements following it, an underestimation would likely occur. Indeed, Sinico et al. (2009) report a reduced illusory shrinkage of the motion path under conditions of constant fixation, compared to conditions where participants were instructed to follow the trajectory with their gaze.

However, the same effect was not observed in those conditions of Experiment 1 where the dot trajectory intersected with other visual stimuli (lines or squares). Under such conditions, the amplitude of the sinusoidal trajectory was overestimated, rather than underestimated. It is hypothesised that this discrepancy is explained by the presence of clear visual reference objects, against which the vertical extent of the dot trajectory can be judged. The judgement of stimulus position in absence of landmark reference objects is known to be poor, leading to the conclusion that human observers typically do not

encode object position in absolute, but in relative coordinates (Deubel, 2004; Deubel, Koch, & Bridgeman, 2010). The absence of such landmarks would then make trajectory perception especially vulnerable to the biases described in the previous paragraph (vector summation of motion vectors, and reduced gain in vertical smooth pursuit eye movements).

With regard to the slalom illusion, it appears paramount to carefully control the vertical extent of all additional display elements close to the dot trajectory. If any differences in vertical extent would arise between conditions, this could presenta confound with the experimental manipulations performed.

5.4. Summary

The inverted slalom display, where the inducing lines are vertical but the dot trajectory is sinusoidal, did not lead to an illusory effect of reduced amplitude, as would be expected from a theoretical account based solely on the angle of intersection between the trajectory and the lines. It is proposed that short-term adaptation of biphasic neurons in area MT of the visual cortex causes the bias towards perpendicular angles to only be relevant in stimulus displays with a straight trajectory, as is the case in the original slalom display. In addition, the presentation of the sinusoidal trajectory in isolation leads to a systematic underreporting of its amplitude, underlining the importance of landmark reference objects in positional judgment tasks.

6. Chapter 6 - Retinal eccentricity

6.1. Introduction

The original study of Cesàro and Agostini (1998) does not report whether an explicit instruction was given to the participants as to the viewing method of the slalom display. Implicitly, however, it is indicated in the introduction to their experiments that participants should maintain their gaze on the moving dot: "*During preliminary observations, we noticed that there was an optimal range of velocities. Outside this range, it was difficult to follow the dot, either because it was too slow or because it was too fast.*" (Cesàro & Agostini, 1998; pp. 519). In the previous studies of the current thesis, a similar instruction to follow the dot was given. The results obtained were all congruent with the original report on the slalom illusion, and were interpreted in terms of the trajectory of the dot across the stimulus display and the motion signals which the moving dot would generate in the visual cortex.

6.1.1. Smooth pursuit eye movements

An alternate explanation could be proposed, however, whereby the instruction to follow the dot would in fact be the cause of the slalom effect. When following a constantly moving object with their gaze, it is known that human observers enter a dedicated mode of eye movement behaviour known as "smooth pursuit" (Keller & Heinen, 1991; Krauzlis & Stone, 1999), that is qualitatively different from the usual alternation of steady fixation periods and rapid saccadic jumps typically employed for scene exploration. The mechanisms underlying smooth pursuit are closely related to the mechanisms of motion perception itself, as they display similar biases (Beutter & Stone,

1998). Indeed, smooth pursuit eye movements cannot be initiated without a moving stimulus. As a consequence of smooth pursuit, however, the projection of the stimulus that is the object of the eye movements will be stabilised on the retina, defying explanations of motion and trajectory perception based only on retinotopic motion signals. To achieve a veridical subjective perception of the dot motion, the visual system then has to integrate its retinal signals with extra-retinal signals, most importantly those originating in the eye muscles and the cortical areas responsible for their motor control (Sperry, 1950; von Holst & Mittelstaedt, 1950; Gauthier et al., 1990; Souman & Freeman, 2008).

In all previous studies on the slalom illusion, a smooth pursuit viewing strategy of the stimulus display was encouraged. It is then possible that the directional motion biases introduced at the points of intersection with the tilted lines, originate in the smooth pursuit path, the extra-retinal signals associated with it, or their integration with retinal signals. As a result, a viewing strategy that requires constant fixation on the stimulus display could eliminate the slalom illusion entirely, putting into serious doubt some of the theoretical interpretations hitherto put forward. Under conditions of fixation the retinal projection of the moving dot would no longer be stabilised in foveal vision, but describe an extended trajectory on the retina that might be more readily veridically interpreted as being straight, despite the presence of the tilted line inducers typical of the slalom illusion.

6.1.2. *Effects of stimulus eccentricity*

However, in the previous experiments reported here the eye movements of participants reporting on the slalom illusion were never measured. It is therefore unknown whether the participants indeed adhered to the instruction to follow the dot or not. Though it

133

appears unlikely that participants would choose to ignore the instruction, the lack of proper eye movement control means that the slalom display in principle could have been viewed in any part of the visual field. Related to this then, is the question of how retinal eccentricity (the distance from the projection of the stimulus on the retina to the fovea centralis) would affect the slalom illusion – if it occurs at all in conditions with a fixational viewing strategy. It is well-known that neurons representing the peripheral visual field have larger receptive fields, and as a consequence have a decreased ability to encode fine detail of object form, orientation or position (Anstis, 1974; Levi, Klein, & Aitsebaomo, 1984, Levi & Waugh, 1994; Mäkelä, Whitaker, & Rovamo, 1993). Although peripheral vision has a relatively preserved overall sensitivity to motion (Cleland & Levick, 1974; Walsh & Polley, 1985; Edwards & Nishida 2004), its impaired position and orientation coding does also impair its ability to finely discriminate between motion signals (Johnson & Scobey, 1980; Orban, 1985; van de Grind, Koenderink, & van Doorn, 1987).

The Poggendorff illusion, as a widely studied static illusion of angle that shares some similarities with the slalom illusion, has been investigated under conditions of different retinal eccentricities. Novak (1966) compared free-viewing conditions to controlled central fixation, and observed a significant reduction in the size of the Poggendorff illusion in the central fixation condition. Greist and Grier (1977) report that the Poggendorff illusion was unaffected by horizontal displacements, but it disappeared when the stimulus was vertically displaced from the centre of fixation. Wenderoth, White, and Beh (1978) however, could not replicate the latter effect, nor the finding of Novak (1966). It can be therefore said that there is mixedevidence that horizontal displacements of the Poggendorff display affect its strength as an illusion – from which it could be concluded that there is no reason to suspect that the angle-of-intersection biases of the slalom illusion, if indeed they share a similar root cause, would be affected.

134

In peripheral vision, however, the slalom display could possibly be susceptible to additional and different visual illusory effects. Anstis (2012) reports a study where a dot was shown to move vertically up and down, across a background grating of high-contrast stripes tilted at a 45° angle. In foveal vision, a veridical percept of this display was achieved. As the eccentricity of the display was increased, the perceived direction of motion was increasingly attracted towards the orientation of the background grating, until at an eccentricity of twenty visual degrees the dot appeared to move parallel to the 45° tilted stripes. This effect was independent of stimulus contrast. Anstis named this the *Furrow Illusion*, whereby the reduced acuity of peripheral vision causes the motion direction of the dot to fall into the 'rut' of the background orientation. He theorises that this effect occurs because peripheral vision is unable to segregate the dot from the background, and confounds the orientation signals of the background with the motion direction of the dot. Similar results were previously obtained by Cormack, Blake, and Hiris (1992). Ito and Yang (2013) report a similar illusion, that more closely resembles the slalom display. In their study, a straight line segment moves rigidly along a straight path across a zig-zag pattern of tilted lines (see Figure 6.1). When viewed in peripheral vision, the participants report a curved trajectory for the short line segment, following the zig-zag pattern of the tilted lines.
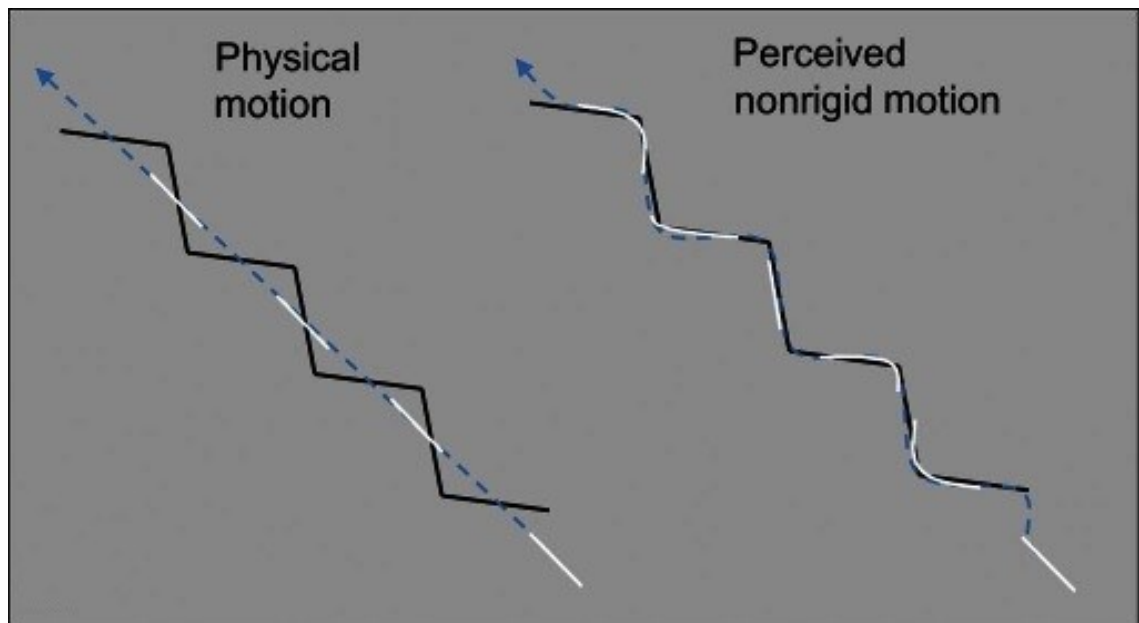
Figure 6.1. The squirm effect as presented by Ito and Yang (2013).

The authors speculate that the *squirming illusion* is closely related to the furrow illusion of Anstis (2012). Interestingly, however, they also offer the following discussion on the slalom illusion: *"Is the squirm effect a version of the slalom effect (Cesàro & Agostini, 1998)? We observed that when the short line segment was tracked by eye movements, the slalom effect was predominant, i.e., the motion path had a phase opposite to that of the zigzag wave. However, in peripheral vision, the path of perceived motion was in phase. Thus, the slalom effect cannot explain the squirm effect"* (Ito & Yang, 2013, pp 142). While the authors offer no data to support this claim, this suggests that the slalom illusion as it is investigated in this thesis could disappear when the display is presented in peripheral vision, as it is overtaken by the furrow/squirming illusion.

While the perceived trajectory described in the squirming illusion of Ito and Yang (2013) is similar to that induced by the slalom illusion, its angle of intersection with regard to the tilted line inducers is different (perpendicular for the slalom illusion, and parallel for the squirming illusion). Indeed, this highlights the fact that Cesàro and

136

Agostini (1998) have not offered data to support the claim that the perceived sinusoidal slalom trajectory occurs as theorized. They do report that "*At the beginning of training, the observers were asked to verbally describe the dot trajectory. This method was used in order to ensure that the observers spontaneously perceived a sinusoidal trajectory*" (pp 520) - but this does not discriminate between a 'slalom' and a 'squirming' type of trajectory.

6.1.3. Goals of the current study

A number of limitations in the current literature on the slalom illusion have been identified and will be addressed in the current experiment. Firstly, the slalom illusion might be rooted in the perceptual consequences of smooth pursuit eye movements, rather than the motion of the dot stimulus itself. If this is the case, the illusion should disappear when constant gaze fixation at a single location in the display is enforced in the experiment. This will be achieved through explicit instruction and through the use of an eye tracker, to measure and store the position of each subject's gaze over the course of each experimental trial.

Secondly, it is unknown whether the slalom illusion, if it occurs at all under conditions of fixation control, is then affected by the retinal eccentricity of the stimulus display. To this end, the slalom display will in the current study be presented at three different horizontal eccentricities: low, mid, and high. The slalom display will also be reduced in size, so as not to extend across different parts of the visual field.Since there is no indication that angle illusions such as the Poggendorff illusion are reduced away from central vision, it is hypothesised that the inducing angles of intersection will similarly not be affected by eccentricity, and the slalom effect will not be reduced. At the same time, however, the veridical straight motion signal could be less reliable in more

eccentric vision. As this signal is corrective to the slalom illusion (see Chapter 3 on partial occlusion of the motion trajectory), it could be expected that the slalom illusion, if it can still be observed, will increase in magnitude towards peripheral vision.

Finally, it has not been established whether the percept of the slalom illusion follows the theorised slalom path, or a 'squirming' path that is similarly sinusoidal but closely following the inducing tilted lines rather than intersecting them. Following the observations of Ito and Yang (2013), it is expected that the slalom path will be present in foveal vision, whereas the squirming path will become more prevalent towards peripheral vision. It remains to be seen whether the slalom illusion can occur at all away from the fovea. To gauge the type of dot trajectory, the participants will be familiarised with both types of trajectories prior to the experiment. In addition to the sinusoidal magnitude response, participants will be and required to indicate the type of display they have perceived (straight, slalom or squirm).

In short, the current investigation will be informative on whether the slalom illusion can occur under conditions of constant fixation, and whether (a) its presence and (b) its magnitude are affected by the eccentricity of the stimulus display relative to the point of fixation.

6.2. Methods
6.2.1. Participants

A sample of 20 participants was recruited from the general student population of Sheffield Hallam University. All participants were undergraduate or postgraduate students and were naïve as to the phenomenon investigated. The inclusion criteria for

the sample were having normal or corrected-to-normal vision and being over 18 years old. Participants were offered a £10 high-street voucher to compensate for their time.

6.2.2. Design

A repeated-measures design was employed, with two independent variables and two dependent variables. The first independent variable, *stimulus type*, has two levels: *tiltedlines* and *vertical lines*. The second independent variable, *eccentricity* has three levels: *low eccentricity* (within 5°)*mid eccentricity* (8.4°), and *higheccentricity* (16.8°). These values are in line with the eccentricities used in the experimental setups of both the furrow illusion (Anstis, 2012) and the squirm effect (Ito & Yang, 2013). The first dependent variable, *amplitude*, is continuous and operationalised as the height of the response line measured in pixels, whereas the second dependent variable, *response type*, is categorical and has three options: *straight*, *slalom,* and *squirm*.

6.2.3. Apparatus and stimuli

The experiment was programmed in MATLAB with Psychtoolbox-3 (Brainard, 1997; Pelli, 1997; Kleiner et al., 2007) and the Tobii SDK. The Tobii Pro T120XL eye tracker was used to record the eye movements. The stimuli were presented on the Tobii Pro T120XL incorporated monitor with a resolution of 1920 x 1200 pixels. The stimuli consisted of four inducing lines (tilted or vertical, depending on condition), forming two modules. The distance between the two lines which make up a module was 1.86 cm, whereas the distance between the two modules was .93 cm. At this size, the stimulus covered the maximum display area that would fit within central vision (5° of visual angle), meaning that the stimuli in their entirety could be placed within the central visual field. For consistency, the same size was maintained for the stimuli presented in the peripheral condition. As in previous experiments, the angle of intersection for all the tilted lines was 40°, whereas for the control vertical lines the angle of intersection was

90°. In all six conditions the moving dot was black, had a diameter of 5 pixels (1.25 mm), and traversed the two modules twice, always from left to right.The position of the stimuli in the experimental display depended on the condition as described below. In the *low eccentricity* conditions, the modules were aligned vertically with the fixation point, and were placed either immediately above or immediately below the fixation point; this ensured both that the fixation point was not incorporated in the stimuli and that the modules were in their entirety within the 5° central vision field. In the *mid eccentricity* conditions, the modules were aligned horizontally with the fixation point, and were placed either to the left, or to the right of it, always at a 8.4° visual angle. In the *high eccentricity* conditions, the modules were aligned horizontally with the fixation point, and were placed either to the left or to the right of it, always at a 16.8° visual angle. (Fig. 6.2).

Figure6.2. All the possible positions of the stimuli on the display screen. Depicted in blue are the *low eccentricity* conditions, in green the *mid eccentricity* conditions, and in red the *high eccentricity* conditions.

6.2.4. Procedure

The procedure was similar to that described for the previous laboratory experiments: participants were provided with information sheets (Appendix 2) and consent forms (Appendix 3) and gave their informed consent prior to commencing the experiment. All participants were informed about their rights as per the university ethics guideline and the Declaration of Helsinki. A chin rest was used, placed at 60 cm from the monitor, to ensure all participants maintained the same visual angle throughout all trials. Before starting the experimental task, participants were assisted by the experimenter in a trial run consisting of ten repetitions of randomised experimental trials. This made the participants familiar with the task and the terminology used (e.g. squirm, slalom), as well as helping with the calibration of the eye tracker. The experimental task consisted of 108 randomised trials (18 repetitions per condition). Any given trial ran in the order depicted in Figure 6.3. Participants were asked to look at the black dot situated in the centre of the screen and to press enter while they are fixating the black dot. If they were fixating, the dot changed its colour to green, indicating that they can proceed with pressing the enter key. After pressing enter, the fixation point remained present on the screen and the stimuli appeared too, consisting of the dot crossing the module of lines twice, always in the same direction (left to right). Following that, the stimuli disappeared and were replaced by the adjustment line used to measure the magnitude of the illusion. The adjustment was made, like in the previous laboratory experiments, by using the up and down keys. After adjusting the line as to represent the perceived vertical displacement of the moving dot, participants had to press the space bar and this lead to the final part of the trial, consisting of choosing between three descriptions of the dot trajectory: 'straight', 'slalom' and 'squirm'. Once this answer was given by using the corresponding key (1, 2, and 3, respectively), the following trial commenced immediately. Participants completed the experimental task at their own pace, and the

duration was about 30 minutes on average, excluding the initial instructions and practice trials. Upon completion, participants were fully debriefed as to the phenomenon investigated and were encouraged to make any comments relating to their experience or to ask any further questions.
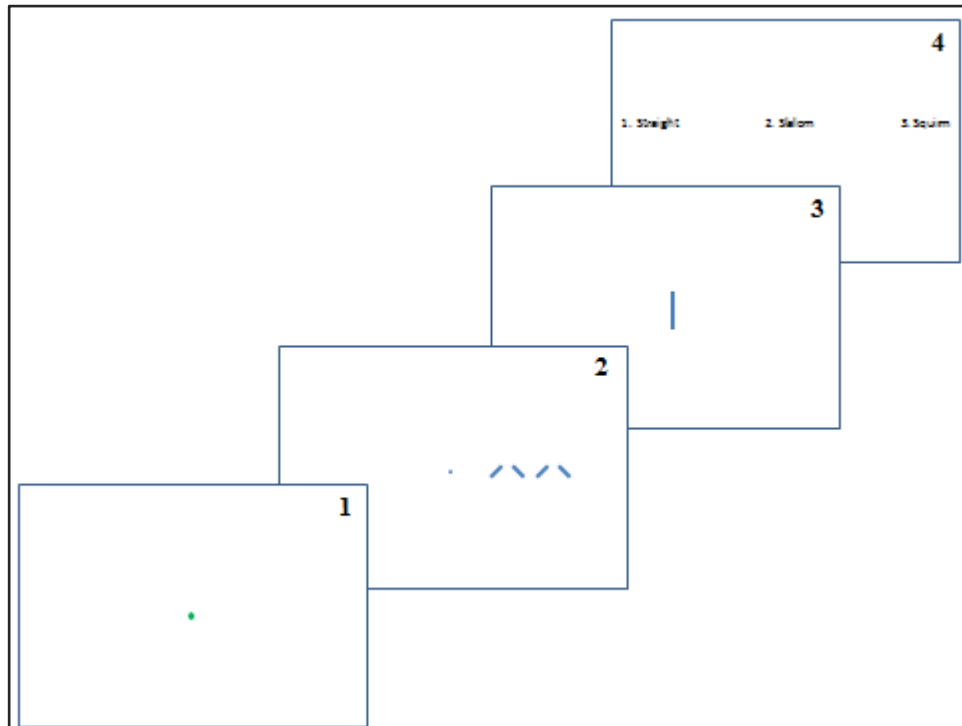

Figure 6.3. The description of an experimental trial, in chronological order: (1) fixation calibration, (2) stimulus presentation, (3) adjustment line for the first dependent variable, and (4) categorical options for the second dependent variable.

6.3. Results

6.3.1. Data preparation

The eye tracking measurements were used to remove trials where participants did not conform to the instruction to fixate on the fixation point. One of the participants completed only 90 trials, whereas the remaining 19 participants each completed all 108 trials. In total, data for 2142 trials were collected over 20 participants. One trial was

removed because no valid eye movement measurements were recorded. Because of theoccurrence of eye tracker measurement errors, some tolerance was given to the fixation accuracy of the participants: trials were removed only when fixation was measured to be maintained less than 80% of the time at the indicated fixation position. 1831 trials across 20 participants remained in the data set after removing trials with inaccurate fixation.

For trials where a straight response type was given, the amplitude was recordedas 0. That is, if they reported the trajectory as being straight, any non-zero amplitude response must have been an inaccuracy introduced by the probe line approximation.On 48.38% of all straight trials, this was already the case. In the other straight trials, an amplitude response of 1.76 pixels on average was given prior to data cleaning. Averaged over all experimental conditions, none of the participants deviated more than three standard deviations from the mean response amplitude, so there were no outliers to be removed. All the analyses reported were performed on the trials remaining after data preparation.

6.3.2. Illusion amplitude

The mean amplitude response was computed per combination of participant and experimental condition, in preparation for repeated-measures statistical tests.

Boxplots (Appendix 27) indicate one possible outlier and the computed Z-scores confirm it ($z_1 = 3.41$). After removing the outlier, the skewness statistic (Appendix 28) and histograms (Appendix 29) showed that the data were normally distributed in three experimental conditions (*tilted mid eccentricity*, *tilted high eccentricity*, and *control high eccentricity*), but were skewed in the remaining three (*tilted low eccentricity*, *control low eccentricity*, *control mid eccentricity*). The data were transformed into their

natural logarithms, and the recalculated skewness statistics confirmed that the transformation corrected the distributions to normality (see Appendix 30).

The means and standard deviations are presented in Table 6.1 and are based on the data prior to their transformation into natural logarithms. The largest amplitude was reported in the tilted mid eccentricity condition, whereas the lowest amplitude was observed in the control low eccentricity condition.

Table 6.1
Mean Amplitudes and Standard Deviations for the Six Experimental Conditions (in Pixels)

Stimulus type	Eccentricity	Means	SDs
	Low	3.79	3.71
Tilted	Mid	6.27	4.16
	High	5.54	3.53
	Low	1.94	1.96
Control	Mid	2.15	1.99
	High	3.25	1.97

The effect of the experimental conditions on the perception of the trajectory was analysed using a two-way repeated-measures ANOVA. All the inferential statistics were calculated based on the computed natural logarithms.

The null hypothesis of sphericity was rejected solely in the case of the eccentricity effect (W = .675, p = .035), so for that condition, a Greenhouse-Geisser correction was applied. The results show that both main effects and their interaction were significant: stimulus type [F (1, 18) = 42.87, p <.001, η_p^2 = .704], eccentricity [F (1.51, 27.17) = 17.29, p <.001, η_p^2 = .490], stimulus type x eccentricity [F (2, 36) = 5.21, p = .010, η_p^2 = .224]. The marginal means for eccentricity were: low = 2.86, mid = 4.21, high = 4.39; the marginal means for stimulus type were tilted = 5.20 and control = 2.45. G*Power (Faul et al., 2009) was used to determine the statistical power of these F tests. Given their respective effect sizes, the power estimates were: >.999 for stimulus type, .985 for eccentricity, and .713 for the interaction effect.
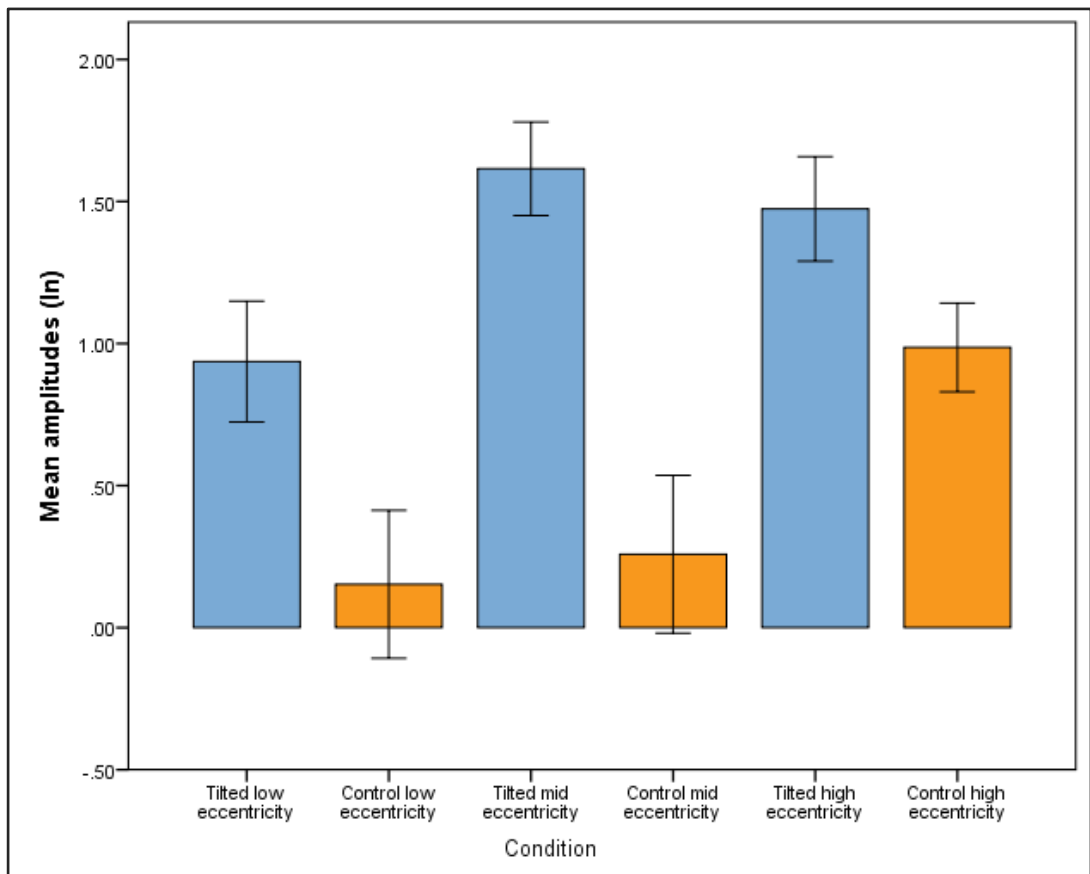
*Figure 6.4.*Mean amplitudes and standard errors for the six background conditions. The tilted conditions are represented in blue, whereas the control conditions are represented in orange.

In order to investigate the interaction of both eccentricity and stimulus type variables,a simple effects analysis was conducted using 15 post hoc paired t-tests. All *p* values associated with the t-tests were interpreted relative to the Bonferroni-corrected alpha level of .003. Table 6.2 shows all the t test scores and their associated significance levels. Notably, within the tilted conditions, there was a significant difference between the low and the mid eccentricities, but not between the low and the high or the mid and the high eccentricities. Within the control conditions, only the difference between the low and the high eccentricity was significant. Within each eccentricity, there was a significant difference between the tilted and the control condition.

Table 6.2

Post-hoc Paired-Samples T Tests and Their Associated Significance Levels

	Tilted low	Tilted mid	Tilted high	Control low	Control mid	Control high
Mean (SD)	.94 (.93)	1.62 (.72)	1.47 (.80)	.15 (1.13)	.26 (1.21)	.99 (.68)
Tilted low		$t(18) =$ -3.71 ***p = .002***	$t(18) =$ -2.53 *p = .021*	$t(18) =$ 3.38 ***p = .003***	$t(18) =$ 3.52 ***p = .002***	$t(18) =$ -.24 *p = .820*
Tilted mid			$t(18) =$ 1.51 *p = .150*	$t(18) =$ 7.53 ***p<.001***	$t(18) =$ 5.43 ***p<.001***	$t(18) =$ 4.70 ***p<.001***
Tilted high				$t(18) =$ 7.86 ***p<.001***	$t(18) =$ 4.91 ***p<.001***	$t(18) =$ 4.38 ***p<.001***
Control low					$t(18) =$ -.58 *p = .566*	$t(18) =$ -5.17 ***p<.001***
Control mid						$t(18) =$ -3.32 *p = .004*

6.3.3. Response type

Three response options were offered to participants to indicate the type of illusion they had perceived: straight (no illusion), slalom (trajectory intersecting the inducing lines), and squirm (trajectory along the inducing lines). Figure 6.5 displays the proportions of responses given in each condition, which necessarily add up to 1. Straight responses were predominant in the control conditions, whereas a larger proportion of Slalom responses were given in the tilted conditions. At mid and high eccentricities for the tilted lines, squirm responses were most common, whereas at low eccentricity nearly half of the responses for the tilted condition were given as straight.
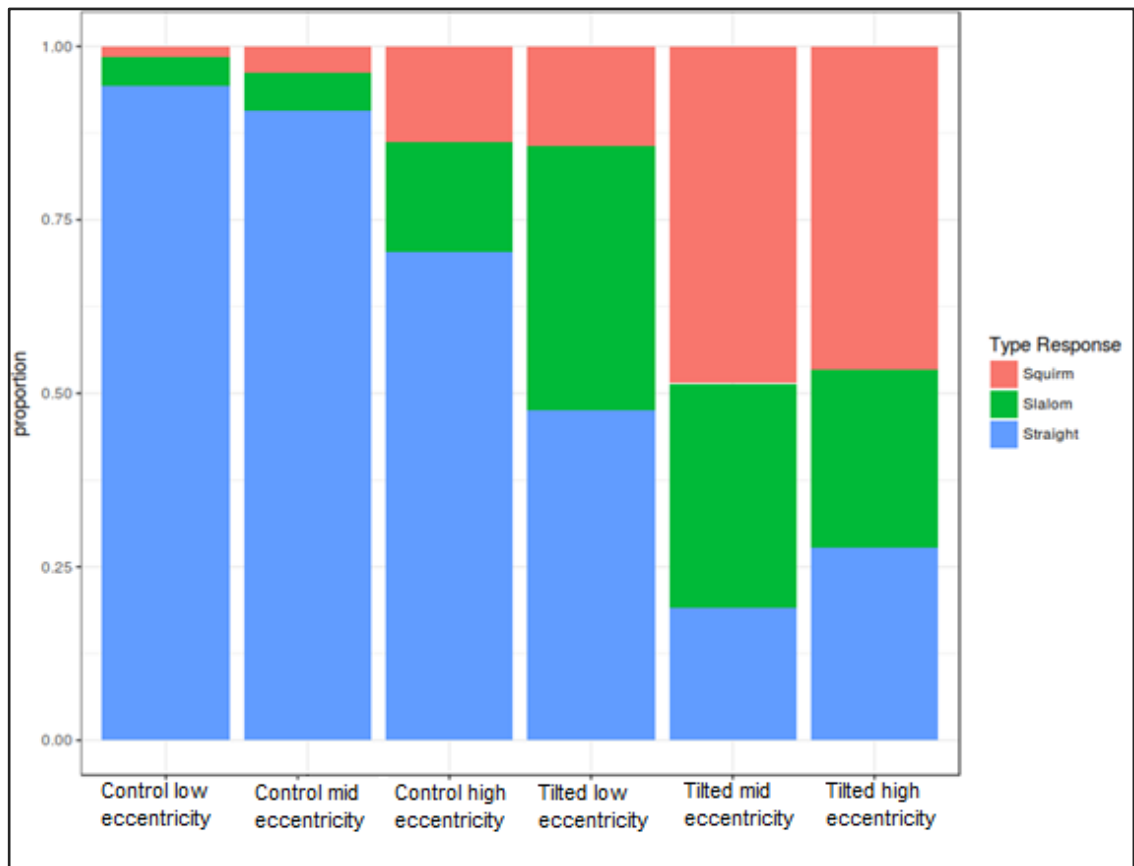
146

*Figure 6.5.*Proportions of response type in each experimental condition.

To analyse the response type data, a multinomial mixed-model logistic regression was performed using the *lme4* package for R. The analysis is *multinomial* because the response variable (the type of illusion perceived) was categorical with three levels (*squirm*, *slalom*, and *straight*). The response variable was dummy-coded and a separate regression was performed for each level. That is, the responses were re-coded as being either a 1 (for instance, 'straight') or a 0 (for instance, 'not straight', so either 'slalom' or 'squirm'). The *logistic regression* model was chosen because ANOVAs do not support categorical response variables. The *mixed-model* nature of the analysis refers to the simultaneous modelling of the random effects of subject variability and the fixed effects of the condition differences. In this it is similar to the repeated measures ANOVAs performed in previous analyses. In a regression analysis, a reference level is to be chosen for each independent variable, with respect to which the regression weights

for the other conditions will be estimated. *mid eccentricity* and *tilted* were chosen as the reference levels for their respective independent variables, since the condition differences with regard to these levels were theoretically deemed the most interesting: it will allow the direct comparison of eccentricities within the tilted conditions, where an illusion can be expected, and it will allow a direct comparison of both the low and the high eccentricity condition to the mid eccentricity condition based on the regression weights. The fitted model parameters for each analysis can be found in Tables 6.2, 6.3, and 6.4.

Table 6.2
Fixed Effects for the Straight Responses

	Regression weight estimate	*p* value
Intercept	-2.45	<.001
Eccentricity Low	2.35	<.001
Eccentricity High	.94	.031
Control	6.32	<.001
Low x Control	-1.58	.024
High x Control	-3.61	<.001

Table 6.3
Fixed Effects for the Slalom Responses

	Regression weight estimate	*p* value
Intercept	-.92	.002
Eccentricity Low	-.04	.913
Eccentricity High	-.25	.301
Control	- 2.58	<.001
Low x Control	-.88	.063
High x Control	1.55	<.001

Table 6.4
Fixed Effects for the Squirm Responses

	Regression weight estimate	*p* value
Intercept	-.07	.817
Eccentricity Low	-2.46	<.001
Eccentricity High	-.09	.695
Control	-3.94	<.001
Low x Control	.80	.253
High x Control	1.87	<.001

For the interpretation of these tables, it is important to note that the regression weights of the main effects are additive to the intercept (the reference level, i.e. the mid eccentricity tilted condition), and the regression weights of the interactions are additive to their respective main effect. A non-significant interaction weight, for instance, only indicates that the condition to which it refers could be fully explained by the sum of the main effects. Most importantly, these results show that in the tilted conditions, the proportion of Slalom responses did not change between the three eccentricity levels. Squirm responses for the tilted conditions increased significantly from low to mid eccentricity, but not from mid to high eccentricity. Straight responses for the tilted conditions increased significantly both from mid to low eccentricity and from mid to high eccentricity. The main effect of the display type was significant for all response types.

In conclusion, no effect of eccentricity on the proportion of slalom responses can be shown for the tilted displays, where the illusion could be expected to occur. However, between the low and the mid eccentricity, straight responses are replaced by squirm responses - and this effect continues to be present at high eccentricity.

6.3.4. Slalom response

In the analysis presented in section 3.2, it was showed that the perceived amplitude significantly increased from low to mid eccentricity in the tilted conditions. For the current analysis, the illusion magnitude responses were processed again, but only for those tilted condition trials on which a slalom response was given by the participants. The aim is to discriminate between a situation where the mean amplitude only increased because fewer straight and more squirm responses were given, and a situation where the amplitude of the slalom illusion itself was affected by retinal eccentricity. For trials at low eccentricity, a mean amplitude response of 1.59 ln(pixels) was observed (N = 14, SD = .50; 4.90 pixels). At mid eccentricity, this was 1.76 ln(pixels) (N = 16, SD = .60; 5.82 pixels), and at high eccentricity, it was 1.87 ln(pixels) (N = 19, SD = .54; 6.51 pixels). This constitutes a monotonic increase of the amplitude with eccentricity. As a consequence of this data filtering, not all participants had data points in all conditions, and therefore not all participants could be taken into an inferential analysis. Six additional participants had to be excluded from this analysis because they did not have observations in all cells of the design, after filtering for slalom responses only. The power of the analysis was therefore reduced, and no significant effect of eccentricity on the magnitude of the slalom illusion was found in a repeated measures ANOVA [$F_{(2, 24)} = 1.13$, $p = .340$, $\eta^2 = .090$]. G*Power (Faul et al., 2009) was used to determine the statistical power of the repeated-measures ANOVA. Given the $\eta_p^2 = .090$ for the effect size, an alpha-level .05 and a total sample of 13, the statistical power was estimated to be .094.

6.4. Discussion

The effect of a fixated viewing strategy, which placed the stimulus display at three different eccentricities in the visual field, was investigated for the slalom illusion. When comparing control displays using vertical lines to displays using tilted lines, the reported perceived magnitude was increased across all eccentricity conditions, indicating that the illusory sinusoidal path remains present under conditions of constant fixation. However, in the mid and high eccentricity tilted line conditions, around half of the responses reported a squirm illusion percept, rather than a slalom illusion. The proportion of slalom responses remained constant across eccentricities, but the proportion of straight responses decreased away from central vision, to be compensated with squirm responses. Although the tilted line display was significantly less often perceived as being straight at mid and high eccentricities as compared to low eccentricity, there was insufficient evidence that the amplitude of the slalom illusion itself was also subject to effects of eccentricity. Finally, there was an increase in non-straight responses to vertical line control displays with vertical at greater eccentricities, which can be interpreted as a consequence of greater perceptual uncertainty at these locations.

These results are a refutation of the alternate hypothesis that the slalom illusion would not occur under conditions of constant fixation, because they are intrinsically linked to smooth eye movements. Even in the absence of eye movements, more slalom responses and greater perceived amplitudes are reported for tilted line displays than for vertical line control displays. This implies that the slalom illusion can result both from a trajectory that is projected across the retina, such as in the current study, and a trajectory that is stabilised on the retina through a smooth pursuit viewing strategy, as in all previous studies. The slalom illusion is therefore likely to originate in areas of the visual cortex which have already integrated the extra-retinal signals that compensate eye

151

movements into the perceptual processing stream. A study by Lebranchu et al. (2010) localises this particular integration between dorsal areas V2 and V3, whereas other studies especially highlight the importance of areas MT and MST in integrating the extra-retinal signals following from smooth pursuit eye movements (e.g. Newsome et al., 1988; Thier & Ilg, 2005; Ilg, 2008).

These data provide further evidence for the existence of the Squirming illusion (Ito & Yang, 2013), a variant of the Furrow illusion (Anstis, 2012; Cormack et al., 1992), outside of central vision. At larger eccentricities, the sinusoidal path of the dot appeared to follow along with the orientation of the tilted-line inducers on around half of the trials recorded, resulting in amplitude responses similar to those obtained with the slalom illusion. The hypothesis according to which the effects measured with the tilted lines are always squirming effects can thus be rejected, as well as the notion that the squirming illusion replaces the slalom illusion completely in peripheral locations of the visual field. Perhaps coincidentally, the proportion of slalom responses remained constant across eccentricities, and squirm responses increased only at the cost of straight responses. This conclusion should not be drawn too strongly, however, since the high eccentricity control conditions indicate a significant amount of uncertainty in the responses – which could potentially lead to a subset of random responses across all illusion type categories.

It was hypothesised prior to the experiment that a combination of a peripherally preserved angle-of-intersection illusion and a reduced reliability of the corrective straight horizontal motion signal would result in an increased slalom illusion at greater eccentricities, similar to what it was observed under conditions of occlusion. Comparing mid and high eccentricities, no significant difference was found lending support to this hypothesis, as both the proportion of slalom responses and the magnitudes reported on slalom responses remained constant. Comparing low and mid eccentricities, the results

at first sight do appear to indicate such an effect, as the proportion of straight responses decreased and related to this, the overall reported amplitude increased. However, as far as could be demonstrated through inferential statistics, this effect could only be attributed to the replacement of straight by squirm responses, not to an increase in the amplitude of the slalom responses themselves. The strong occurrence of the squirming illusion outside of central vision interferes with the assessment of eccentricity effects on the slalom illusion, leaving us with the preliminary conclusion that neither the occurrence, nor the magnitude of the latter is affected by the eccentricity of the stimulus display.

6.5. Summary

The slalom illusion is present under experimental conditions of constant fixation, and could not be shown to depend on the eccentricity of presentation. The slalom illusion can be clearly distinguished from the squirming illusion, the latter strongly manifesting itself when participants are presented with classic slalom displays away from central vision.

7. Chapter 7 - General discussion

7.1. Summary of the experimental chapters

Over the course of five experimental chapters, empirical and theoretical aspects of the slalom illusion have been investigated. The goal was not only to define the boundary conditions of this illusion in particular, but also to explore the more general mechanisms of object trajectory perception as it integrates a sequence of local motion signals into a global path. The clear discrepancy in the slalom illusion between the veridical local motion signals, that are always horizontal, and the illusory sinusoidal trajectory that is typically observed by experimental participants made it a promising candidate for this investigation.

In Chapter 2, the original slalom illusion was replicated in two experiments, both using a tablet computer setup where responses were collected directly as sinusoidal finger movements across the screen, and a psychophysical setup where the magnitude of the illusion was estimated using a probe line. To determine whether the illusion is crucially dependent on the local information at the points of intersection between the dot trajectory and the tilted lines, illusory contours were created using Kanizsa-like inducers. In addition, experimental conditions were included where real contours were used, but at different contrast levels. The illusory tilted lines did not elicit a strong slalom illusion, and the illusion's magnitude remained unaffected by even a strong reduction in contrast.

In Chapter 3, it was investigated whether the illusory slalom trajectory can be perceptually completed behind an occluding shape, and whether the size of the illusion is affected by this manipulation. When presented with filled triangles instead of alternating tilted lines, the participants reported an increased rather than a decreased

illusion. This not only indicates that the perceptual completion of the dot trajectory is not that of the shortest, straight path behind the occluding shape, but also that the partial removal of the veridical straight trajectory significantly increases the weight of the bias induced by the tilted lines in the final percept of the display. Participants reported that the dot re-appeared faster than expected from behind the occluding shapes.

In Chapter 4, the occluded slalom illusion was compared to a classic effect in apparent motion, known as Korte's third law (Korte, 1915), whereby longer inter-stimulus intervals elicit the perception of longer apparent motion trajectories. Whereas the dot speed across the visible part of the slalom display was kept constant, the time spent behind the triangular occluders was manipulated to be either shorter or longer than would result from a trajectory at continuous speed. The shorter ISIs decreased the slalom illusion, but the longer ISIs did not increase it. The main interpretation of these results was that while the maximal magnitude of the slalom illusion is bound by the angle of the tilted inducing lines, its trajectory can also be re-interpreted by the visual system after the fact, based on the time spent behind the occluder and an assumption of constant speed. Because shorter ISIs only allow for shorter trajectories, a shorter trajectory also becomes more likely when the ISI is short.

In Chapter 5, the slalom illusion was inverted. A sinusoidal veridical dot trajectory was superimposed on a display of vertical lines. If a bias towards a perpendicular angle of intersection underlies the slalom illusion, a reduced amplitude would then be expected. Instead, the slalom illusion was not affected when comparing vertical inducing lines to tilted inducing lines, and the effect of the angle of intersection appears exclusive to veridically straight trajectories. This could be attributed to a rapid adaption in neurons tuned to the constant motion direction of the classic slalom illusion, increasing the relative salience of the biased motion signals around the points of intersection. In

addition, the presence of static reference objects was found to be of significant influence on the magnitude of the slalom illusion.

In Chapter 6, the effect of eye movements and retinal eccentricity on the slalom illusion was investigated. The slalom effect was shown to still occur when participants were instructed to keep the gaze fixated at a constant position, instead of following the dot with their eyes. Given the markedly different retinal effects of these fixational strategies, the slalom illusion then appears likely to be rooted at a stage of visual processing where abstraction has already been made of retinal coordinates. Even though the size of the amplitude responses increased outside of foveal vision, no evidence was found that retinal eccentricity affected the magnitude of the slalom illusion. Instead, the veridical percepts of a straight trajectory were towards the periphery replaced by a different type of visual illusion, the squirming illusion, while the amplitude responses remained constant across eccentricities when the slalom illusion was perceived to be present.

These results will now be discussed from three different perspectives: the empirical determinants of the slalom illusion, the theoretical consequences of the current findings, and suggestions for future research.

7.2. Determinants of the slalom illusion

In the original slalom display of Cesàro and Agostini (1998), participants were presented with 13 tilted black lines of alternating orientations, a width of .3 mm and a vertical height of 8 mm, on a white background. A black dot with a diameter of .5 mm moved horizontally for 230 mm across this set of lines at a default speed of 1.55°/s (12.1 seconds), and intersected them at their middle points. Participants were seated at a distance of 700 mm from a fixed CTR computer screen, and were instructed to follow

the dot with their gaze. They could indicate the perceived size of the illusion by adjusting the size of a vertical probe line. The effect size of the slalom illusion was shown to depend strongly on the incidence angle, ranging from 2 mm for 30° to .8 mm for 60°. A dependence on the speed of the dot was also observed, with a +-20% smaller amplitude being reported at a speed of 3.1°/s, and a +-20% greater amplitude at .8°/s. Speed and angle effects did not interact. Outside of the speed range tested, the participants of Cesàro and Agostini (1998) reportedly experienced problems following the dot. The horizontal distance between the middle points of the tilted lined similarly affected the magnitude of the illusion; an increase and a decrease of the distance by 50% respectively decreased and increased the reported amplitude by 20%.

7.2.1. Robustness

Since all the reported manipulations performed by Cesàro and Agostini (1998) affected the magnitude of the illusion, they did not deliver any empirical data on the factors to which the slalom illusion is robust. In the current work, new empirical conditions have been explored to which the magnitude of the slalom illusion remained invariant.

First, it was shown that the slalom illusion can also be measured using a portable tablet device, whereby the response is given by re-tracing the perceived trajectory of the dot on the tablet screen. Apart from the classic slalom effect; the additional effects of Chapter 2 and Chapter 3 were replicated on both a tablet device and on a psychophysical setup using a CRT screen. While of limited theoretical consequence, this does show that the slalom effect is robust, does not require the adjustable probe line to be measured, and data on the effect can also easily be collected outside of the laboratory.

Second, the slalom illusion was observed to occur in a variety of experimental displays, for instance placing circles at the end of the tilted lines (Chapter 2), or at a greatly

reduced spatial extent of the total trajectory (Chapter 6). Although these changes might have affected the size of the slalom illusion between experiments, the illusion itself never failed to occur in those conditions that were designed to be the analogue of the classic slalom illusion, in any of the experimental chapters. The slalom effect is not only strong in its magnitude, but also robust to the exact type of display design.

Third, the magnitude of the slalom illusion is invariant to the contrast of the inducing lines (Chapter 2), at least down to a Michelson contrast of .17. It can, however, not yet be excluded that the magnitude will decrease when the contrast is reduced further. Similarly, in Chapter 3, it was observed that there was no significant difference between the non-occluding triangle condition where the triangle was solid grey, and the condition where only a black outline of the triangle was presented. Given the central importance of the tilted lines in producing the effect and the systematic dependence of the effect on all display parameters investigated by Cesàro and Agostini (1998), the robustness to contrast manipulations is a notable finding.

Fourth, the slalom illusion is robust to the eye movement strategy used (Chapter 6). Although no direct comparison between the classic follow-the-dot instruction and a fixed gaze position was made, the illusion occurred with both strategies.

Fifth, the magnitude of the slalom illusion, when it is perceived as following a slalom trajectory, was statistically invariant to retinal eccentricity (Chapter 6). It should be noted however that the proportion of Straight responses decreased away from foveal vision, to be replaced with squirm responses that were associated with a greater amplitude. Moreover, the statistical power for detecting a dependence of the magnitude of the slalom illusion on retinal eccentricity was limited in Chapter 6.

7.2.2. Boundary conditions

The study of Cesàro and Agostini (1998) did not have a control condition, whereby no illusory sinusoidal modulation of the path would be expected, and the response bias of the participants in the context of the experimental task could be assessed. As such, it cannot be concluded from their manipulations of angle, speed or distance that the slalom illusion was in the condition with the lowest reported amplitude (60° angle, 3.11°/s, 24 mm distance – .46 pixel effect) merely reduced, rather than absent. In the current experiments, control conditions were employed, both with vertical lines and without line inducers (Chapter 2). It was regularly observed that even in the control conditions a non-zero amplitude was reported, and the magnitude of the slalom illusion was taken to be the difference between a non-control and the control condition.

Given the equivalence of the control condition with vertical lines and the control condition without lines in Chapter 2, a plausible conclusion is that the slalom illusion does not occur for line displays with an incidence angle of 90°. For an incidence angle of 60°, an amplitude greater than the minimum observed was reported by Cesàro and Agostini (1998). For angles between 60° and 90°, since a recent search (March 2018)[1] showed that Cesàro and Agostini are still the only authors to have provided empirical results on the slalom illusion, no data are available to establish the precise empirical boundary conditions for the effect to be observed. Similarly, no data are available for incidence angles below 30°, but it is possible to infer that a sequence of aligned horizontal lines (incidence angle of 0°) will not elicit the slalom illusion. Chapter 2 in addition demonstrated that a physical tilted line contour was required to be present for the slalom illusion to occur. Illusory or subjective contours elicit only a small effect compared to one control condition, but not compared to the second control condition. It is possible, however, that stronger emanations of illusory contours are

---

[1] The search was done by querying Google Scholar for papers citing the original slalom illusion paper by Cesàro and Agostini.

more effective. For instance, when using full illusory Kanizsa figures, rather than just illusory lines.

A straight trajectory is required for the path to be modulated by its repeated intersection with lines that are tilted with regard to its motion direction. As shown in Chapter 5, the inverted slalom illusion did not produce the expected result, i.e. a reduction in the magnitude of the illusion. This clearly demonstrates that incidence angle, while a main determinant of the slalom illusion, is effective only *conditionally*. It should be noted however that no measurements were recorded for experimental conditions where the trajectory was straight but not horizontal. The possibility cannot strictly be excluded that it is the non-horizontal, rather than the non-straight, property of the inverse slalom trajectory that prevented the occurrence of the illusion.

Finally, it was also observed that continuous visibility of the dot is not required for the slalom illusion to occur (Chapter 3). When an occluding triangular shape was positioned in between the tilted lines of the original slalom display, the illusory sinusoidal trajectory could be perceptually completed behind an occluder, at an increased magnitude.

7.2.3. Modulatory influences

The known modulatory influences of angle, speed, and distance and their interactions were not investigated further in the current experiments. Despite the lack of control conditions in the original study of Cesàro and Agostini (1998), they were considered to be established to a sufficient degree of certainty. Some further observations were however made on those factors that affected the slalom illusion, but did not prevent its occurrence altogether.

Partial occlusion of the dot trajectory increased the magnitude of the slalom illusion (Chapter 3). A similar increase did not occur when the dot moved in front of an object of a similar size. This finding could perhaps be compared to the effect of distance in the paper of Cesàro and Agostini (1998), whereby the illusion magnitude also increased when the straight trajectory between the tilted lines was simply made shorter. However when the time spent behind the occluder (ISI; Chapter 4) was in addition made shorter, the illusion magnitude decreased again. This effect therefore has the same direction as the speed modulation of Cesàro and Agostini (1998), whereby higher speeds decreased the reported amplitude.

The presence of visual references modulates the estimation of sinusoidal trajectories. When non-occluding triangles were used as inducing elements (Chapter 3), the size of the illusion was decreased. It could be speculated that this is to be attributed to the presence of a horizontal line at the base of the triangle, which makes it easier for the observer to estimate the true vertical extent of sinusoidal modulation of the trajectory. In Chapter 5, participants were presented with a veridically sinusoidal trajectory, of which the amplitude was to be estimated. If vertical or tilted lines were present in the display, with a vertical extent greater than the amplitude of the trajectory, the amplitude was slightly overestimated. When they were removed, however, the amplitude was strongly underestimated. While such reference effects do not *cause* the slalom illusion, they should be closely controlled when designing conditions for future experiments, so that confounds can be avoided.

Finally, retinal eccentricity did affect the size of the overall mean amplitude responses when participants were presented with the slalom display (Chapter 6). However, this could not be shown to be attributable to either an increase in the propensity of the

slalom illusion, nor the magnitude of the slalom illusion itself. Instead, the main variation was introduced by Straight and Squirm interpretations of the stimulus display.

7.3. Theoretical implications

Human visual perception is often characterised as a hierarchical analysis of the retinal input image, starting from local features limited in spatial and temporal extent, and integrating them across space and time into the global percept that is consciously perceived by the observer. While Gestalt psychologists have posited for over a century that the 'whole' is more than, different from, and dominant over the sum of the 'parts' (Wertheimer, 1912, 1938; Köhler, 1920; Koffka, 1935), more recent advances in vision science have also shown that the representation of the local, detailed features in the brain is itself in turn actively influenced by the global analysis of the stimulus (Navon, 1977; Murray et al., 2002; Johnson & Olshausen, 2003). Motion in particular is a salient quality of visual perception, which is analysed from the earliest stages of visual perception up to the complex interpretation and anticipation of object trajectories – often in dedicated cortical areas, such as area MT and MST. The slalom illusion offers a privileged view into this process.

The local features underlying the slalom illusion are the position and the motion direction of the dot, at any moment in time. It is proposed that the encoding of motion direction is biased towards perpendicularity around the points of intersection with the tilted lines (Cesàro & Agostini, 1998). The main argument for this is the dependence of the magnitude of the illusion on the angle of the lines, with no illusion occurring in the case of vertical lines, as well as the prevalence of a perpendicularity bias in other types of stimulus displays (Fineman & Melingonis, 1977; Wenderoth & Johnson, 1983; Khuu, 2012; Khuu & Kim, 2013). The exact origin of this bias in the context of the slalom

162

illusion is unclear. Among the potential candidate explanations, the aperture problem (Stumpf, 1911; Wallach, 1935; Wuerger et al., 1996) in primary visual cortex applies to the motion direction of lines, not of dots. It could perhaps be speculated that the motion energy of the dot is confounded with that of the tilted line it intersects with, and that the perpendicular motion of the line is then in turn mis-assigned to the dot. However, there is no evidence for this. Another possible root cause for the perpendicularity bias in primary visual cortex could be surround suppression of neighbouring orientation columns (Blakemore et al., 1970; see section 2.3 of the general introduction). This mechanism was demonstrated by the authors using static line stimuli, however, and it is yet to be shown in empirical research whether it could generalise to the interception angle between a moving object and a static line.

The subjective Kanizsa line contours of Chapter 2 were used to test whether the tilted lines need to be locally defined, as can be expected to be a prerequisite to localise the root cause of the slalom illusion early in the visual stream, or whether the perpendicularity bias arises at a higher and later level of contour representation. The slalom illusion could indeed only be clearly elicited by real line contours, but it was also noted that the induction of the subjective line contours was possibly too weak to allow a fair comparison. The invariance of the slalom illusion to the contrast of the tilted lines in Chapters 2 and 3, however, is not reminiscent of the signal processing properties of primary visual cortex, where the strength of neuronal responses is strongly contrast-dependent (if not their selectivity – see Skottun, Bradley, Sclar, Ohzawa, & Freeman, 1987). It can be concluded that there is reason to suggest a higher-level origin than V1 for the local perpendicularity bias in the case of the slalom illusion.

Interestingly, Chapter 5 demonstrated that the perpendicularity bias does not generalise to cause an inverted slalom illusion, where the veridical motion path is sinusoidal and

the intersecting lines are vertical. At the very least, this demonstrates that the perpendicularity bias does not by itself suffice to cause a motion illusion that is as strong as the slalom illusion. It is suggested that the manner in which middle temporal (MT) cortex encodes motion information could be the second fundamental piece of the puzzle, in addition to the perpendicularity bias. Priebe and Lisberger (2002) describe a neural circuitry in MT which leads to a short-term adaptation, and thus loss of response strength, within 20-80 ms after the motion onset. This adaptation is tuned to the direction, but also the speed of the motion. This circuitry would suppress the neuronal responses to the constant horizontal motion of the classic slalom illusion, but not that of the constantly changing veridically sinusoidal motion path of the inverted slalom illusion.

Given the building blocks of on the one hand a rapidly suppressed horizontal motion signal, and on the other hand motion signals locally biased towards perpendicularity at the intersections with the tilted lines, how could the slalom illusion arise? An important finding in this regard is the occurrence of the slalom illusion using both a smooth pursuit eye movement strategy in Chapters 2 to 5, and a constant fixation strategy in Chapter 6. At the retinal level, following the dot and fixating the gaze result in a very different input – the first with little motion and positional signals on the retina, the latter with many. This suggests that the integration process of the trajectory must take place at a level in the visual processing stream where stimulus representations have become independent of their position on the retina. That is, they must have incorporated the motor signals of eye movement into the visual representation, so that the motion can still be seen even when the moving dot has been stabilised on the retina by the smooth pursuit eye movements. This has been found to be case for only some cells in area MT, but most cells in area MST (Ong & Bisley, 2011; Hartmann, Bremmer, Albright, & Krekelberg, 2011; Chukoskie & Movshon, 2009). Interestingly, the middle-superior

164

temporal area (MST) of the visual cortex has also been implicated in the processing of object shape, in cooperation with the shape-sensitive lateral-occipital complex LOC (Kourtzi, Bülthoff, Erb, & Grodd, 2002). This makes MST a good candidate for the representation of the sinusoidally modulated trajectory shape, which participants reported on in the experimental tasks of the current research.

A simple motion integration mechanism to explain the slalom illusion is vector summation or averaging within a sliding temporal integration window, where each vector represents the direction and neuronal strength of the dot motion at each moment in time. If the horizontal motion signal is indeed strongly suppressed by short-term adaptation, then the motion signals biased towards perpendicularity at the points of intersection gain a great weight in the integration window, affecting the averaged motion direction over an extended period of time. This by itself could result in a smoothly evolving average motion direction, following a sinusoidal pattern. If part of the unbiased horizontal trajectory is removed, then the biased direction signals gain even greater weight, and the magnitude of the illusion is increased. Indeed, in Chapter 3 it was found that the partial occlusion of the slalom display resulted in larger reported amplitudes for the slalom illusion.

This passive mechanism of vector summation cannot, however, account for all aspects of the amodal completion of the dot trajectory. First, participants reported that the dot appeared to 'jump out' from behind the occluder, as if they had expected it to take longer to complete its trajectory. This is consistent with a greater amplitude, but also implies a more active process of prediction, whereby the visual system attempts to make sense of its inputs as they arrive, through assumptions based on past knowledge and recent inputs. The predictive coding (Rao & Ballard, 1999) framework formalises this view. The visual system is modelled as a continuous generator of predictions which are

fed back to and subtracted from the lower levels of representation. What is represented in neuronal activity is the error signal between the expected input and the actual input. The goal of visual processing is to constantly update predictions, and iteratively reduce error and therefore low-level neuronal activity (Murray et al., 2002). The salient 'jumping out' of the dot from behind the occluder may then represent a momentary error signal.

Second, in Chapter 4 shorter ISIs behind the occluder resulted in a reduced illusion magnitude. This is reminiscent of observations made in the apparent motion literature (Korte, 1915), whereby longer ISIs allow for the possibility of longer trajectories in the interpretation of the stimulus. Since the ISI is only known after the occluded trajectory has been travelled, this was interpreted as an example of post-diction, whereby the interpretation of the stimulus that reached conscious perception is not computed on-line, but after the fact (Eagleman & Sejnowski, 2000; 2003). At the same time, longer ISIs did not increase the magnitude of the illusion, as would have been predicted by this model. It was proposed that the amplitude of the slalom trajectory may have been limited by a ceiling effect in this condition.

An inconsistency appears to be present in the attempt to offer a coherent explanation of the empirical effects observed with the slalom illusion. If the dot stimulus is temporarily occluded, could this not release the suppression of the horizontal motion signal by short-term adaptation in MT neurons, and reduce the magnitude of the illusion? However, given the very short time needed for this adaption to occur (20-80 ms), the effect of its temporary release would probably be limited. In Experiment 4 of Chapter 3, the trajectory took 7.5 seconds in total to complete, and 660 ms for each visible part between the triangles. Therefore, only 3-12% of the visible dot trajectory would be free from adaptation to the constant motion direction.

A central aspect of the slalom illusion and other motion illusions is the necessary coupling between motion and position. Whereas the view put forward here argues its point mainly in terms of biased motion direction signals and their integration over time, the report given by the experimental participants of the current experiments is always in terms of changes in the vertical dot position. This implied dominance of motion information over position information is remarkable, because motion by itself is a rather elusive aspect of a visual perception, as demonstrated by Wertheimer's surprise upon discovering it as an independent quality, whereas few aspects of visual perception appear to be more real and more actionable than object position. From a neurophysiological perspective, however, it has been well established that motion direction signals in area MT do strongly bias the encoding of object position (Whitney, 2002; Maus et al., 2013; Nishida & Johnston, 1999; McGraw et al., 2002). Interestingly, Watanabe (2015) demonstrated in a binocular rivalry experiment that this misperception of object position due to a motion direction bias only occurs when the stimulus is consciously perceived. In binocular rivalry, a different image is shown to each eye, but only the dominant image is perceived. The other image is still processed by the visual system, but not consciously perceived. The same could then hold true for the slalom illusion, in that the trajectory modulation might only occur exclusively when the participants are consciously observing the slalom display.

Lastly, the effect of reference objects should not be ignored. Human observers are surprisingly poor at estimating the absolute position of visual stimuli in isolation, and accurately detecting displacements of such stimuli, especially when their motion transient is masked or not attended to (Bridgeman et al., 1994; Deubel, 2004; Deubel et al., 2010; Higgins, Irwin, Wang, & Thomas, 2009; Higgins & Wang, 2010). In Chapter 5, it was indeed observed that the sinusoidal amplitude of a dot trajectory in isolation was underestimated, whereas the presence of accompanying stimuli leads to a slight

overestimation. This implies that the final amplitude responses given by experimental participants should not only be explained through the subjective motion vectors of the dot, but also through the general layout characteristics of the display as a whole, including the tilted lines. A future quantitative model of the slalom illusion which does not take the effects of spatial references into account, will necessarily be incomplete.

7.4. Suggestions for future research

The results of the experiments conducted for this thesis have given rise to new questions that can be operationalised into a number of follow-up studies. The proposed experiments will both shed more light on the invariances, boundary conditions and modulatory influence of the slalom illusion, and on its theoretical underpinnings.

7.4.1. Smooth pursuit eye movements as a dependent variable

Both in the study of Cesàro and Agostini (1998) and in Chapters 2-5 of the current thesis, an instruction was given to the participants in the experiments to follow the dot with their eyes. That is, to perform smooth pursuit eye movements. However, these eye movements were never measured during the task.

A central question of interest is whether the smooth pursuit eye movements display a sinusoidal pattern, even though the veridical motion direction is straight, and whether this is the case already from the beginning of the trajectory or not. Unlike the reported perception of the amplitude of the trajectory, smooth pursuit eye movements are on-line, steered only by the visual information that is available either currently or in the past. In the case of a partially occluded trajectory (see Chapter 3) and manipulated ISIs during occlusion (see Chapter 4), the proposed effects on the trajectory amplitude during occlusion could similarly be measured indirectly through smooth pursuit eye

movements. If the increased amplitude that was observed during occlusion is a predictive effect, smooth pursuit eye movements could follow the pattern of results found in Chapter 3. If it is postdictive and takes effect only after the dot re-appears from behind the occluder, as was proposed for the ISI effect on occluded trajectories in Chapter 4, it should not affect the amplitude of the eye movements.

Although smooth pursuit eye movements are not required for the slalom illusion to occur (see Chapter 6), it is possible they play a causal role in some of the effects observed in the current thesis, or in the magnitude of the illusion. That is, the perception of the trajectory can be biased in the direction into which the eye motor control is biased. To investigate this, replication attempts can be made for the main findings of Chapters 2-5, but under fixated gaze conditions. If smooth pursuit eye movements do not play a causal role, these effects should still occur.

7.4.2. Effect of the length and vertical extent of the inducing lines

In the study of Cesàro and Agostini (1998), the incidence angle of the dot and the lines was manipulated between 30° and 60°, and the vertical extent of the lines was kept constant. However, this is only possible if the length of the lines covaries with the angle: for an identical vertical extent, a more tilted line must also be longer.

The confounding factor of length needs to be experimentally disentangled from the effect of angle. This implies that the vertical extent will be manipulated, too. Given the suggested importance of visual reference on the estimation of trajectory amplitude (Chapter 3 and Chapter 5), this is a factor of interest in its own right. Additional elements could be added to the display to separate reference effects from line length and angle. For instance, the circular markers of Chapter 2 proved to be equally effective as a reference for vertical extent as full vertical lines. In addition, since Cesàro and Agostini only explored incidence angles between 30° and 60°, the full range of incidence angles

between 0° and 90° can be tested in the context of this proposed study (using 90° as the control condition).

7.4.3. Separating offset from occlusion

In Chapter 3 of the current thesis, the dot trajectory was partially invisible as it appeared to be occluded by a triangular shape. This manipulation increased the perceived amplitude of the trajectory, whereas the magnitude of the illusion did not increase when the dot passed in front of a similar shape. The interpretation made focused on the partial unavailability of the veridically straight dot trajectory, otherwise compensating the biased directional signals at the line intersections.

However, the partial unavailability of the trajectory can be manipulated separately from amodal completion of the trajectory by a shape. In condition A, an occluding black triangle such as in Chapter 3 could be displayed. In condition B, the original layout of the tilted lines can be used, but the dot would disappear during those parts of the trajectory where it was occluded in condition A. It can then be observed whether amodal completion is a necessary condition for the trajectory to be integrated across an interruption, or whether a temporary disappearance without occlusion suffices to elicit an identical increase in reported magnitude of the illusion.

Stimulus onset and offset can also be manipulated independent of the tilted line positions. If indeed the temporary disappearance of the dot elicits the same effects as occlusion, a follow-up experiment could manipulate the onset and offset of the dot to occur at other positions in the display than at the intersection with the tilted lines, so as to investigate what the main driving factors of the original occlusion effect are (for instance, the total visible trajectory regardless of the number of onset and offset events). If temporary disappearance and occlusion did not result in similar effects, occlusion can also be introduced at positions that do not coincide with the tilted lines - for instance by

placing black rectangles on parts of the trajectory. The results from this experiment will show whether the occlusion and/or disappearance effects are only effective immediately following the biased local motion signals at the intersections, or not.

7.4.4. A challenge to the hypothesis of locally biased motion signals

The root cause of the slalom illusion is proposed to lie in the points of intersection between the dot trajectory and the tilted lines. To test this hypothesis, the local intersections could be removed without removing the general context of the tilted lines. This can be done in two different ways.

First, temporally the tilted lines can be briefly blanked at the time of intersection, retaining the approach of the dot to the lines but removing the moment of intersection itself. Second, a gap could be introduced in the middle of the tilted lines, similarly retaining the lines but not the intersection signal. In both cases, it is expected that the slalom illusion will disappear compared to a control condition. If it does not, further investigations should be performed into the general context effects imposed by the tilted line modules.

7.4.5. Oc*clusion behind strong Kanizsafigures*

In Chapter 2, the slalom illusion was not observed when inducing illusory contours using a line variant of the Kanizsa figure, as an analogue of the classic slalom illusion. It can be suspected that the induced percept of lines was not strong, however, compared to the perceptually filled-in shapes of traditional Kanizsa figures. In Chapter 3, it was observed that the slalom illusion manifested itself even stronger when the motion path was partially occluded by a shape.

A new type of slalom display can then be created, where the triangular shapes of Chapter 3 are perceptually induced using classic Kanizsa inducers. The strong

perceptual presence of the figure can be determined independently, for instance by measuring the associated apparent brightening of the surface of the triangle. If the findings of Chapter 2 are again replicated using a strong Kanizsa figure, it can be asserted with greater certainty that an intersection with a locally defined contour is necessary to elicit the slalom illusion.

7.4.6. Independent manipulation of the speed between and behind occluders

In Chapter 4 it was found that shorter ISIs behind occluders caused a reduced magnitude of the slalom illusion. Cesàro and Agostini (1998) showed, however, that faster speed in general reduces the effect. There is a clear difference between these situations: in Chapter 4 the speed manipulation is not directly visible, in the work of Cesàro and Agostini it affects the entire visible trajectory. The speed effect of Cesàro and Agostini could then possibly be attributed to a reduced short-term adaptation at greater speeds for the horizontal motion signals, whereas this would not apply to speed increases for occluded trajectories. The speed between and behind occluders could be manipulated independently within the same display, to empirically chart their independent contribution and their interaction.

7.4.7. Disentangling straight from horizontal paths in the inverted slalom illusion

In Chapter 5, participants did not report smaller trajectory amplitudes when a veridically sinusoidal path intersected with vertical lines (inverted slalom illusion), even though this could have been expected from the hypothesis that motion direction is biased towards perpendicular angles at the points of intersection. It was concluded that the slalom illusion requires a veridically straight trajectory.

However, an alternate hypothesis could be that the path should in particular be horizontally straight. The general rotation of the slalom display was never manipulated. In this follow-up study, a horizontal condition could be compared to vertical and oblique rotations. It is interesting here to note that smooth pursuit eye movements have the greatest accuracy for horizontal motion (Rottach et al., 1996). If eye movements play a role in the strength of the slalom illusion – which is yet to be shown - it could potentially be demonstrated that rotation effects in the slalom illusion are also influenced by the degree of eye movement control in each direction.

7.4.8. Exploration of the contrast space, and manipulating the reliability of the trajectory

In Chapter 2, a reduced contrast of the inducing lines did not reduce the magnitude of the illusion. It would be interesting to explore this effect in a more systematic manner, and determine the contrast threshold at which it will start to affect the slalom illusion. According to the view put forward in the current thesis, this should only occur at a very low contrast.

The contrast of the moving dot was not manipulated in the current thesis. In a Bayesian view of visual perception, low contrast is often suggested to reduce the reliability of the immediate veridical information, in favour of biases from other sources (e.g. Weiss et al., 2002). By gradually and dynamically manipulating the contrast of the dot over the course of the trajectory, the reliability of the proposed 'veridical' and 'biased' parts of the trajectory could be systematically manipulated, allowing for clear predictions. For instance, according to the view put forward in the current thesis, the slalom effect should be larger if the dot contrast is higher around the line intersections. More generally, it could then be inferred which parts of the dot trajectory contribute positively, and which parts contribute negatively to the magnitude of the slalom illusion.

7.5. Conclusions

The motion path of an object is more than a contiguous sequence of position and motion direction signals. The slalom illusion demonstrates this, as a veridically horizontal dot trajectory is perceived as following a sinusoidal path, across a set of tilted lines alternatingly oriented in opposite directions. As a result of the findings presented in the current thesis, it was argued that the effect finds its origin in the intersection points of the trajectory and the tilted lines, but not at the earliest stages of the visual system. It is suggested that the motion path is integrated across occluders in a postdictive fashion, interpreting the motion direction signals as a coherent trajectory after the fact, in motion-sensitive areas of the visual cortex that have already transformed their visual inputs from a retinotopic coordinate system to spatiotopic coordinates. Indeed, the eye movement strategy used does not affect the occurrence of the illusion. The modulation of the motion path by the line pattern is dependent on the veridical trajectory being straight, leading to speculation that it relies on short-term adaptation in bi-phasic neurons to the constant motion direction. The postdictive motion path integration mechanism is proposed to reach a final trajectory interpretation by weighing the motion direction signals by their neuronal strength. Positional signals are easily overruled by the dot's positions implied by these motion direction signals. Finally, the slalom illusion is equally prevalent and equally large in magnitude across different retinal eccentricities.

Seen in a broader context, the slalom illusion is also more than merely a mistaken perception. It is a demonstration of the object motion path as a Gestalt, a coherent holistic analysis that is not just adding to its constituent input signals of position and motion direction, localised in space and time, but superseding them. A continued research program has been outlined, that will not only further elucidate empirical aspects of the illusion itself, but also contribute to the general understanding of the

174

visual perception of motion, position, and shape: how eye movements are abstracted from retinal inputs, signals become a Gestalt, and prediction relates to postdiction. With its combination of single-object trajectory motion and geometrical determinants, in full foveal view, the slalom illusion is a pertinent showcase of visual perception as an active reconstruction of reality.

Word count: **45,837**

8. References

Aaen-Stockdale, C., & Thompson, B. (2012). Visual motion: From cortex to percept. In S. Molotchnikoff & J. Rouat (Eds.), *Visual cortex - current status and perspectives*. Rijeka: InTech.

Adelson, E. H., & Movshon, J. A. (1982).Phenomenal coherence of moving visual patterns.*Nature*, *300*(5892), 523.

Akselrod, M., Herzog, M. H., & Öğmen, H. (2014).Tracing path-guided apparent motion in human primary visual cortex V1.*Scientific Reports*, *4*, 6063.

Alais, D., Apthorp, D., Karmann, A., & Cass, J. (2011). Temporal integration of movement: The time-course of motion streaks revealed by masking. *PLOS ONE*, *6*(12), e28675.

Albert, M. K. (2007). Mechanisms of modal and amodal interpolation.*Psychological Review*, *114*(2), 455–469.

Albrecht, D. G. (1995). Visual cortex neurons in monkey and cat: effect of contrast on the spatial and temporal phase transfer functions. *Visual Neuroscience*, *12*(6), 1191–121.

Albright, T. D., Desimone, R., & Gross, C. G. (1984).Columnar organization of directionally selective cells in visual area MT of the macaque.*Journal of Neurophysiology*, *51*(1), 16–31.

Allman, J. M., & Kaas, J. H. (1971).A representation of the visual field in the caudal third of the middle tempral gyrus of the owl monkey (Aotus trivirgatus). *Brain Research*, *31*(1), 85–105.

Allman, J., Miezin, F., & McGuinness, E. (1985).Direction- and velocity-specific responses from beyond the classical receptive field in the middle temporal visual area (MT).*Perception*, *14*(2), 105–126.

Amano, K., Edwards, M., Badcock, D. R., & Nishida, S. (2009). Adaptive pooling of visual motion signals by the human visual system revealed with a novel multi-element stimulus. *Journal of Vision*, *9*(3), 4.

Amano, K., Takeda, T., Haji, T., Terao, M., Maruya, K., Matsumoto, K., Nishida, S. (2012). Human neural responses involved in spatial pooling of locally ambiguous motion signals. *Journal of Neurophysiology*, *107*(12), 3493–3508.

Anstis, S. (2012). The furrow illusion: peripheral motion becomes aligned with stationary contours. *Journal of Vision*, *12*(12), 12.

Anstis, S. M. (1974). Letter: A chart demonstrating variations in acuity with retinal position. *Vision Research*, *14*(7), 589–592.

Anstis, S. M., & Ramachandran, V. S. (1985). Kinetic occlusion by apparent movement.*Perception*, *14*(2), 145–149.

Anstis, S., Verstraten, F. A. J., & Mather, G. (1998). The motion aftereffect.*Trends in Cognitive Sciences*, *2*(3), 111–117.

Avidan, G., Harel, M., Hendler, T., Ben-Bashat, D., Zohary, E., & Malach, R. (2002). Contrast sensitivity in human visual areas and its relationship to object recognition. *Journal of Neurophysiology*, *87*(6), 3102–3116.

Bahill, A.T., Clark, M.R., & Stark, L. (1975).The main sequence, a tool for studying human eye movements.*Mathematical Biosciences*, *24*, 191–204.

Bair, W., & Movshon, J. A. (2004).Adaptive temporal integration of motion in direction-selective neurons in macaque visual cortex.*The Journal of Neuroscience*, *24*(33), 7305–7323.

Baldwin, J., Burleigh, A., Pepperell, R., & Ruta, N. (2016).The perceived size and shape of objects in peripheral vision.*I-Perception*, *7*(4), 20416695166619.

Bar, M. (2003). A cortical mechanism for triggering top-down facilitation in visual object recognition.*Journal of Cognitive Neuroscience*, *15*(4), 600–609.

Becker, W., & Fuchs, A. F. (1985).Prediction in the oculomotor system: smooth pursuit during transient disappearance of a visual target. *Experimental Brain Research*, *57*(3), 562–575.

Beutter, B. R., & Stone, L. S. (1998). Human motion perception and smooth eye movements show similar directional biases for elongated apertures. *Vision Research*, *38*(9), 1273–1286.

Blakemore, C., Carpenter, R. H. S., & Georgeson, M. A. (1970). Lateral inhibition between orientation detectors in the human visual system. *Nature*, *228*(5266), 37.

Brainard, D. H. (1997).The Psychophysics Toolbox.*Spatial Vision*, *10*(4), 433–436.

Bremner, J. G., Johnson, S. P., Slater, A., Mason, U., Foster, K., Cheshire, A., &Spring, J. (2005). Conditions for young infants' perception of object trajectories. *Child Development*, *76*(5), 1029–1043.

Bridgeman, B., Heijden, A. H. C. V. der, & Velichkovsky, B. M. (1994). A theory of visual stability across saccadic eye movements.*Behavioral and Brain Sciences*, *17*, 247–292.

Bridgeman, B., Hendry, D., & Stark, L. (1975). Failure to detect displacement of the visual world during saccadic eye movements.*Vision Research*, *15*, 719–722.

Bullier, J. (2001).Integrated model of visual processing.*Brain Research. Brain Research Reviews*, *36*(2–3), 96–107.

Burke, L. (1952). On the tunnel effect.*Quarterly Journal of Experimental Psychology*, *4*(3), 121–138.

Burr, D. C. (1981).Temporal summation of moving images by the human visual system.*Proceedings of the Royal Society of London B*, *211*(1184), 321–339.

Burr, D. C., & Santoro, L. (2001). Temporal integration of optic flow, measured by contrast and coherence thresholds. *Vision Research*, *41*(15), 1891–1899.

Campbell, F. W., & Robson, J. G. (1968).Application of Fourier analysis to the visibility of gratings.*The Journal of Physiology*, *197*(3), 551–566.

Carandini, M. (2007).Melting the iceberg: Contrast invariance in visual cortex.*Neuron*, *54*(1), 11–13.

Carandini, M., Heeger, D. J., & Movshon, J. A. (1997). Linearity and normalization in simple cells of the macaque primary visual cortex.*The Journal of Neuroscience*, *17*(21), 8621–8644.

Carman, G. J., & Welch, L. (1992). Three-dimensional illusory contours and surfaces.*Nature*, *360*(6404), 585–587.

Cavanagh, P., Hunt, A. R., Afraz, A., & Rolfs, M. (2010). Visual stability based on remapping of attention pointers. *Trends in Cognitive Sciences*, *14*(4), 147–153.

Cesàro, A. L., & Agostini, T. (1998). The trajectory of a dot crossing a pattern of tilted lines is misperceived. *Perception & Psychophysics*, *60*(3), 518–523.

Changizi, M. A. (2001). 'Perceiving the present' as a framework for ecological explanations of the misperception of projected angle and angular size.*Perception*, *30*(2), 195–208.

Changizi, M. A., & Widders, D. M. (2002). Latency correction explains the classical geometrical illusions. *Perception*, *31*(10), 1241–1262.

Chukoskie, L., & Movshon, J. A. (2009). Modulation of visual signals in macaque MT and MST neurons during pursuit eye movement.*Journal of Neurophysiology*, *102*(6), 3225–3233.

Clark, A. (2013). Whatever next? Predictive brains, situated agents, and the future of cognitive science. *The Behavioral and Brain Sciences*, *36*(3), 181–204.

Cleland, B. G., & Levick, W. R. (1974).Properties of rarely encountered types of ganglion cells in the cat's retina and an overall classification.*The Journal of Physiology*, *240*(2), 457–492.

Clifford, C. W. G. (2014). The tilt illusion: Phenomenology and functional implications. *Vision Research*, *104*, 3–11.

Coren, S., & Girgus, J. S. (1978).*Seeing is deceiving: The psychology of visual illusions.* Oxford, England: Lawrence Erlbaum.

Cormack, R., Blake, R., & Hiris, E. (1992).Misdirected visual motion in the peripheral visual field.*Vision Research*, *32*(1), 73–8.

Crawford, J. D., & Vilis, T. (1991).Axes of eye rotation and Listing's law during rotations of the head.*Journal of Neurophysiology*, *65*(3), 407–423.

Davies, A. J., Chaplin, T. A., Rosa, M. G. P., & Yu, H.-H. (2016). Natural motion trajectory enhances the coding of speed in primate extrastriate cortex. *Scientific Reports*, *6*, 19739.

De Weerd, P., Vandenbussche, E., De Bruyn, B., & Orban, G. A. (1990).Illusory contour orientation discrimination in the cat.*Behavioural Brain Research*, *39*(1), 1–17.

DeAngelis, G. C., & Newsome, W. T. (1999).Organization of disparity-selective neurons in macaque area MT.*The Journal of Neuroscience*, *19*(4), 1398–1415.

Desimone, R., Schein, S. J., Moran, J., & Ungerleider, L. G. (1985). Contour, color and shape analysis beyond the striate cortex. *Vision Research*, *25*(3), 441–452.

Deubel, H. (2004). Localization of targets across saccades: Role of landmark objects. *Visual Cognition*, *11*(2–3), 173–202.

Deubel, H., Koch, C., & Bridgeman, B. (2010). Landmarks facilitate visual space constancy across saccades and during fixation. *Vision Research*, *50*(2), 249–259.

DeYoe, E. A., & Van Essen, D. C. (1985). Segregation of efferent connections and receptive field properties in visual area V2 of the macaque. *Nature*, *317*(6032), 58–61.

DeYoe, E. A., & Van Essen, D. C. (1988). Concurrent processing streams in monkey visual cortex. *Trends in Neurosciences*, *11*(5), 219–226.

Dorr, M., Martinetz, T., Gegenfurtner, K. R., & Barth, E. (2010). Variability of eye movements when viewing dynamic natural scenes. *Journal of Vision*, *10*(10), 28.

Dubner, R., & Zeki, S. M. (1971). Response properties and receptive fields of cells in an anatomically defined region of the superior temporal sulcus in the monkey. *Brain Research*, *35*(2), 528–532.

Duffy, C. J. (1998). MST neurons respond to optic flow and translational movement. *Journal of Neurophysiology*, *80*(4), 1816–1827.

Dürsteler, M. R., & Wurtz, R. H. (1988). Pursuit and optokinetic deficits following chemical lesions of cortical areas MT and MST. *Journal of Neurophysiology*, *60*(3), 940–965.

Dzhafarov, E. N., Sekuler, R., & Allik, J. (1993). Detection of changes in speed and direction of motion: reaction time analysis. *Perception & Psychophysics*, *54*(6), 733–75.

Eagleman, D. M., & Sejnowski, T. J. (2000). Motion integration and postdiction in visual awareness. *Science*, *287*(5460), 2036–2038.

Eagleman, D. M., & Sejnowski, T. J. (2003). The line-motion illusion can be reversed by motion signals after the line disappears. *Perception*, *32*(8), 963–968.

Edwards, M., & Crane, M. F. (2007). Motion streaks improve motion detection. *Vision Research*, *47*(6), 828–833.

Edwards, M., & Nishida, S. (2004). Contrast-reversing global-motion stimuli reveal local interactions between first- and second-order motion signals. *Vision Research*, *44*(16), 1941–195.

Emerson, R. C., & Gerstein, G. L. (1977). Simple striate neurons in the cat. I. Comparison of responses to moving and stationary stimuli. *Journal of Neurophysiology*, *40*(1), 119–135.

Enns, J. T., & Di Lollo, V. (2000). What's new in visual masking? *Trends in Cognitive Sciences*, *4*(9), 345–352.

Fahle, M., & Wehrhahn, C. (1991).Motion perception in the peripheral visual field.*Graefe's Archive for Clinical and Experimental Ophthalmology*, *229*(5), 430–436.

Faubert, J., & Herbert, A. M. (1999). The peripheral drift illusion: a motion illusion in the visual periphery. *Perception*, *28*(5), 617–621.

Faul, F., Erdfelder, E., Buchner, A., & Lang, A.-G. (2009). Statistical power analyses using G*Power 3.1: tests for correlation and regression analyses. *Behavior Research Methods*, *41*(4), 1149–116.

Feldman, J. (2009). Bayes and the simplicity principle in perception.*Psychological Review*, *116*(4), 875–887.

Fennema, C. L., & Thompson, W. B. (1979).Velocity determination in scenes containing several moving objects.*Computer Graphics and Image Processing*, *9*(4), 301–315.

Fineman, M. B., & Melingonis, M. P. (1977).The effect of a moving dot transversal on the Poggendorff illusion.*Perception & Psychophysics*, *21*(2), 153–156.

Freyd, J. J., & Finke, R. A. (1984). Representational momentum.*Journal of Experimental Psychology: Learning, Memory, and Cognition*, *10*(1), 126–132.

Friedman, H. S., Zhou, H., & von der Heydt, R. (2003). The coding of uniform colour figures in monkey visual cortex. *The Journal of Physiology*, *548*(2), 593–613.

Friston, K. (2010). The free-energy principle: a unified brain theory? *Nature Reviews Neuroscience*, *11*(2), 127–138.

Gauthier, G. M., Nommay, D., & Vercher, J. L. (1990).The role of ocular muscle proprioception in visual localization of targets.*Science*, *249*(4964), 58–61.

Geisler, W. S. (1999). Motion streaks provide a spatial code for motion direction. *Nature*, *400*(6739), 65–69.

Geisler, W. S., Albrecht, D. G., Crane, A. M., & Stern, L. (2001). Motion direction signals in the primary visual cortex of cat and monkey. *Visual Neuroscience*, *18*(4), 501–516.

Genç, E., Bergmann, J., Singer, W., & Kohler, A. (2011). Interhemispheric connections shape subjective experience of bistable motion. *Current Biology*, *21*(17), 1494–1499.

Ghim, H.-R. (1990). Evidence for perceptual organization in infants: Perception of subjective contours by young infants. *Infant Behavior and Development*, *13*(2), 221–248.

Gibson, J. J. (1950). The Perception of Visual Surfaces.*The American Journal of Psychology*, *63*(3), 367–384.

Gibson, J. J., & Radner, M. (1937). Adaptation, after-effect and contrast in the perception of tilted lines. I. Quantitative studies. *Journal of Experimental Psychology*, *20*(5), 453–467.

Glasser, D. M., Tsui, J. M. G., Pack, C. C., & Tadin, D. (2011). Perceptual and neural

consequences of rapid motion adaptation.*Proceedings of the National Academy of*

Sciences of the United States of America, *108*(45), E1080-1088.

Goodale, M. A., & Milner, A. D. (1992). Separate visual pathways for perception and action.

Trends in Neurosciences, *15*(1), 20–25.

Gregory, R. L. (1972). Cognitive Contours.*Nature*, *238*(5358), 51–52.

Greist, S. M., & Grier, J. B. (1977). The effect of retinal location on the magnitude of the

Poggendorff illusion.*Perception & Psychophysics*, *21*(3), 249–252.

Grosof, D. H., Shapley, R. M., & Hawken, M. J. (1993). Macaque V1 neurons can signal

'illusory' contours. *Nature*, *365*(6446), 550–552.

Grossberg, S., & Mingolla, E. (1985). Neural dynamics of perceptual grouping: Textures,

boundaries, and emergent segmentations. *Perception & Psychophysics*, *38*(2), 141–171.

Grzywacz, N. M., Watamaniuk, S. N. J., & Mckee, S. P. (1995).Temporal coherence theory

for the detection and measurement of visual motion.*Vision Research*, *35*(22), 3183–

3203.

Halko, M. A., Mingolla, E., & Somers, D. C. (2008).Multiple mechanisms of illusory

contour perception.*Journal of Vision*, *8*(11), 17.

Harrington, D. O. (1981).*The visual fields: Textbook and atlas of clinical perimetry.* St.

Louis: C. V. Mosby.

Hartmann, T. S., Bremmer, F., Albright, T. D., & Krekelberg, B. (2011). Receptive field

positions in area MT during slow eye movements.*The Journal of Neuroscience*, *31*(29),

10437–10444.

Hasson, U., Yang, E., Vallines, I. Heeger, D. J., & Rubin, N. (2008).A hierarchy of temporal receptive windows in human cortex. The Journal of Neuroscience, 28(10), 2539-255.

Hawken, M. J., Shapley, R. M., & Grosof, D. H. (1996).Temporal-frequency selectivity in monkey visual cortex.*Visual Neuroscience*, *13*(3), 477–492.

Hess, null, & Field, null. (1999). Integration of contours: new insights. *Trends in Cognitive Sciences*, *3*(12), 480–486.

Hess, R. F., & Dakin, S. C. (1997).Absence of contour linking in peripheral vision.*Nature*, *390*(6660), 602–604.

Higgins, J. S., Irwin, D. E., Wang, R. F., & Thomas, L. E. (2009).Visual direction constancy across eyeblinks.*Attention, Perception & Psychophysics*, *71*(7), 1607–1617.

Higgins, J. S., & Wang, R. F. (2010). A landmark effect in the perceived displacement of objects.*Vision Research*, *50*(2), 242–248.

Hochberg, J., & McAlister, E. (1953).A quantitative approach to figural 'goodness'.*Journal of Experimental Psychology*, *46*(5), 361.

Hochstein, S., & Ahissar, M. (2002). View from the top: hierarchies and reverse hierarchies in the visual system. *Neuron*, *36*(5), 791–804.

Hohnsbein, J., & Mateeff, S. (1998). The time it takes to detect changes in speed and direction of visual motion. *Vision Research*, *38*(17), 2569–2573.

Howe, C. Q., & Purves, D. (2005). Natural-scene geometry predicts the perception of angles and line orientation. *Proceedings of the National Academy of Sciences of the United States of America*, *102*(4), 1228–1233.

Hubbard, T. L. (1995). Environmental invariants in the representation of motion: Implied dynamics and representational momentum, gravity, friction, and centripetal force. *Psychonomic Bulletin & Review*, *2*(3), 322–338.

Hubel, D. H., & Wiesel, T. N. (1959). Receptive fields of single neurones in the cat's striate cortex. *The Journal of Physiology*, *148*(3), 574–591.

Hubel, D. H., & Wiesel, T. N. (1968). Receptive fields and functional architecture of monkey striate cortex. *The Journal of Physiology*, *195*(1), 215–243.

Ilg, U. J. (2008).The role of areas MT and MST in coding of visual motion underlying the execution of smooth pursuit.*Vision Research*, *48*(20),

Irwin, D. E., Yantis, S., & Jonides, J. (1983).Evidence against visual integration across saccadic eye movements.*Perception & Psychophysics*, *34*, 49–57.

Ito, H., & Yang, X. (2013). A short line segment squirms along a zigzag line. *I-Perception*, *4*(2), 141–143.

Johnson, C. A., & Scobey, R. P. (1980).Foveal and peripheral displacement thresholds as a function of stimulus luminance, line length and duration of movement.*Vision Research*, *20*(8), 709–715.

Johnson, J. S., & Olshausen, B. A. (2003).Timecourse of neural signatures of object recognition.*Journal of Vision*, *3*(7), 499–512.

Johnson, S. P., & Aslin, R. N. (1998).Young infants' perception of illusory contours in dynamic displays.*Perception*, *27*(3), 341–353.

Kanizsa, G. (1955). Margini quasi-percettivi in campi con stimolazione omogenea. *Rivista Di Psicologia*, *49*, 7–3.

Kanizsa, G. (1976). Subjective contours. *Scientific American*, *234*(4), 48–52.

Keller, E. L., & Heinen, S. J. (1991).Generation of smooth-pursuit eye movements: neuronal mechanisms and pathways. *Neuroscience Research*, *11*(2), 79–107.

Kelly, D. H., & Martinez-Uriegas, E. (1993). Measurements of chromatic and achromatic afterimages.*Journal of the Optical Society of America. A, Optics and Image Science*, *10*(1), 29–37.

Kerzel, D. (2003). Centripetal force draws the eyes, not memory of the target, toward the center. *Journal of Experimental Psychology. Learning, Memory, and Cognition*, *29*(3), 458–466.

Keysers, C., Xiao, D. K., Földiák, P., & Perrett, D. I. (2001).The speed of sight.*Journal of Cognitive Neuroscience, 13*(1), 90–101.

Khuu, S. K. (2012). The role of motion streaks in the perception of the kinetic Zollner illusion. *Journal of Vision*, *12*(6), 19

Khuu, S. K., & Kim, D. D. (2013). Using the kinetic Zollner illusion to quantify the interaction between form and motion information in depth.*Vision Research*, *83*, 48–55.

Kim, S.-H., Feldman, J., & Singh, M. (2012).Curved apparent motion induced by amodal completion. *Attention, Perception & Psychophysics*, *74*(2), 350–364.

Kim, S.-H., Feldman, J., & Singh, M. (2013).Perceived causality can alter the perceived trajectory of apparent motion. *Psychological Science*, *24*(4), 575–582.

Kleiner, M., Brainard, D., & Pelli, D. (2007). What's new in Psychtoolbox-3?Perception, 36, ECVP Abstract Supplement 14.

Koffka, K. (1935). *Principles of Gestalt psychology.*London, England: Lund Humphries.

Köhler, W. (1920). *Die physischen Gestalten in Ruhe und im stationären Zustand. Eine natur-philosophische Untersuchung*. Braunschweig, Germany: Vieweg und Sohn.

Komatsu, H., & Wurtz, R. H. (1989). Modulation of pursuit eye movements by stimulation of cortical areas MT and MST.*Journal of Neurophysiology*, *62*(1), 31–47.

Korte, A. (1915). *Kinematoskopische Untersuchungen*. Hogrefe.

Kourtzi, Z., Bülthoff, H. H., Erb, M., & Grodd, W. (2002). Object-selective responses in the human motion area MT/MST.*Nature Neuroscience*, *5*(1), 17–18.

Kourtzi, Z., & Kanwisher, N. (2001).Representation of perceived object shape by the human lateral occipital complex.*Science*, *293*(5534), 1506–1509.

Krauzlis, R. J., & Stone, L. S. (1999).Tracking with the mind's eye.*Trends in Neurosciences*, *22*(12), 544–55.

Krukowski, A. E., Pirog, K. A., Beutter, B. R., Brooks, K. R., & Stone, L. S. (2003). Human discrimination of visual direction of motion with and without smooth pursuit eye movements.*Journal of Vision*, *3*(11), 831–84.

Kumbhani, R. D., El-Shamayleh, Y., & Movshon, J. A. (2015). Temporal and spatial limits of pattern motion sensitivity in macaque MT neurons. *Journal of Neurophysiology*, *113*(7), 1977–1988.

Lamme, V. A., & Roelfsema, P. R. (2000).The distinct modes of vision offered by feedforward and recurrent processing.*Trends in Neurosciences*, *23*(11), 571–579.

Larsen, A., Madsen, K. H., Lund, T. E., & Bundesen, C. (2006). Images of illusory motion in primary visual cortex.*Journal of Cognitive Neuroscience*, *18*(7), 1174–118.

Lebranchu, P., Bastin, J., Pelegrini-Issac, M., Lehericy, S., Berthoz, A., & Orban, G. A. (2010). Retinotopic coding of extraretinal pursuit signals in early visual cortex. *Cerebral Cortex*, *20*(9), 2172–2187.

Lee, T. S., & Mumford, D. (2003).Hierarchical Bayesian inference in the visual cortex.*Journal of the Optical Society of America. A, Optics, Image Science, and Vision*, *20*(7), 1434–1448.

Lee, T. S., & Nguyen, M. (2001).Dynamics of subjective contour formation in the early visual cortex.*Proceedings of the National Academy of Sciences*, *98*(4), 1907–1911.

Leeuwenberg, E., & Boselie, F. (1988).Against the likelihood principle in visual form perception.*Psychological Review*, *95*(4), 485–491.

Lesher, G. W. (1995). Illusory contours: Toward a neurally based perceptual theory.*Psychon Bull Rev*, *2*(3), 279–321.

Levi, D. M., Klein, S. A., & Aitsebaomo, P. (1984). Detection and discrimination of the direction of motion in central and peripheral vision of normal and amblyopic observers.*Vision Research*, *24*(8), 789–8.

Levi, D. M., & Waugh, S. J. (1994). Spatial scale shifts in peripheral vernier acuity. *Vision Research*, *34*(17), 2215–2238.

Li, X., Cave, K. R., & Wolfe, J. M. (2008). Kanizsa-type subjective contours do not guide attentional deployment in visual search but line termination contours do. *Perception & Psychophysics*, *70*(3), 477–488.

Lisberger, S. G., Morris, E. J., & Tychsen, L. (1987).Visual motion processing and sensory-motor integration for smooth pursuit eye movements.*Annual Review of Neuroscience*, *10*(1), 97–129.

Lisberger, S. G., & Westbrook, L. E. (1985).Properties of visual inputs that initiate horizontal smooth pursuit eye movements in monkeys. *The Journal of Neuroscience*, *5*(6), 1662–1673.

Liu, J., Harris, A., & Kanwisher, N. (2002). Stages of processing in face perception: an MEG study. *Nature Neuroscience*, *5*(9), 910–916.

Liu, J., & Newsome, W. T. (2003). Functional organization of speed tuned neurons in visual area MT. *Journal of Neurophysiology*, *89*(1), 246–256.

Löw, A., Bentin, S., Rockstroh, B., Silberman, Y., Gomolla, A., Cohen, R., & Elbert, T. (2003).Semantic categorization in the human brain: Spatiotemporal dynamics revealed by magnetoencephalography. *Psychological Science*, *14*(4), 367–372.

MacKay, D. M. (2003).*Information Theory, Inference and Learning Algorithms*. Cambridge: Cambridge University Press.

Macknik, S. L., & Martinez-Conde, S. (2008). The role of feedback in visual masking and visualprocessing.*Advances in Cognitive Psychology*, *3*(1–2), 125–152.

Mäkelä, P., Whitaker, D., & Rovamo, J. (1993).Modelling of orientation discrimination across the visual field.*Vision Research*, *33*(5–6), 723–73.

Marcar, V. L., Zihl, J., & Cowey, A. (1997). Comparing the visual deficits of a motion blind patient with the visual deficits of monkeys with area MT removed. *Neuropsychologia*, *35*(11), 1459–1465.

Maunsell, J. H., & van Essen, D. C. (1983). The connections of the middle temporal visual area (MT) and their relationship to a cortical hierarchy in the macaque monkey.*The Journal of Neuroscience*, *3*(12), 2563–2586.

Maunsell, J. H., & Van Essen, D. C. (1987).Topographic organization of the middle temporal visual area in the macaque monkey: representational biases and the relationship to callosal connections and myeloarchitectonic boundaries. *The Journal of Comparative Neurology*, *266*(4), 535–555.

Maus, G. W., Fischer, J., & Whitney, D. (2013).Motion-dependent representation of space in area MT+.*Neuron*, *78*(3), 554–562.

McGraw, P. V., Whitaker, D., Skillen, J., & Chung, S. T. L. (2002). Motion adaptation distorts perceived visual position. *Current Biology*, *12*(23), 2042–2047.

McLeod, P. (1996). Preserved and impaired detection of structure from motion by a 'motion-blind' patient. *Visual Cognition*, *3*(4), 363–392.

Melcher, D. (2005). Spatiotopic transfer of visual-form adaptation across saccadic eye movements. *Current Biology*, *15*(19), 1745–1748.

Meyer, G. E., & Garges, C. (1979).Subjective contours and the Poggendorff illusion.*Perception & Psychophysics*, *26*(4), 302–304.

Michotte, A. (1946). *La perception de la causalité*. Louvain: Institut Superieur de Philosophie.

Michotte, A., Thinès, G. O., & Crabbé, G. (1964).*Les compléments amodaux des structures perceptives*. Louvain: Publications Universitaires.

Mital, P. K., Smith, T. J., Hill, R. L., & Henderson, J. M. (2011). Clustering of gaze during dynamic scene viewing is predicted by motion. *Cognitive Computation*, *3*(1), 5–24.

Montemayor, C., & Haladjian, H. H. (2015).*Consciousness, attention, and conscious attention*.MIT Press.

Morgan, M. J. (1999). The Poggendorff illusion: a bias in the estimation of the orientation of virtual lines by second-stage filters. *Vision Research*, *39*(14), 2361–238.

Movshon, J. A., & Newsome, W. T. (1996).Visual response properties of striate cortical neurons projecting to area MT in macaque monkeys.*The Journal of Neuroscience*, *16*(23), 7733–7741.

Movshon, J., Adelson, E. H., Gizzi, M. S., & Newsome, W. T. (1985).The analysis of moving visual patterns.In C. Chagas, R. Gattass, C.Gross (Eds.), *Pattern Recognition Mechanisms*.Rome: Vatican Press.

Muckli, L., Kohler, A., Kriegeskorte, N., & Singer, W. (2005). Primary visual cortex activity along the apparent-motion trace reflects illusory perception. *PLOS Biology*, *3*(8), e265.

Murray, M. M., Foxe, D. M., Javitt, D. C., & Foxe, J. J. (2004). Setting boundaries: brain dynamics of modal and amodal illusory shape completion in humans. *The Journal of Neuroscience*, *24*(31), 6898–6903.

Murray, M. M., & Herrmann, C. S. (2013). Illusory contours: a window onto the neurophysiology of constructing perception. *Trends in Cognitive Sciences*, *17*(9), 471–481.

Murray, S. O., & He, S. (2006). Contrast invariance in the human lateral occipital complex depends on attention. *Current Biology*, *16*(6), 606–611.

Murray, S. O., Kersten, D., Olshausen, B. A., Schrater, P., & Woods, D. L. (2002).Shape perception reduces activity in human primary visual cortex. *Proceedings of the National Academy of Sciences*, *99*(23), 15164–15169.

Nakajima, Y., & Sakaguchi, Y. (2016).Perceptual shrinkage of a one-way motion path with high-speed motion.*Scientific Reports*, *6*, 30592.

Navon, D. (1977). Forest before trees: The precedence of global features in visual perception. *Cognitive Psychology*, *9*(3), 353–383.

Newsome, W. T., & Paré, E. B. (1988).A selective impairment of motion perception

    following lesions of the middle temporal visual area (MT).*The Journal of*

    Neuroscience,8(6), 2201–2211.

Newsome, W. T., Wurtz, R. H., & Komatsu, H. (1988). Relation of cortical areas MT and

    MST to pursuit eye movements. II. Differentiation of retinal from extraretinal inputs.

    Journal of Neurophysiology, *60*(2), 604–62.

Nieder, A., & Wagner, H. (1999).Perception and neuronal coding of subjective contours in

    the owl.*Nature Neuroscience*, *2*(7), 660–663.

Nijhawan, R. (2002). Neural delays, visual motion and the flash-lag effect. *Trends in*

    Cognitive Sciences, *6*(9), 387.

Nishida, S., & Johnston, A. (1999). Influence of motion signals on the perceived position of

    spatial pattern. *Nature*, *397*(6720), 610–612.

Novak, S. (1966).Effects of free inspection and fixation on magnitude of Poggendorff

    illusion.*Perceptual and Motor Skills*, *23*(2), 663.

Nundy, S., Lotto, B., Coppola, D., Shimpi, A., & Purves, D. (2000). Why are angles

    misperceived? *Proceedings of the National Academy of Sciences of the United States of*

    America, *97*(10), 5592–5597.

Okuyama-Uchimura, F., & Komai, S. (2016).Mouse ability to perceive subjective

    contours.*Perception*, *45*(3), 315–327.

Ong, W. S., & Bisley, J. W. (2011).A lack of anticipatory remapping of retinotopic receptive

    fields in area MT.*The Journal of Neuroscience, 3*1(29), 10432-10436.

Orban, G. A. (1985). Velocity tuned cortical cells and human velocity discrimination. In

    Brain Mechanisms and Spatial Vision (pp. 371–388). Dordrecht: Springer.

Orban, G. A., Kennedy, H., & Bullier, J. (1986). Velocity sensitivity and direction selectivity of neurons in areas V1 and V2 of the monkey: influence of eccentricity. *Journal of Neurophysiology*, *56*(2), 462–48.

Otsuka, Y., & Yamaguchi, M. K. (2003).Infants' perception of illusory contours in static and moving figures.*Journal of Experimental Child Psychology*, *86*(3), 244–251.

Pack, C. C., Berezovskii, V. K., & Born, R. T. (2001). Dynamic properties of neurons in cortical area MT in alert and anaesthetized macaque monkeys.*Nature*, *414*(6866), 905–908.

Pack, C. C., & Born, R. T. (2001). Temporal dynamics of a neural solution to the aperture problem in visual area MT of macaque brain.*Nature*, *409*(6823), 1040–1042.

Pack, C. C., Conway, B. R., Born, R. T., & Livingstone, M. S. (2006). Spatiotemporal structure of nonlinear subunits in macaque visual cortex.*The Journal of Neuroscience*, *26*(3), 893–907.

Pack, C. C., Livingstone, M. S., Duffy, K. R., & Born, R. T. (2003). End-stopping and the aperture problem: two-dimensional motion signals in macaque V1. *Neuron*, *39*(4), 671–68.

Parker, D. M. (1974).Evidence for the inhibition hypothesis in expanded angle illusion.*Nature*, *250*(5463), 265–266.

Parovel, G., & Casco, C. (2006).The psychophysical law of speed estimation in Michotte's causal events.*Vision Research*, *46*(24), 4134–4142.

Pearson, P. M., & Kingdom, F. a. A. (2002). Texture-orientation mechanisms pool colour and luminance contrast. *Vision Research*, *42*(12), 1547–1558.

Pelli, D. G. (1997). The VideoToolbox software for visual psychophysics: transforming numbers into movies. *Spatial Vision*, *10*(4), 437–442.

Perge, J. A., Borghuis, B. G., Bours, R. J. E., Lankheet, M. J. M., & van Wezel, R. J. A. (2005). Temporal dynamics of direction tuning in motion-sensitive macaque area MT. *Journal of Neurophysiology*, *93*(4), 2104–2116.

Peterhans, E., & von der Heydt, R. (1989). Mechanisms of contour perception in monkey visual cortex. II. Contours bridging gaps. *The Journal of Neuroscience*, *9*(5), 1749–1763.

Pirenne, M. H., Compbell, F. W., Robson, J. G., & Mackay, D. M. (1958). Moving visual images produced by regular stationary patterns. *Nature*, *181*(4605), 362–363.

Pola, J., & Wyatt, H. J. (1997). Offset dynamics of human smooth pursuit eye movements: Effects of target presence and subject attention. *Vision Research*, *37*(18), 2579–2595.

Price, N. S. C., & Prescott, D. L. (2012). Adaptation to direction statistics modulates perceptual discrimination. *Journal of Vision*, *12*(6), 1-17.

Priebe, N. J., Churchland, M. M., & Lisberger, S. G. (2002). Constraints on the source of short-term motion adaptation in macaque area MT. I. the role of input and intrinsic mechanisms.*Journal of Neurophysiology*, *88*(1), 354–369.

Priebe, N. J., & Lisberger, S. G. (2002). Constraints on the source of short-term motion adaptation in macaque area MT. II.tuning of neural circuit mechanisms. *Journal of Neurophysiology*, *88*(1), 370–382.

Prince, S. J., Pointon, A. D., Cumming, B. G., & Parker, A. J. (2000). The precision of single neuron responses in cortical area V1 during stereoscopic depth judgments.*The Journal of Neuroscience*, *20*(9), 3387–34.

Ramachandran, V. S., & Anstis, S. M. (1986).The perception of apparent motion.*Scientific American*, *254*(6), 102–109.

Rao, R. P., & Ballard, D. H. (1999). Predictive coding in the visual cortex: a functional interpretation of some extra-classical receptive-field effects. *Nature Neuroscience*, *2*(1), 79–87.

Rashbass, C. (1961). The relationship between saccadic and smooth tracking eye movements.*The Journal of Physiology*, *159*(2), 326–338.

Recanzone, G. H., & Wurtz, R. H. (1999). Shift in smooth pursuit initiation and MT and MST neuronal activity under different stimulus conditions. *Journal of Neurophysiology*, *82*(4), 1710–1727.

Robinson, D. A. (1965). The mechanics of human smooth pursuit eye movement. *The Journal of Physiology*, *180*(3), 569–591.

Rodman, H. R., Gross, C. G., & Albright, T. D. (1989).Afferent basis of visual response properties in area MT of the macaque. I. Effects of striate cortex removal. *The Journal of Neuroscience*, *9*(6), 2033–205.

Rottach, K. G., Zivotofsky, A. Z., Das, V. E., Averbuch-Heller, L., Discenna, A. O., Poonyathalang, A., & Leigh, R. J. (1996). Comparison of horizontal, vertical and diagonal smooth pursuit eye movements in normal human subjects.*Vision Research*, *36*(14), 2189–2195.

Sceniak, M. P., Hawken, M. J., & Shapley, R. (2001).Visual spatial characterization of macaque V1 neurons.*Journal of Neurophysiology*, *85*(5), 1873–1887.

Sceniak, M. P., Ringach, D. L., Hawken, M. J., & Shapley, R. (1999). Contrast's effect on spatial summation by macaque V1 neurons.*Nature Neuroscience*, *2*(8), 733–739.

Schenk, T.,& McIntosh, R. D. (2010). Do we have independent visual streams for
perception and action? *Cognitive Neuroscience*, *1*(1), 52–62.

Scherzer, T. R., & Ekroll, V. (2009). Intermittent occlusion enhances the smoothness of
sampled motion. *Journal of Vision*, *9*(10), 16–16.

Schira, M. M., Tyler, C. W., Breakspear, M., & Spehar, B. (2009).The foveal confluence in
human visual cortex.*Journal of Neuroscience*, *29*(28), 9050–9058.

Schmider, E., Ziegler, M., Danay, E., Beyer, L., & Bühner, M. (2010). Is it really robust?
Reinvestigating the robustness of ANOVA against violations of the normal distribution
assumption.*Methodology: European Journal of Research Methods for the Behavioral
and Social Sciences*, *6*(4), 147–151.

Schumann, F. (1900). Beiträge zur Analyse der Gesichtswahrnehmungen. Zur Schätzung
räumlicher Grössen. *Zeitschrift Für Psychologie Und Physiologie Der Sinnersorgane*,
24, 1–33.

Schwarzkopf, D. S., Song, C., & Rees, G. (2011). The surface area of human V1 predicts the
subjective experience of object size. *Nature Neuroscience*, *14*(1), 28–3.

Sekuler, A. B., Sekuler, R., & Sekuler, E. B. (1990). How the visual system detects changes
in the direction of moving targets. *Perception*, *19*(2), 181–195.

Shannon, C. E. (1948). A mathematical theory of communication.*Bell System Technical
Journal*, *27*(3), 379–423.

Shepard, R. N., & Zare, S. L. (1983).Path-guided apparent motion.*Science*, *220*(4597), 632–
634.

Sigman, E., & Rock, I. (1974). Stroboscopic movement based on perceptual intelligence.
Perception, *3*(1), 9–28.

Simoncelli, E. P., & Heeger, D. J. (1998). A model of neuronal responses in visual area MT. *Vision Research*, *38*(5), 743–761.

Singh, M. (2004). Modal and amodal completion generate different shapes. *Psychological Science*, *15*(7), 454–459.

Singh, M., & Fulvio, J. M. (2005).Visual extrapolation of contour geometry.*Proceedings of the National Academy of Sciences*, *102*(3), 939–944.

Sinico, M., Parovel, G., Casco, C., & Anstis, S. (2009). Perceived shrinkage of motion paths.*Journal of Experimental Psychology. Human Perception and Performance*, *35*(4), 948–957.

Skottun, B. C., Bradley, A., Sclar, G., Ohzawa, I., & Freeman, R. D. (1987). The effects of contrast on visual orientation and spatial frequency discrimination: a comparison of single cells and behavior. *Journal of Neurophysiology*, *57*(3), 773–786.

Smeets, J., & Brenner, E. (2004). Curved movement paths and the Hering illusion: Positions or directions? *Visual Cognition*, *11*(2–3), 255–274.

Souman, J., & Freeman, T. (2008). Motion perception during sinusoidal smooth pursuit eye movements: signal latencies and non-linearities. *Journal of Vision*, *8*(14:10), 1–14.

Sovrano, V. A., & Bisazza, A. (2009). Perception of subjective contours in fish.*Perception*, *38*(4), 579–59.

Sperry, R. W. (1950). Neural basis of the spontaneous optokinetic response produced by visual inversion.*Journal of Comparative and Physiological Psychology*, *43*, 482–489.

Spillmann, L., Otte, T., Hamburger, K., & Magnussen, S. (2006). Perceptual filling-in from the edge of the blind spot.*Vision Research*, *46*(25), 4252–4257.

Stone, L. S., & Krauzlis, R. J. (2003).Shared motion signals for human perceptual decisions and oculomotor actions. *Journal of Vision*, *3*(11), 725–736.

Stone, L. S., Watson, A. B., & Mulligan, J. B. (1990).Effect of contrast on the perceived direction of a moving plaid.*Vision Research*, *30*(7), 1049–1067.

Stumpf, P. (1911). Über die Abhängigkeit der visuellen Bewegungsrichtung und negativen Nachbildes von den Reizvorgangen auf der Netzhaut. *Zeitschrift Fur Psychologie*, *59*, 321–33.

Sumner, P., Anderson, E. J., Sylvester, R., Haynes, J.-D., & Rees, G. (2008).Combined orientation and colour information in human V1 for both L-M and S-cone chromatic axes.*NeuroImage*, *39*(2), 814–824.

Swanston, M. T. (1984). Displacement of the path of perceived movement by intersection with static contours.*Perception & Psychophysics*, *36*(4), 324–328.

Tabachnick, B. G., & Fidell, L. S. (2007). Using Multivariate Statistics (5th ed.). *New York: Allyn and Bacon.*

Tadin, D., & Lappin, J. S. (2005). Optimal size for perceiving motion decreases with contrast. *Vision Research*, *45*(16), 2059–2064.

Tapia, E., Breitmeyer, B. G., & Jacob, J. (2011).Metacontrast masking with texture-defined second-order stimuli.*Vision Research*, *51*(23), 2453–2461.

Thier, P., & Ilg, U. J. (2005). The neural basis of smooth-pursuit eye movements.*Current Opinion in Neurobiology*, *15*(6), 645–652.

Thorpe, S., Fize, D., & Marlot, C. (1996). Speed of processing in the human visual system. *Nature*, *381*(6582), 520–522.

Tibber, M. S., Melmoth, D. R., & Morgan, M. J. (2008). Biases and sensitivities in the Poggendorff effect when driven by subjective contours. *Investigative Ophthalmology & Visual Science*, *49*(1), 474–478.

Tong, F. (2003). Primary visual cortex and visual awareness.*Nature Reviews. Neuroscience*, *4*(3), 219–229.

Tulunay-Keesey, U. (1982). Fading of stabilized retinal images.*Journal of the Optical Society of America*, *72*(4), 440–447.

Ungerleider, L., & Mishkin, M. (1982).Two cortical visual systems.In D. J. Ingle, M. A. Goodale, & R. J. W. Mansfield (Eds.), *Analysis of visual behavior (pp. 549-586)*. Cambridge: MIT Press.

Valenza, E., & Bulf, H. (2007).The role of kinetic information in newborns' perception of illusory contours.*Developmental Science*, *10*(4), 492–501.

van de Grind, W. A., Koenderink, J. J., & van Doorn, A. J. (1987). Influence of contrast on foveal and peripheral detection of coherent motion in moving random-dot patterns. *Journal of the Optical Society of America. A, Optics and Image Science*, *4*(8), 1643–1652.

Van der Helm, P. (2014). *Simplicity in vision: A multidisciplinary account of perceptual organization*. Cambridge: Cambridge University Press.

Van Essen, D. C., Maunsell, J. H., & Bixby, J. L. (1981). The middle temporal visual area in the macaque: myeloarchitecture, connections, functional properties and topographic organization. *The Journal of Comparative Neurology*, *199*(3), 293–326.

Verghese, P., & McKee, S. P. (2002).Predicting future motion.*Journal of Vision*, *2*(5), 413–423.

Verghese, P., Watamaniuk, S. N., McKee, S. P., & Grzywacz, N. M. (1999). Local motion detectors cannot account for the detectability of an extended trajectory in noise. *Vision Research*, *39*(1), 19–3.

Vogels, R. (1999). Categorization of complex visual images by rhesus monkeys. Part 2: single-cell study. *European Journal of Neuroscience*, *11*(4), 1239–1255.

von der Heydt, R., Peterhans, E., & Baumgartner, G. (1984). Illusory contours and cortical neuron responses.*Science*, *224*(4654), 1260–1262.

von Helmholtz, H. (1924). *Helmholtz's treatise on physiological optics, Vol. 1, Translation from the 3rd German edition.* Rochester: Optical Society of America.

von Holst, E., & Mittelstaedt, H. (1950). Das Reafferenzprinzip. *Naturwissenschaften*, *37*(20), 464–476.

Wagemans, J., Elder, J. H., Kubovy, M., Palmer, S. E., Peterson, M. A., Singh, M., & von der Heydt, R. (2012). A century of Gestalt psychology in visual perception I. Perceptual grouping and figure-ground organization.*Psychological Bulletin*, *138*(6), 1172–1217.

Wallach, H. (1935). Über visuell wahrgenommene Bewegungsrichtung. *Psychologische Forschung*, *20*(1), 325–38.

Walsh, C., & Polley, E. H. (1985).The topography of ganglion cell production in the cat's retina.*The Journal of Neuroscience*, *5*(3), 741–75.

Watamaniuk, S. N. J. (2005). The predictive power of trajectory motion.*Vision Research*, *45*(24), 2993–3003.

Watamaniuk, S. N. J., & McKee, S. P. (1995).Seeing motion behind occluders.*Nature*, *377*(6551), 729–73.

Watamaniuk, S. N. J., & Sekuler, R. (1992).Temporal and spatial integration in dynamic random-dot stimuli.*Vision Research*, *32*(12), 2341–2347.

Watanabe, K. (2005). The motion-induced position shift depends on the visual awareness of motion. *Vision Research*, *45*(19), 2580–2586.

Wehrhahn, C., & Westheimer, G. (1990). How vernier acuity depends on contrast. *Experimental Brain Research*, *80*(3), 618–62.

Weiss, Y., Simoncelli, E. P., & Adelson, E. H. (2002).Motion illusions as optimal percepts.*Nature Neuroscience*, *5*(6), 598–604.

Wenderoth, P., & Johnson, M. (1983). Relationships between the kinetic, alternating-line, and Poggendorff illusions: The effects of interstimulus interval, inducing parallels, and fixation. *Perception & Psychophysics*, *34*(3), 273–279.

Wenderoth, P., White, D., & Beh, H. (1978).The effects of peripheral and central fixation on a Poggendorff-like vernier alignment task.*Perception & Psychophysics*, *24*(4), 377–386.

Wertheimer, M. (1912). Experimentelle Studien über das Sehen von Bewegung. *Zeitschrift Für Psychologie Und Physiologie Der Sinnesorgane*, *61*, 161–265.

Wertheimer, M. (1938).Gestalt theory.In W. D. Ellis (Ed.), *A source book of Gestalt psychology* (pp. 1–11). London, England: Routledge & Kegan Paul.

Westheimer, G., & Wehrhahn, C. (1997).Real and virtual borders in the Poggendorff illusion.*Perception*, *26*(12), 1495–1501.

Whitney, D. (2002). The influence of visual motion on perceived position.*Trends in Cognitive Sciences*, *6*(5), 211–216.

Williams, L. R., & Jacobs, D. W. (1997). Stochastic completion fields; a neural model of illusory contour shape and salience.*Neural Computation*, *9*(4), 837–858.

Wilming, N., Onat, S., Ossandón, J. P., Açık, A., Kietzmann, T. C., Kaspar, K., König, P. (2017). An extensive dataset of eye movements during viewing of complex images.*Scientific Data*, *4*, 160126.

Wilson, H. R., Ferrera, V. P., & Yo, C. (1992).A psychophysically motivated model for two-dimensional motion perception.*Visual Neuroscience*, *9*(1), 79–97.

Wuerger, S., Shapley, R., & Rubin, N. (1996). 'On the visually perceived direction of motion' by Hans Wallach: 60 years later. *Perception*, *25*(11), 1317–1367.

Yantis, S. (1995). Perceived continuity of occluded visual objects.*Psychological Science*, *6*(3), 182–186.

Yasui, S., & Young, L. R. (1975).Perceived visual motion as effective stimulus to pursuit eye movement system.*Science*, *190*(4217), 906–908.

Yo, C., & Wilson, H. R. (1992). Perceived direction of moving two-dimensional patterns depends on duration, contrast and eccentricity. *Vision Research*, *32*(1), 135–147.

Zago, M., McIntyre, J., Senot, P., & Lacquaniti, F. (2009). Visuo-motor coordination and internal models for object interception. *Experimental Brain Research*, *192*(4), 571–604.

Zanforlin, M. (1981).Visual perception of complex forms (anomalous surfaces) in chicks.*Italian Journal of Psychology*, *8*(1), 1–16.

Zihl, J., Von Cramon, D., & Mai, N. (1983). Selective disturbance of movement vision after bilateral brain damage.*Brain*, *106*(2), 313–34.

Zirnsak, M., & Moore, T. (2014). Saccades and shifting receptive fields: anticipating consequences or selecting targets? *Trends in Cognitive Sciences*, *18*(12), 621–628.

9. Appendices

Appendix 1. Ethical approval for the research project

Sheffield Hallam University

Our Ref AM/KW/21C-2014
11June 2014

t.gheorghes@shu.ac.uk
Development and Society

INTERNAL
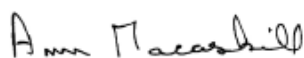
Dear Tamara,

Request for Ethical Approval of Research Project

Your research project entitled "The effect of context on the perceived trajectory of a moving object" has been submitted for ethical review to the Faculty's rapporteurs and I am pleased to confirm that they have approved your project.

I wish you every success with your research project.

Yours sincerely

Professor A Macaskill
Chair
Faculty Research Ethics Committee

Office address :
Business Support Team
Faculty of Development & Society
Sheffield Hallam University
Unit 4, Sheffield Science Park
Howard Street, Sheffield, S1 1WB
Tel: 0114-225 3308
E-mail: DS-ResearchEthics@shu.ac.uk

Appendix 2. Participant information sheet

The effect of context on the perceived trajectory of a moving object

Participant information sheet

We would like to invite you to take part in our research study. Before you decide, we would like you to understand why the research is being done and what it would involve.

What is the purpose of this study?
The aim of this study is to investigate how visual perception is affected by changes in the visual context.

Why have I been invited to take part? In order to take part in this study, you need to be at least 18 year old and have normal, or corrected to normal, vision.

Do I have to take part? Your participation is voluntary. You can leave the study at any time without being penalised or disadvantaged in any way, even if you have already completed some or all of the tasks. If you choose to leave the study before completion, your data will be destroyed and not used in any subsequent analyses. Please note that once the task has been completed, your personal results will no longer be traceable, and thus it will be impossible to withdraw them afterwards.

What will I do if I decide to participate? If you decide to participate in this study, you will be presented with some visual stimuli on a computer monitor. You will be asked to judge the trajectory of a moving dot, or a moving line, and input your answer by using the computer keyboard. The process should not take longer than 30 minutes.

Who has reviewed the study? This research project has been reviewed and approved by the Research Ethics Committee at Sheffield Hallam University.

What are the risks and advantages of participating? There are no known risks associated with participating in this study. The task is behavioural, there are no invasive procedures and no sensitive information will be presented to you or asked from you.

Will my taking part in the study be kept confidential? Any information you provide is confidential, and will only be available to the principal researcher. Once collected, the data you provide will be coded so as to be anonymous. No information that could lead to your identification will be disclosed. Data will be stored securely on the premises of Sheffield Hallam University and in the researcher's computer. Aggregated results may be published in academic journals and made available to the wider community by being deposited in appropriate data archives.

For further information about this research project, please contact the researcher Tamara Gheorghes.
E-mail: t.gheorghes@shu.ac.uk **Tel**: 01142252217
Address: Sheffield Hallam University, Collegiate Campus, Room HC1.05, Heart of the Campus Building, S10 2BQ

Appendix 3. Participant consent form

205

CONSENT FORM

Title of Project: The effect of context on the perceived trajectory of a moving object

Name of Researcher: Tamara Gheorghes

Please initial each box:

1. I confirm that I have read and understand the Information Sheet for the above study.

2. I have had the opportunity to consider the information and ask any questions and I understand that I may ask further questions at any point.

3. I understand that all information I give will be confidential and only accessible to the research team.

4. I understand that my participation is voluntary and that I am free to withdraw at any time without giving a reason.

5. I agree to take part in the above research project under the conditions set out in the Information Sheet.

6. I consent to the information collected for the purposes of this research study, once anonymised, to be used in future studies and publications.

Participant's Name: _____

Participant's Signature:_____ Date_____

Researcher's Name:_____

Researcher's Signature:_____

Researcher's contact details:
Tamara Gheorghes
t.gheorghes@shu.ac.uk
01142252217
Sheffield Hallam University, Collegiate Campus, Room HC1.05, Heart of the Campus Building, S10 2BQ
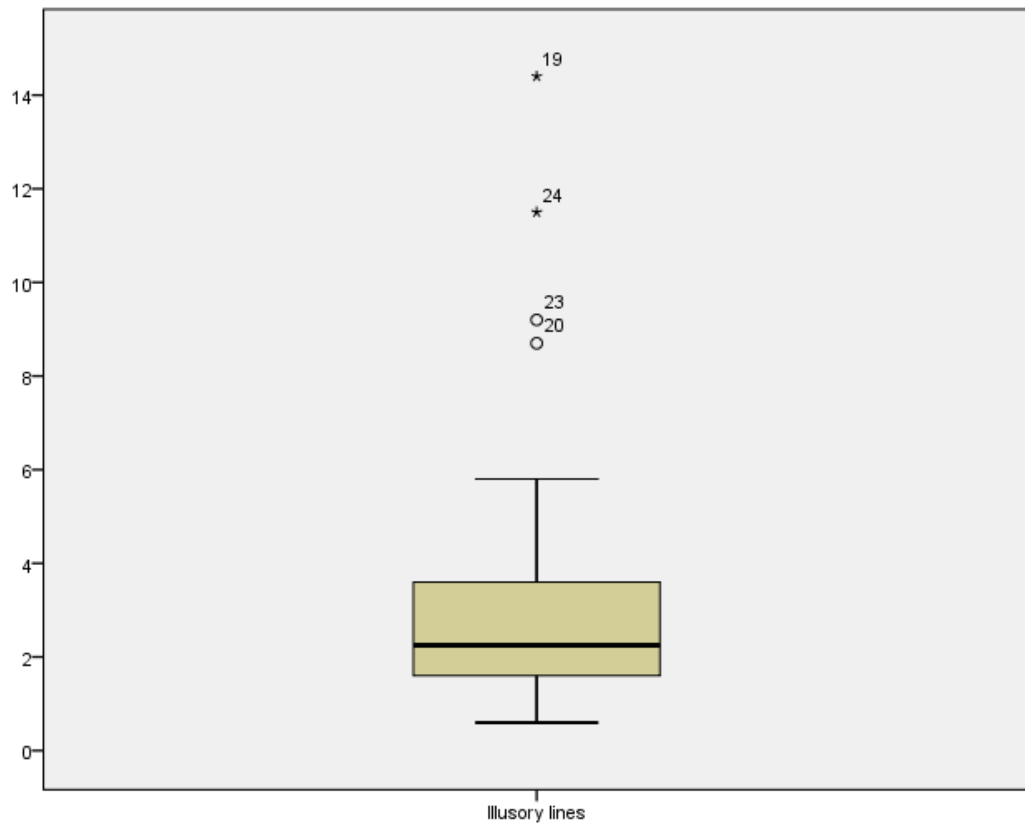
Appendix 4.Boxplots for the data from Experiment 1 Chapter 2.
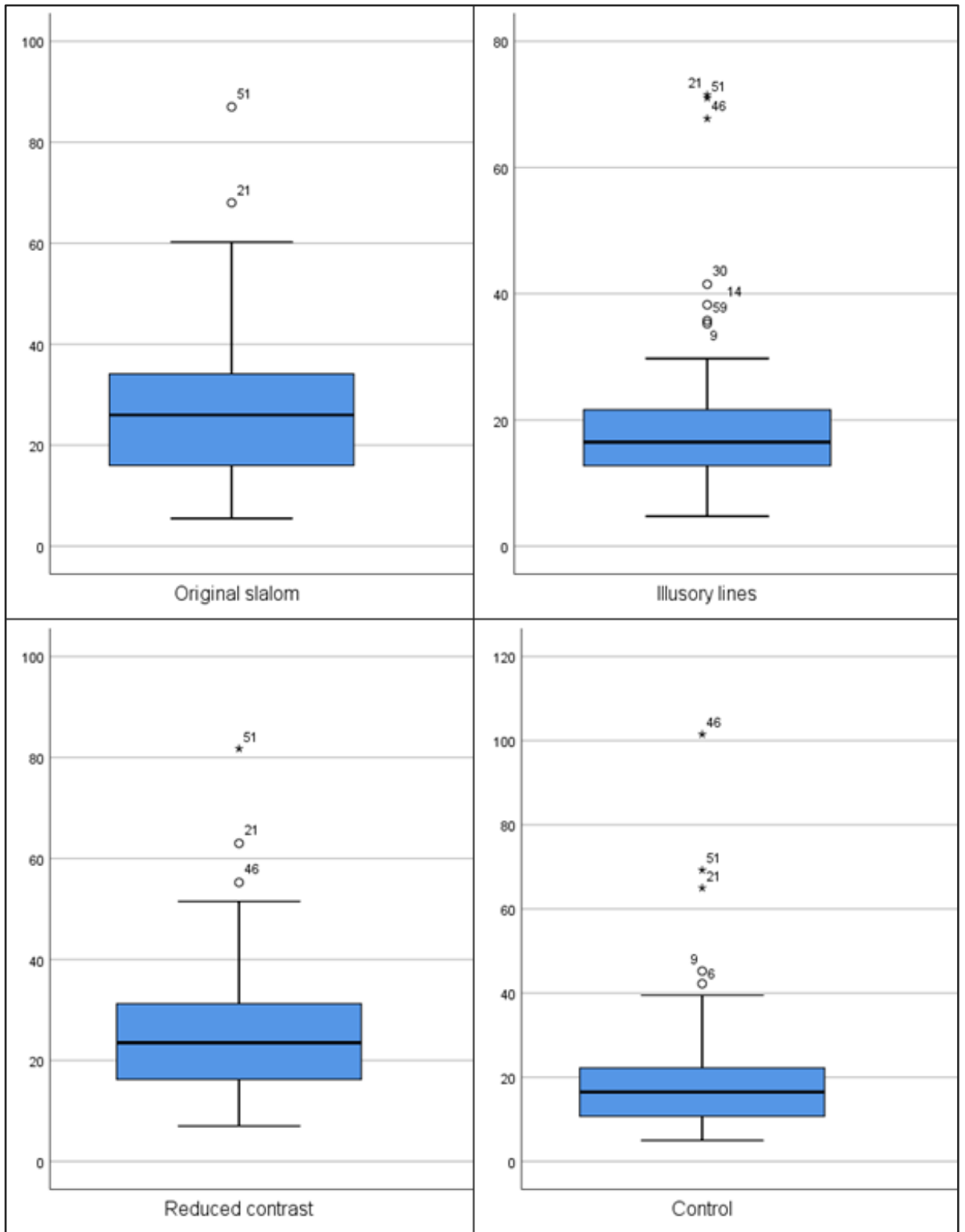
Appendix 5.Descriptive statistics for the data from Experiment 1 Chapter 2, after the
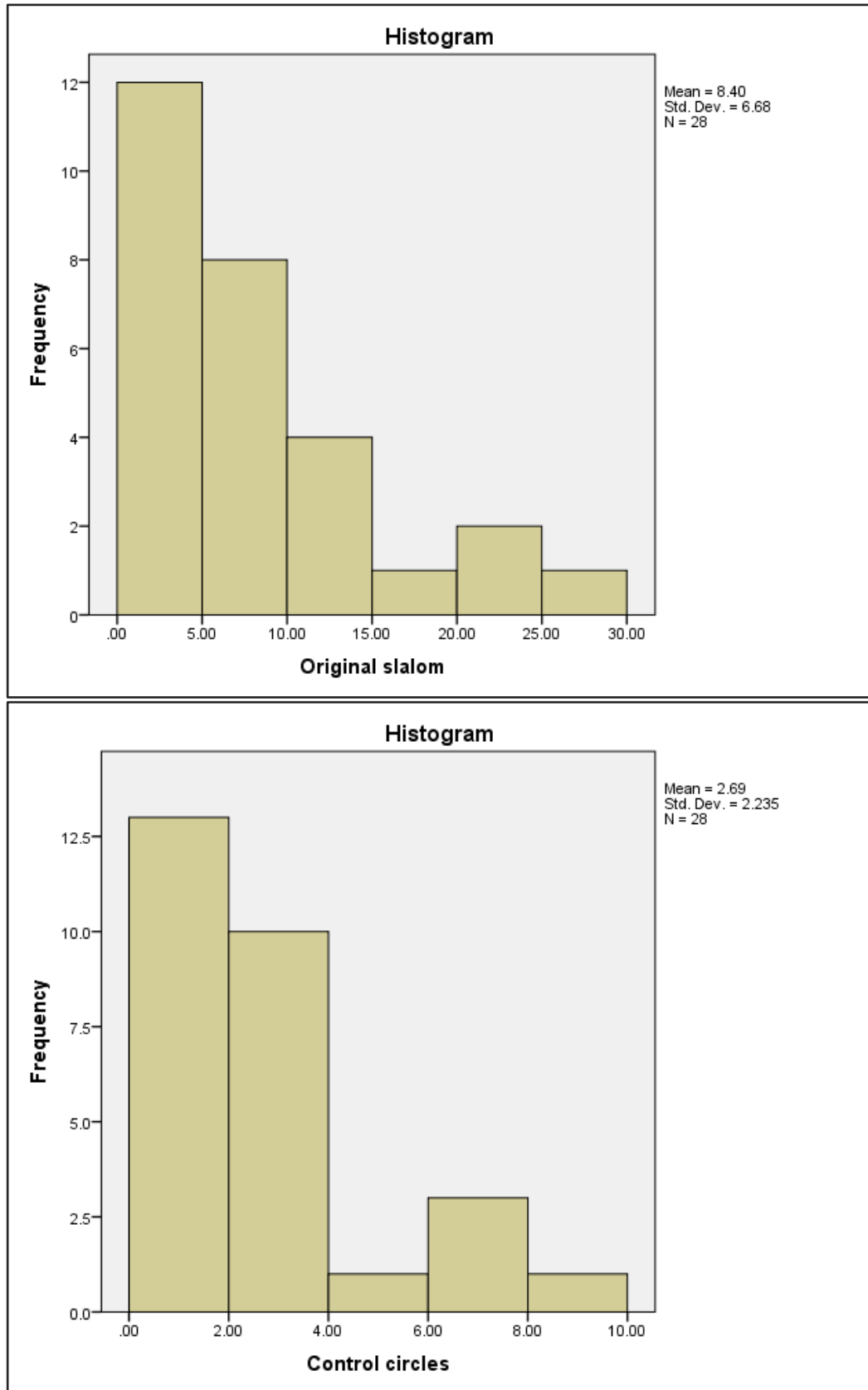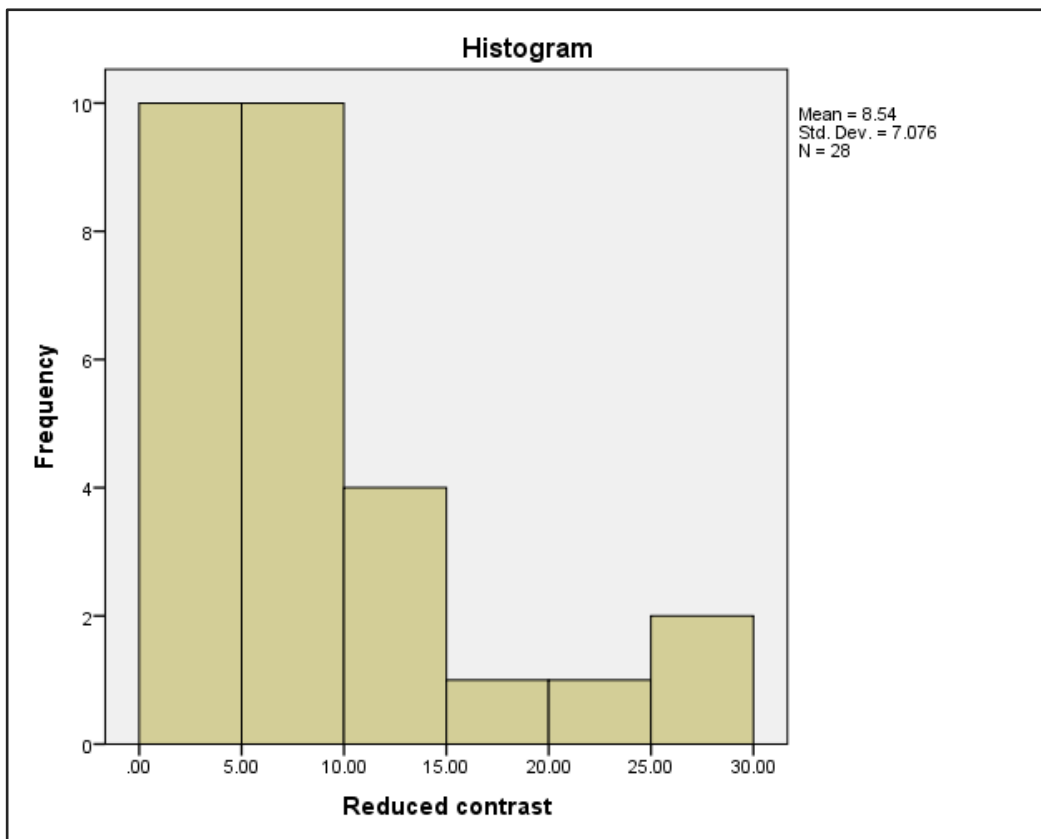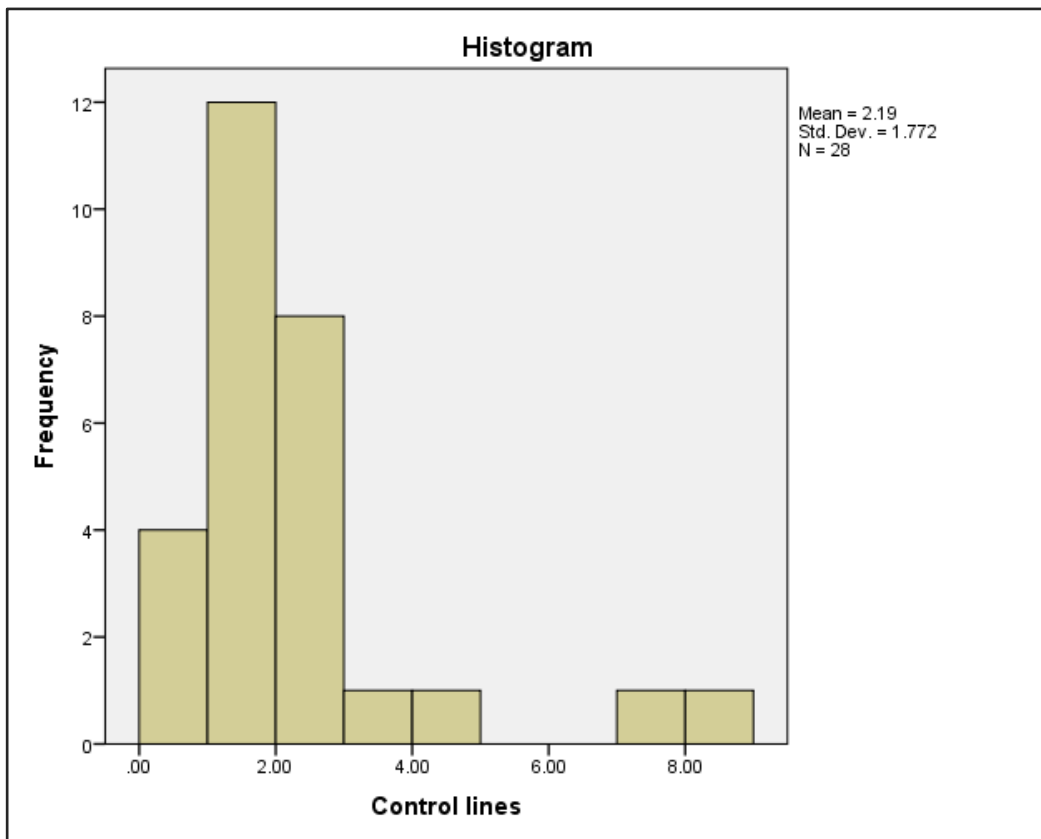
outliers were removed.

Descriptives

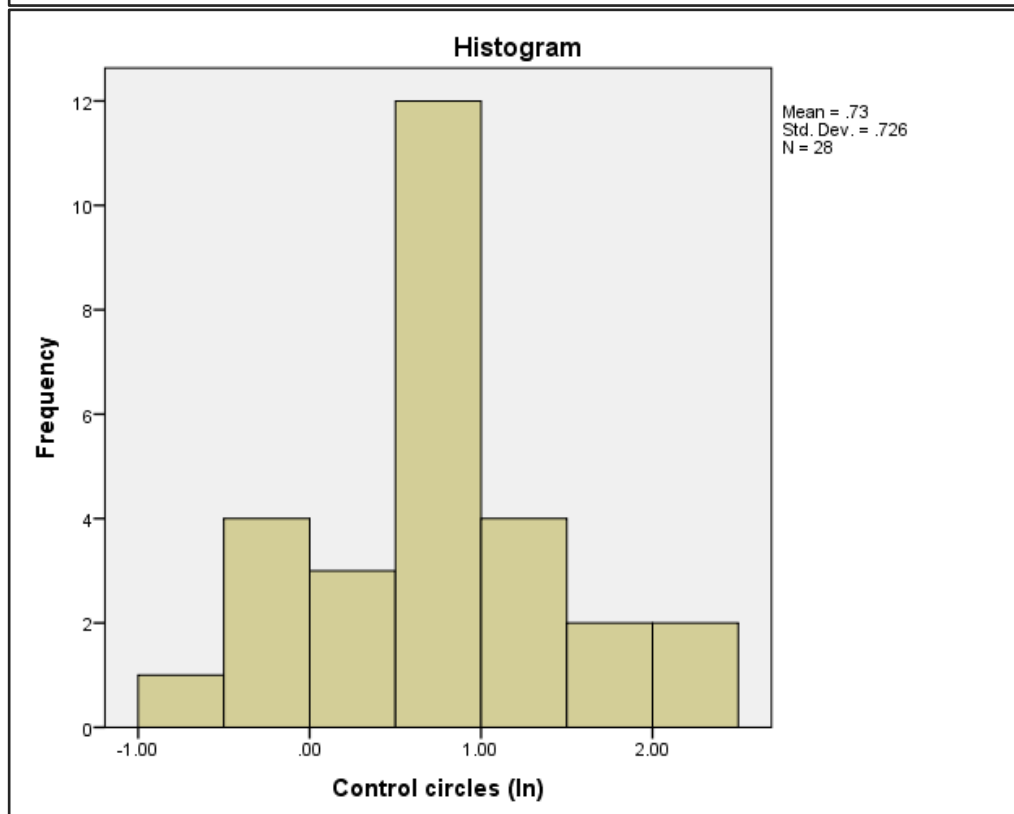|			Statistic	Std. Error
Original slalom	Mean		24.7344	1.34501
	95% Confidence Interval for Mean	Lower Bound	22.0466	
		Upper Bound	27.4222	
	5% Trimmed Mean		24.6085	
	Median		25.3750	
	Variance		115.780	
	Std. Deviation		1.76009	
	Minimum		5.50	
	Maximum		49.25	
	Range		43.75	
	Interquartile Range		17.25	
	Skewness		.033	.299
	Kurtosis		-.886	.590
Illusory lines	Mean		17.4492	.93384
	95% Confidence Interval for Mean	Lower Bound	15.5831	
		Upper Bound	19.3154	
	5% Trimmed Mean		16.9436	
	Median		16.5000	
	Variance		55.812	
	Std. Deviation		7.47073	
	Minimum		4.75	
	Maximum		41.50	
	Range		36.75	
	Interquartile Range		7.56	
	Skewness		1.225	.299
	Kurtosis		1.837	.590
Reduced contrast	Mean		23.7656	1.31597
	95% Confidence Interval for Mean	Lower Bound	21.1359	
		Upper Bound	26.3954	
	5% Trimmed Mean		23.2465	
	Median		21.6250	
	Variance		11.833	
	Std. Deviation		1.52773	
	Minimum		7.00	
	Maximum		51.50	
	Range		44.50	
	Interquartile Range		14.44	
	Skewness		.700	.299
	Kurtosis		.175	.590
Control	Mean		17.1406	1.14789

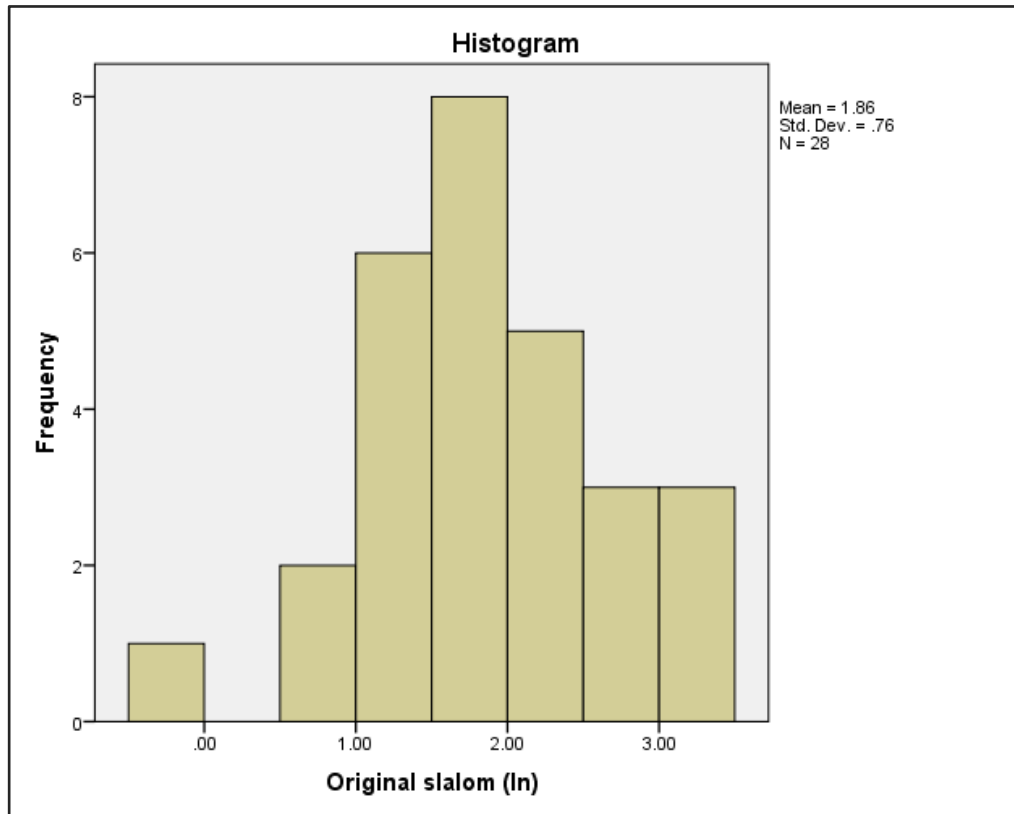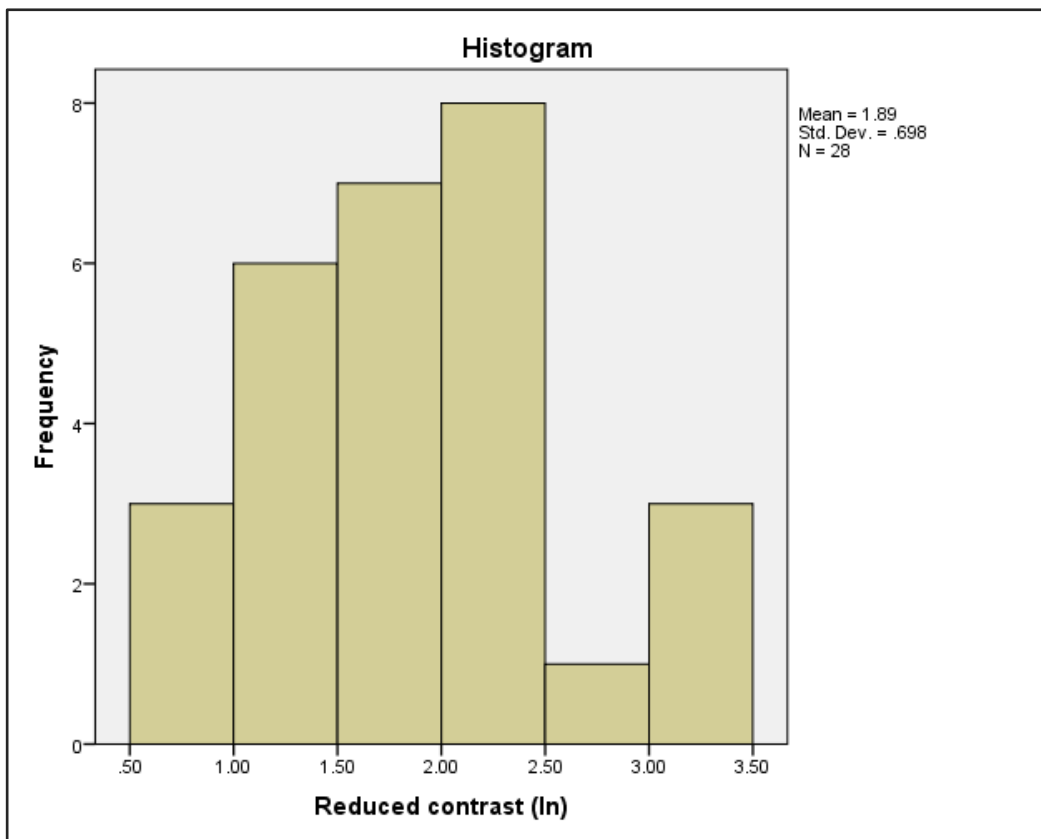|			
95% Confidence Interval for Mean	Lower Bound	14.8468	
	Upper Bound	19.4345	
5% Trimmed Mean		16.3906	
Median		15.6250	
Variance		84.329	
Std. Deviation		9.18309	
Minimum		5.00	
Maximum		45.25	
Range		4.25	
Interquartile Range		1.81	
Skewness		1.278	.299
Kurtosis		1.460	.590

Appendix 6.Histograms showing the distribution of the data from Experiment 1
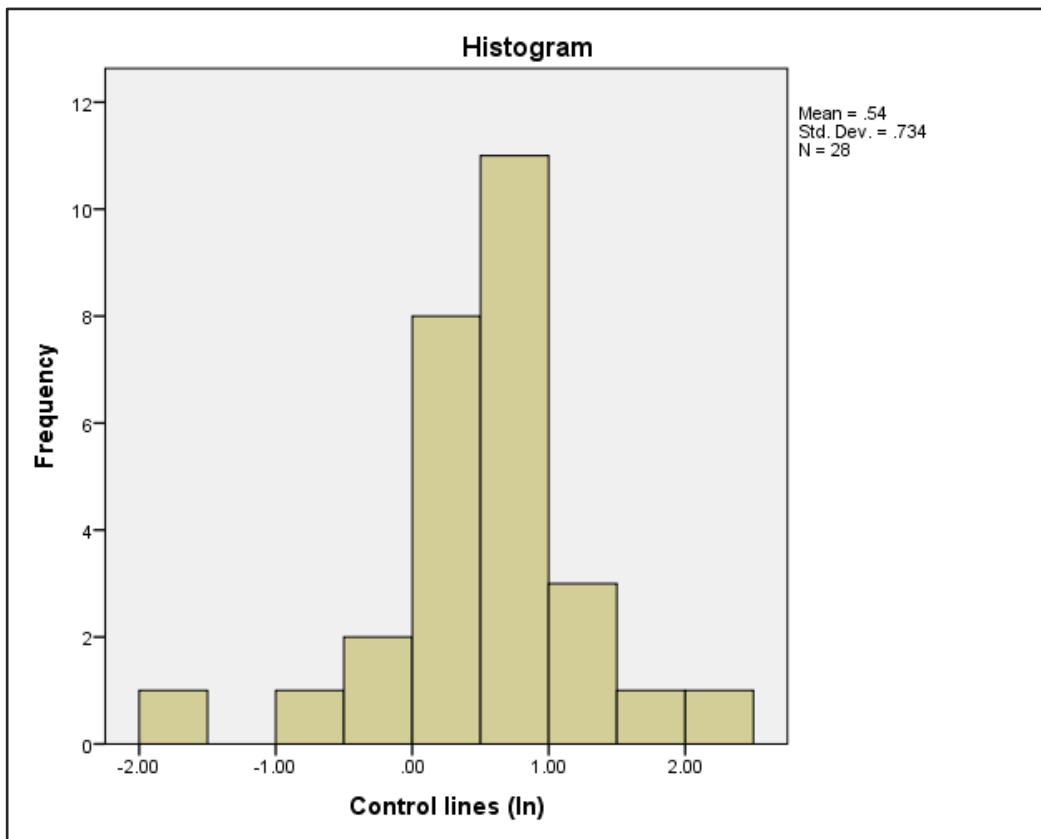
Chapter 2, after the outliers were removed.

Histogram

Mean = 24.73
Std. Dev. = 10.76
N = 64

Original slalom

Histogram

Mean = 17.45
Std. Dev. = 7.471
N = 64

Illusory lines

210

Histogram

Mean = 23.77
Std. Dev. = 10.528
N = 64

Reduced contrast

Histogram

Mean = 17.14
Std. Dev. = 9.183
N = 64

Control
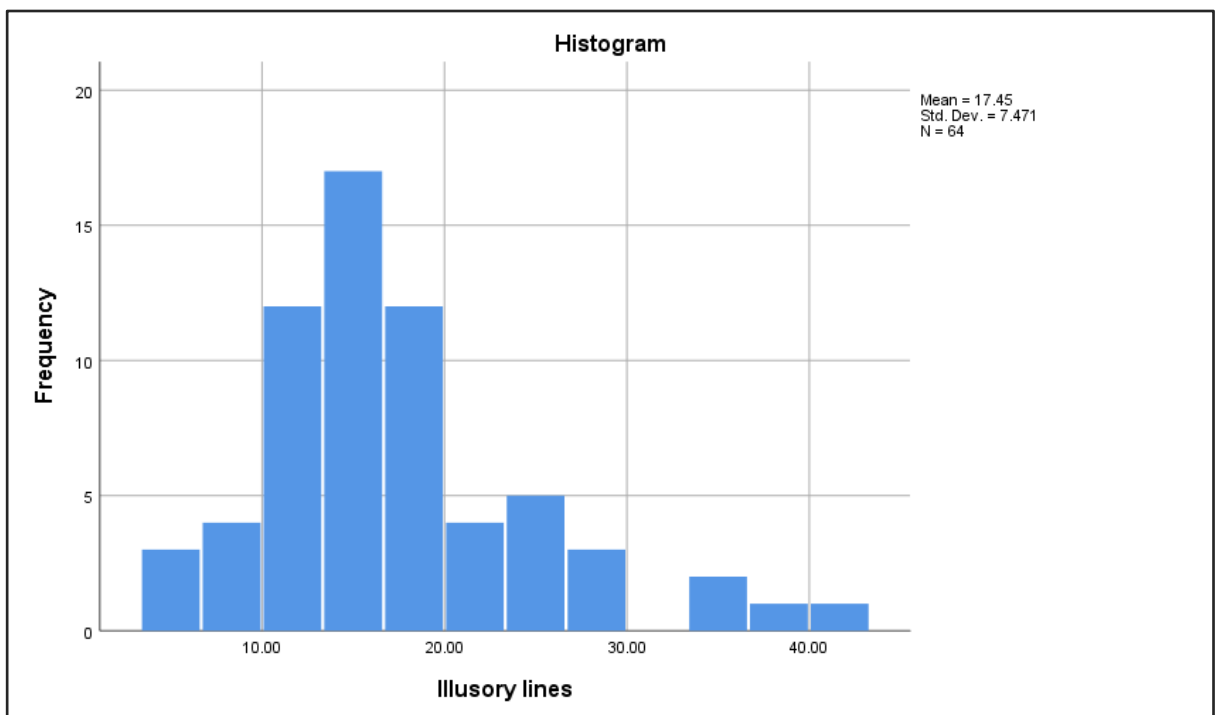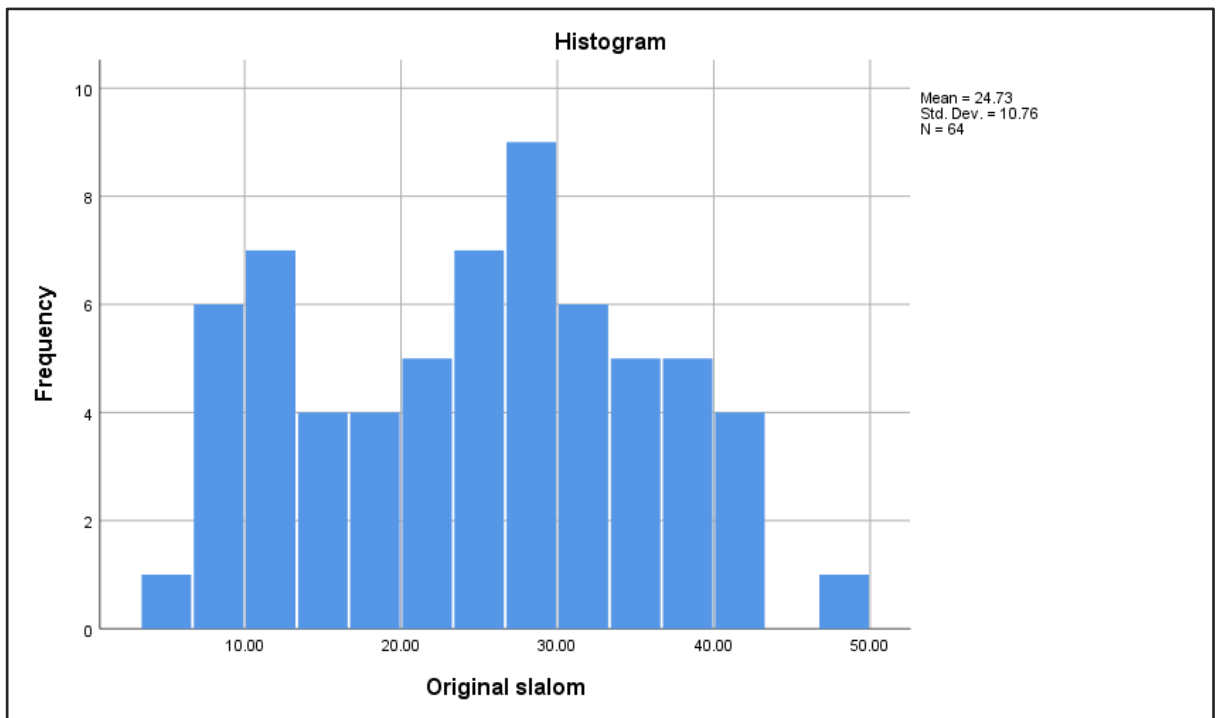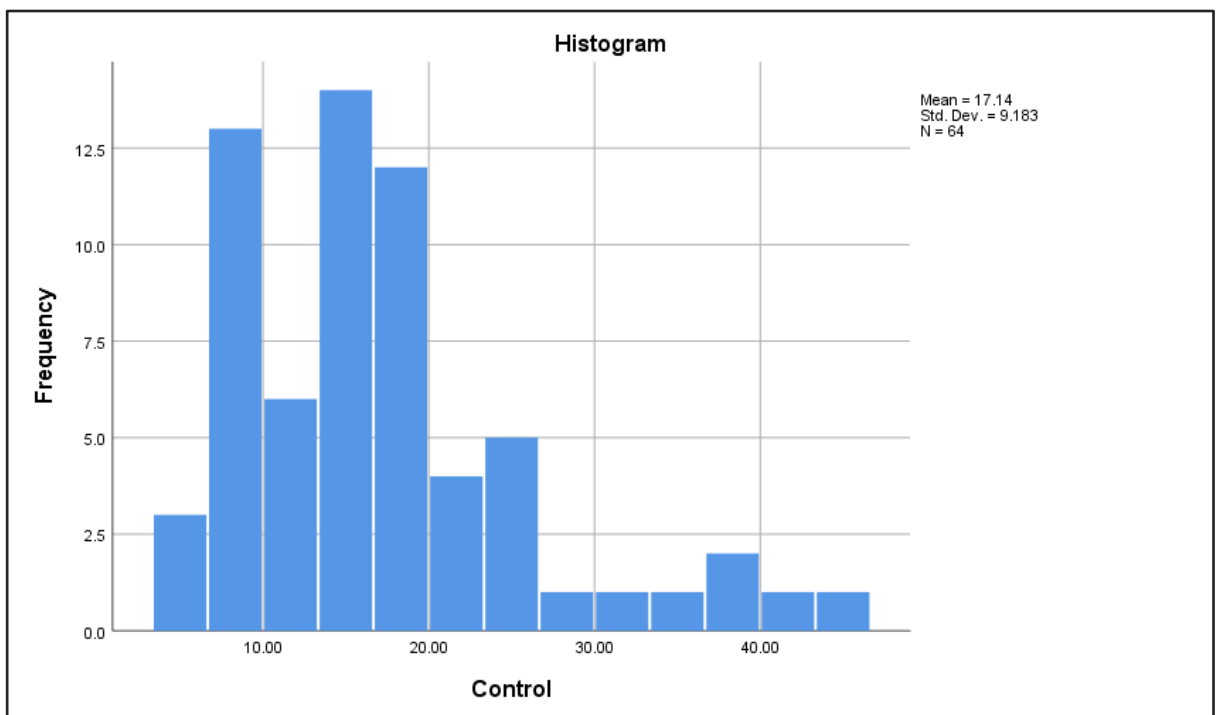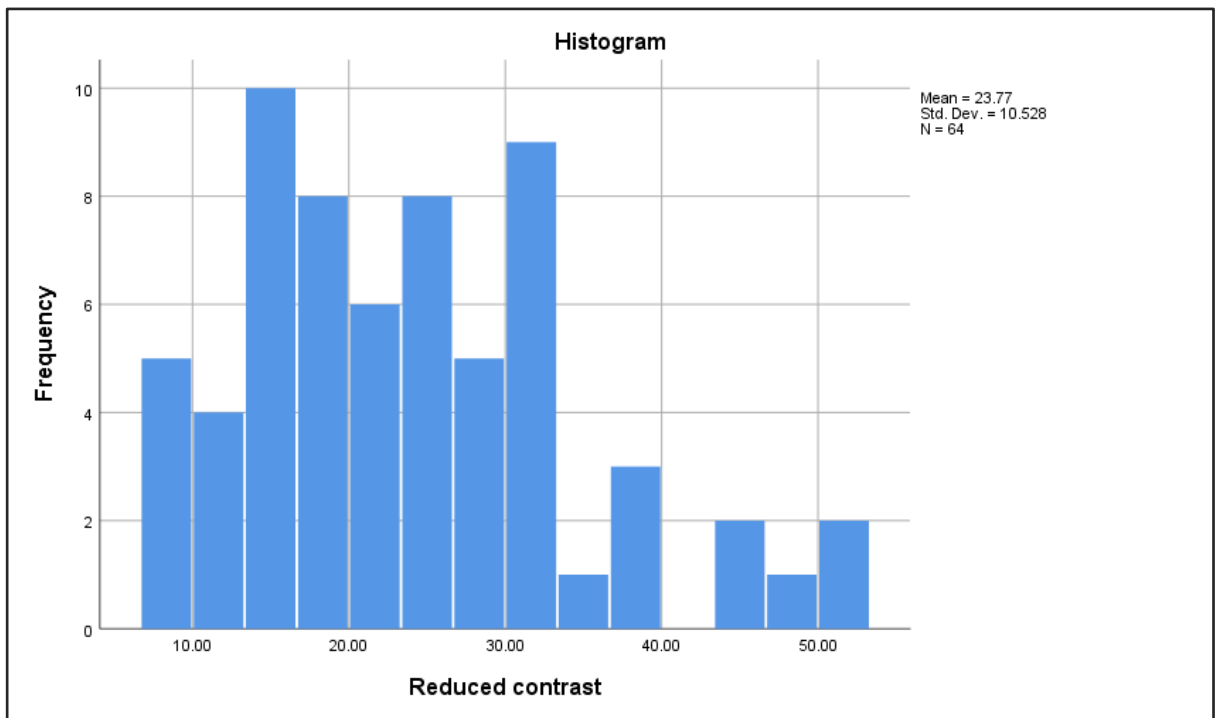
Appendix 7.Boxplots for the data from Experiment 2 Chapter 2.

Control lines

Reduced contrast
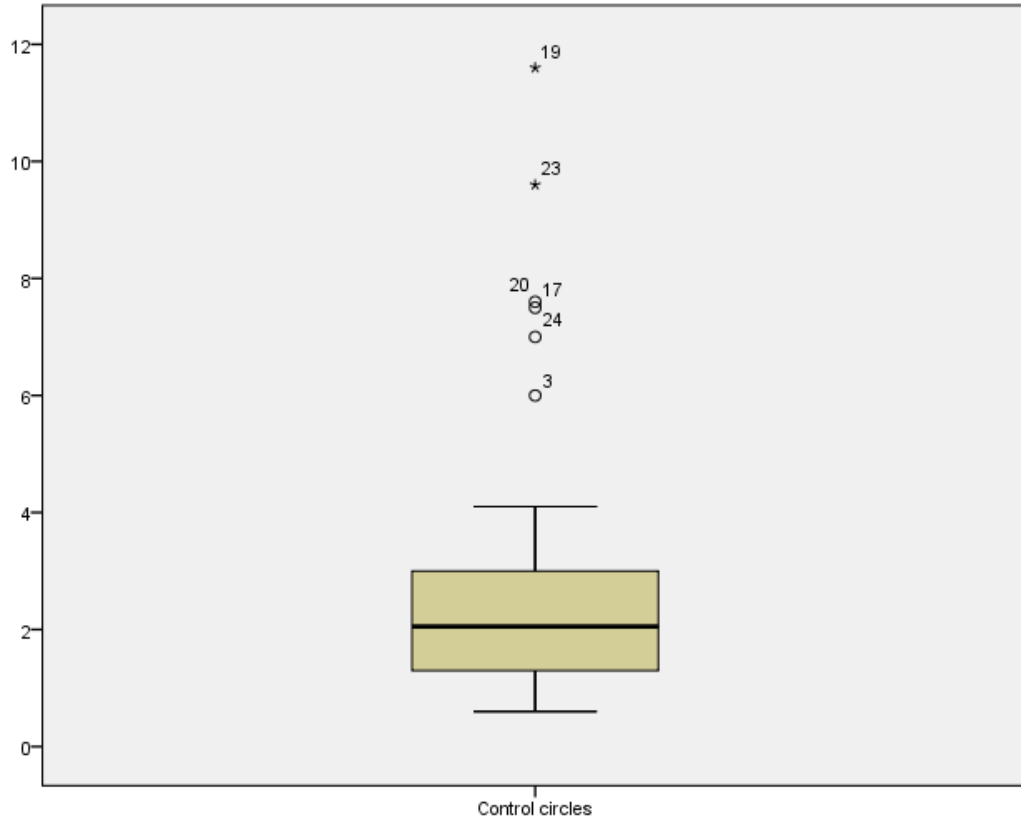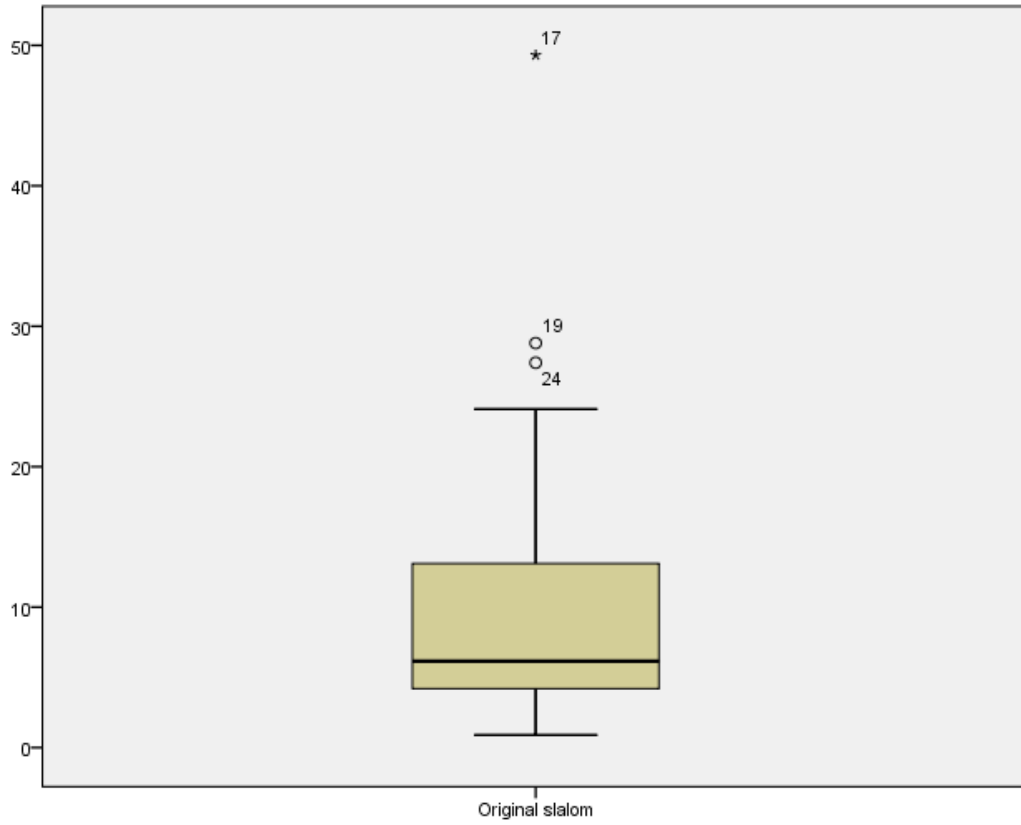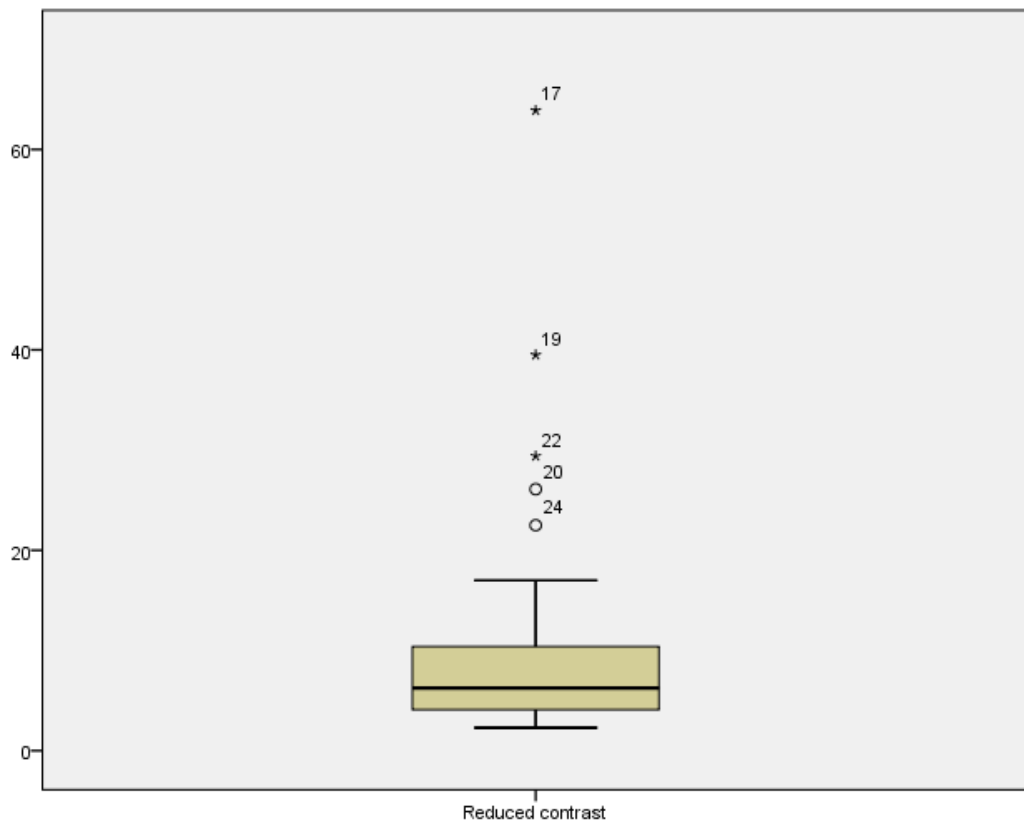
Appendix 8. Descriptive statistics for the data from Experiment 2 Chapter 2 after the
outliers were removed.

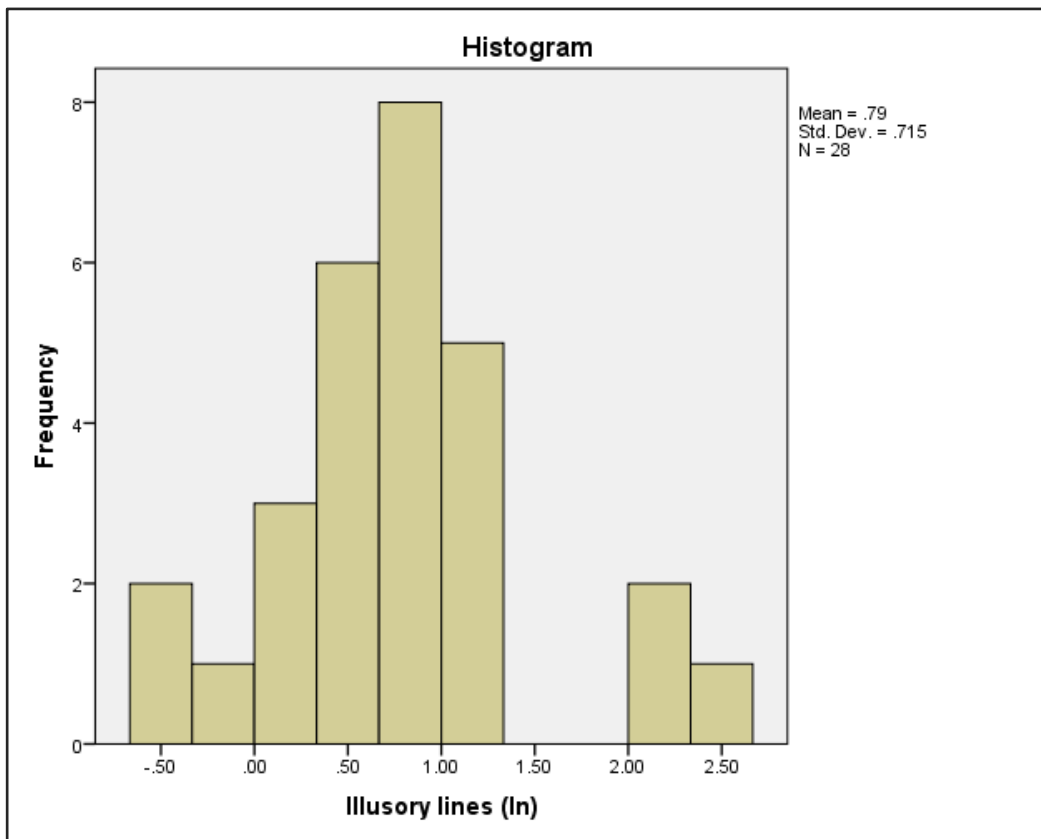**Descriptives**

			Statistic	Std. Error
Original slalom	Mean		8.3964	1.26247
	95% Confidence Interval for Mean	Lower Bound	5.8061	
		Upper Bound	1.9868	
	5% Trimmed Mean		7.7841	
	Median		5.4000	
	Variance		44.627	
	Std. Deviation		6.68035	
	Minimum		.90	
	Maximum		27.40	
	Range		26.50	
	Interquartile Range		6.63	
	Skewness		1.557	.441
	Kurtosis		1.900	.858
Control circles	Mean		2.6929	.42232
	95% Confidence Interval for Mean	Lower Bound	1.8263	
		Upper Bound	3.5594	
	5% Trimmed Mean		2.4556	
	Median		2.0000	
	Variance		4.994	
	Std. Deviation		2.23473	
	Minimum		.60	
	Maximum		9.60	
	Range		9.00	
	Interquartile Range		1.73	
	Skewness		1.837	.441
	Kurtosis		2.976	.858
Control lines	Mean		2.1929	.33480
	95% Confidence Interval for Mean	Lower Bound	1.5059	
		Upper Bound	2.8798	
	5% Trimmed Mean		1.9794	
	Median		1.9000	
	Variance		3.138	
	Std. Deviation		1.77157	
	Minimum		.20	
	Maximum		8.20	
	Range		8.00	

|				
	Interquartile Range		1.43	
	Skewness		2.328	.441
	Kurtosis		5.939	.858
Reduced contrast	Mean		8.5429	1.33724
	95% Confidence Interval for Mean	Lower Bound	5.7991	
		Upper Bound	11.2866	
	5% Trimmed Mean		7.7817	
	Median		5.4000	
	Variance		5.070	
	Std. Deviation		7.07601	
	Minimum		2.30	
	Maximum		29.40	
	Range		27.10	
	Interquartile Range		6.20	
	Skewness		1.830	.441
	Kurtosis		2.833	.858
Illusory lines	Mean		2.8821	.49527
	95% Confidence Interval for Mean	Lower Bound	1.8659	
		Upper Bound	3.8984	
	5% Trimmed Mean		2.5667	
	Median		2.1000	
	Variance		6.868	
	Std. Deviation		2.62072	
	Minimum		.60	
	Maximum		11.50	
	Range		1.90	
	Interquartile Range		1.75	
	Skewness		2.281	.441
	Kurtosis		4.844	.858

Appendix 9. Histograms showing the distribution of the data from Experiment 2

Chapter 2 after the outliers were removed.

Histogram

Mean = 2.19
Std. Dev. = 1.772
N = 28

Control lines

Histogram

Mean = 8.54
Std. Dev. = 7.076
N = 28

Reduced contrast

Histogram

Mean = 2.88
Std. Dev. = 2.621
N = 28
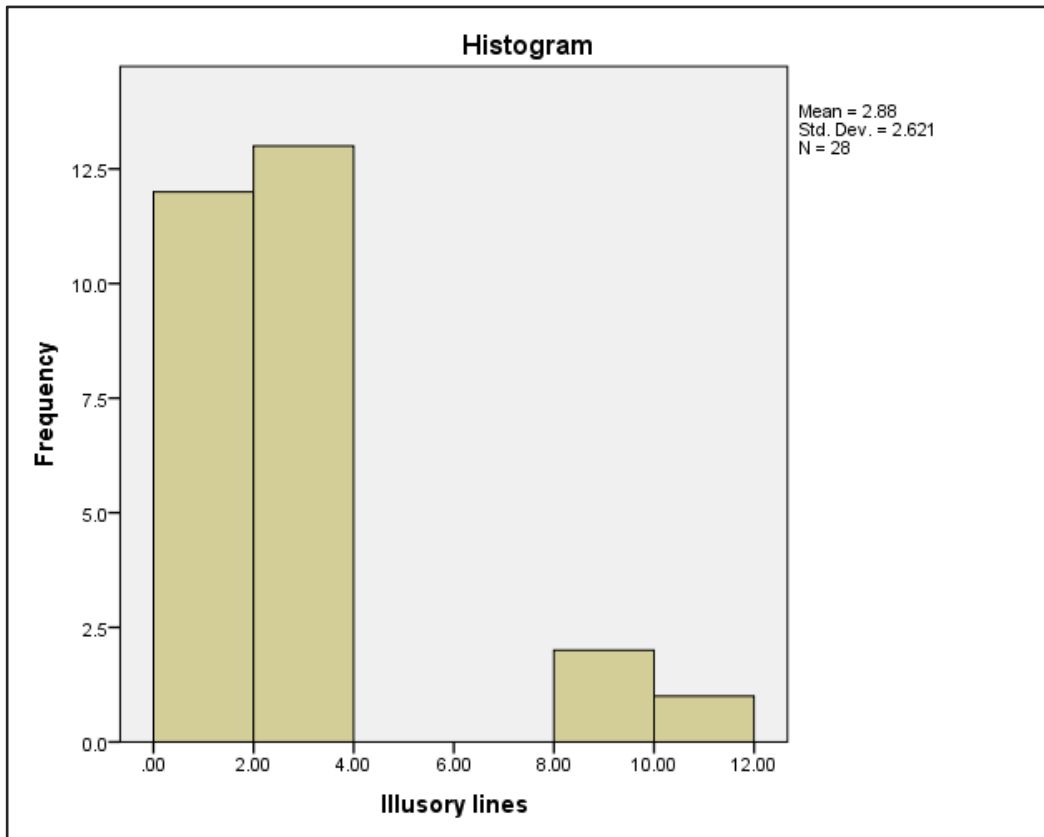
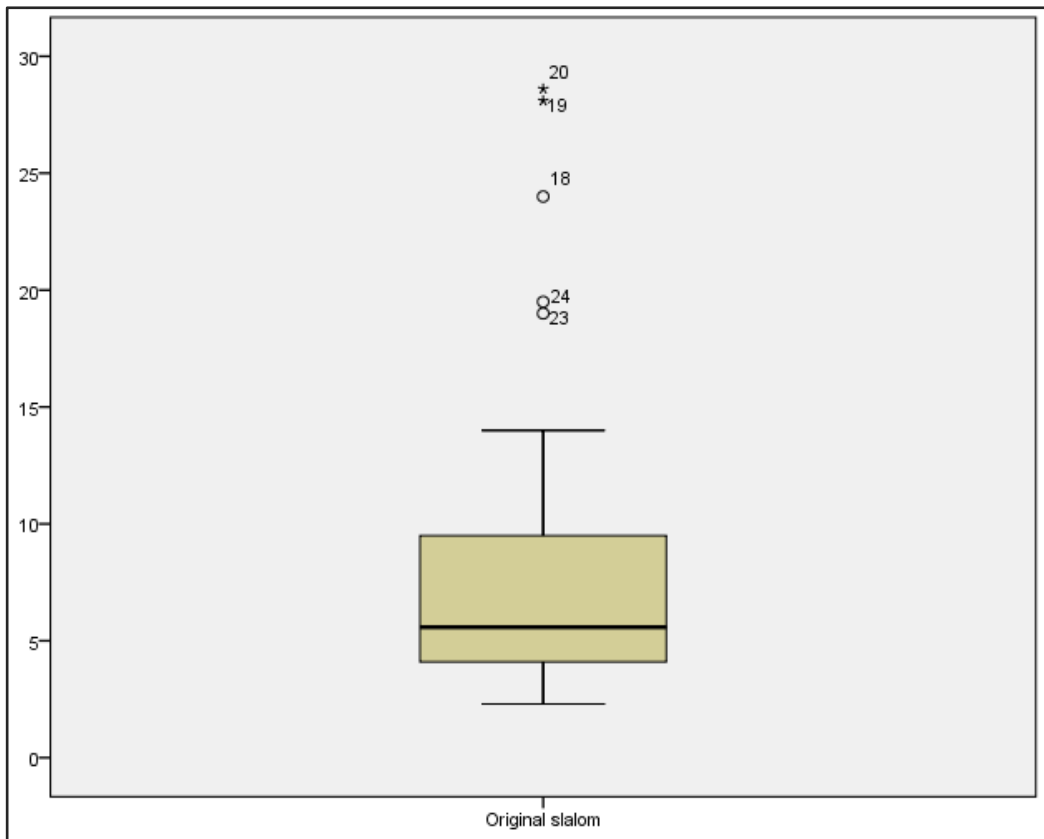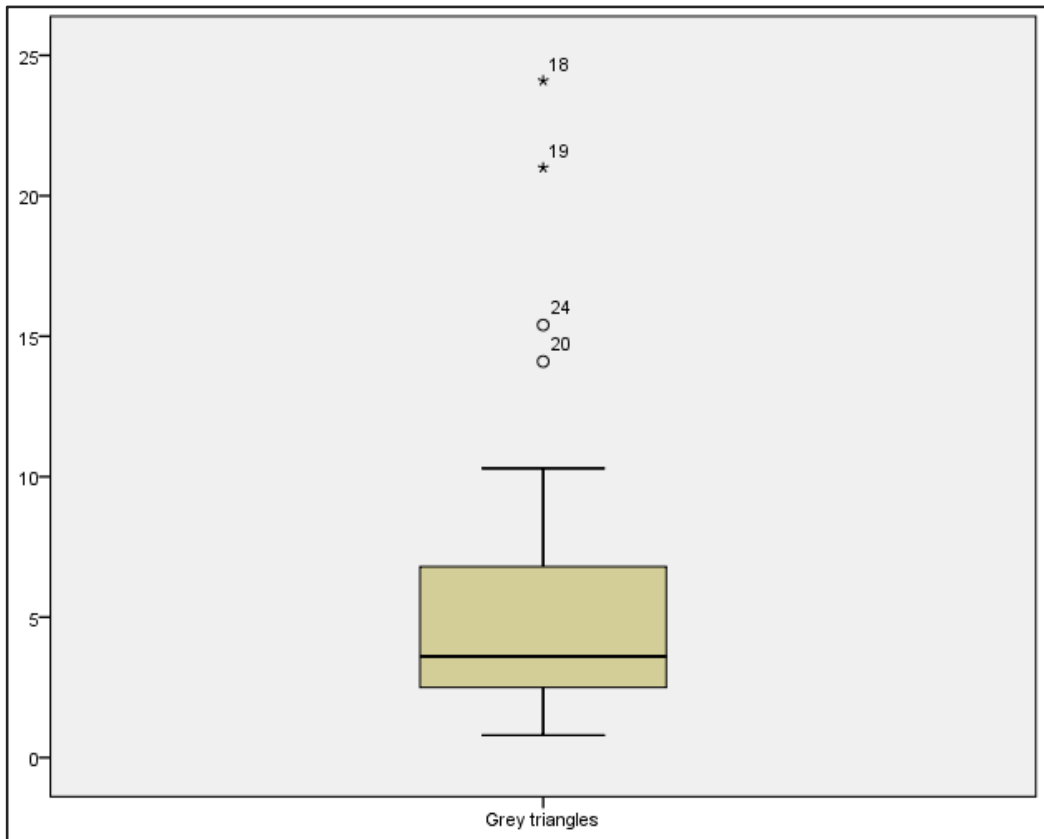**Appendix 1.** Histograms showing the distribution of the data from Experiment 2 Chapter 2 after the outliers were removed and the data were transformed into their natural logarithms.

Histogram

Mean = .54
Std. Dev. = .734
N = 28

Frequency — Control lines (ln)

Histogram

Mean = 1.89
Std. Dev. = .698
N = 28

Frequency — Reduced contrast (ln)

221

Histogram

Mean = .79
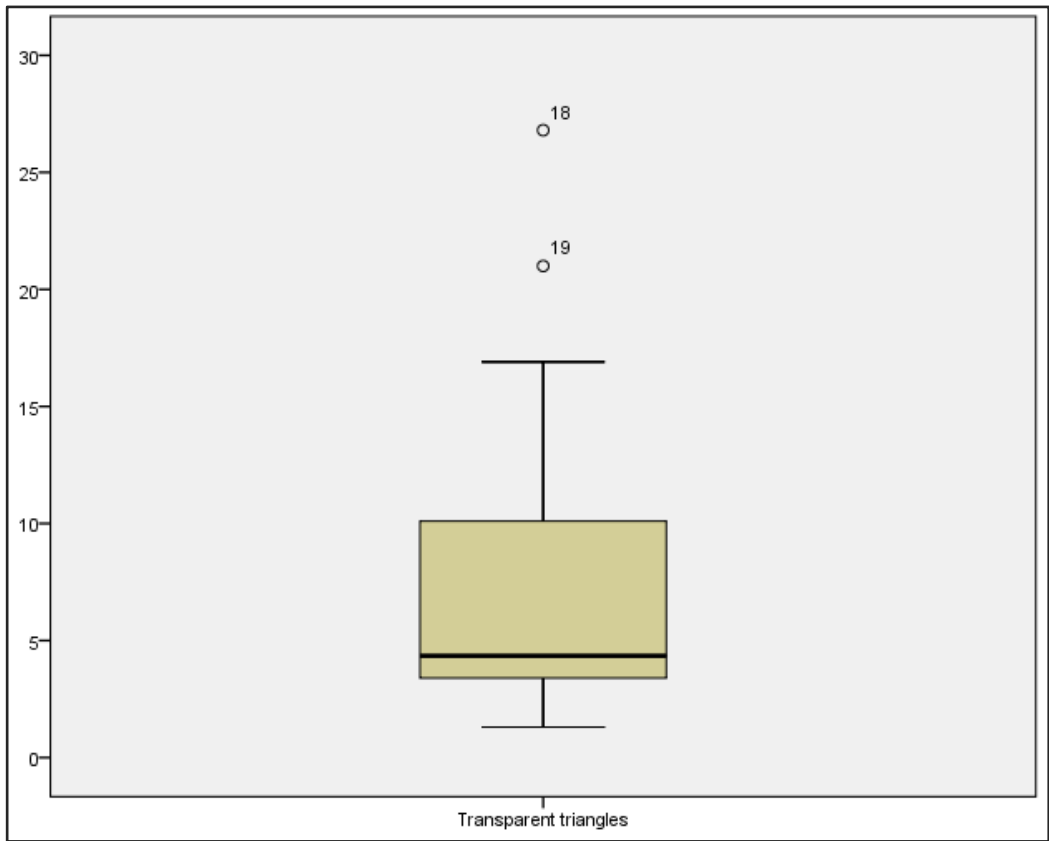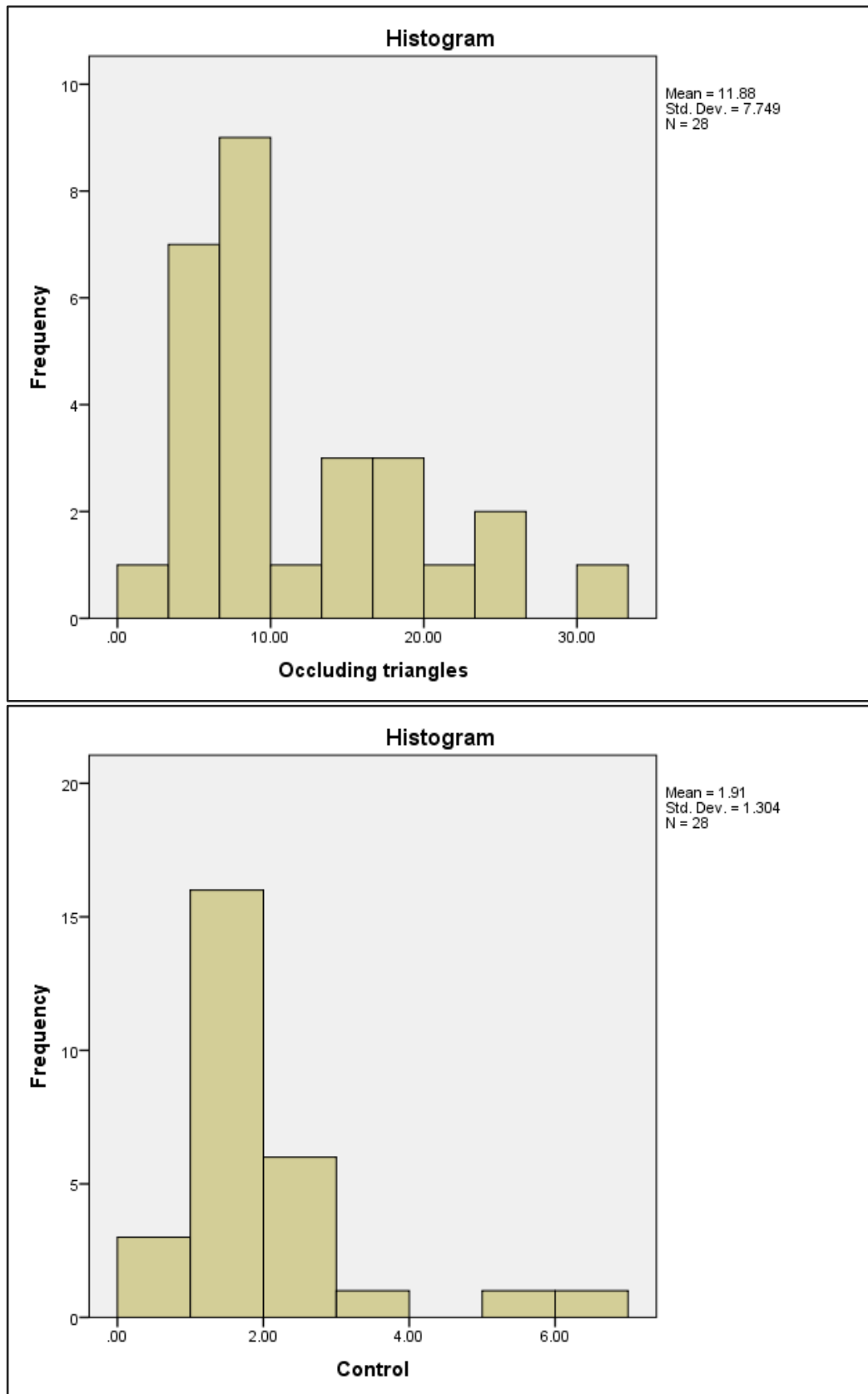Std. Dev. = .715
N = 28

Illusory lines (ln)

Appendix 11.Boxplots showing the distribution of the data from Experiment 1 Chapter 3.
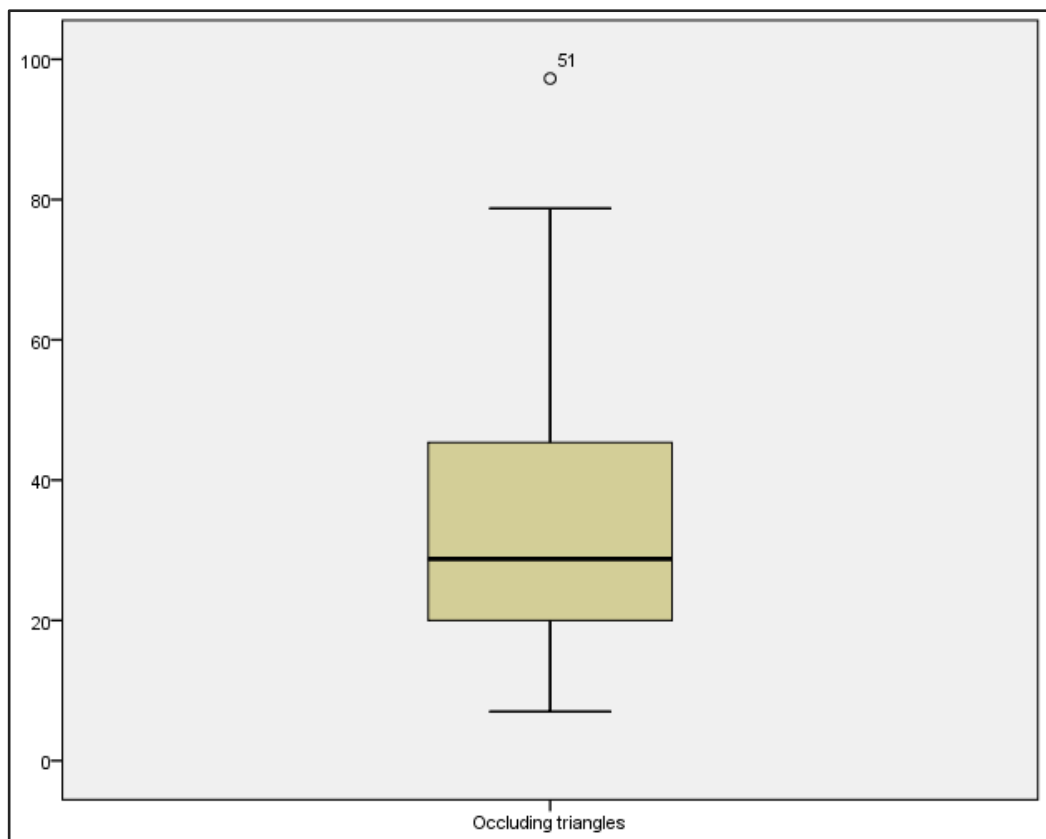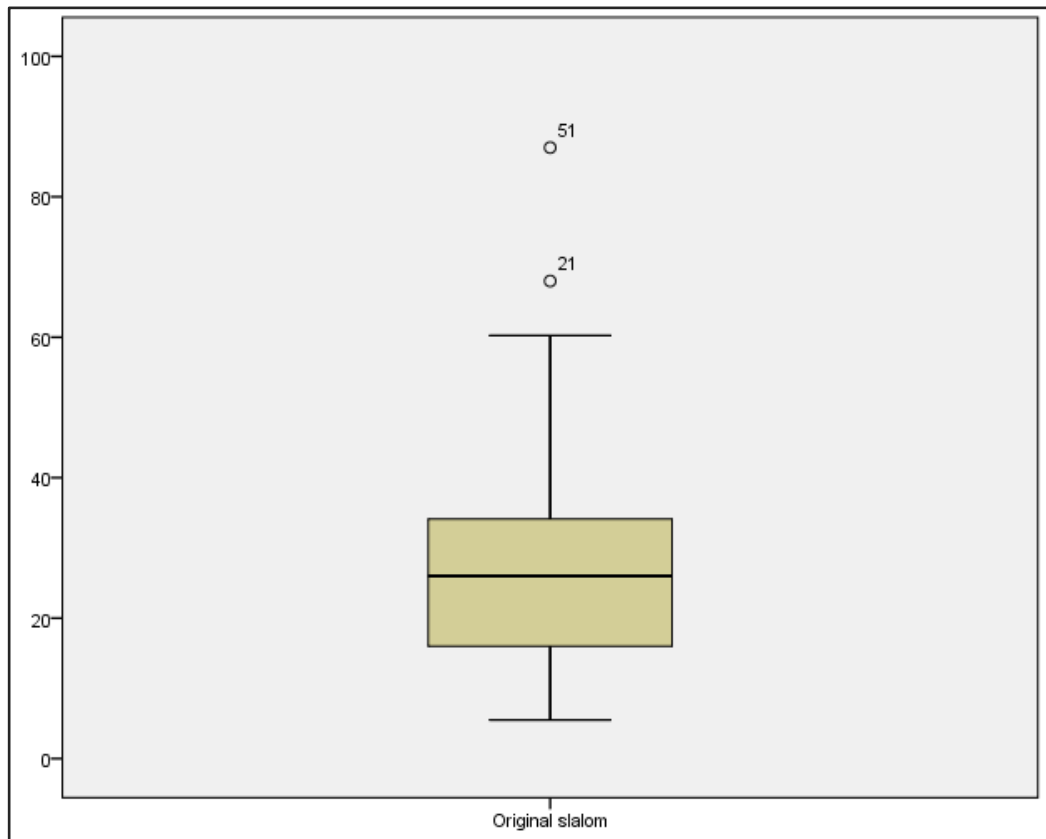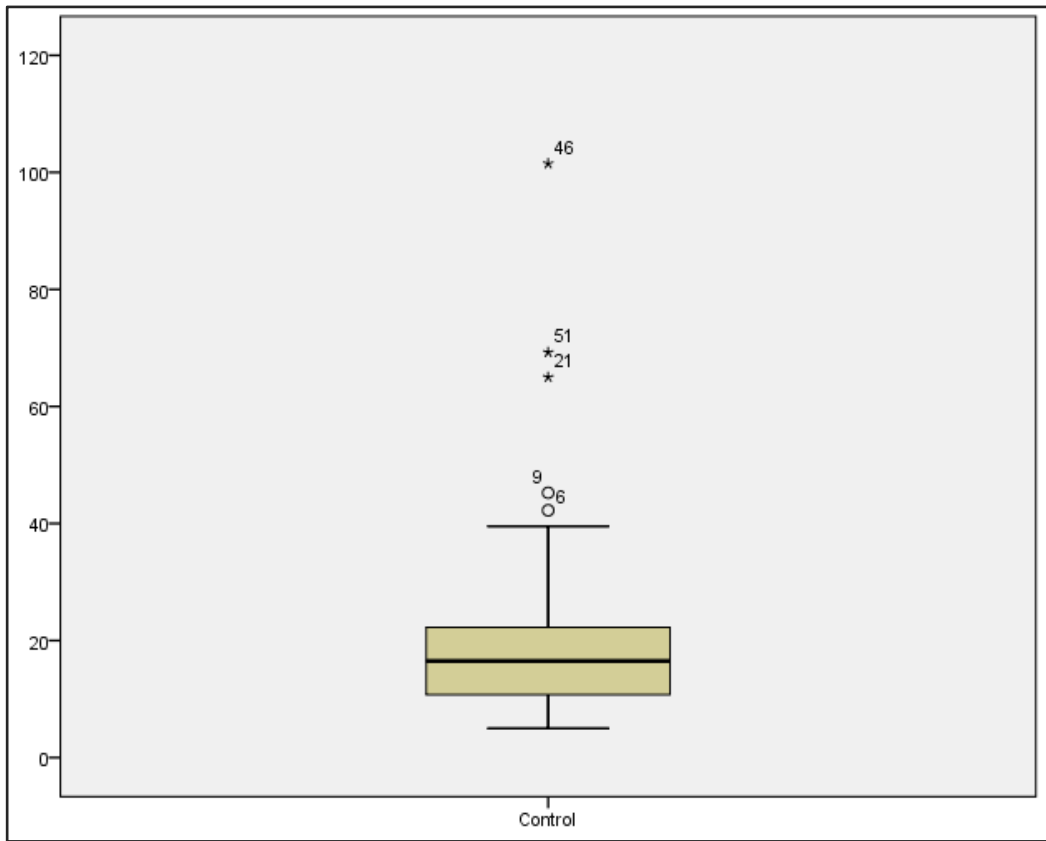
Appendix 12.Descriptive statistics for the data from Experiment 1 Chapter 3.

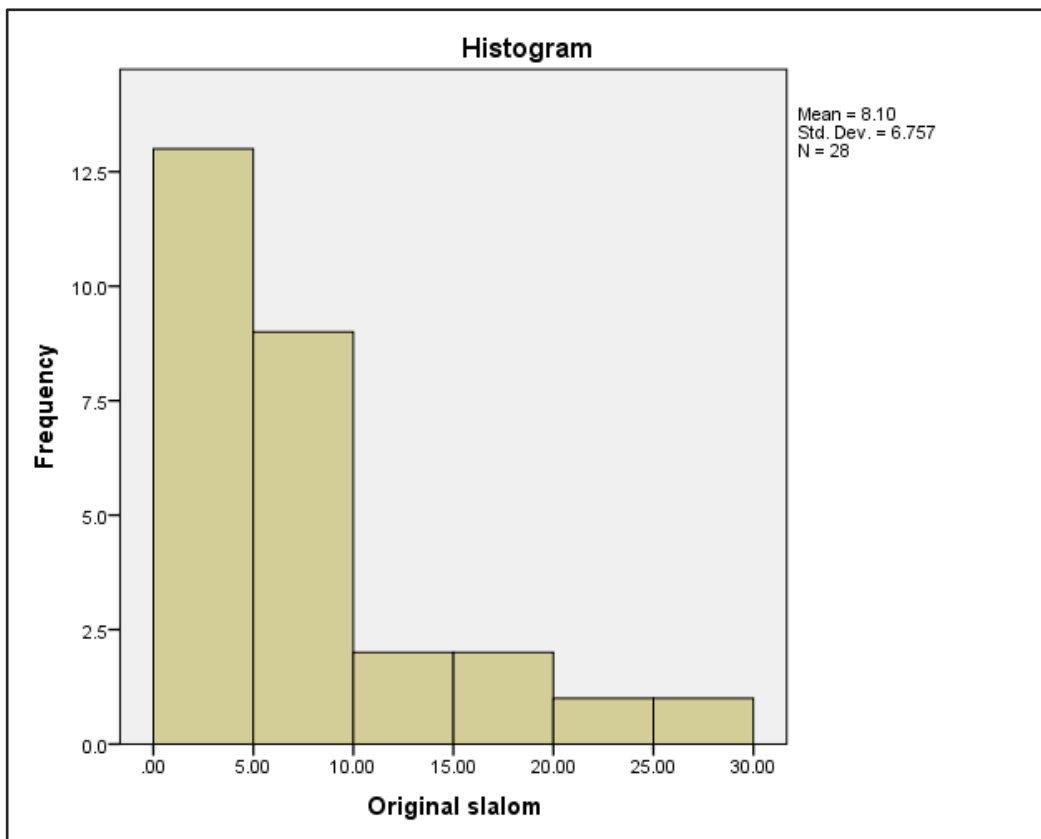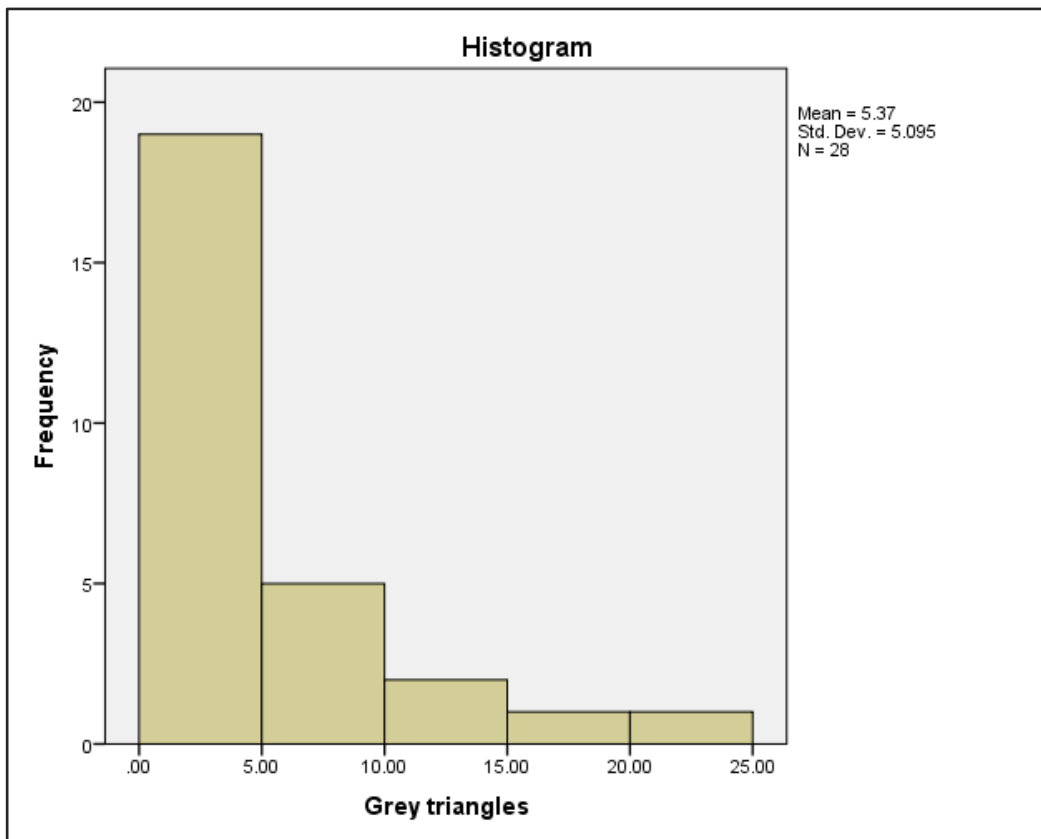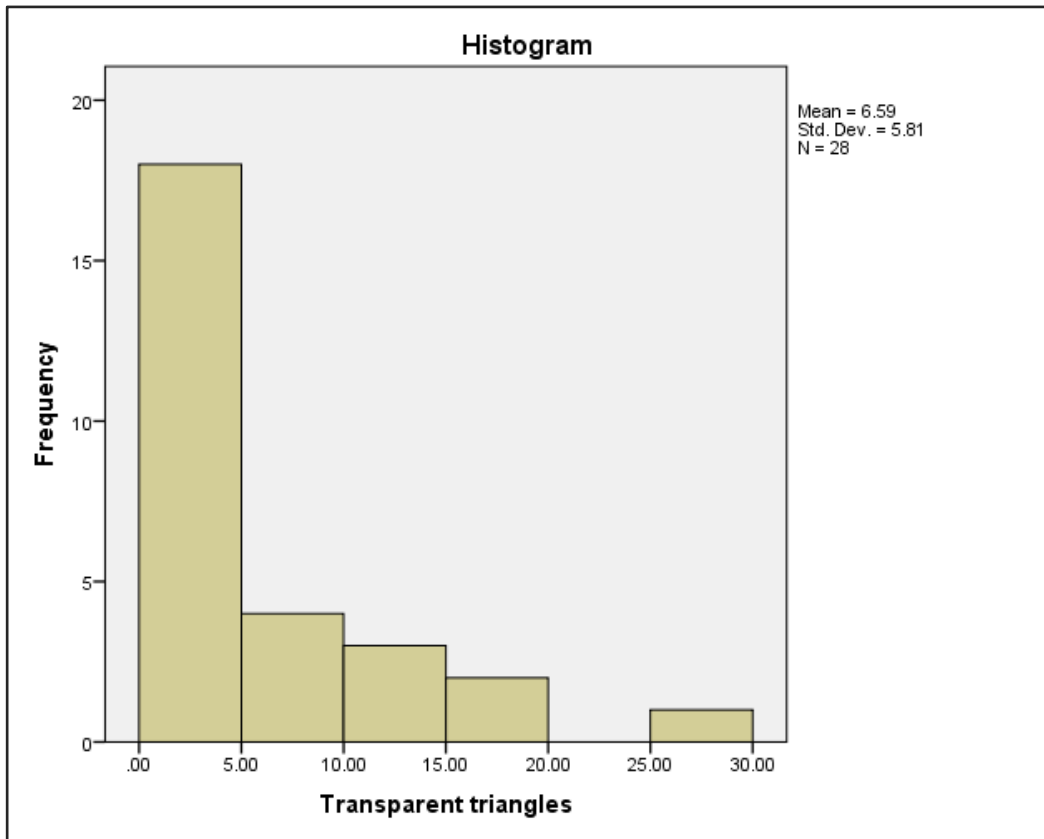|			Statistic	Std. Error
Original slalom	Mean		25.4000	1.48204
	95% Confidence Interval for Mean	Lower Bound	22.4393	
		Upper Bound	28.3607	
	5% Trimmed Mean		24.8942	
	Median		25.7500	
	Variance		142.769	
	Std. Deviation		11.94860	
	Minimum		5.50	
	Maximum		68.00	
	Range		62.50	
	Interquartile Range		17.50	
	Skewness		.617	.297
	Kurtosis		1.100	.586
Occluding triangles	Mean		32.1846	1.99190
	95% Confidence Interval for Mean	Lower Bound	28.2053	
		Upper Bound	36.1639	
	5% Trimmed Mean		31.5823	
	Median		27.5000	
	Variance		257.899	
	Std. Deviation		16.05923	
	Minimum		7.00	
	Maximum		78.75	
	Range		71.75	
	Interquartile Range		25.25	
	Skewness		.609	.297
	Kurtosis		-.240	.586
Control	Mean		17.8769	1.34879
	95% Confidence Interval for Mean	Lower Bound	15.1824	
		Upper Bound	2.5714	
	5% Trimmed Mean		16.7703	
	Median		16.0000	
	Variance		118.250	
	Std. Deviation		1.87429	
	Minimum		5.00	
	Maximum		65.00	
	Range		6.00	
	Interquartile Range		11.25	
	Skewness		1.922	.297
	Kurtosis		5.012	.586

Appendix 13. Histograms showing the distribution of the data from Experiment 1
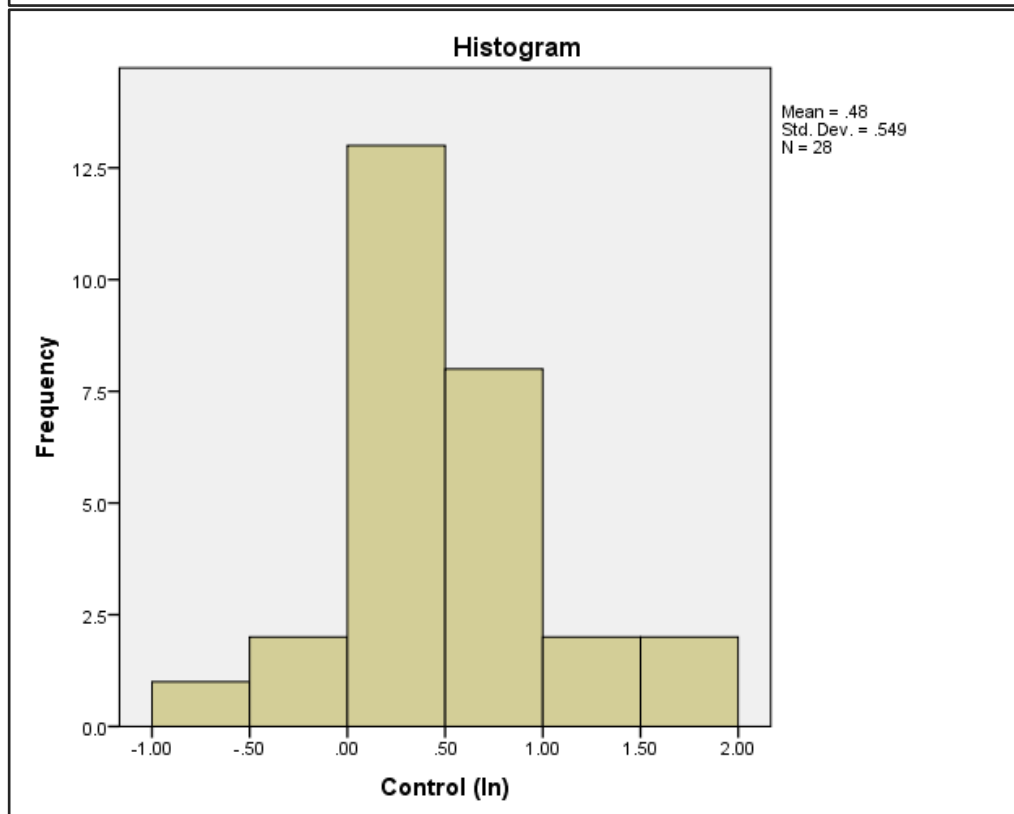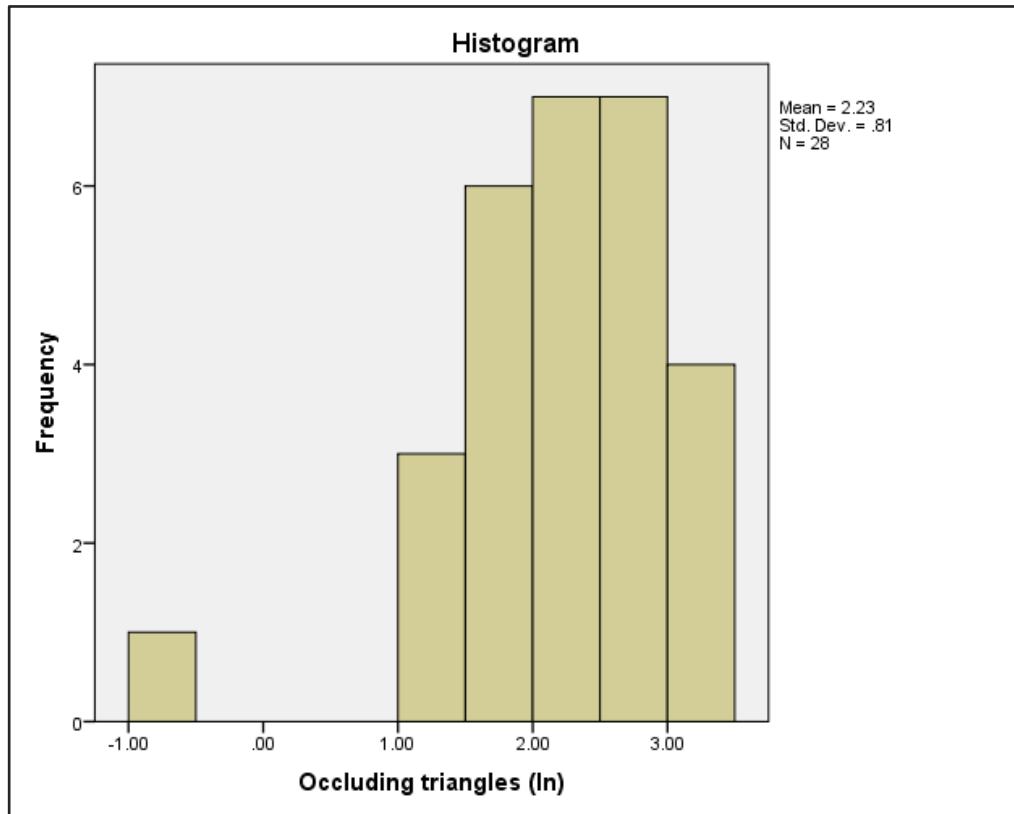
Chapter 3 after the outliers were removed.

Histogram

Mean = 17.88
Std. Dev. = 10.874
N = 65
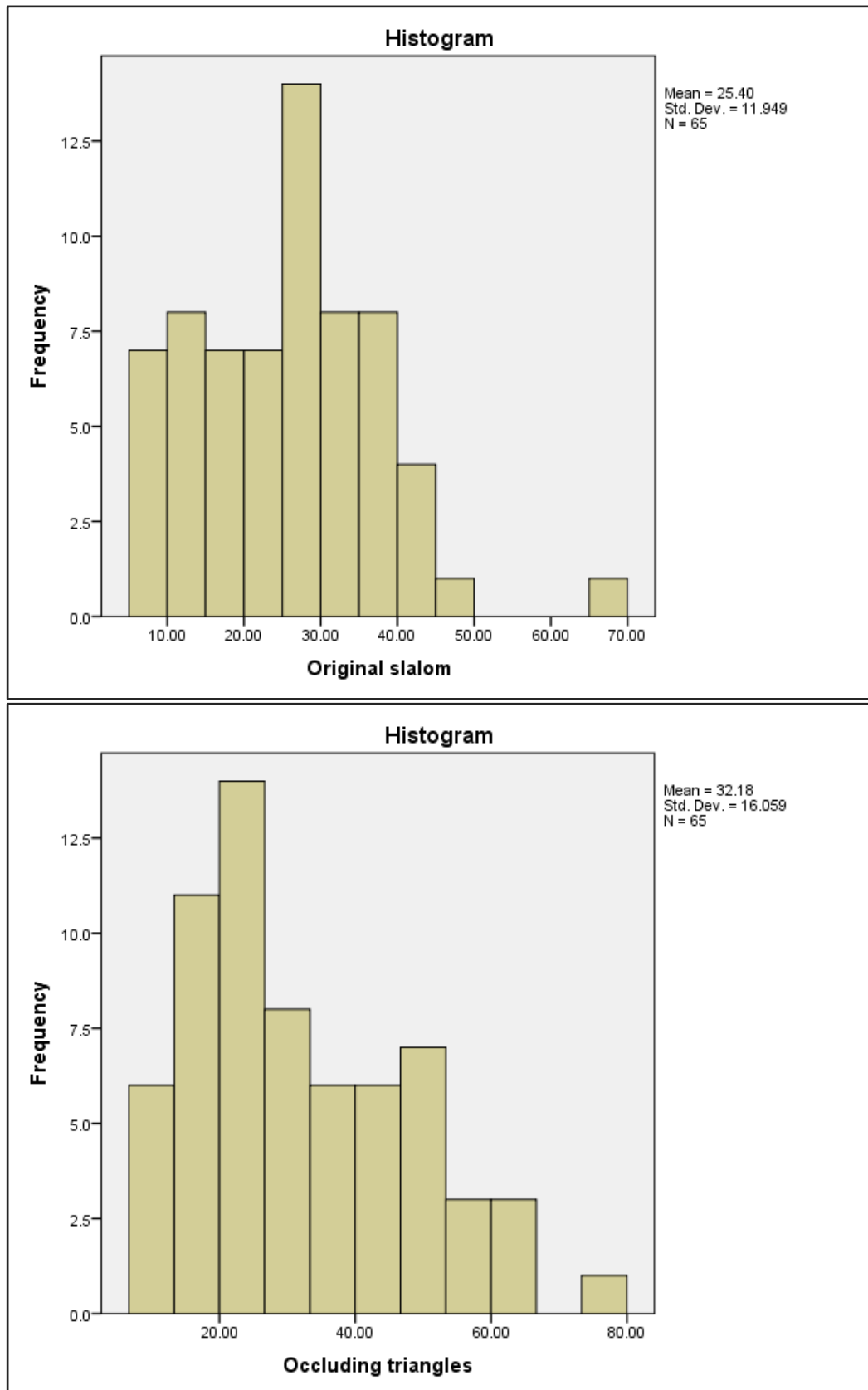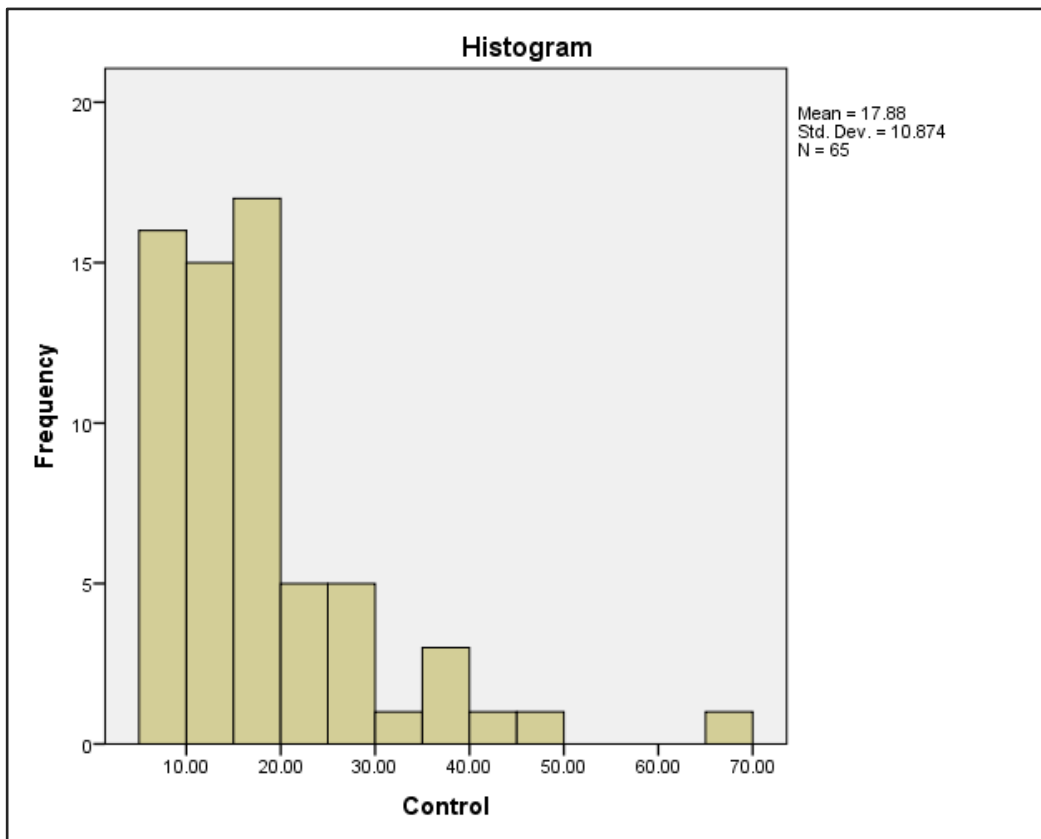
Appendix 14.Boxplots showing the distribution of the data from Experiment 2 Chapter 3.

229

Transparent triangles
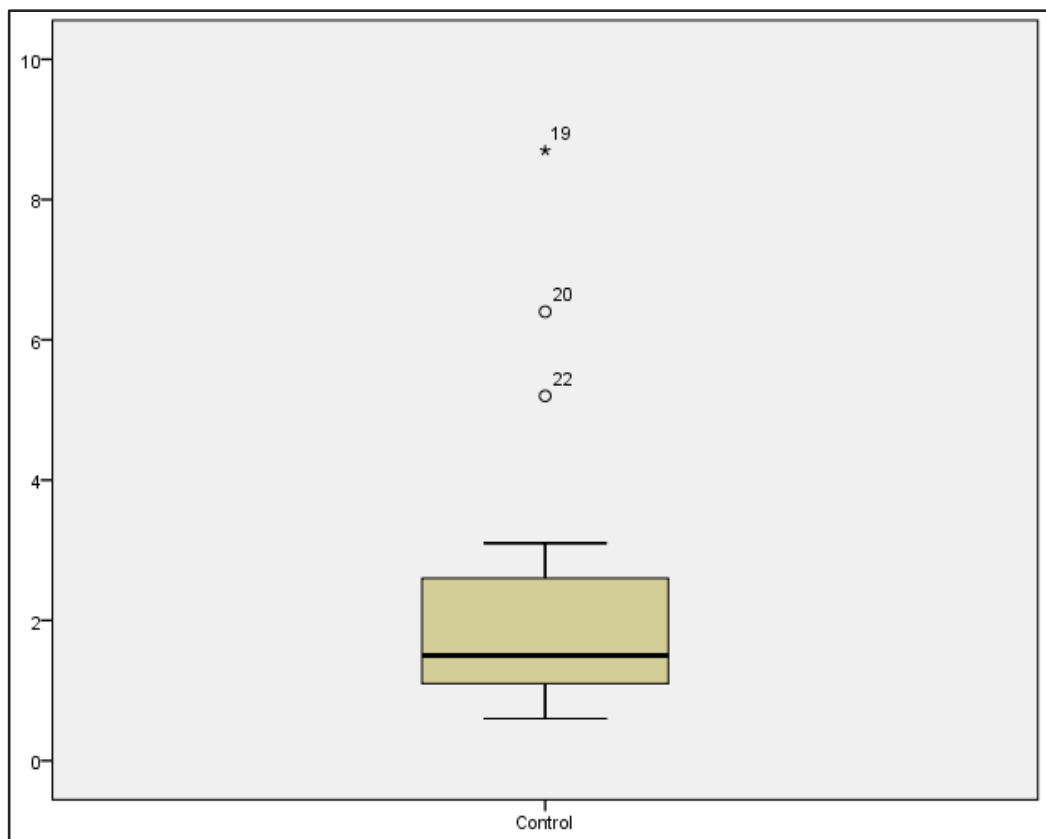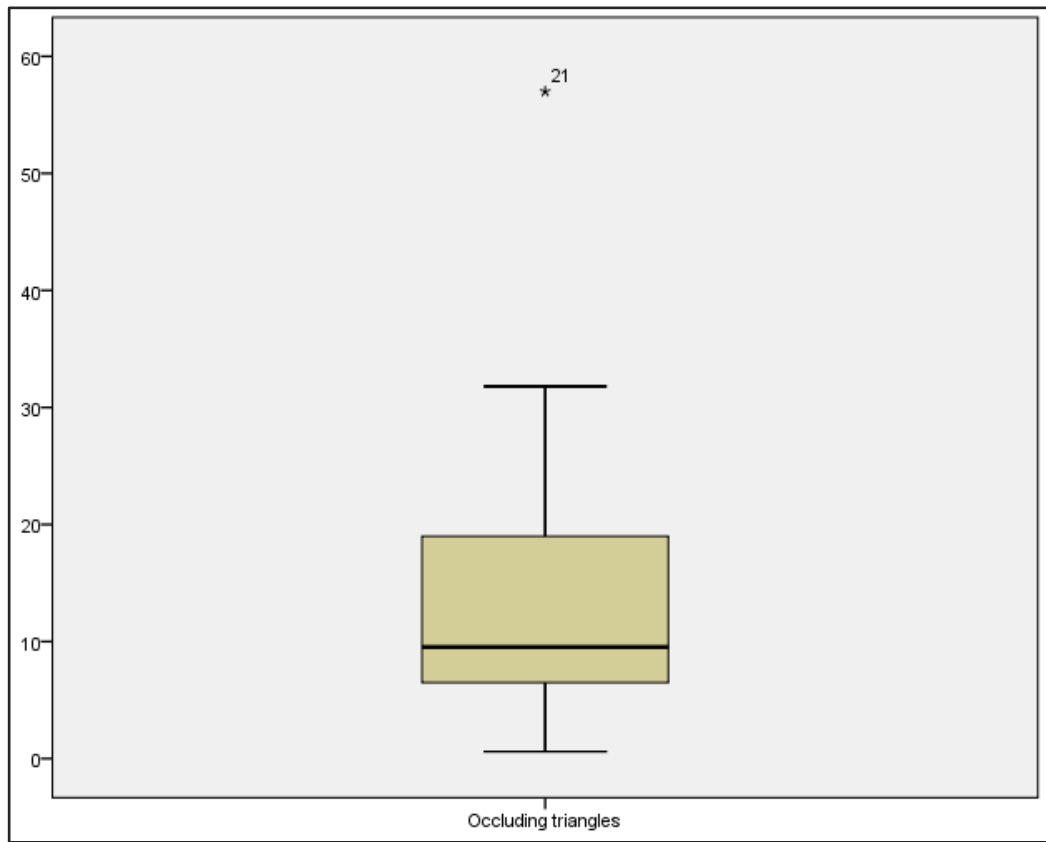
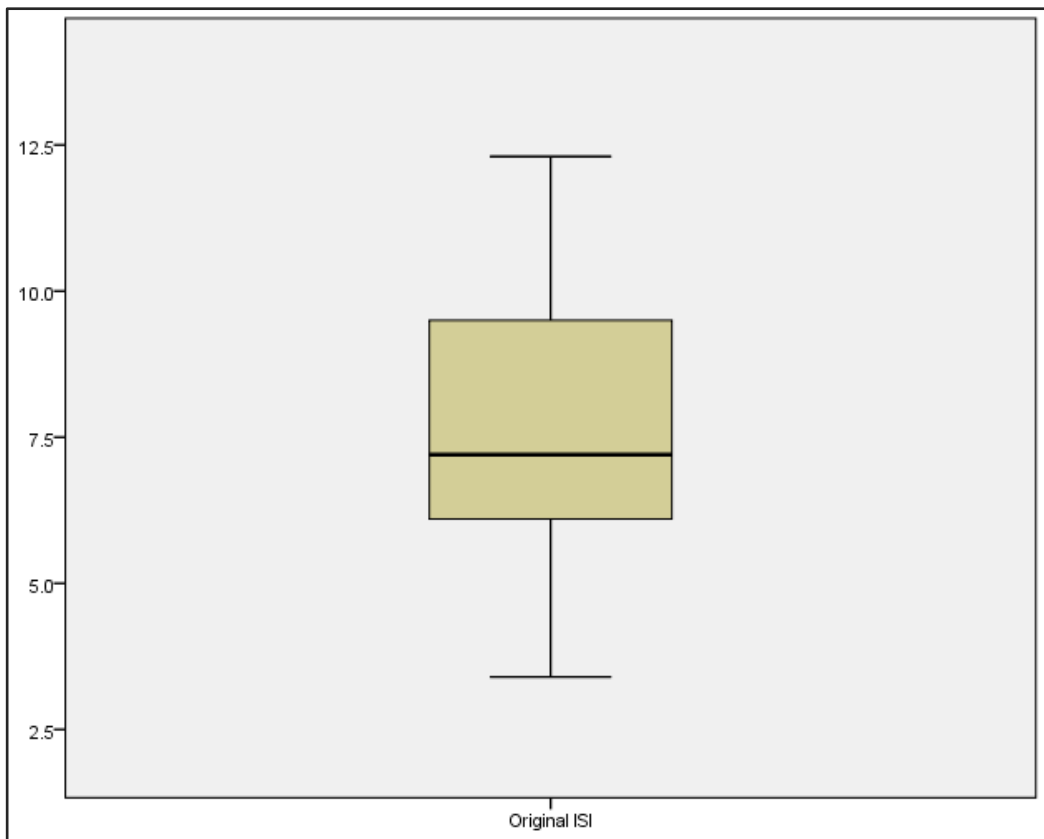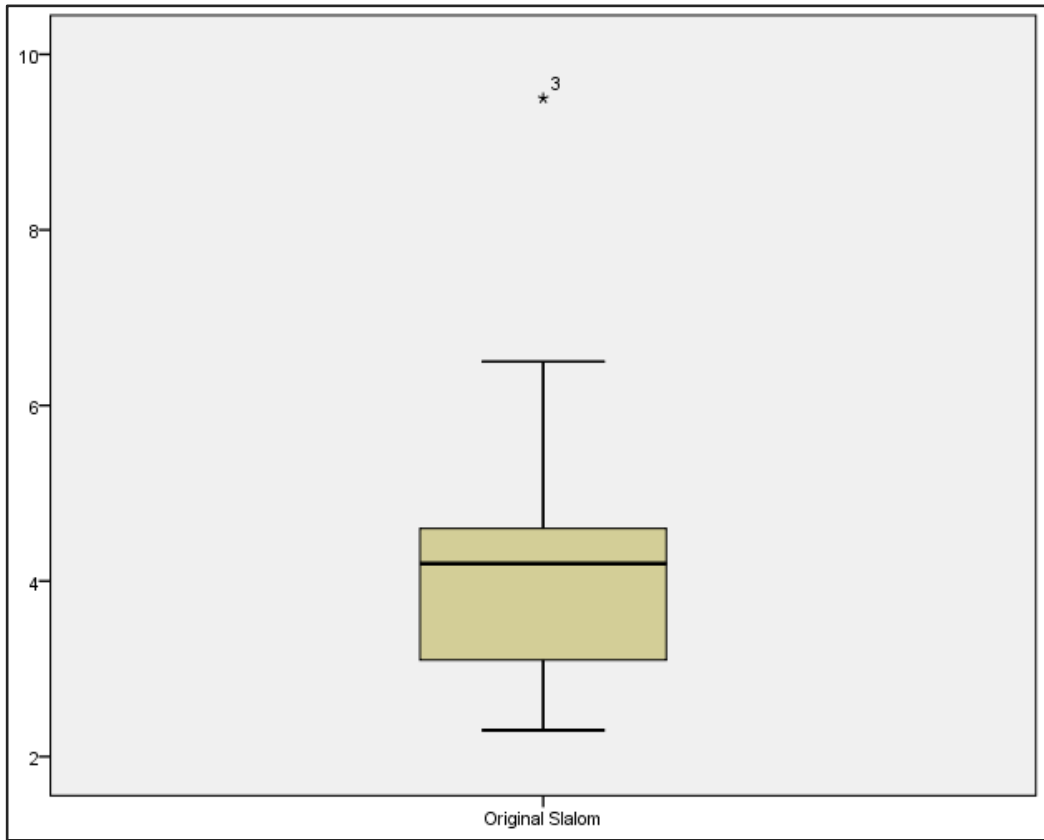**Appendix 15**. Histograms showing the distribution of the data from Experiment 2

Chapter 3 after the outliers were removed.

Histogram

Mean = 5.37
Std. Dev. = 5.095
N = 28

Histogram

Mean = 8.10
Std. Dev. = 6.757
N = 28

232

Histogram

Mean = 6.59
Std. Dev. = 5.81
N = 28

Appendix 16. Descriptive statistics for the data from Experiment 2 Chapter 3 after the
outliers were removed.

Descriptives

			Statistic	Std. Error
Occluding triangles	Mean		11.8843	1.46439
	95% Confidence Interval for Mean	Lower Bound	8.8796	
		Upper Bound	14.8890	
	5% Trimmed Mean		11.4794	
	Median		9.3500	
	Variance		6.044	
	Std. Deviation		7.74883	
	Minimum		.60	
	Maximum		31.40	
	Range		3.80	
	Interquartile Range		1.78	
	Skewness		.881	.441
	Kurtosis		.042	.858
Control	Mean		1.9054	.24651
	95% Confidence Interval for Mean	Lower Bound	1.3996	
		Upper Bound	2.4112	
	5% Trimmed Mean		1.7440	
	Median		1.4000	
	Variance		1.702	
	Std. Deviation		1.30443	
	Minimum		.60	
	Maximum		6.40	
	Range		5.80	
	Interquartile Range		1.48	
	Skewness		2.177	.441
	Kurtosis		5.252	.858
Grey triangles	Mean		5.3700	.96286
	95% Confidence Interval for Mean	Lower Bound	3.3944	
		Upper Bound	7.3456	
	5% Trimmed Mean		4.7151	
	Median		3.6000	
	Variance		25.959	
	Std. Deviation		5.09496	
	Minimum		.80	
	Maximum		24.10	
	Range		23.30	

	Interquartile Range		4.00	
	Skewness		2.390	.441
	Kurtosis		6.336	.858
Original slalom	Mean		8.0989	1.27686
	95% Confidence Interval for Mean	Lower Bound	5.4790	
		Upper Bound	1.7188	
	5% Trimmed Mean		7.3671	
	Median		5.5850	
	Variance		45.651	
	Std. Deviation		6.75652	
	Minimum		2.30	
	Maximum		28.10	
	Range		25.80	
	Interquartile Range		5.10	
	Skewness		1.780	.441
	Kurtosis		2.459	.858
Transparent triangles	Mean		6.5868	1.09799
	95% Confidence Interval for Mean	Lower Bound	4.3339	
		Upper Bound	8.8397	
	5% Trimmed Mean		5.9083	
	Median		4.3000	
	Variance		33.756	
	Std. Deviation		5.81000	
	Minimum		1.30	
	Maximum		26.80	
	Range		25.50	
	Interquartile Range		6.00	
	Skewness		2.026	.441
	Kurtosis		4.514	.858

Appendix 17. Histograms showing the distributions of the data from Experiment 2 Chapter 3 after the outliers were removed and the data was transformed into their natural logarithms.
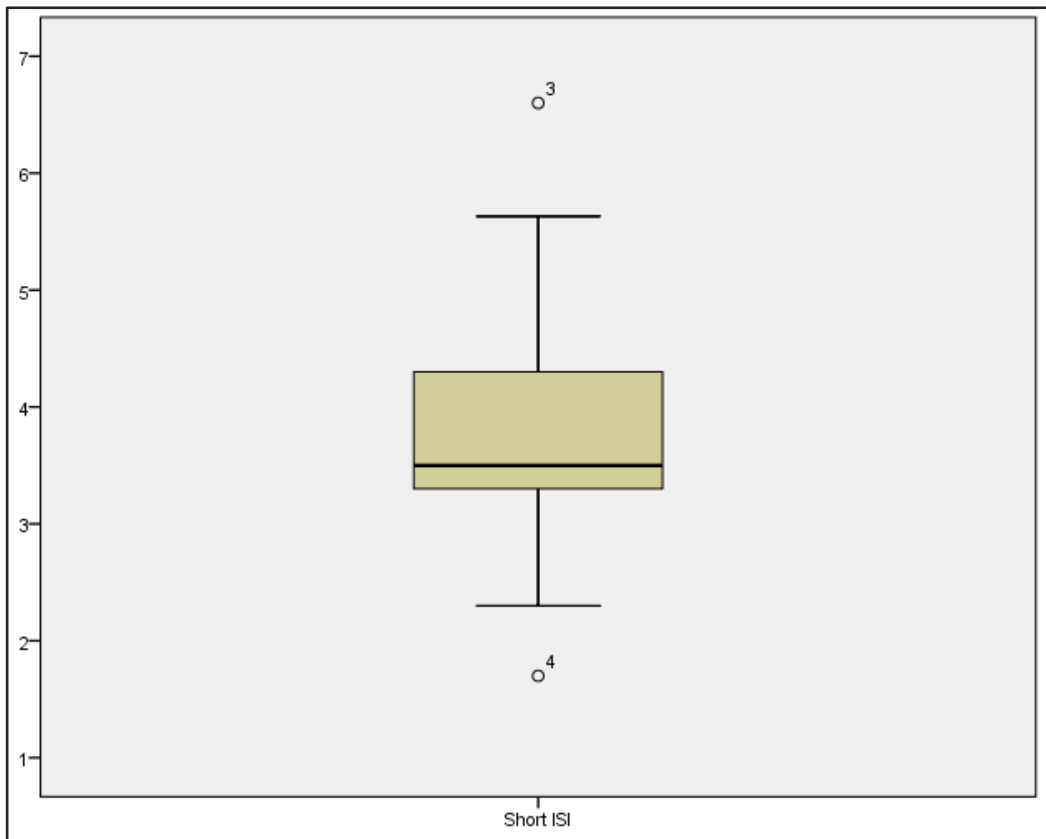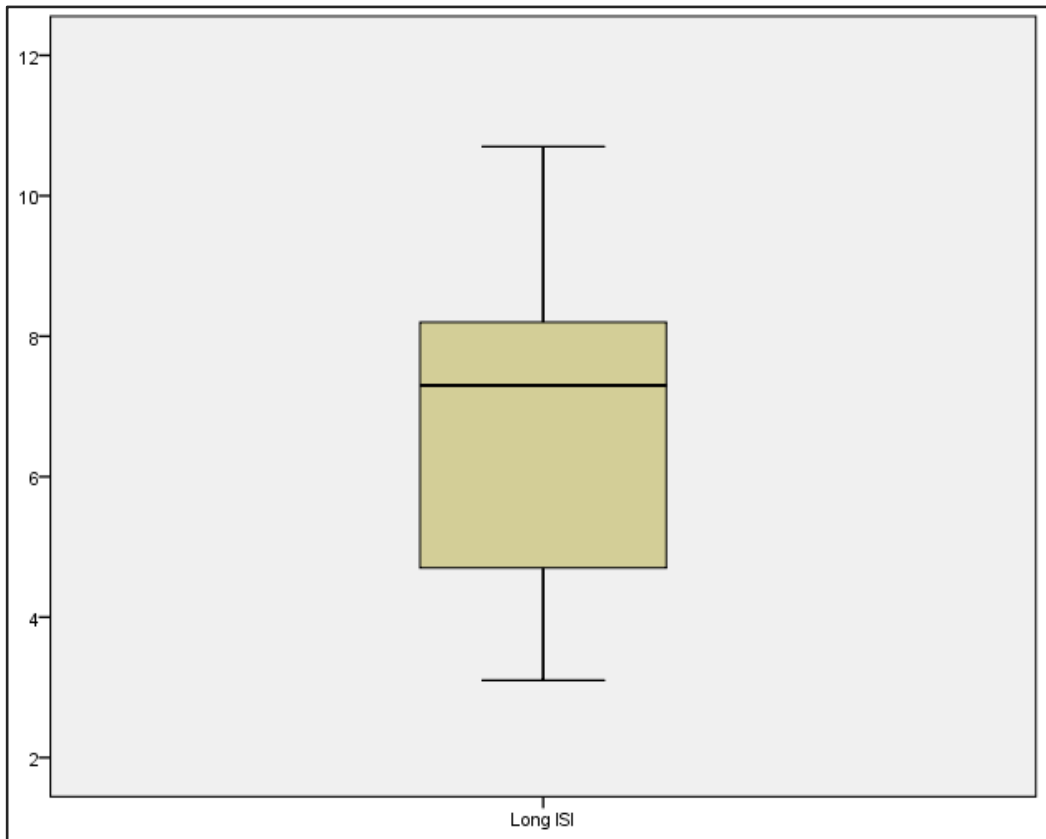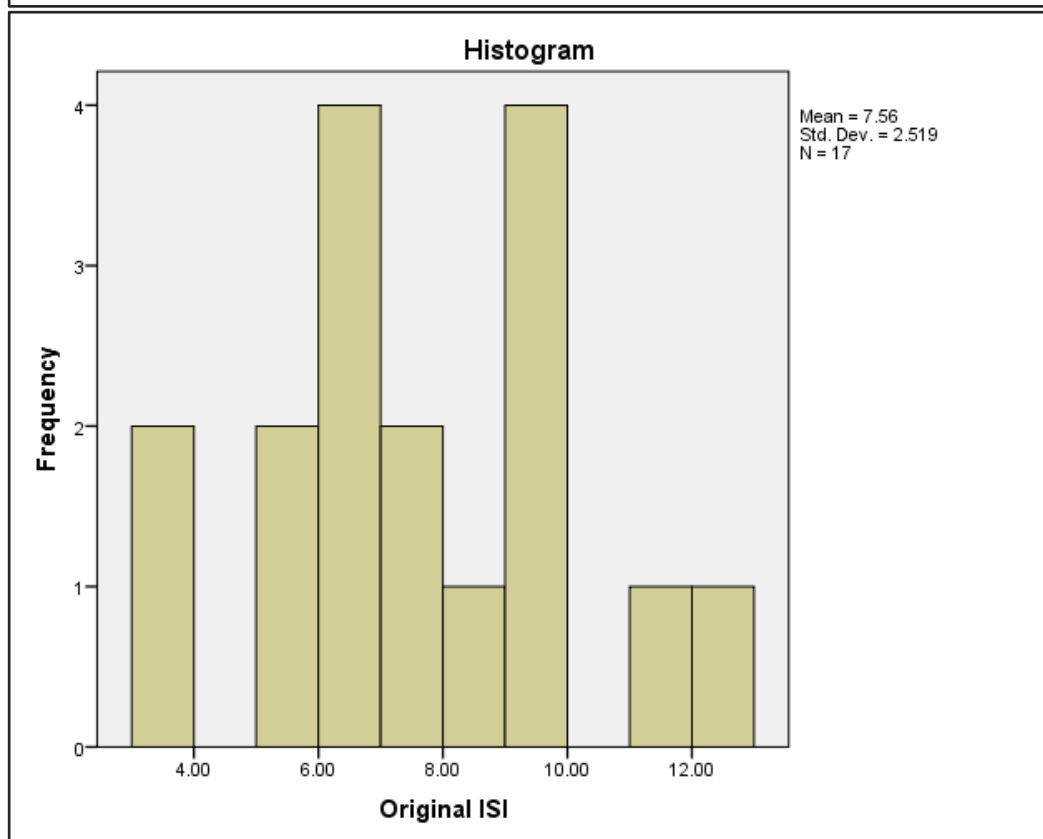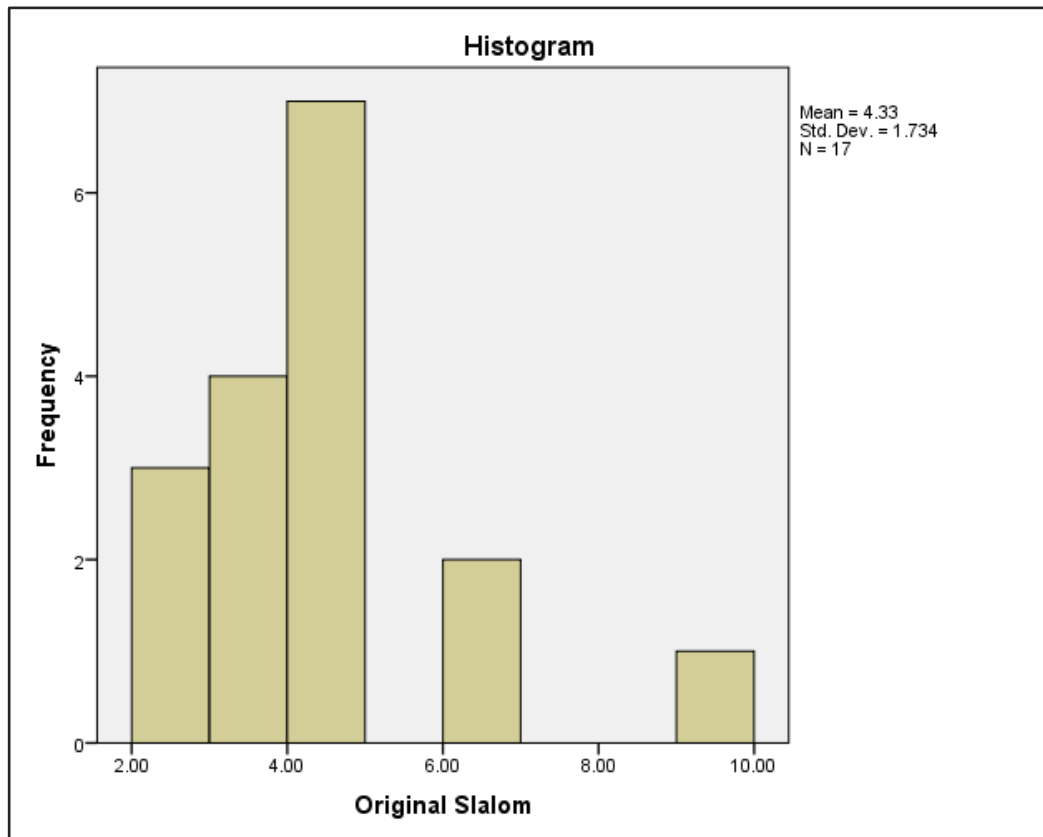
Histogram

Mean = 1.37
Std. Dev. = .772
N = 28

Grey triangles (ln)

Histogram

Mean = 1.84
Std. Dev. = .683
N = 28

Original slalom (ln)

237

Histogram

Mean = 1.60
Std. Dev. = .742
N = 28
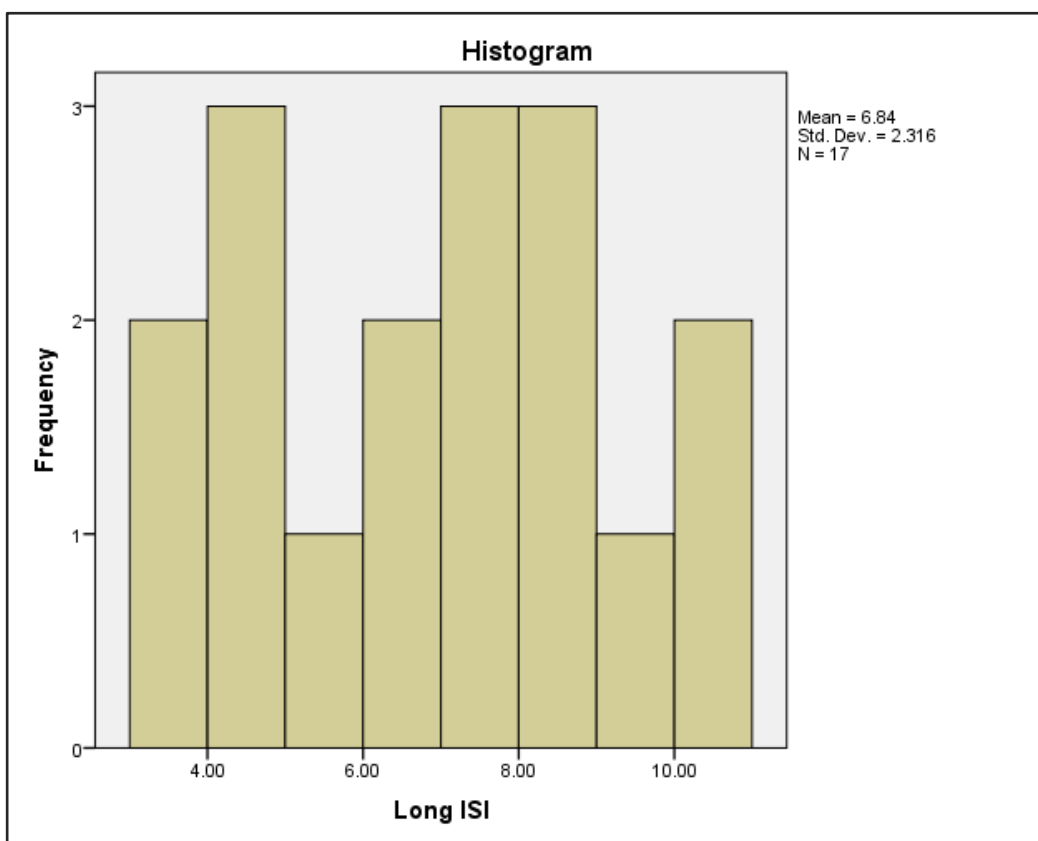
Frequency

Transparent triangles (ln)
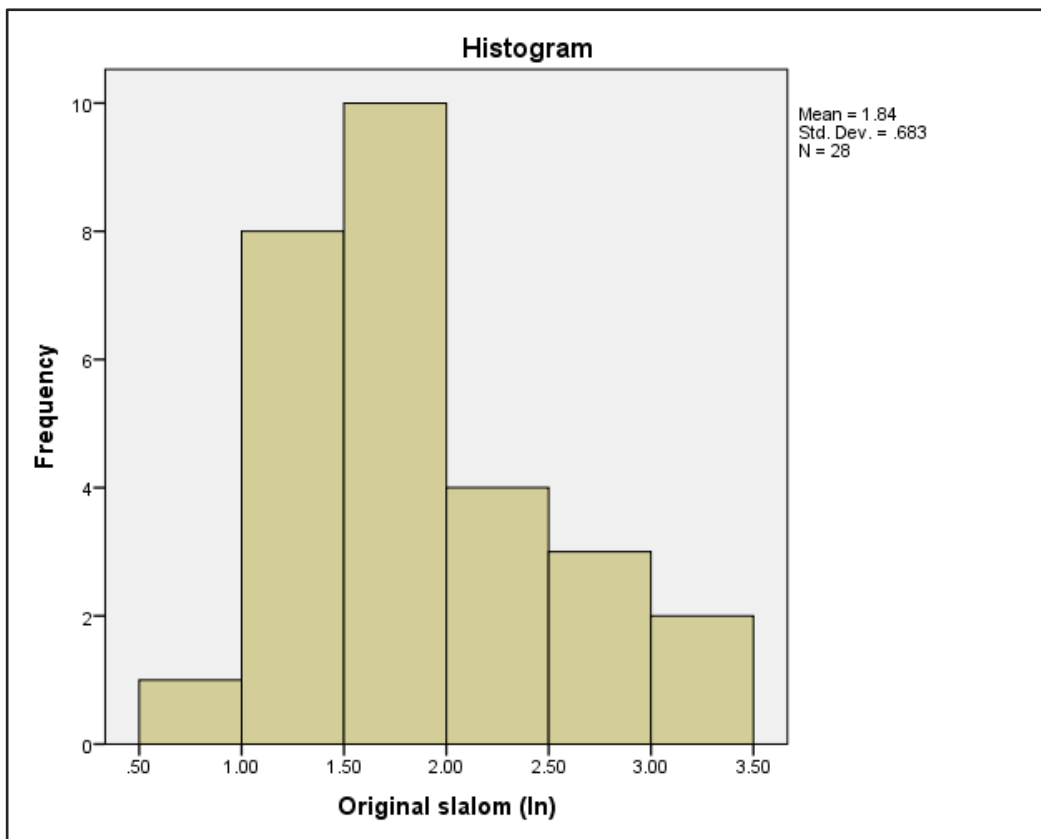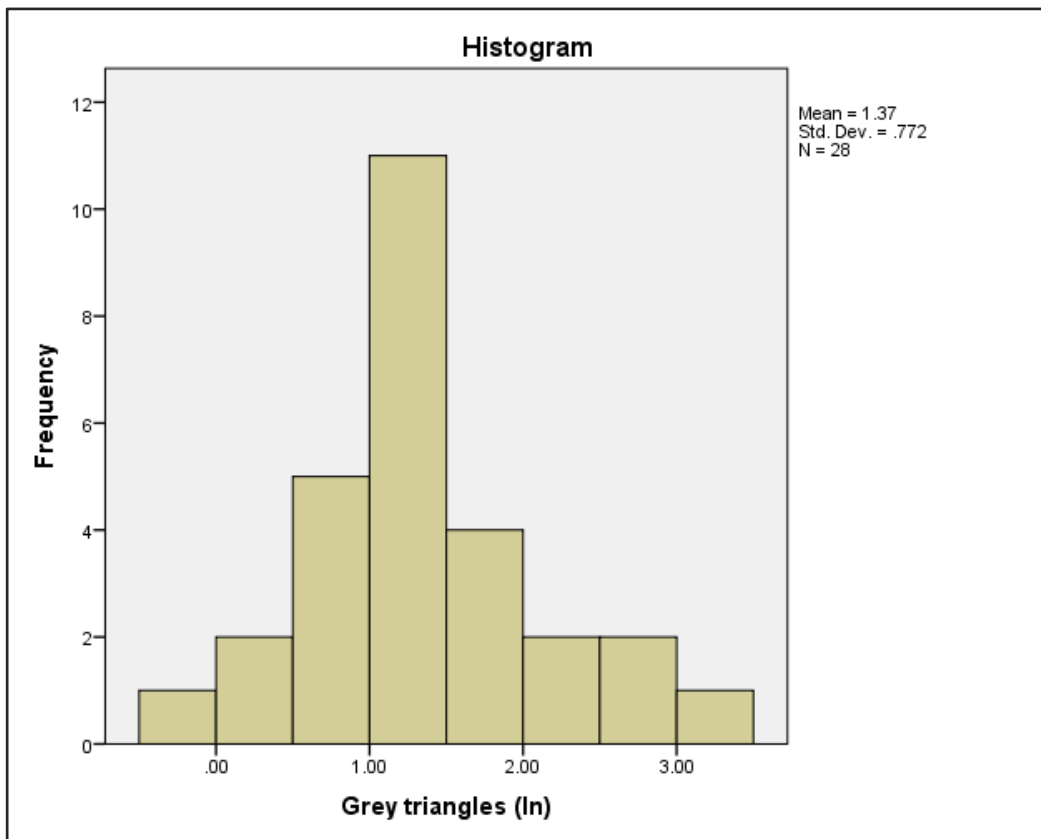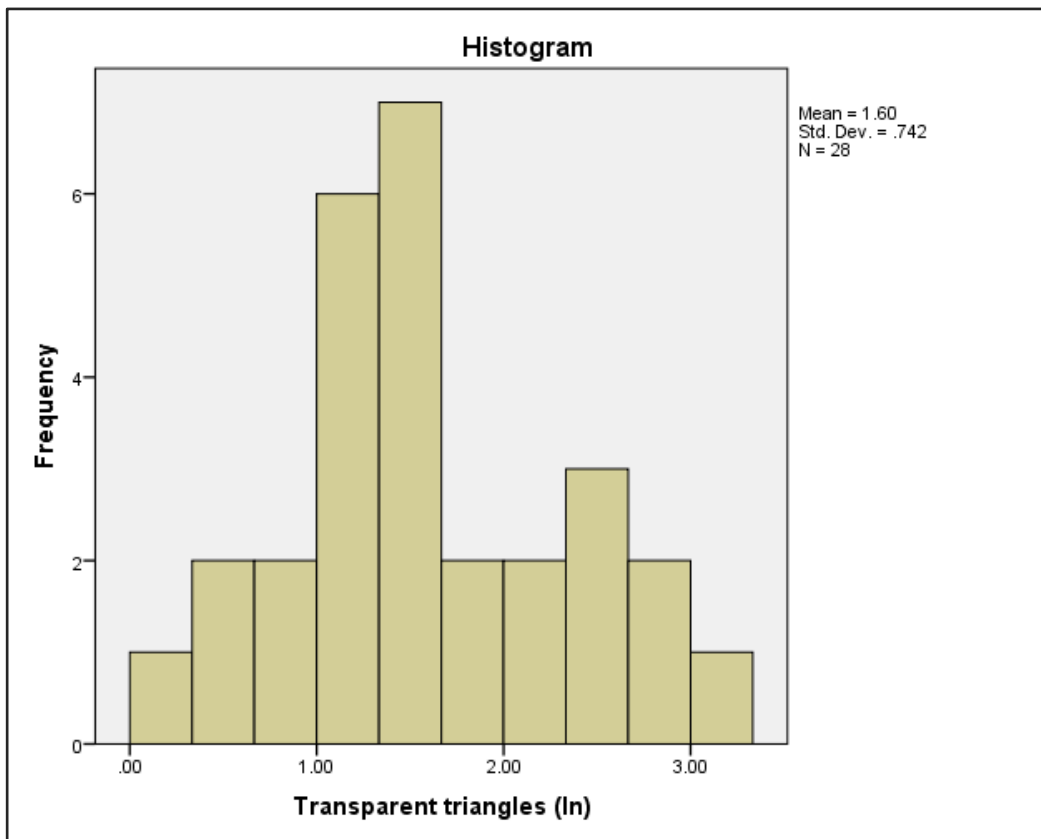
Appendix 18.Boxplots showing the distribution of the data from the experiment in

Chapter 4.

Appendix 19.Histograms showing the distribution of the data from the experiment in

Chapter 4.

Histogram

Mean = 6.84
Std. Dev. = 2.316
N = 17

Long ISI

Histogram

Mean = 3.72
Std. Dev. = 1.20
N = 17

Short ISI

242
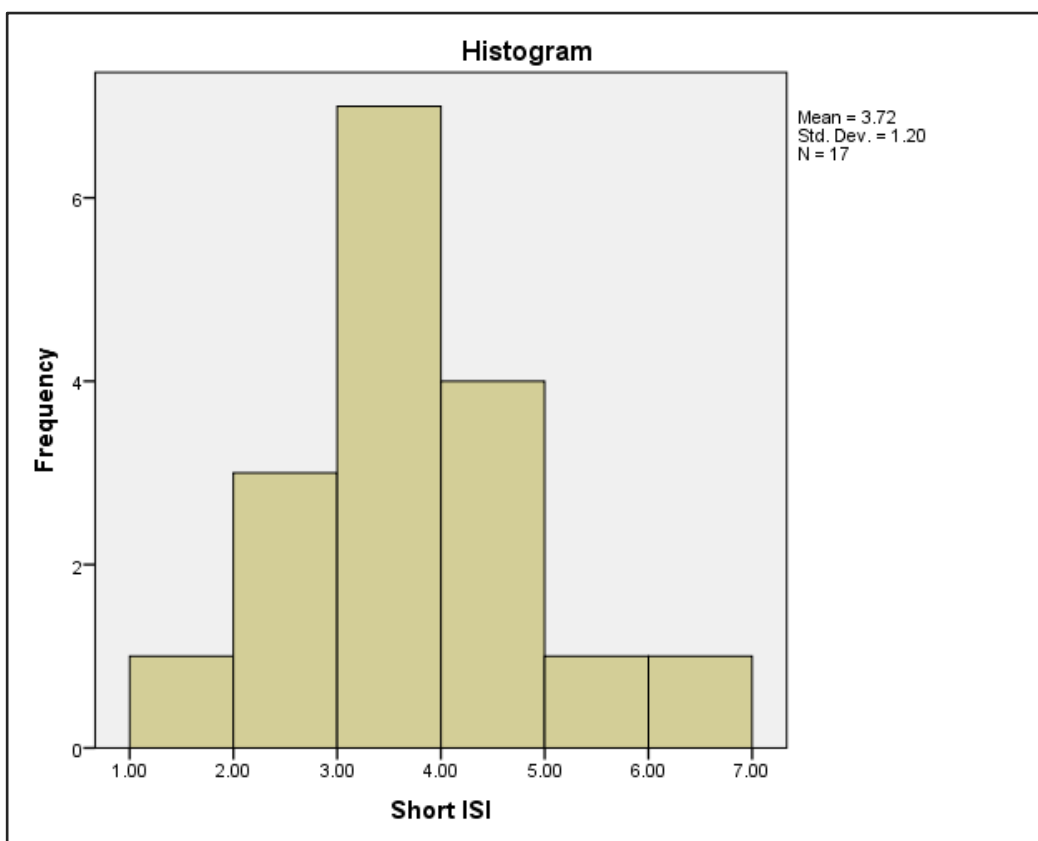
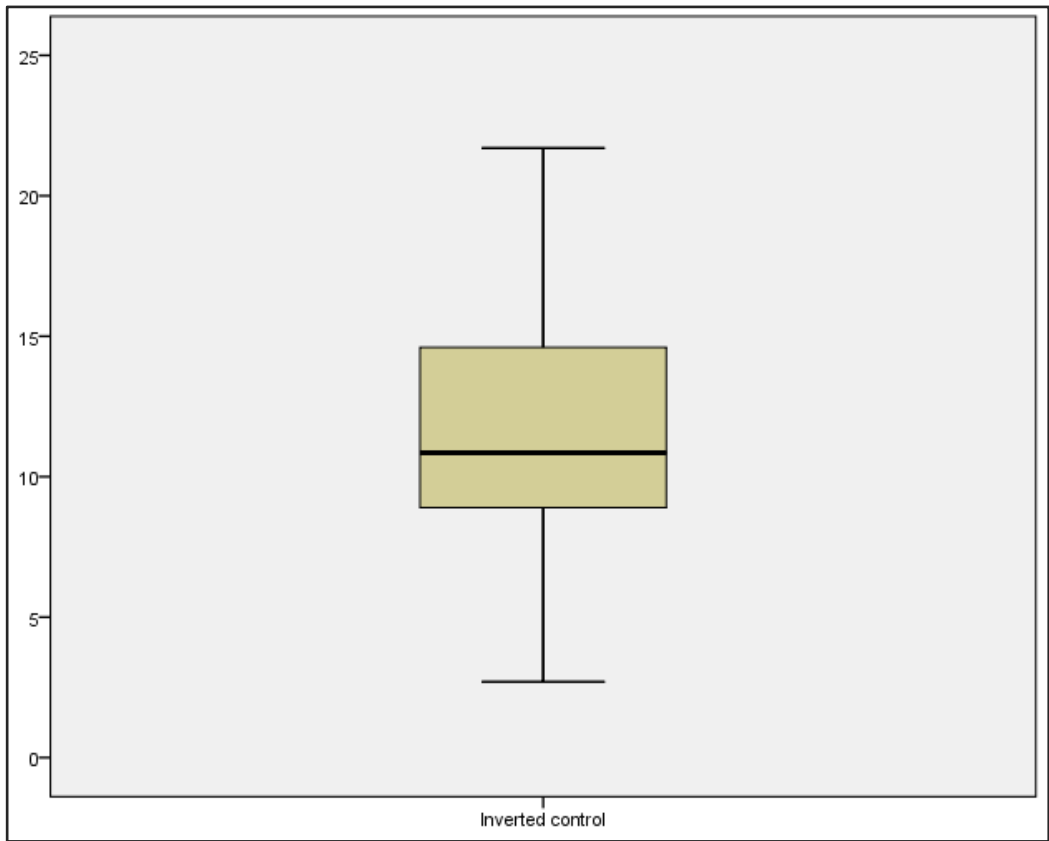**Appendix 20.** Descriptive statistics for the data from the experiment in Chapter 4.

Descriptives

			Statistic	Std. Error
Original Slalom	Mean		4.3324	.42045
	95% Confidence Interval for Mean	Lower Bound	3.4410	
		Upper Bound	5.2237	
	5% Trimmed Mean		4.1582	
	Median		4.2000	
	Variance		3.005	
	Std. Deviation		1.73358	
	Minimum		2.30	
	Maximum		9.50	
	Range		7.20	
	Interquartile Range		1.60	
	Skewness		1.796	.550
	Kurtosis		4.176	1.063
Original ISI	Mean		7.5565	.61105
	95% Confidence Interval for Mean	Lower Bound	6.2611	
		Upper Bound	8.8518	
	5% Trimmed Mean		7.5239	
	Median		7.2000	
	Variance		6.347	
	Std. Deviation		2.51942	
	Minimum		3.40	
	Maximum		12.30	
	Range		8.90	
	Interquartile Range		3.63	
	Skewness		.157	.550
	Kurtosis		-.442	1.063
Long ISI	Mean		6.8400	.56166
	95% Confidence Interval for Mean	Lower Bound	5.6493	
		Upper Bound	8.0307	
	5% Trimmed Mean		6.8333	
	Median		7.3000	
	Variance		5.363	
	Std. Deviation		2.31579	
	Minimum		3.10	
	Maximum		1.70	
	Range		7.60	
	Interquartile Range		3.80	
	Skewness		-.081	.550

	Kurtosis		-.899	1.063
Short ISI	Mean		3.7194	.29103
	95% Confidence Interval for Mean	Lower Bound	3.1024	
		Upper Bound	4.3364	
	5% Trimmed Mean		3.6716	
	Median		3.5000	
	Variance		1.440	
	Std. Deviation		1.19996	
	Minimum		1.70	
	Maximum		6.60	
	Range		4.90	
	Interquartile Range		1.30	
	Skewness		.682	.550
	Kurtosis		1.117	1.063

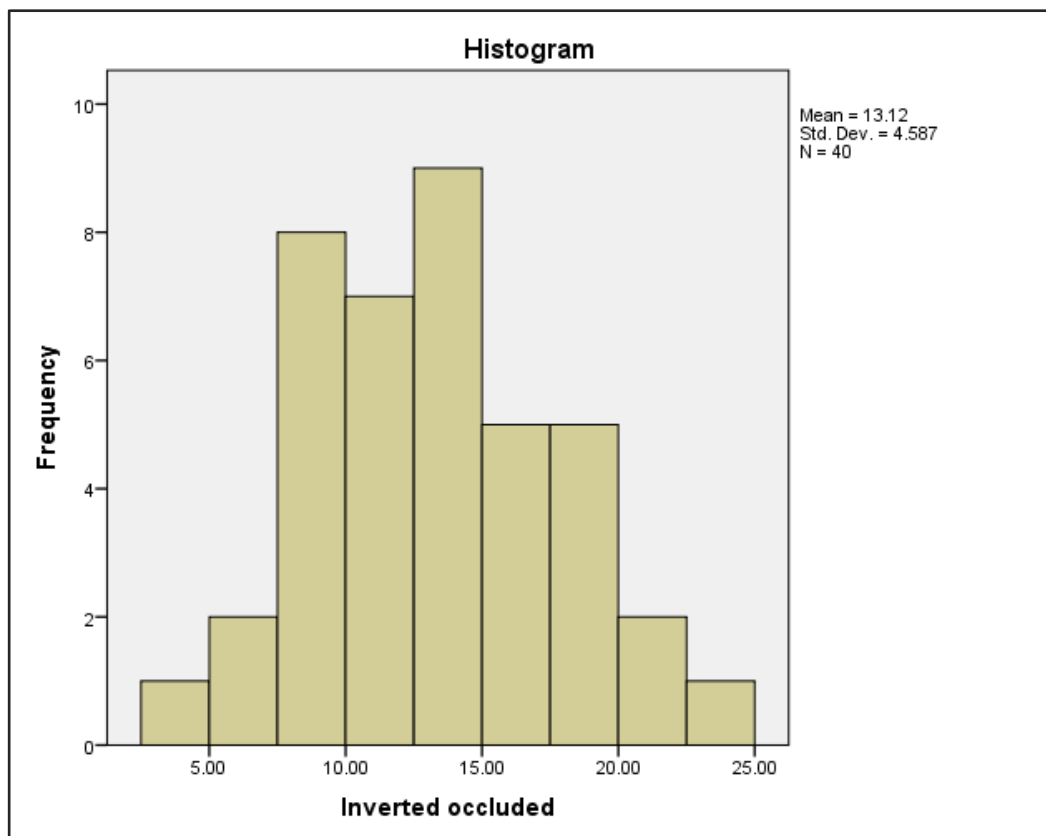**Appendix 21**.Boxplots showing the distribution of the data from Experiment 1 Chapter 5.
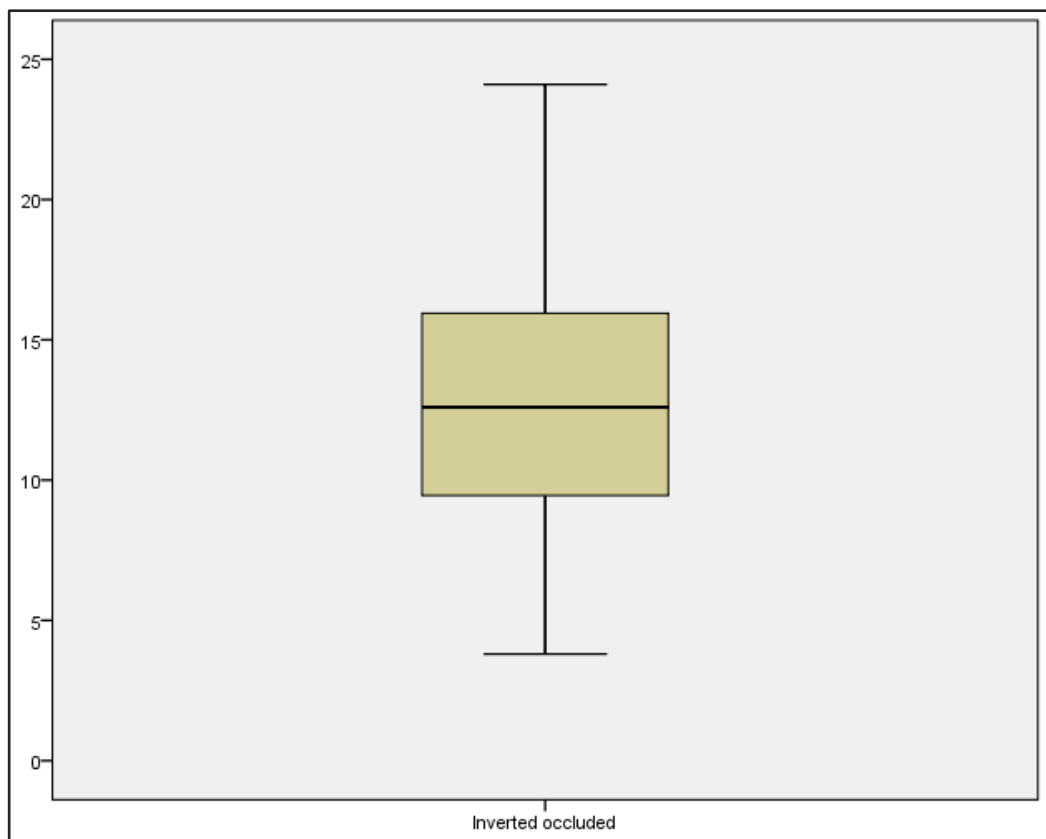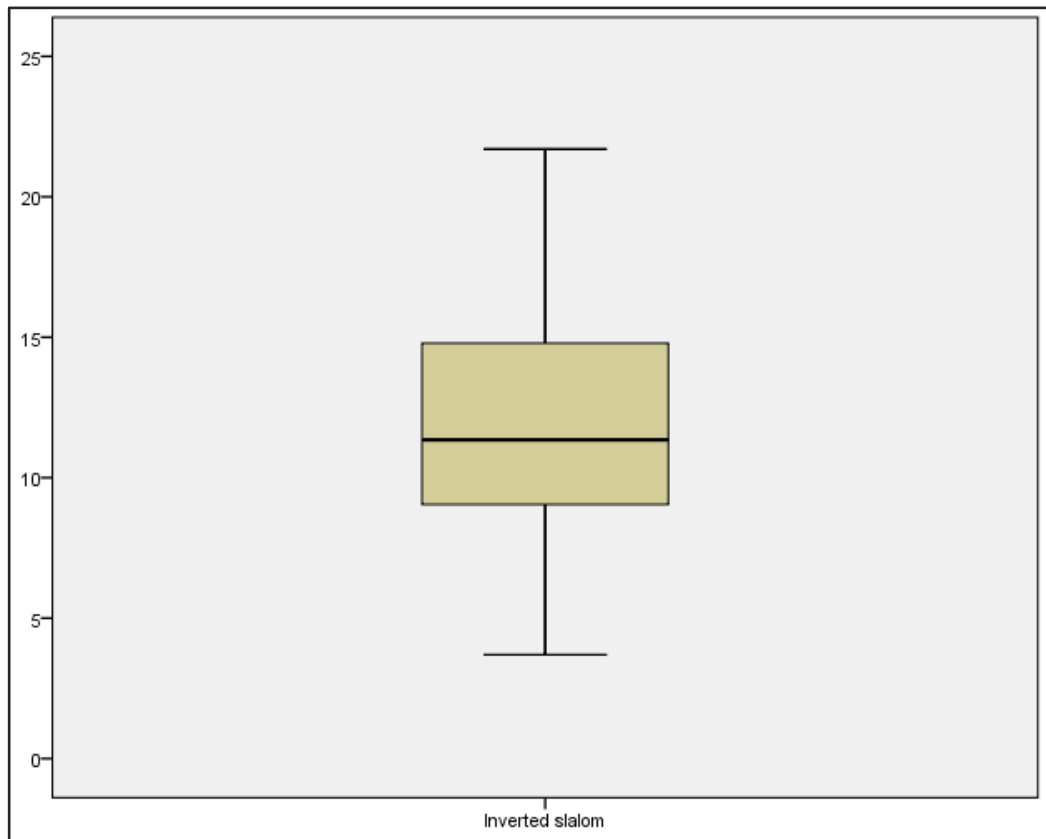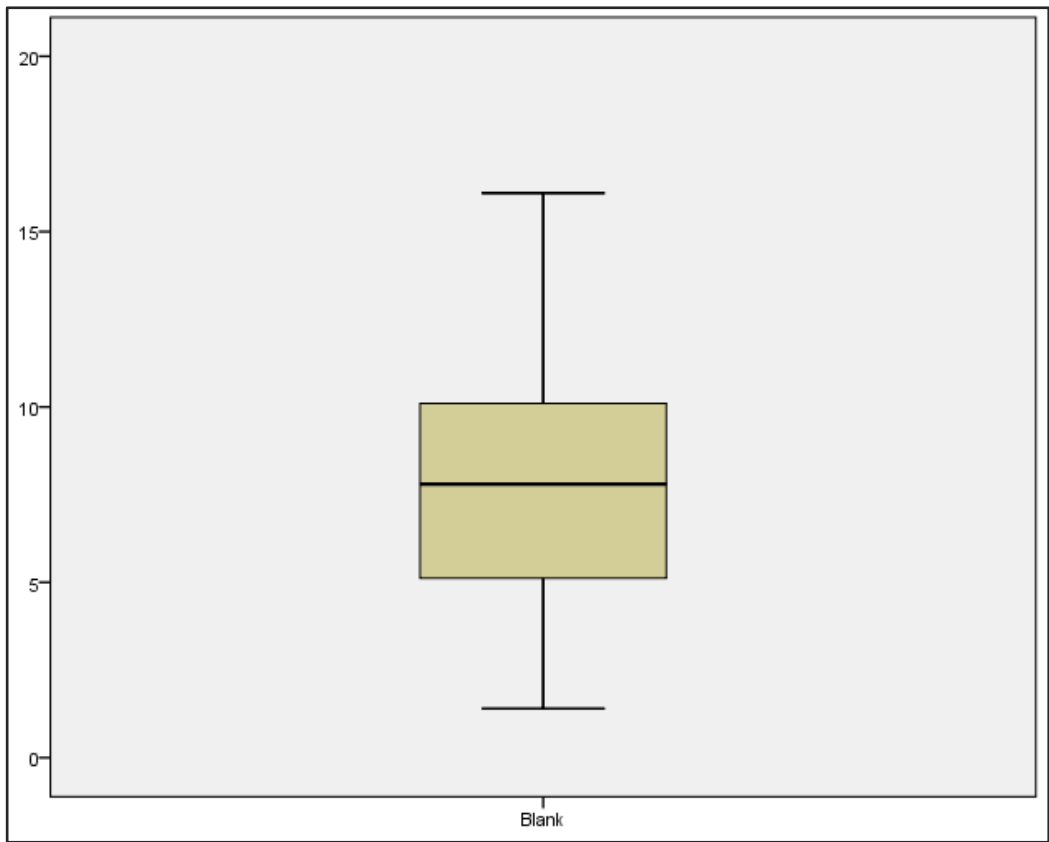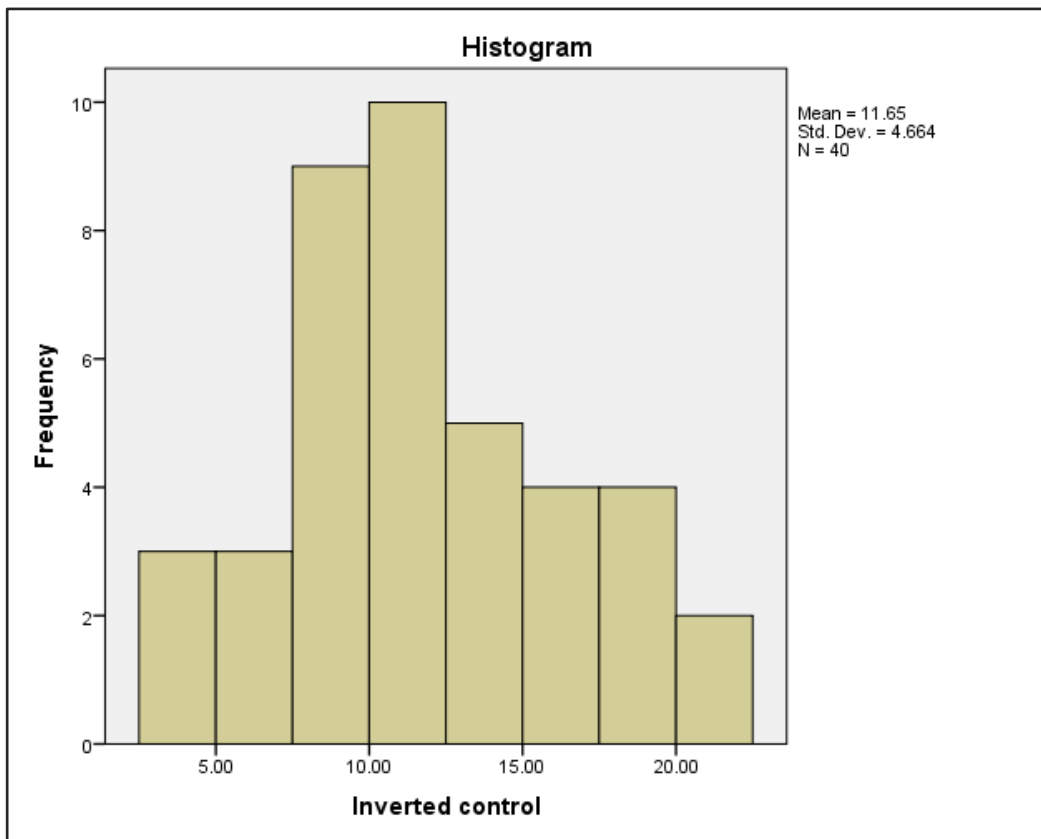
Appendix 22.Histograms showing the distribution of the data from Experiment 1

Chapter 5.

Histogram

Mean = 11.65
Std. Dev. = 4.664
N = 40

Inverted control

Histogram

Mean = 7.73
Std. Dev. = 3.609
N = 40

Blank

248
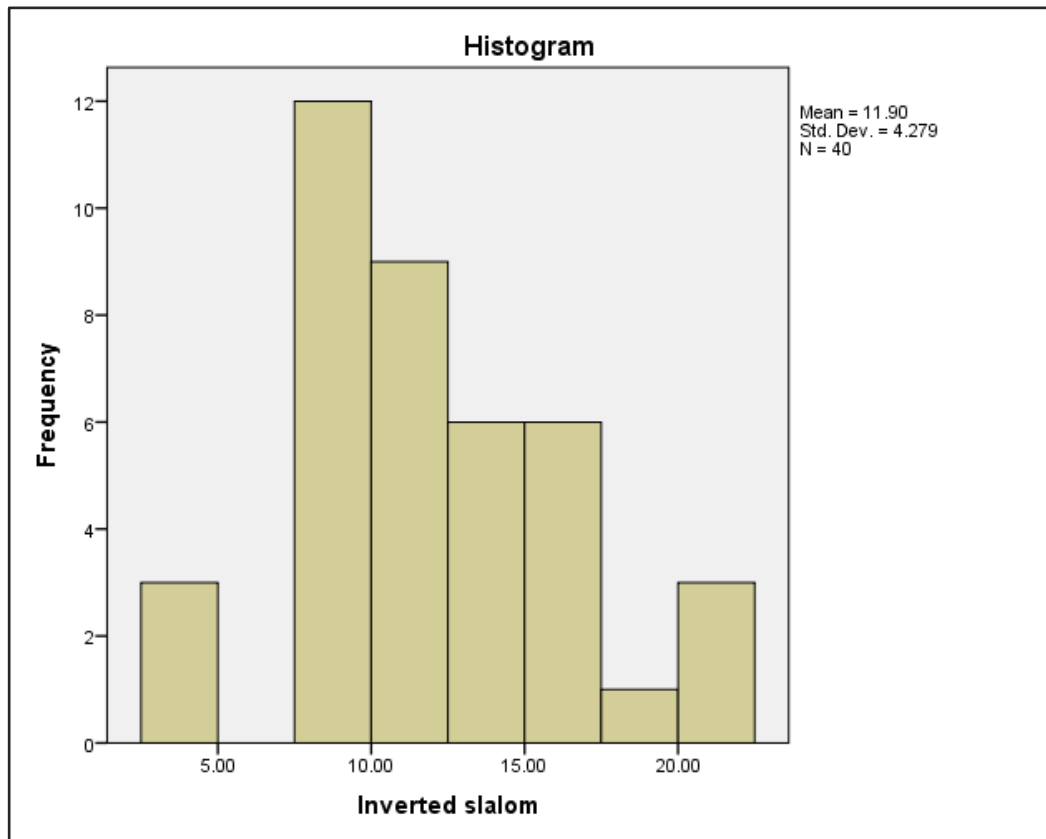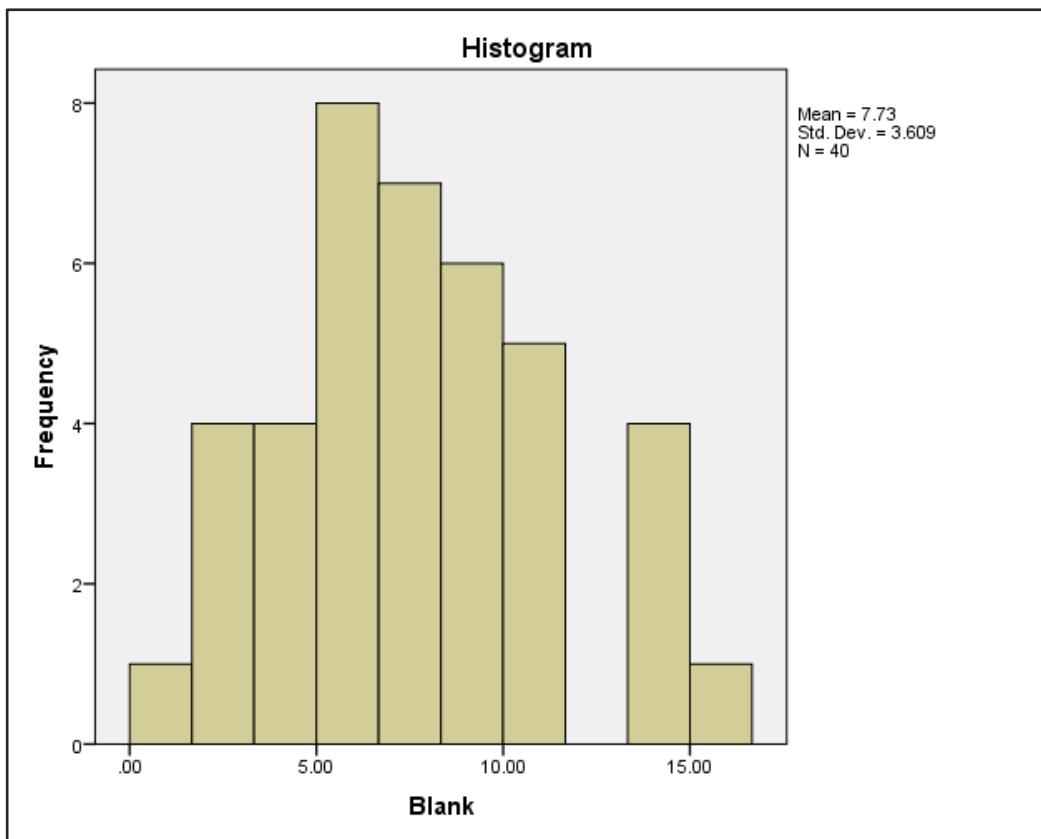
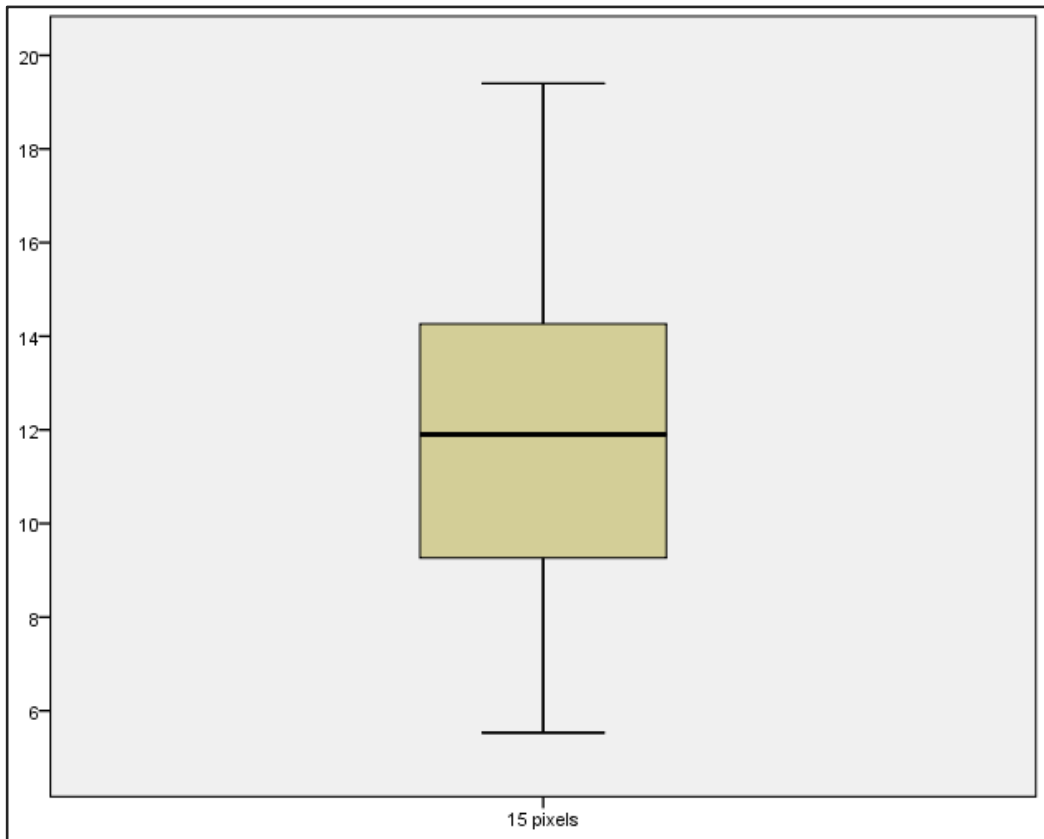**Appendix 23**.Descriptive statistics for the data from Experiment 1 Chapter 5.

Descriptives

			Statistic	Std. Error
Inverted slalom	Mean		11.8960	.67663
	95% Confidence Interval for Mean	Lower Bound	1.5274	
		Upper Bound	13.2646	
	5% Trimmed Mean		11.7925	
	Median		11.3500	
	Variance		18.313	
	Std. Deviation		4.27937	
	Minimum		3.70	
	Maximum		21.70	
	Range		18.00	
	Interquartile Range		6.30	
	Skewness		.487	.374
	Kurtosis		-.026	.733
Inverted occluded	Mean		13.1188	.72522
	95% Confidence Interval for Mean	Lower Bound	11.6519	
		Upper Bound	14.5856	
	5% Trimmed Mean		13.0319	
	Median		12.6000	
	Variance		21.038	
	Std. Deviation		4.58668	
	Minimum		3.80	
	Maximum		24.10	
	Range		2.30	
	Interquartile Range		6.75	
	Skewness		.368	.374
	Kurtosis		-.205	.733
Inverted control	Mean		11.6490	.73746
	95% Confidence Interval for Mean	Lower Bound	1.1573	
		Upper Bound	13.1407	
	5% Trimmed Mean		11.5847	
	Median		1.8500	
	Variance		21.754	
	Std. Deviation		4.66412	
	Minimum		2.70	
	Maximum		21.70	
	Range		19.00	
	Interquartile Range		5.95	
	Skewness		.314	.374

	Kurtosis		-.277	.733
Blank	Mean		7.7343	.57071
	95% Confidence Interval for Mean	Lower Bound	6.5799	
		Upper Bound	8.8886	
	5% Trimmed Mean		7.6631	
	Median		7.8000	
	Variance		13.028	
	Std. Deviation		3.60947	
	Minimum		1.40	
	Maximum		16.10	
	Range		14.70	
	Interquartile Range		5.04	
	Skewness		.395	.374
	Kurtosis		-.267	.733

Appendix 24.Boxplots showing the distribution of the data from Experiment 2 Chapter 5.
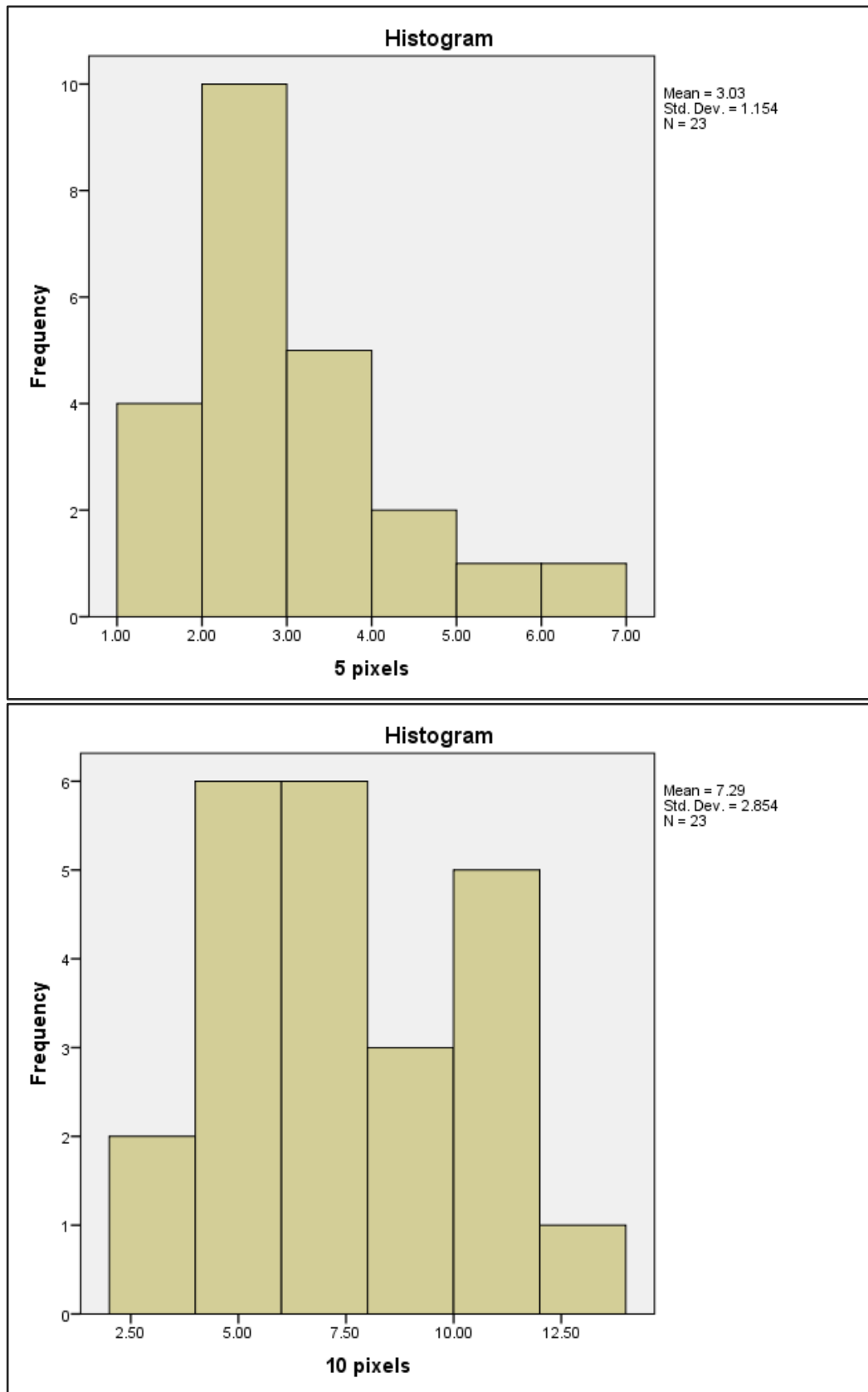
15 pixels

20 pixels

252
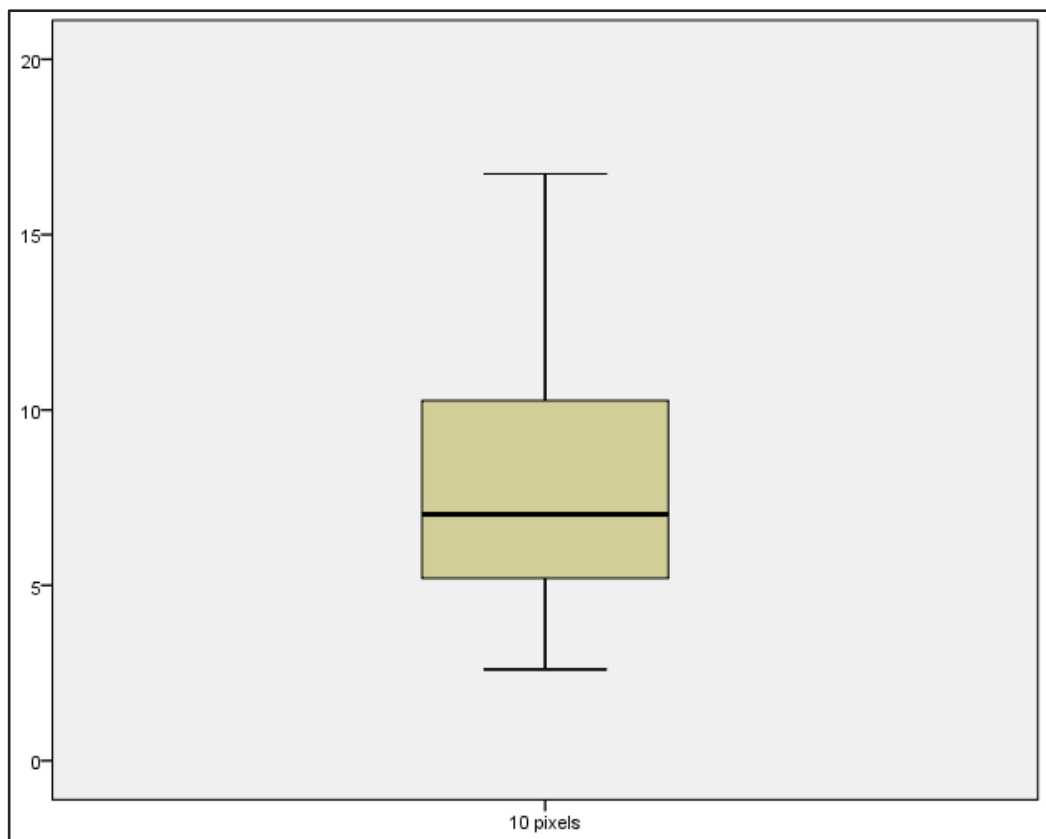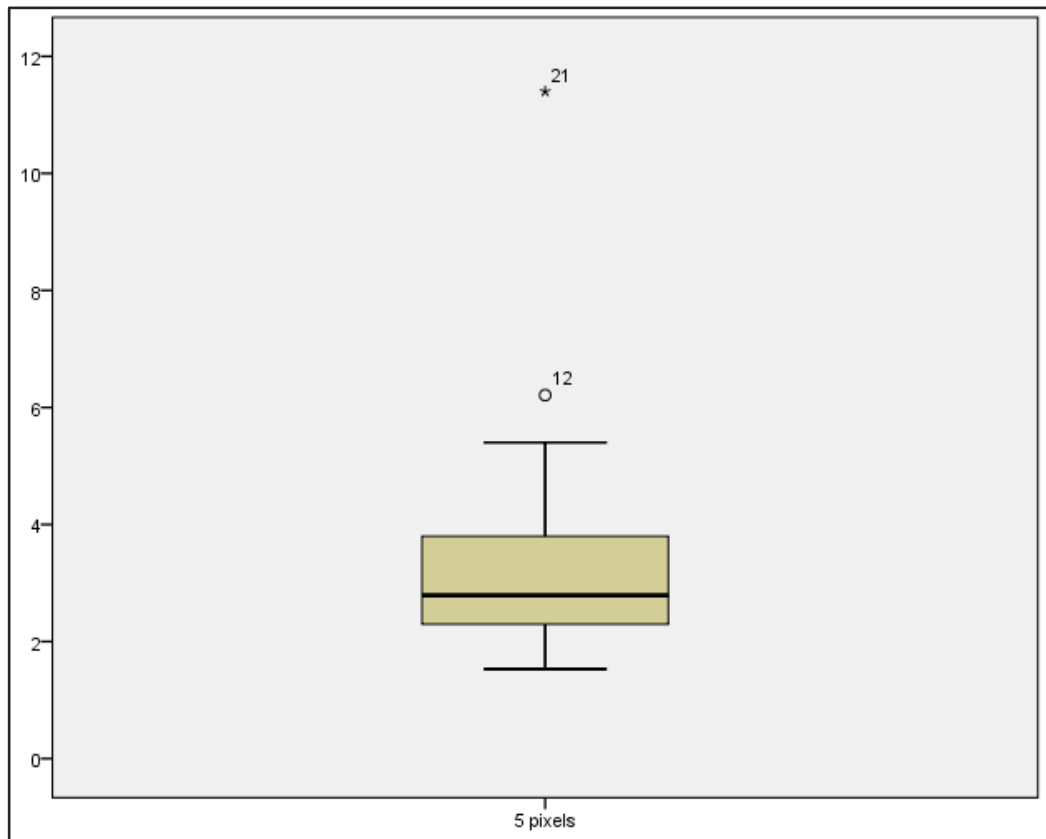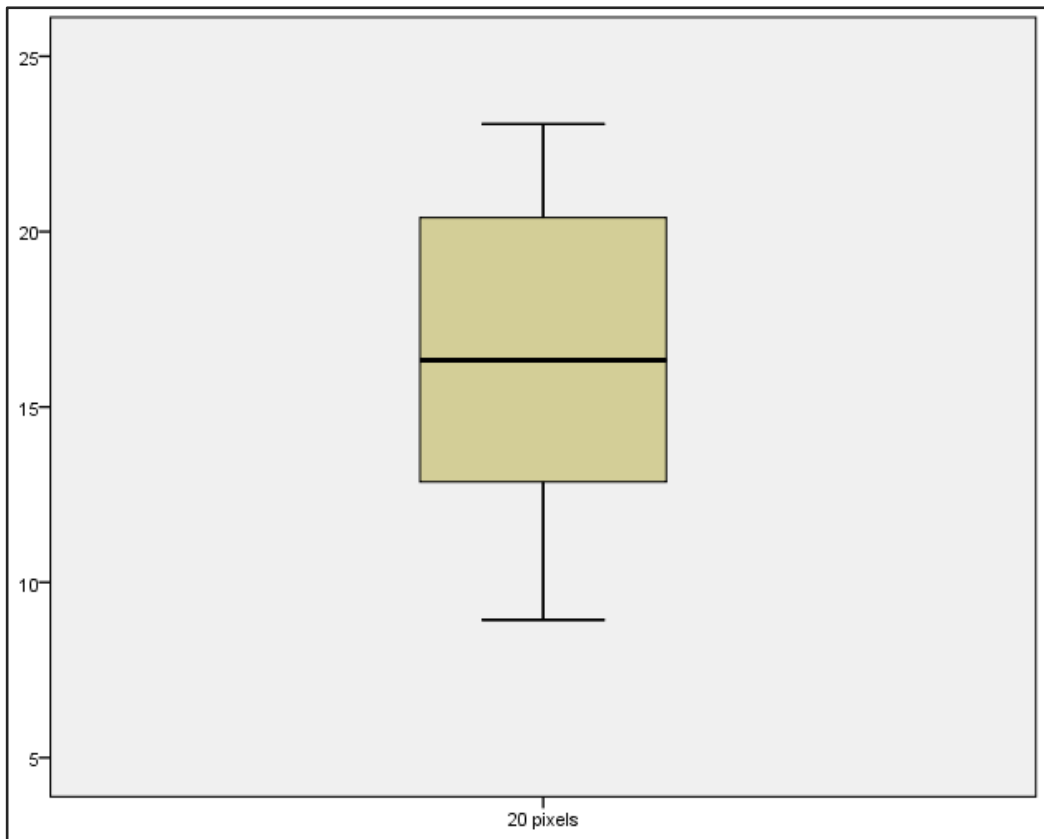
Appendix 25. Descriptive statistics for the data from Experiment 2 Chapter 5 after the outlier was removed.

Descriptives

			Statistic	Std. Error
5 pixels	Mean		3.0287	.24063
	95% Confidence Interval for Mean	Lower Bound	2.5297	
		Upper Bound	3.5277	
	5% Trimmed Mean		2.9391	
	Median		2.7300	
	Variance		1.332	
	Std. Deviation		1.15402	
	Minimum		1.53	
	Maximum		6.21	
	Range		4.68	
	Interquartile Range		1.47	
	Skewness		1.286	.481
	Kurtosis		1.664	.935
10 pixels	Mean		7.2904	.59509
	95% Confidence Interval for Mean	Lower Bound	6.0563	
		Upper Bound	8.5246	
	5% Trimmed Mean		7.2773	
	Median		6.8700	
	Variance		8.145	
	Std. Deviation		2.85393	
	Minimum		2.60	
	Maximum		12.33	
	Range		9.73	
	Interquartile Range		5.00	
	Skewness		.166	.481
	Kurtosis		-.934	.935
15 pixels	Mean		11.7826	.74895
	95% Confidence Interval for Mean	Lower Bound	1.2294	
		Upper Bound	13.3358	
	5% Trimmed Mean		11.7903	
	Median		11.4400	
	Variance		12.901	
	Std. Deviation		3.59184	
	Minimum		5.53	
	Maximum		17.67	
	Range		12.14	

	Interquartile Range		5.07	
	Skewness		.270	.481
	Kurtosis		-.897	.935
20 pixels	Mean		16.0983	.87613
	95% Confidence Interval for Mean	Lower Bound	14.2813	
		Upper Bound	17.9153	
	5% Trimmed Mean		16.1164	
	Median		16.2700	
	Variance		17.655	
	Std. Deviation		4.20179	
	Minimum		8.93	
	Maximum		22.93	
	Range		14.00	
	Interquartile Range		7.60	
	Skewness		-.049	.481
	Kurtosis		-1.169	.935

**Appendix 26**.Histograms showing the distribution of the data from Experiment 2

Chapter 5 after the outlier was removed.

Histogram

Mean = 11.78
Std. Dev. = 3.592
N = 23

15 pixels

Histogram
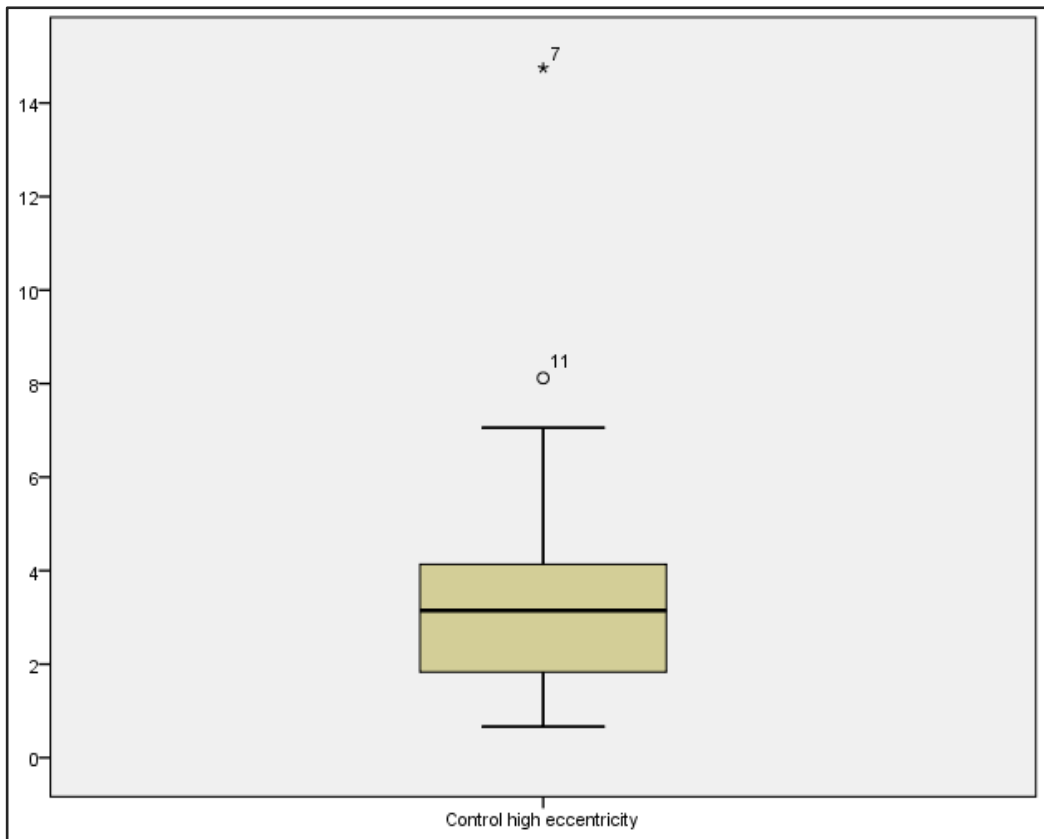
Mean = 16.10
Std. Dev. = 4.202
N = 23

20 pixels

256
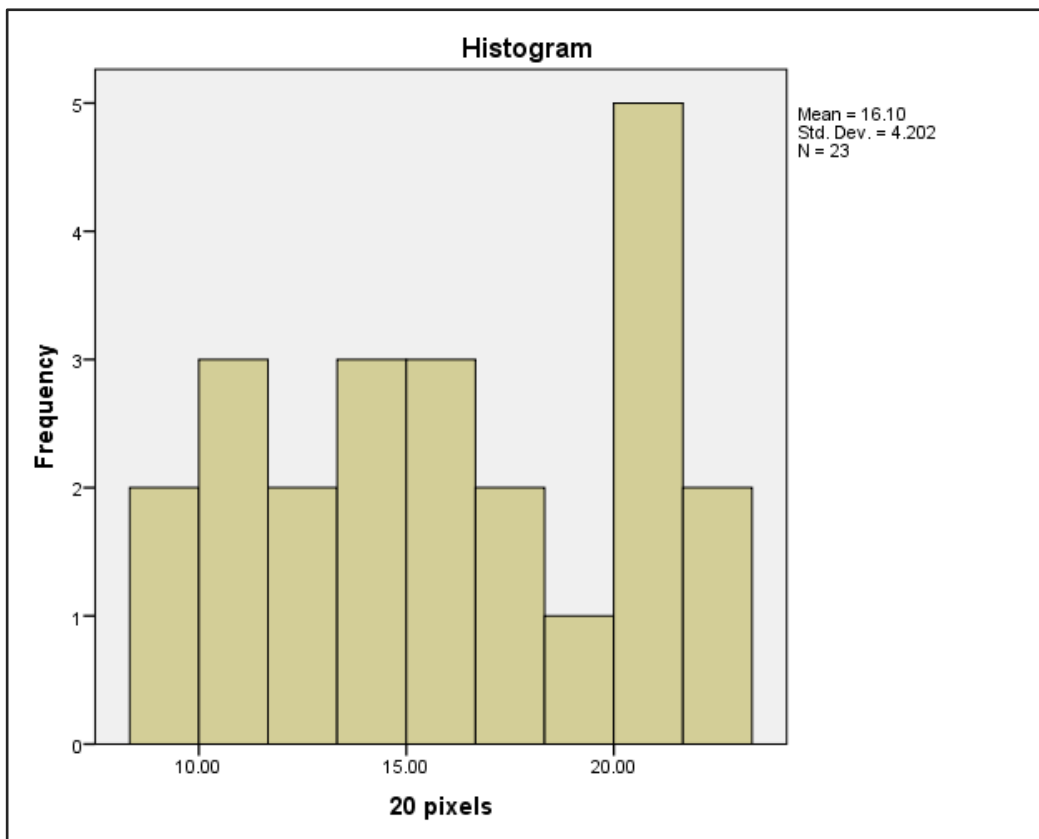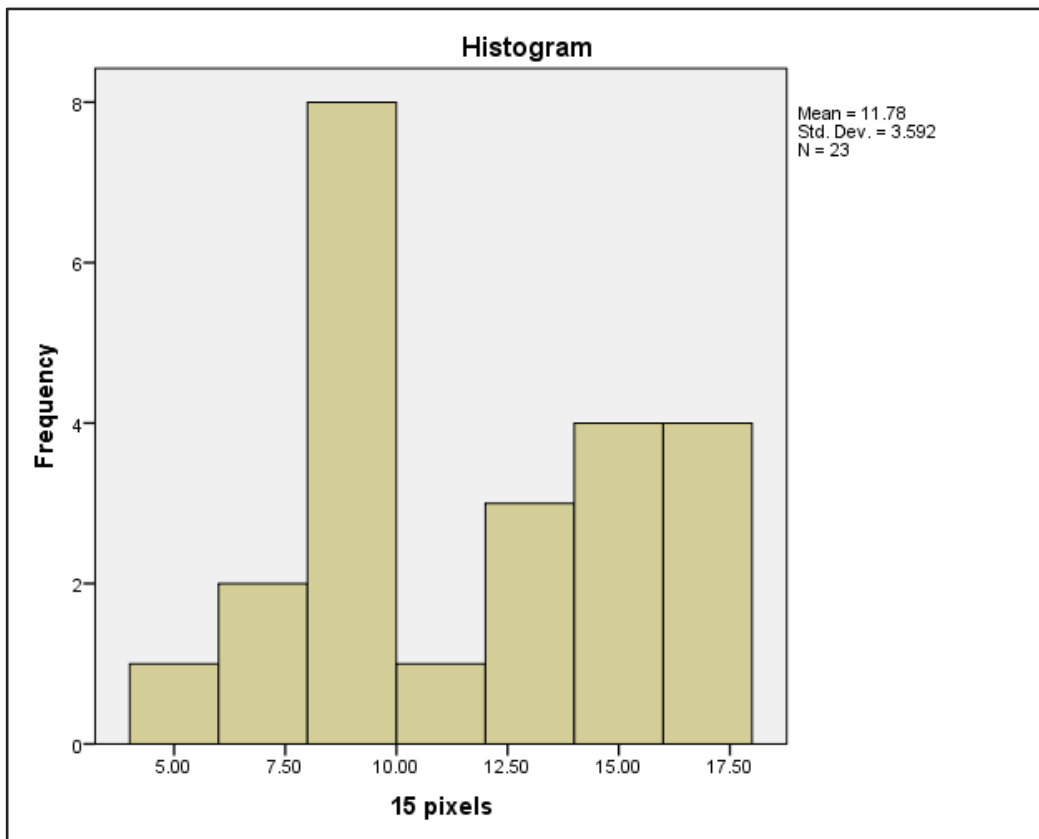
Appendix 27.Boxplots showing the distribution of the amplitude data from the

experiment in Chapter 6.

Control mid eccentricity
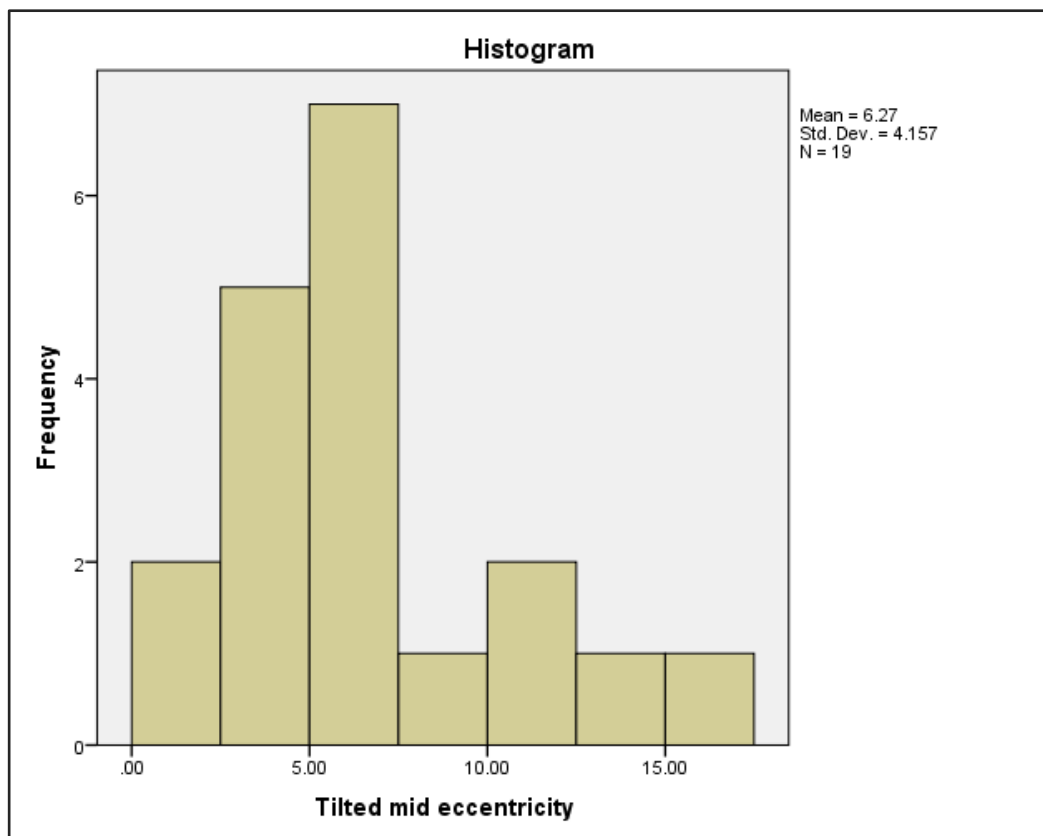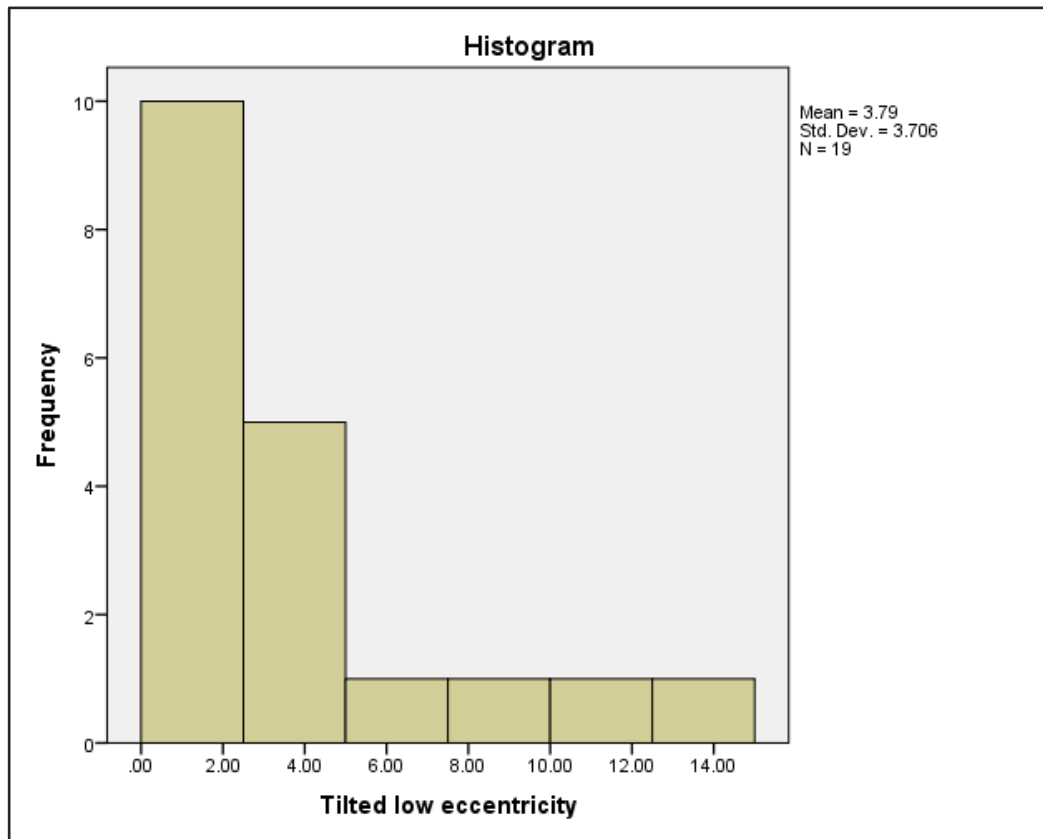

Control high eccentricity
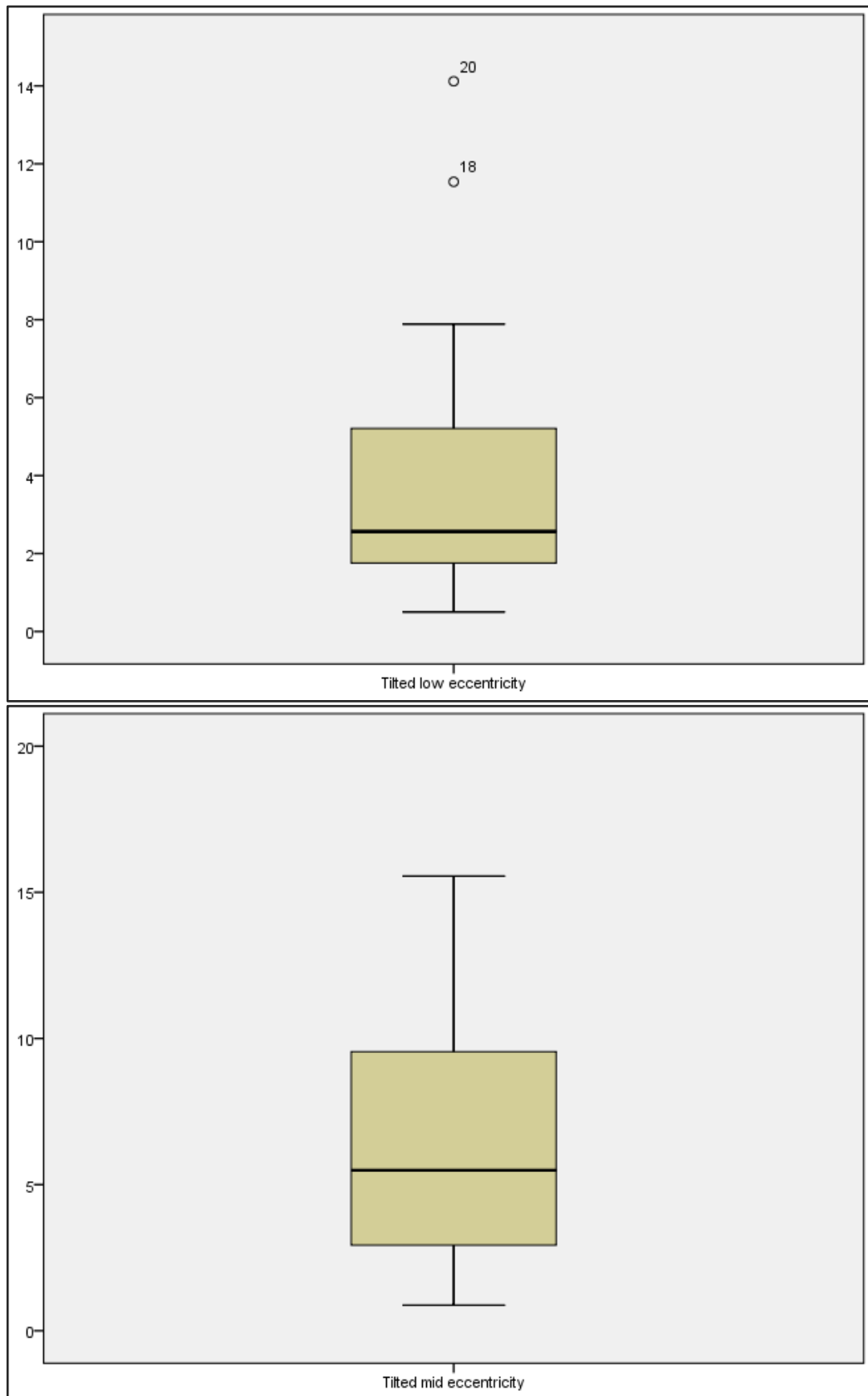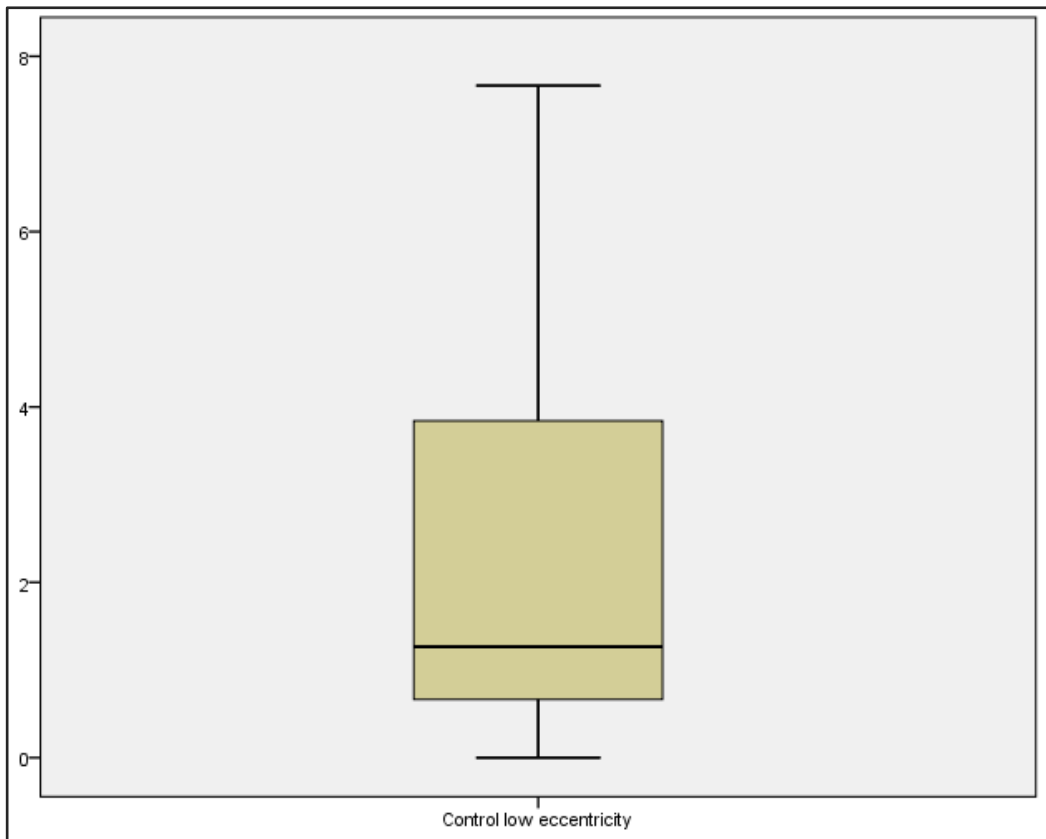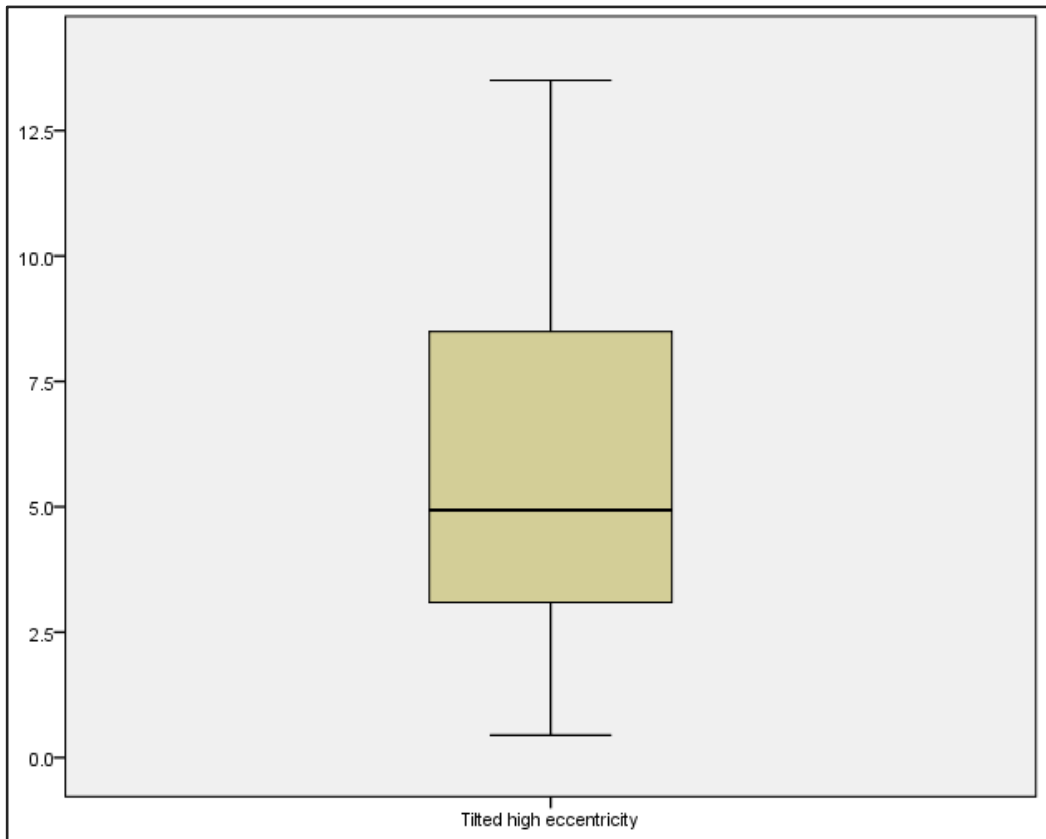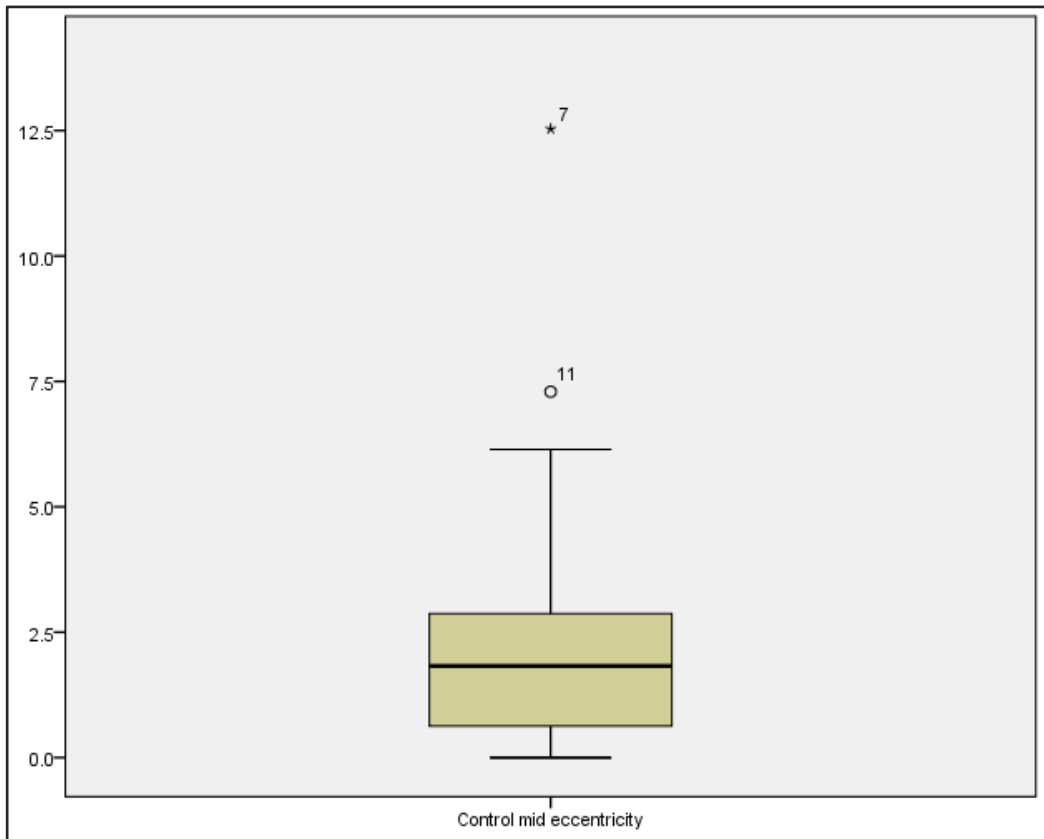
Appendix 28. Descriptive statistics for the amplitude data from the experiment in

Chapter 6 after the outlier was removed.

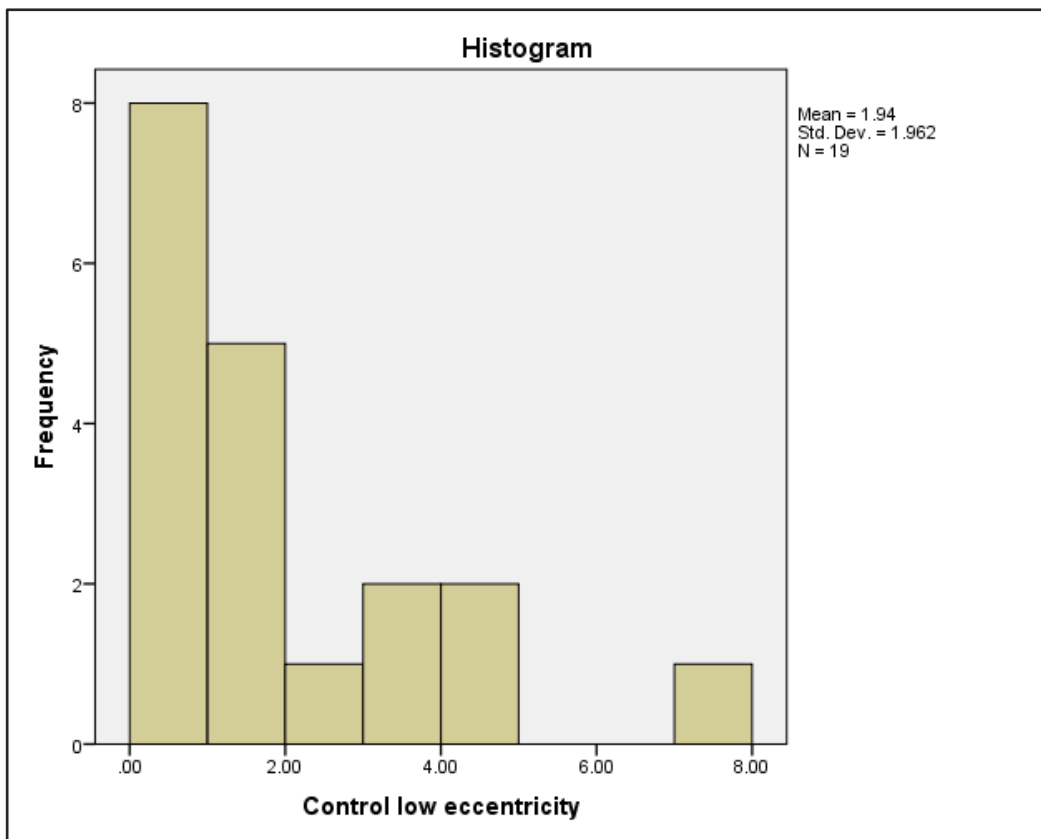**Descriptives**

			Statistic	Std. Error
Tilted low eccentricity	Mean		3.7885	.85031
	95% Confidence Interval for Mean	Lower Bound	2.0020	
		Upper Bound	5.5749	
	5% Trimmed Mean		3.3973	
	Median		2.3529	
	Variance		13.738	
	Std. Deviation		3.70642	
	Minimum		.50	
	Maximum		14.12	
	Range		13.62	
	Interquartile Range		3.00	
	Skewness		1.816	.524
	Kurtosis		2.892	1.014
Tilted mid eccentricity	Mean		6.2688	.95371
	95% Confidence Interval for Mean	Lower Bound	4.2651	
		Upper Bound	8.2724	
	5% Trimmed Mean		6.0525	
	Median		5.4118	
	Variance		17.282	
	Std. Deviation		4.15714	
	Minimum		.88	
	Maximum		15.56	
	Range		14.68	
	Interquartile Range		5.31	
	Skewness		1.001	.524
	Kurtosis		.136	1.014
Tilted high eccentricity	Mean		5.5437	.80929
	95% Confidence Interval for Mean	Lower Bound	3.8435	
		Upper Bound	7.2440	
	5% Trimmed Mean		5.3964	
	Median		4.5333	
	Variance		12.444	
	Std. Deviation		3.52762	
	Minimum		.44	
	Maximum		13.29	
	Range		12.85	

	Interquartile Range		4.81	
	Skewness		.858	.524
	Kurtosis		.224	1.014
Control low eccentricity	Mean		1.9426	.45017
	95% Confidence Interval for Mean	Lower Bound	.9968	
		Upper Bound	2.8883	
	5% Trimmed Mean		1.7325	
	Median		1.2000	
	Variance		3.850	
	Std. Deviation		1.96226	
	Minimum		.00	
	Maximum		7.67	
	Range		7.67	
	Interquartile Range		3.18	
	Skewness		1.603	.524
	Kurtosis		2.686	1.014
Control mid eccentricity	Mean		2.1453	.45602
	95% Confidence Interval for Mean	Lower Bound	1.1872	
		Upper Bound	3.1033	
	5% Trimmed Mean		1.9784	
	Median		1.7778	
	Variance		3.951	
	Std. Deviation		1.98773	
	Minimum		.00	
	Maximum		7.29	
	Range		7.29	
	Interquartile Range		2.08	
	Skewness		1.387	.524
	Kurtosis		1.698	1.014
Control high eccentricity	Mean		3.2533	.45092
	95% Confidence Interval for Mean	Lower Bound	2.3060	
		Upper Bound	4.2006	
	5% Trimmed Mean		3.1268	
	Median		3.0000	
	Variance		3.863	
	Std. Deviation		1.96551	
	Minimum		.67	
	Maximum		8.12	
	Range		7.45	
	Interquartile Range		2.59	
	Skewness		.993	.524
	Kurtosis		1.139	1.014

Appendix 29.Histograms showing the amplitude data from the experiment in Chapter 6 after the outlier was removed.

Histogram

Mean = 5.54
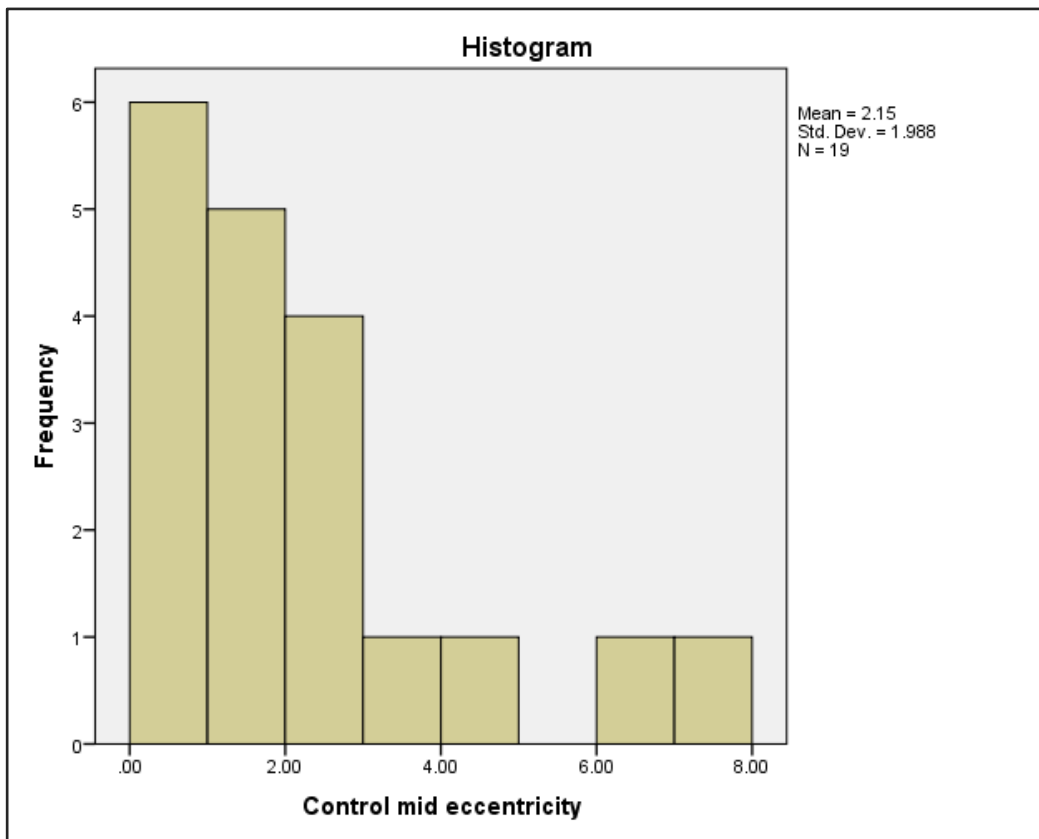Std. Dev. = 3.528
N = 19

Tilted high eccentricity

Histogram

Mean = 1.94
Std. Dev. = 1.962
N = 19

Control low eccentricity

263

Mean = 2.15
Std. Dev. = 1.988
N = 19

Mean = 3.25
Std. Dev. = 1.966
N = 19
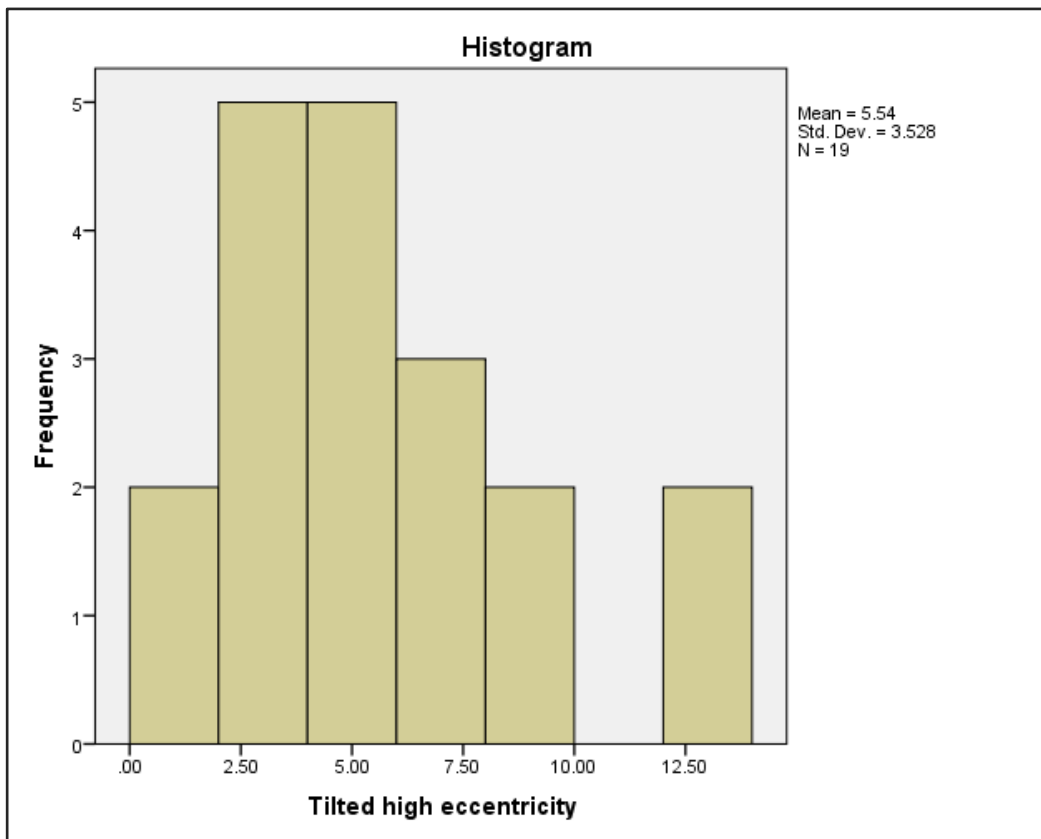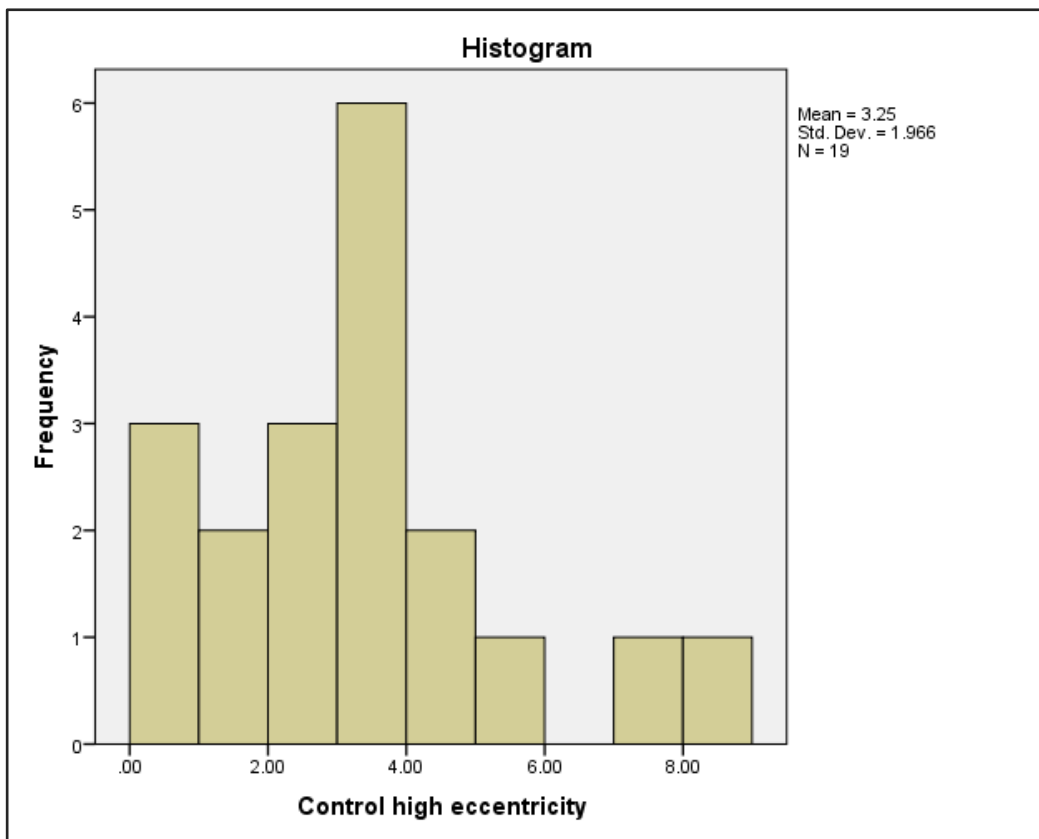
Appendix 30. Descriptive statistics for the amplitude data from the experiment in

Chapter 6 after the data were transformed into their natural logarithms.

			Statistic	Std. Error
Tilted low eccentricity	Mean		1.0544	.21406
	95% Confidence Interval for Mean	Lower Bound	.6006	
		Upper Bound	1.5082	
	5% Trimmed Mean		1.0506	
	Median		1.0217	
	Variance		.779	
	Std. Deviation		.88261	
	Minimum		-.47	
	Maximum		2.65	
	Range		3.12	
	Interquartile Range		1.06	
	Skewness		.019	.550
	Kurtosis		-.195	1.063
Tilted mid eccentricity	Mean		1.5917	.18349
	95% Confidence Interval for Mean	Lower Bound	1.2027	
		Upper Bound	1.9807	
	5% Trimmed Mean		1.6235	
	Median		1.6487	
	Variance		.572	
	Std. Deviation		.75655	
	Minimum		-.13	
	Maximum		2.74	
	Range		2.88	
	Interquartile Range		1.21	
	Skewness		-.349	.550
	Kurtosis		.134	1.063
Tilted high eccentricity	Mean		1.5070	.20467
	95% Confidence Interval for Mean	Lower Bound	1.0731	
		Upper Bound	1.9409	
	5% Trimmed Mean		1.5758	
	Median		1.6740	
	Variance		.712	
	Std. Deviation		.84388	
	Minimum		-.81	
	Maximum		2.59	
	Range		3.40	
	Interquartile Range		1.11	

	Skewness		-1.306	.550
	Kurtosis		2.402	1.063
Control low eccentricity	Mean		.3262	.24523
	95% Confidence Interval for Mean	Lower Bound	-.1936	
		Upper Bound	.8461	
	5% Trimmed Mean		.3297	
	Median		.2877	
	Variance		1.022	
	Std. Deviation		1.01113	
	Minimum		-1.45	
	Maximum		2.04	
	Range		3.48	
	Interquartile Range		1.68	
	Skewness		-.201	.550
	Kurtosis		-.655	1.063
Control mid eccentricity	Mean		.5597	.20768
	95% Confidence Interval for Mean	Lower Bound	.1194	
		Upper Bound	.9999	
	5% Trimmed Mean		.5659	
	Median		.6286	
	Variance		.733	
	Std. Deviation		.85629	
	Minimum		-.98	
	Maximum		1.99	
	Range		2.97	
	Interquartile Range		1.13	
	Skewness		-.236	.550
	Kurtosis		-.526	1.063
Control high eccentricity	Mean		1.0615	.15205
	95% Confidence Interval for Mean	Lower Bound	.7391	
		Upper Bound	1.3838	
	5% Trimmed Mean		1.0696	
	Median		1.1921	
	Variance		.393	
	Std. Deviation		.62690	
	Minimum		-.12	
	Maximum		2.09	
	Range		2.21	
	Interquartile Range		.83	
	Skewness		-.448	.550
	Kurtosis		-.204	1.063